

**Homology modeling-guided medium-throughput screening of
novel hydrolases among *Pseudomonas aeruginosa* genes
of unknown function**

Inaugural-Dissertation

zur Erlangung des Doktorgrades
der Mathematisch-Naturwissenschaftlichen Fakultät
der Heinrich-Heine-Universität Düsseldorf

vorgelegt von

Nikolina Babić

aus Belgrad in Serbien

Düsseldorf, November 2021

Aus dem Institut für Molekulare Enzymtechnologie
der Heinrich-Heine-Universität Düsseldorf

Diese Arbeit wurde durch die Graduiertenschule „Moleküle der Infektion“ (MOI) III von
Jürgen Manchot Stiftung sowie den strategischen Forschungsfonds der Heinrich-Heine-
Universität Düsseldorf gefördert.

Gedruckt mit der Genehmigung der
Mathematisch-Naturwissenschaftlichen Fakultät der
Heinrich-Heine-Universität Düsseldorf

Referent: Prof. Dr. Karl-Erich Jäger
Korreferent: Prof. Dr. Michael Feldbrügge
Tag der mündlichen Prüfung: 25.04.2022

Eidesstattliche Versicherung

Ich versichere an Eides Statt, dass die Dissertation mit dem Thema „Homology modeling-guided medium-throughput screening of novel hydrolases among *Pseudomonas aeruginosa* genes of unknown function“ von mir selbständig und ohne unzulässige fremde Hilfe unter Beachtung der „Grundsätze zur Sicherung guter wissenschaftlicher Praxis an der Heinrich-Heine-Universität Düsseldorf“ erstellt worden ist. Die Dissertation wurde bei keiner anderen Fakultät eingereicht und ich habe bisher keine erfolglosen Promotionsversuche unternommen. Es handelt sich bei allen von mir eingereichten Dissertationsschriften um in Wort und Bild völlig übereinstimmende Exemplare. Weiterhin erkläre ich, dass digitale Abbildungen nur die originalen Daten enthalten und in keinem Fall inhaltsverändernde Bildbearbeitungen vorgenommen wurden.

Düsseldorf, den 18.11.2022

Nikolina Babić

„What is research but a blind date with knowledge?“

Will Harvey

To Ljiljana Sudar and Dragan Dimitrijević

Acknowledgements

I would like to thank my supervisor, Prof. Karl-Erich Jäger, for accepting me in this project and giving me the opportunity to develop my scientific skills in an international environment in the field that I was keen on. Thank you very much for the valuable discussions, important insights, check-points, personal support, and understanding.

I would like to thank my second supervisor, Prof. Michael Feldbrügge, for useful discussions, advice and support during MOI yearly symposia and supervision meetings and for accepting being a coreferee in my thesis.

I would like to thank my mentor, Dr. Filip Kovačić, for the given trust to work on this project and be part of the Bacterial Enzymology group. I am very grateful for the perfect balancing between setting the scientific criteria, which require deep understanding and creativity in problem solving, and simultaneously a very supportive, friendly, and pleasant working atmosphere. Thank you very much for reading the draft of this thesis, your constant support, shared expertise, and countless fruitful and interesting discussions!

I would like to thank our collaborating partner Dr. Sebastian Felgner from the group of Prof. Susanne Häußler for performing *G. mellonella* virulence assays and providing *P. aeruginosa* transposon mutants. Many thanks to Dr. Katherina Bücher and Prof. Laura Hartmann for the successful collaboration and discussions regarding the LecB project.

Thank you Esther Knieps-Grünhagen for sharing your expertise with HPLC, positive attitude and assistance in plasmid purification.

I am thankful to my former students Karina Wolf, Sebastian Schröder, Rolland Oben and Diana Lorenz for their contribution to this project. I am deeply grateful to Diana Lorenz for her diligence during practical help in the last experiments in the project.

I would like to thank my long-term lab-mates Andrea, Talip and Christoph for knowledge sharing, mutual understanding, and advice that made the beginning of my life in Germany easier and for the funny moments. Thanks to Diana, Saji and Matea for the pleasant working atmosphere and support.

I am very grateful to my parents, brother Miloš and sisters Milica, Marija and Jelena for their support, which came from deep within their hearts, and my friends Jelena, Milija, Aleksandra, Milica, Ivana and Christina for the nice moments, support and understanding.

Thank you all!

Publications in the frame of Ph.D. Thesis

Articles

1. Bücher KS, **Babic N**, Freichel T, Kovacic F, Hartmann L. *Monodisperse sequence-controlled α -l-fucosylated glycooligomers and their multivalent inhibitory effects on LecB*. Macromol Biosci, 2018. 18(12): 1800337.
2. Kovacic F, **Babic N**, Krauss U, Jaeger K. *Classification of lipolytic enzyme from bacteria. Aerobic Utilization of Hydrocarbons, Oils, and Lipids*, 2019. 24: 255-89.
3. **Babic N**, Kovacic F. *Predicting drug targets by homology modeling of Pseudomonas aeruginosa proteins of unknown function*. PloS ONE, 2021. 16: e0258385.
4. **Babic N**, Lorenz D, Felgner S, Kovacic F, Jaeger K. *Extending the repertoire of Pseudomonas aeruginosa lipolytic enzymes revealed putative virulence factors*. In preparation.

Poster presentations

1. **Nikolina Babic**, Karl Erich Jaeger and Filip Kovacic. *Hydrolytic enzymes of Pseudomonas aeruginosa as potential virulence factors*. March 2020, Annual Conference of the Association for General and Applied Microbiology, Leipzig, Germany.
2. **Nikolina Babic**, Karl Erich Jaeger and Filip Kovacic. *Characterization of Pseudomonas aeruginosa genes of unknown function*. March 2019, Annual Conference of the Association for General and Applied Microbiology, Mainz, Germany.
3. **Nikolina Babic**, Tobias Schwabroch, Katharina Bücher, Laura Hartmann, Karl Erich Jaeger and Filip Kovacic. *Synthetic oligomers as inhibitors of Pseudomonas aeruginosa virulence factor lectin LecB*. April 2018, Annual Conference of the Association for General and Applied Microbiology, Wolfsburg, Germany.

Table of contents

Publications in the frame of Ph.D. Thesis.....	VI
List of abbreviations (alphabetically ordered)	XI
List of tables	XIII
List of figures	XIV
Abstract	1
Zusammenfassung.....	3
1. Introduction.....	5
1.1. Pathogenic bacterium <i>P. aeruginosa</i>	5
1.2. <i>P. aeruginosa</i> virulence and pathogenicity	6
1.2.1. Type IV pili	7
1.2.2. Flagellum	8
1.2.3. Lipopolysaccharide	9
1.2.4. Alginate.....	9
1.2.5. Biofilm.....	9
1.2.6. Lectins.....	10
1.2.7. Secretion systems.....	11
1.2.8. Pyocyanin	12
1.2.9. Rhamnolipids	13
1.3. Antibiotic resistance in <i>P. aeruginosa</i>	13
1.3.1. Intrinsic antibiotic resistance	14
1.3.2. Acquired antibiotic resistance	15
1.3.3. Adaptive antibiotic resistance and tolerance.....	16
1.4. Global significance and emerging antimicrobial strategies against <i>P. aeruginosa</i>	17
1.4.1. Anti-resistance therapy	18
1.4.2. Anti-virulence therapy.....	21
1.5. <i>P. aeruginosa</i> hydrolytic enzymes and their potential as antimicrobial targets.....	23
1.5.1. Esterases.....	24
1.5.2. Lipases	24
1.5.3. Phospholipases	25
1.5.4. Acyl-CoA thioesterases.....	27
1.5.5. Phosphatases.....	27
1.5.6. Phosphoric-diester hydrolases	28
1.5.7. Glycosylases.....	28
1.5.8. Peptidases	29
1.5.9. Hydrolases acting on non-peptide C-N bond	30

1.6. Aims of the study.....	31
2. Material and methods.....	33
2.1. Chemicals	33
2.2. <i>In silico</i> methods.....	33
2.2.1. Databases	33
2.2.2. Servers	33
2.2.3. The Basic Local Alignment Search Tool (BLAST)	34
2.2.4. Programs	34
2.2.5. Design of primers for PCR amplification of GUFs	35
2.3. DNA methods	35
2.3.1. Touchdown polymerase chain reaction (TD-PCR).....	35
2.3.2. Trypsin treatment of the PCR products.....	36
2.3.3. Isolation of genomic DNA.....	36
2.3.4. Isolation of plasmid DNA	37
2.3.5. Purification of DNA.....	37
2.3.6. Endonuclease hydrolysis and dephosphorylation of pGUF vector	38
2.3.7. Purification of linearized pGUF with the anion exchange chromatography	38
2.3.8. Gibson assembly cloning	38
2.3.9. Endonuclease hydrolysis and phosphorylation of GUFs in 96-well plates.....	39
2.3.10. Ligation in 96-well plates.....	39
2.3.11. Agarose gel electrophoresis	39
2.3.12. Colony PCR.....	39
2.3.13. DNA sequencing	40
2.4. Cultivation and manipulation of bacteria	40
2.4.1. Used media, bacterial strains, and plasmids.....	40
2.4.2. Cultivation of bacteria	55
2.4.3. Storage of bacteria	56
2.4.4. Preparation of chemically competent <i>E. coli</i>	56
2.4.5. Preparation of chemically competent <i>P. aeruginosa</i> PA01.....	56
2.4.6. Chemical transformation of bacteria	56
2.5. Protein methods.....	57
2.5.1. Protein expression in <i>E. coli</i>	57
2.5.2. Protein expression in <i>P. aeruginosa</i>	58
2.5.3. Preparation of bacterial cell lysates	58
2.5.4. Dot-blot	59
2.5.5. SDS-polyacrylamide gel electrophoresis (SDS-PAGE).....	59

2.5.6. Western blot.....	60
2.6. Enzyme assays	60
2.6.1. Esterase activity assay	61
2.6.2. Lipase activity assay.....	61
2.6.3. Phosphatase activity assay	61
2.6.4. Phosphodiesterase activity assay	61
2.6.5. Phospholipase C activity assay	62
2.6.6. Protease activity assay	62
2.6.7. Glucosidase activity assay	62
2.6.8. Thioesterase activity assay	62
2.6.9. Phospholipase and lipase assay using non-esterified fatty acid (NEFA) kit	63
2.6.10. Phospholipase A2 assay.....	63
2.7. Modified enzyme-linked lectin assay (mELLA)	63
2.8. Biological assays	64
2.8.1. Biofilm formation assay.....	64
2.8.2. <i>Galleria mellonella</i> virulence assay	64
3. Results	66
3.1. Bioinformatic analysis of <i>P. aeruginosa</i> genes of unknown function (GUFs)	66
3.1.1. Identification of <i>P. aeruginosa</i> GUFs.....	66
3.1.2. Comparative genomic analysis of <i>P. aeruginosa</i> GUFs	67
3.1.3. <i>In silico</i> assignment of putative biochemical and biological functions to <i>P. aeruginosa</i> PUFs	68
3.2. Novel expression vector pGUF enables functional protein expression in <i>E. coli</i> and <i>P. aeruginosa</i>	74
3.2.1. Novel expression plasmid pGUF is constructed by the Gibson cloning	74
3.2.2. Validation of the cloning strategy and pGUF functionality	76
3.3. Development of medium-throughput cloning pipeline and generation of the expression plasmid library.....	79
3.3.1. Optimization of medium-throughput cloning	79
3.3.2. Generation of the expression plasmid library	81
3.3.3. Preparing linear pGUF vector for the library construction	82
3.3.4. Medium-throughput TD-PCR amplification of GUFs	83
3.3.5. Identification of positive pGUF constructs	85
3.4. Screening of hydrolase activities.....	89
3.4.1. Expression of putative hydrolases.....	89
3.4.2. Enzyme activity screening revealed promising novel hydrolases	93
3.5. Validation of hydrolase activities identified in the screening.....	120

3.6. Biological roles of characterized <i>P. aeruginosa</i> GUFs	135
3.6.1. Novel <i>P. aeruginosa</i> biofilm effectors	135
3.6.2. Novel <i>P. aeruginosa</i> virulence factors in the <i>Galleria mellonella</i> model	137
3.7. Inhibition of virulence factor LecB sugar-binding activity by glycoamidoamines.....	138
4. Discussion.....	140
4.1. Structure homology modeling guided deciphering the functions of <i>P. aeruginosa</i> GUFs.....	140
4.2. The pGUF is a novel cloning and expression vector.....	145
4.3. Medium-throughput cloning of <i>P. aeruginosa</i> GUFs	148
4.4. Medium-throughput <i>P. aeruginosa</i> PUFs production and enzyme activity screening	152
4.5. Novel <i>P. aeruginosa</i> hydrolases and their biological significance.....	156
4.6. Glycoamidoamines as <i>P. aeruginosa</i> lectin LecB inhibitors	164
5. Supplementary data	166
6. References	203

List of abbreviations (alphabetically ordered)

Acyl-acyl carrier proteins	ACP
Acyl-CoA thioesterase	AT
α -Benzoyl-L-arginine- <i>p</i> -nitroanilide	BA- <i>p</i> -NA
Basic local alignment search tool	BLAST
Conserved Domain Database (CDD)	CDD
(6R,7R)-3-[(3-Carboxy-4-nitrophenyl)sulfanylmethyl]-8-oxo-7-[(2-thiophen-2-ylacetyl)amino]-5-thia-1-azabicyclo[4.2.0]oct-2-ene-2-carboxylic acid	CENTA
Coenzyme A	CoA
Cystic fibrosis	CF
Dimethyl sulfoxide	DMSO
1,2-dipalmitoyl-sn-glycero-3-phosphocholine	16:0 PC
1,2-dipalmitoyl-sn-glycero-3-phosphoethanolamine	16:0 PE
1,2-dipalmitoyl-sn-glycero-3-phospho-(1'-rac-glycerol)	16:0 PG
5,5-Dithio-bis-(2-nitrobenzoic acid)	DTNB
Deep 96-well plate	DWP
Extracellular polysaccharide	EPS
Extended-spectrum beta-lactamases	ESLB
Extracellular DNA	eDNA
Gene ontology	GO
Glyceryl tridecanoate	GTD
Infectious Diseases Society of America	IDSA
Isopropyl β -D-1-thiogalactopyranoside	IPTG
Lysogeny broth	LB
L-leucine- <i>p</i> -nitroanilide	Leu- <i>p</i> -NA
Lipopolysaccharide	LPS
Multivalent adhesion molecule-7	MAM-7
Metallo beta-lactamases	MBL
Multiple cloning site	MCS
Multi-drug resistant	MDR
Modified enzyme-linked lectin assay	mELLA
Minimal inhibitory concentration	MIC
Microtiter plates	MTP
Non-esterified fatty acid	NEFA
Not determined	n.d.
Optical density	OD
Outer membrane	OM
Open reading frame	ORF
Poly-acetyl-arginyl-glucosamine	PAAG
Polymerase chain reaction	PCR
Protein database	PDB
Peptidoglycan	PG
Pseudomonas genome database	PGD
Protein homology/analogy recognition engine	Phyre
Phospholipases A1	PLA1
Phospholipases A2	PLA2

Phospholipases B	PLB
Phospholipases C	PLC
Phospholipases D	PLD
Patatin-like phospholipase	PLP
Peptide nucleic acid	PNA
<i>p</i> -Nitrophenyl butyrate	p-NPB
<i>p</i> -Nitrophenyl decanoate	<i>p</i> -NPdec
<i>p</i> -Nitrophenyl phosphate	<i>p</i> -NPP
<i>p</i> -nitrophenyl phosphorylcholine	<i>p</i> -NPPC
Room temperature	r.t.
Resistance nodulation-cell division	RND
Small multidrug resistance	SMR
Super optimal broth with catabolite repression	SOC
The sum of average activity and the standard deviation	Ave.+S.D.
Toxin-antitoxin system	TA
Touchdown polymerase chain reaction	TD-PCR
Extensively drug-resistant	XDR

List of tables

Table 1. Used bacterial strains.

Table 2. Used plasmids.

Table 3. Composition of SDS-polyacrylamide gels.

Table 4: Keywords used for textual mining of templates used to build reliable structural models by Phyre2 homology modeling.

Table 5: Keywords used for textual mining of templates with virulence and antibiotic resistance-related functions.

Table 6. Sequence alignments of pGUF backbone and walking primer Sanger sequencing results.

Table 7. Summarized sequencing data for pGUF-*guf* expression plasmids containing genes < 1000 bp.

Table 8. Summarized sequencing data for pGUF-*guf* expression plasmids containing genes \geq 1000 bp.

Table 9. PUFs with high and moderate activities in hydrolase enzyme screenings.

Table 10. Phyre2 models and Uniprot annotations of proteins with validated *in vitro* hydrolase activities.

Table 11. Comparison of plasmid libraries validation results.

Table S1. Used oligonucleotides.

Table S2. Sequencing results of pGUF-*guf* expression plasmids obtained using forward primer.

Table S3. Positive Sanger sequencing results of genes \geq 1000 bp obtained with the reverse primer.

Table S4. Organization of GUFs expressed from corresponding pGUF constructs in DWP and analyzed by dot-blot and hydrolase assays.

Table S5. PUFs with low activities in hydrolase enzyme screening.

List of figures

- Fig. 1. An arsenal of virulence factors produced by *Pseudomonas aeruginosa*.
- Fig. 2. Modified TD-PCR cycling protocol for amplification of GUFs in 96-well plate.
- Fig. 3. *P. aeruginosa* genes of unknown function.
- Fig. 4. Pathogen-specific, essential, virulence factors and genes with human homologs among GUFs.
- Fig. 5. Pie charts showing success of homology modeling of 2137 *P. aeruginosa* PUFs using the Phyre2 server.
- Fig. 6. Pipeline for automatic analysis of results obtained after homology modeling of 2137 PUFs with Phyre2 server.
- Fig. 7. Predicted biochemical functions for *P. aeruginosa* PUFs by Phyre2 homology modeling.
- Fig. 8. Subclassification of predicted biochemical functions by Phyre2 homology modeling and superimposition of 3D structures of model and corresponding template for three selected PUFs.
- Fig. 9. Predicted virulence-related biological functions for *P. aeruginosa* proteins of unknown function.
- Fig. 10. Design and construction of pGUF vector.
- Fig. 11. Verification of pGUF sequence.
- Fig. 12. Cloning strategy for the generation of pGUF constructs.
- Fig. 13. Validation of pGUF-*plaf* expression vector in *E. coli* and *P. aeruginosa*.
- Fig. 14. Optimization of TD-PCR conditions for GUFs amplification in 96-well plates.
- Fig. 15. Scheme of cloning pipeline in 96-well plates.
- Fig. 16. Large-scale purification of linear pGUF plasmid by Mono Q™ anion exchange chromatography.
- Fig. 17. Agarose gel electrophoresis of GUFs amplified by optimized TD-PCR in 96-well PCR plate.
- Fig. 18. Screening of positive clones.
- Fig. 19. Sequencing results indicate that mismatches and gaps often arose as the consequence of unreliable signals in the sequencing chromatogram.
- Fig. 20. Western blot analysis of recombinant PUFs expression in *E. coli* BL21(DE3).
- Fig. 21. Dot-blot analysis of expression of PUFs from plates HY I and HY II.
- Fig. 22. Dot-blot analysis of PUFs expression in plates HY III and HY IV.
- Fig. 23. Dot-blot analysis of PUFs expression in plates HY V and HY VI.
- Fig. 24. Fingerprint showing a screening of esterase activity with *p*-nitrophenyl butyrate.
- Fig. 25. Fingerprint showing a screening of thioesterase activity measured with acetyl-CoA and palmitoyl-CoA.
- Fig. 26. Fingerprint showing a screening of lipase activity measured with *p*-nitrophenyl decanoate.
- Fig. 27. Fingerprint showing a screening of lipase activity measured with glyceryl tridecanoate.
- Fig. 28. Fingerprint showing a screening of phospholipase A/B activities measured with 16:0 PC, 16:0 PE, and 16:0 PG cocktail.
- Fig. 29. Fingerprint showing a screening of phospholipase C activity measured with *p*-nitrophenyl phosphorylcholine.
- Fig. 30. Fingerprint showing a screening of phosphodiesterase activity measured with bis-*p*-nitrophenyl phosphate.
- Fig. 31. Fingerprint showing a screening of phosphatase activity with *p*-nitrophenyl phosphate.
- Fig. 32. Fingerprint showing a screening of protease activity measured with α -benzoyl-L-arginine-*p*-nitroanilid and L-leucine-*p*-nitroanilide.
- Fig. 33. Fingerprint showing a screening of α/β -glucosidase activity measured with *p*-nitrophenyl- α -D-glucopyranosid and *p*-nitrophenyl- β -D-glucopyranosid.
- Fig. 34. Esterase activity and Western blot signal of recombinant PA2315 expressed from pGUF-*pa2315* vector in *E. coli* BL21(DE3).
- Fig. 35. Esterase activity of recombinant PA2689 expressed from pGUF-*pa2689* vector in *E. coli* BL21(DE3).

- Fig. 36. Esterase activity of recombinant PA3615 expressed from pGUF-*pa3615* vector in *E. coli* BL21(DE3).
- Fig. 37. Esterase (A) and thioesterase (B) activity of recombinant PA2693 expressed from pGUF-*pa2693* vector in *E. coli* BL21(DE3).
- Fig. 38. Esterase (A) and lipase (B) activity of recombinant PA3518 expressed from pGUF-*pa3518* vector in *E. coli* BL21(DE3).
- Fig. 39. Esterase (A) and lipase (B) activity of recombinant PA0829 expressed from pGUF-*pa0829* vector in *E. coli* BL21(DE3).
- Fig. 40. Phospholipase A2 activity of recombinant PA3750 expressed from pGUF-*pa3750* vector in *E. coli* BL21(DE3).
- Fig. 41. Phospholipase A2 activity of recombinant PA2419 expressed from pGUF-*pa2419* vector in *E. coli* BL21(DE3).
- Fig. 42. Phospholipase A2 activity of recombinant PA2660 expressed from pGUF-*pa2660* vector in *E. coli* BL21(DE3).
- Fig. 43. Phospholipase A2 activity of recombinant PA0484 expressed from pGUF-*pa0484* vector in *E. coli* BL21(DE3).
- Fig. 44. Phospholipase A activity of recombinant PA1193 expressed from pGUF-*pa1193* vector in *E. coli* BL21(DE3).
- Fig. 45. Phospholipase A activity of recombinant PA5535 expressed from pGUF-*pa5535* vector in *E. coli* BL21(DE3).
- Fig. 46. Phospholipase C activity of recombinant PA4961 expressed from pGUF-*pa4961* vector in *E. coli* BL21(DE3).
- Fig. 47. Phospholipase C activity of recombinant PA0285 expressed from pGUF-*pa0285* vector in *E. coli* BL21(DE3).
- Fig. 48. Phosphodiesterase activity of recombinant PA5028 expressed from pGUF-*pa5028* vector in *E. coli* BL21(DE3).
- Fig. 49. Phosphodiesterase (A) and phosphatase (B) activity of recombinant PA0543 expressed from pGUF-*pa0543* vector in *E. coli* BL21(DE3).
- Fig. 50. Phosphodiesterase (A) and phosphatase (B) activity of recombinant PA3074 expressed from pGUF-*pa3074* vector in *E. coli* BL21(DE3).
- Fig. 51. Phosphatase activity of recombinant PA1089 expressed from pGUF-*pa1089* vector in *E. coli* BL21(DE3).
- Fig. 52. Biofilm formation assay with *P. aeruginosa* transposon mutants (Tn).
- Fig. 53. Kaplan-Meier plots of *P. aeruginosa* transposon mutant strains of PA0285 (A) and PA1784 (B) in *G. mellonella* virulence assay.
- Fig. 54. Inhibition of LecB binding to α -L-fucose-PAA-biotin by glycoamidoamines.
- Fig. 55. Biofilm formation assay with *P. aeruginosa* incubated with glycoamidoamine inhibitors.
- Fig. 56. Secondary structures of T-7 terminator RNA sequences.
- Fig. 57. Comparison of the cloning pipelines used in high/medium-throughput projects.
- Fig. 58. Multiple protein sequence alignment of PA2315 and three esterases from lipolytic enzyme family VIII.
- Fig. 59. Protein sequence alignment between PA4961 and *Pasteurella multocida*AhpA (Q9L8J3).
- Fig. 60. Multiple protein sequence alignment between PA0829, lipolytic enzymes from family V and Phyre2 structural templates.
- Fig. 61. Multiple protein sequence alignment between PA3750 and lipolytic enzymes from family II.
- Fig. 62. Multiple protein alignment between PA0285 and Phyre2 templates.

Abstract

A rising threat to human health emerges from antibiotic-resistant bacteria, which are already a significant cause of morbidity and mortality. One of the most problematic nosocomial pathogens, a member of the ESKAPE pathogens, is *P. aeruginosa*. The notorious status of *P. aeruginosa* is due to its capacity to produce a plethora of different virulence factors and cause severe infections in immunocompromised patients and the existence of multidrug-resistant clones, which have become prevalent worldwide. Although antibiotic resistance is a natural phenomenon, it is highly accelerated by human activities. The main concern is that the development of novel antibiotics significantly lags behind the emergence of resistant clones. The global urge for faster development of novel antibiotics is reflected in the announcement of the World Health Organization, which published a list of bacteria that are the most critical for introducing novel antibiotics. Since clones resistant to the new β -lactam imipenem have been identified, *P. aeruginosa* is listed in the most critical group. The way to confront this issue is to identify novel therapeutic strategies, drug targets, and their inhibitors (drugs). An obstacle on that road represents the fact that nearly 40 % of the *P. aeruginosa* genome consists of genes whose functions are still unknown. This often hampers the interpretation of various global proteomics and transcriptomics studies and generally limits our knowledge about bacterial pathology and physiology. Simultaneously, this pool of genes represents a valuable source for research on novel drug targets, possibly revealing novel structures, mechanisms, or metabolic pathways. Moreover, the functional deciphering of genes of unknown function (GUFs) has general significance, as these genes represent a burden in the databases in the current genomic era.

In the present work, medium-throughput *in silico* and experimental characterization of *P. aeruginosa* GUFs was performed to identify novel drug targets. The comparative genomic analysis revealed 106 GUFs as a drug-target research priority group based on their sequence similarity to other virulence factors, pathogen-specific genes, essential roles, and the absence of homologues among human genes. Furthermore, putative biochemical functions were assigned to 1267 *P. aeruginosa* GUFs based on 3D structural homology modelling. This analysis revealed that more than 1000 proteins of unknown function (PUFs) had putative enzyme functions, including 566 putative hydrolases. Since many essential, virulence-related, and antibiotic resistance proteins have hydrolase functions, this set of genes was further experimentally characterized. To that end, the novel broad-host-range pGUF vector

was assembled and used to generate an expression plasmid library consisting of 606 pGUF-*guf* constructs. The medium-throughput expression of 460 GUFs from pGUF-*guf* constructs, including 429 putative hydrolases, was conducted in *E. coli* with an expression success rate of 76 %. The screening of hydrolase activities using *E. coli* cell lysates and 15 different substrates resulted in 57 positives. Finally, in a separate experiment, 18 novel hydrolase activities were confirmed, including five esterases, one thioesterase, two lipases, six phospholipases A, two phospholipases C and three phosphodiesterases and phosphatases. Further analysis of these genes led to the identification of two putative virulence factors and three biofilm effectors, representing novel candidates for drug targets.

Zusammenfassung

Eine zunehmende Bedrohung der menschlichen Gesundheit geht von antibiotikaresistenten Bakterien aus, die bereits eine bedeutende Ursache für Morbidität und Mortalität darstellen. Eines der problematischsten nosokomialen Pathogene, ein Mitglied der ESKAPE-Erreger, ist *P. aeruginosa*. Der berühmte Status von *P. aeruginosa* ist auf seine Fähigkeit zurückzuführen, eine Vielzahl verschiedener Virulenzfaktoren zu produzieren und schwere Infektionen bei immungeschwächten Patienten zu verursachen, sowie auf das Vorhandensein von multiresistenten Klonen, die sich weltweit verbreitet haben. Obwohl die Antibiotikaresistenz ein natürliches Phänomen ist, wird sie durch menschliche Aktivitäten stark beschleunigt. Das Hauptproblem ist, dass die Entwicklung neuer Antibiotika deutlich hinter dem Auftreten resistenter Klone zurückbleibt. Das weltweite Drängen auf eine schnellere Entwicklung neuer Antibiotika spiegelt sich in der Ankündigung der Weltgesundheitsorganisation, in der die Pathogene, die für die Einführung neuer Antibiotika am kritischsten sind, veröffentlicht wurden. Seit der Identifizierung von Klonen, die gegen das neue β -Lactam, Imipenem, resistent sind, wird *P. aeruginosa* in der kritischsten Gruppe geführt. Der Weg zur Lösung dieses Problems besteht darin, neue therapeutische Strategien, therapeutische Ansatzpunkte und deren Inhibitoren (Medikamente) zu identifizieren. Ein Hindernis auf diesem Weg ist die Tatsache, dass fast 40 % des Genoms von *P. aeruginosa* aus Genen besteht, deren Funktionen noch unbekannt sind. Dies erschwert häufig die Interpretation verschiedener globaler Proteom- und Transkriptomstudien und schränkt unser Wissen über die Pathologie und Physiologie der Bakterien generell ein. Gleichzeitig stellt diese Gengruppe eine wertvolle Quelle für die Erforschung neuer Arzneimittelziele dar, die möglicherweise neue Strukturen, Mechanismen oder Stoffwechselwege offenbaren. Darüber hinaus ist die funktionelle Entschlüsselung von Genen mit unbekannter Funktion (GUFs) von allgemeiner Bedeutung, da diese Gene im gegenwärtigen Zeitalter der Genomik eine Belastung für die Datenbanken darstellen.

In der hier vorgestellten Arbeit wurde eine *in silico* und experimentelle Charakterisierung von *P. aeruginosa*-GUFs mit mittlerem Durchsatz durchgeführt, um neue Arzneimittelziele zu identifizieren. Die vergleichende Genomanalyse ergab, dass 106 GUFs aufgrund ihrer Sequenzähnlichkeit mit anderen Virulenzfaktoren, pathogen-spezifischer Genen, essenzieller Funktionen und des Fehlens von Homologen unter menschlichen Genen eine vorrangige Gruppe für die Arzneimittelforschung darstellen. Darüber hinaus wurden 1267 *P.*

aeruginosa-GUFs auf Grundlage der 3D-Strukturhomologiemodellierung mutmaßliche biochemische Funktionen zugewiesen. Diese Analyse ergab, dass mehr als 1000 Proteine mit unbekannten Funktionen (PUFs) mutmaßliche Enzymfunktionen haben, darunter 566 mutmaßliche Hydrolasen. Da viele essenzielle virulenzbezogene und antibiotikaresistente Proteine Hydrolasefunktionen haben, wurde diese Gruppe von Genen weiter experimentell charakterisiert. Zu diesem Zweck wurde der neuartige pGUF-Vektor mit breiter Wirtsreichweite zusammengesetzt und zur Erzeugung einer Expressionsplasmidbibliothek verwendet, die aus 606 pGUF-*guf*-Konstrukten besteht. Die Expression von 460 GUFs aus pGUF-*guf*-Konstrukten, darunter 429 mutmaßliche Hydrolasen, wurde im mittleren Durchsatz in *E. coli* mit einem Expressionserfolg von 76 % durchgeführt. Das Screening der Hydrolaseaktivitäten unter Verwendung von *E. coli*-Zelllysaten und 15 verschiedenen Substraten ergab 57 positive Klone. In einem separaten Experiment wurden schließlich 18 neue Hydrolaseaktivitäten bestätigt, darunter fünf Esterasen, eine Thioesterase, zwei Lipasen, sechs Phospholipasen A, zwei Phospholipasen C und drei Phosphodiesterasen und Phosphatasen. Die weitere Analyse dieser Gene führte zur Identifizierung von zwei mutmaßlichen Virulenzfaktoren und drei Biofilm-Effektoren, die neue Kandidaten für Arzneimittel sind.

1. Introduction

1.1. Pathogenic bacterium *P. aeruginosa*

P. aeruginosa is a rod-shaped, monoflagellated, heterotrophic bacterium and is one of 144 species of the largest gram-negative bacterium genus, *Pseudomonas*, belonging to the gamma-Proteobacterium phylum. [1, 2] *P. aeruginosa* is a pathogenic bacterium capable of infecting plants, animals, and insects and is the epitome of a human opportunistic bacterium. [3] Infections with *P. aeruginosa* can occur in almost every human tissue in patients with primary or acquired immunodeficiencies and chronic conditions such as cystic fibrosis, burns, cancer, tuberculosis, and AIDS. [4] Community-acquired *P. aeruginosa* infections include ulcerative keratitis correlated with contact lens application and ear and skin infections often found in *diabetes mellitus* patients. [5] Regarding hospital-acquired infections, including pneumonia, urinary tract, bloodstream, and surgical site infections, *P. aeruginosa* is considered one of the most important nosocomial pathogens, causing 10-20 % of infections in most hospitals and being associated with high morbidity and mortality rates. [5-8]

The two *P. aeruginosa* reference strains, PAO1 and PA14, both isolated from patient wounds, are commonly used in laboratories worldwide. The genomes of both strains are highly similar, except that PA14 contains two additional pathogenicity islands and a mutation in the *ladS* gene, which correlates with the increased virulence of PA14 in comparison to PAO1, which is moderately virulent. [9] Sequencing the complete *P. aeruginosa* PAO1 genome comprised of 6.3 million base pairs on a single circular chromosome revealed its atypical complexity in comparison to other bacteria, making it more similar to the simple eukaryote *Saccharomyces cerevisiae*. [10] Among the 5570 identified ORFs, there are a large number of enzymes participating in almost 1000 metabolic pathways, allowing the bacteria to catabolize over 100 different organic molecules, including polycyclic aromatic hydrocarbons, under aerobic or anaerobic conditions. [2, 4, 11] In addition to metabolic versatility, the richness of the genome is reflected in the high proportion of regulatory genes, i.e., 8-9 % of *P. aeruginosa* genes encode transcriptional regulators or regulatory two-component system proteins. [10] This enables bacterial adaptation and thriving in different and challenging habitats, such as soil, water, various plant and animal tissues, and even in soap and antiseptic solutions, distilled water, cosmetics, and hot tubs. [2, 4, 12] *P. aeruginosa* can grow in a relatively broad temperature range, 4–42 °C, while survival at 42 °C differentiates *P. aeruginosa* from other species of this genus. [13]

Although long considered ubiquitous, recent studies indicate that the bacterium is more likely to be found in environmental samples close to humans. [14] *P. aeruginosa* exists in nature in biofilm communities attached to surfaces or in a fast-swimming unicellular planktonic form. [4] When cultivated in laboratory conditions, the strains obtained from soil and aquatic habitats form small and rough colonies, while large and smooth colonies are observed from clinical isolates and are additionally very slimy if isolated from respiratory and urinary secretions due to the production of the exopolysaccharide alginate. [4] The characteristic blue-green colour of *P. aeruginosa* originates from the pigment pyocyanin, which has an important role in virulence and whose derivative pyochelin, together with the fluorescent pigment pyoverdine, are siderophores important for bacterial growth in iron-depleted environments. [15, 16] *P. aeruginosa* produces additional pigments: pyoverdine (yellow, green, and fluorescent), pyomelanin, which is light brown, and reddish-brown pyorubrin. [17, 18]

1.2. *P. aeruginosa* virulence and pathogenicity

Although *P. aeruginosa* is not a typical pathogen, due to its genomic plasticity and complex regulatory and signalling networks, it can adapt to various host tissues with compromised immunity or damaged epithelial barriers, causing acute or chronic infections. [19-21] *P. aeruginosa* infection is a spatially and temporally organized process occurring in stages: bacterial attachment, colonization, local invasion, and bloodstream dissemination. [22, 23] Between these stages and in the transition from acute to chronic infection, there are phenotypic switches with respect to the core metabolism, production of virulence factors, genomic stability, growth rate, motility, lifestyle, etc. [24-26] Moreover, genetically and phenotypically diverse clones often exist in one population at the same time, as shown by comparative genomics and biological characterization of subsequent isolates of the same ancestral strain from a cystic fibrosis patient. [26, 27] Phenotypic diversity emerges from the bacterial tendency to maximize its survival during interaction with the host. The phenotypic alterations are orchestrated *via* quorum sensing, chemotaxis, hypermutability, and various signalling and regulatory pathways, including c-di-GMP signalling and two-component regulatory systems such as cAMP/Vfr and Gac/Rsm. [24, 25, 28, 29] Quorum sensing represents the cell-to-cell communication system in which the cells share and receive information about their population density *via* a specific molecule, the autoinducer, which then regulates the expression of certain genes, including virulence factors. [30] The most important quorum-

sensing systems in *P. aeruginosa* are the *las* and *rhl* systems, which use l-homoserine lactone derivatives as autoinducers. [30]

Key players in the first stages of infection and during acute infection are virulence factors specific to the host and localization of the infection. The consequences of their actions are damaged tissues and abolishment of the host immune response, which results in pathogenesis.[29] Virulence factors are classified as cell-associated virulence factors, including pili, flagellum, lipopolysaccharide (LPS), and extracellular virulence factors, which are mainly toxic effectors secreted through one of five secretion systems (Fig. 1). [25]

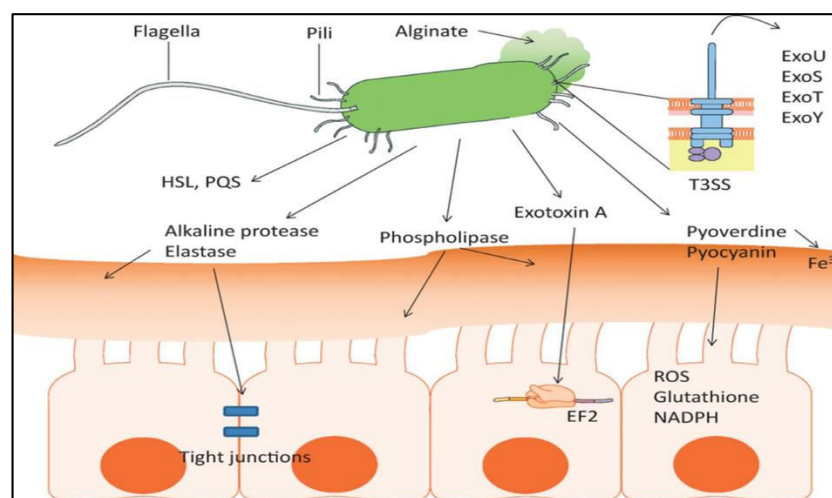


Fig. 1. An arsenal of virulence factors is produced by the *Pseudomonas aeruginosa*. The figure is adopted from Gellatly *et al.* (2013) [61] with the permission of Oxford University press (licence nr. 5185380517169). Cell-associated virulence factors include flagella and type 4 pili, which are the main adhesion and motility determinants. Extracellular virulence factors include polysaccharide alginate, which has protective role against host immune components; toxins secreted through T3SS (exotoxins U, S, T and Y) and exotoxin A, which disrupts host translation process by inactivating elongation factor 2; hydolytic enzymes including phospholipases which damage host cell membranes and proteases which disrupt epithelial cell tight junctions facilitating bacterial invasion; pyocyanin that interferes with host cell electron transport pathways inducing ROS-mediated host cell damage; pyoverdine which enables bacterial adaptation to the iron-depleted environments. The regulation of virulence factors is achieved by quorum sensing systems PQS and HSL. EF2 - elongation factor 2, ROS - reactive oxygen species, NADPH - reduced nicotinamide adenine dinucleotide phosphate, HSL-homoserine lactone, PQS - *Pseudomonas* quinolone signal.

1.2.1. Type IV pili

Type IV pili (T4P) are polar surface fibres whose assembly (polymerization of PilA protein monomer) and retraction (depolymerization) are achieved by two ATPases anchored at the base. [31-33] These retraction dynamics of pili polymerization represent twitching motility, which bacteria use in surface sensing, mobility, and attachment. [34] T4P have many virulence roles. They are important to prevent bacterial opsonization by host surfactant protein

A (SP-A) [35] The attachment of T4P to host cells leads to the activation of many genes, including virulence determinants such as T2SS and T3SS, and LasR quorum sensing. [36] Twitching motility has been shown to be important in tissue invasion by facilitating bacterial translocation through epithelial layers. [37] Moreover, T4P has a role in the formation of mushroom-like biofilm structures. [38] Components of T4P, PilT, and PilU are involved in T3SS activity and are therefore important in exerting cytotoxicity. [39]

1.2.2. Flagellum

P. aeruginosa flagellum is composed of basal bodies (rotary motor) transversing the inner and outer membranes, the hook consisting of FlgE, helicoidally polymerized flagellin FliC that constitutes the filament (helical propeller), and the cap consisting of FliD. [40, 41] The primary role of the flagellum is swimming in low-density surroundings achieved by force generated by the corkscrew-like rotation of the flagellum powered by proton flux. [42] Importantly, the direction of swimming is driven by chemotaxis, in which the binding of a certain attractant or repellent molecule to one of the 26 identified receptors (methyl-accepting chemotaxis proteins, MCPs) activates the kinase/phosphatase intracellular cascade, ultimately leading to the phosphorylation/dephosphorylation of the flagellar motor protein FliM. [43] This allows the bacteria to quickly move towards desirable and away from detrimental temperature, pH, and nutrient gradients. The importance of the flagellum in virulence was shown in a mouse model of subcutaneous infection, in which bacterial invasion and persistence were dependent on the flagellum. [44] Furthermore, 25 % of the mice developed pneumonia when inoculated with a *fliC* deletion mutant *P. aeruginosa* strain. [45] Similar to T4P, flagellum also has dual functions: motility and adhesion. The flagellar components are identified as adhesins responsible for binding to glycolipids and proteoglycans localized on human epithelial cells (FliC), [46, 47] human respiratory mucin MUC-1 (FliD), [46] and SP-A surfactant (FliC). [48] The flagellum is an important antigen determinant (H-antigen) [49] that can induce an innate immune response by inducing pro-inflammatory cytokines *via* flagellin recognition by TLR (toll-like receptors). [50] Interestingly, it was shown that flagellum-mediated motility, but not the presence of flagellum *per se*, is needed to trigger phagocytosis, [51] which could explain the existence of nonmotile phenotypes isolated from chronically infected cystic fibrosis patients. [52]

1.2.3. Lipopolysaccharide

Lipopolysaccharide (LPS) is a major component of the outer membrane, consisting of the hydrophobic glycolipid (lipid A), the core oligosaccharide region, and long O-polysaccharide (O-antigen), which protrudes into the extracellular space. [53] LPS represents an additional protection barrier: its lipid moiety together with the phospholipid membrane prevents the passage of polar molecules, while polar sugar groups repel nonpolar molecules. [54] LPS strongly stimulates host immune cells but also muscle and endothelial cells to produce potent mediators of inflammation, such as interleukins-1 and 6, reactive oxygen species (ROS), nitric oxide, and thromboxane A₂. [55] Therefore, when present in large amounts, LPS leads to extensive host tissue damage and possibly septic shock, which categorizes it as an endotoxin. [55] LPS has roles in bacterial attachment and biofilm formation, as concluded from Lipid A mutants. [56] Additionally, the O-polysaccharide chain of LPS protects the bacteria from phagocytosis. [57]

1.2.4. Alginate

Alginate is an exopolysaccharide consisting of acylated D-mannuronic and L-guluronic acids, whose acyl groups bind water and nutrients, resulting in mucoid consistency. [25] In addition to scavenging ROS [58] and preventing phagocytosis, [59] it has a significant role in the maturation and stability of biofilms. [60]

1.2.5. Biofilm

Biofilms are organized bacterial communities embedded in a matrix composed of polysaccharides, protein polymers, and extracellular DNA released from bacterial cells. [62] Biofilm formation occurs in five stages: flagella and type IV pili-assisted reversible adhesion to the abiotic or biotic surface and exopolysaccharide biosynthesis; transition to irreversible attachment; formation of microcolonies; formation of mushroom-like aggregates (biofilm maturation); and biofilm dispersion, which implies liberation of a certain number of bacteria through the cavity formed by dead cells. [62] The dispersed cells transit to a planktonic lifestyle and initiate biofilm formation at new surfaces. The virulence role of biofilms is reflected in ensuring successful colonization, protecting the bacteria from host immune responses, e.g., phagocytosis and oxidative stress, and generally increasing the survival rate under disturbing external factors, such as temperature and nutrient fluctuations. [62] Moreover, bac-

teria that are dispersed from the mature biofilm have a highly virulent phenotype. [63] In addition to protection from the host immune response, biofilm organization has enormous importance in antibiotic resistance, which is elaborated in the Chapter 1.3.1.

1.2.6. Lectins

Lectins are carbohydrate-binding proteins present in all organisms. [64] *P. aeruginosa* produces lectins LecA (PA-IL) and LecB (PA-III) during the stationary growth phase and under the control of the quinolone quorum-sensing system. [65] LecA binds D-galactose and N-acetyl-D-galactosamine, while LecB has a high affinity for L-fucose and lower affinities for L-mannose, L-arabinose, L-galactose, and other saccharides. [66] It was shown that there is an increase in bacterial virulence in strains expressing higher levels of both lectins. [67] This is at least partially due to their implicated role in adhesion to host cells and biofilm formation [68] and their inhibitory effect on ciliary beating, which is an important defence mechanism during lung infection. [67]

LecB is a posttranslational glycosylated protein with a homotetrameric quaternary structure. [69] Each subunit consists of 115 amino acids with a size of 11.9 kDa, enclosing one sugar-binding site. [69] Each sugar-binding site has two Ca^{2+} ions that are coordinated by Asp and Asn residues. The binding of the sugar is achieved *via* the coordination of two Ca^{2+} ions to three hydroxyl groups of the monosaccharide. [70] Additionally, seven hydrogen bonds are formed between these hydroxyl groups and ring oxygens of fucose and acidic residues of the calcium-binding site, together with hydrophobic interactions between the methyl group of fucose and Thr45. [69] LecB is anchored to the outer membrane by the interaction with the porin OprF. [67] The significance of LecB in biofilm formation was confirmed in an experiment with a *P. aeruginosa* *lecB*-deletion mutant [71] and by inhibition of LecB with a D2 dendrimer. [72] In addition, it was shown that LecB is required for the proper assembly of type IV pili and the activity of virulence-related protease IV. [73] LecB is also involved in haemagglutination by binding to blood group carbohydrates. [74] Regarding the role of LecB in adhesion to host cells, the literature data are not always straightforward, as they vary with the type of host cell or exopolysaccharide, e.g. *Pseudomonas* strains with mutations in *lecB* (and *lecA*) were significantly impaired in binding to human A549 epithelial cells, but binding to host mucin glycoproteins was not affected. [66] The involvement of lectins in *P. aeruginosa* adhesion might be either direct through the interaction with glycan structures on the cell

surface or indirect through involvement in the assembly, secretion, and functioning of other adhesins, such as type IV pili. [66]

1.2.7. Secretion systems

Secretion systems are multiprotein nanomachines that distribute biologically active molecules across the bacterial membrane into the extracellular space or directly into the cytosol of host cells. [75] Among the eight protein secretion systems identified in bacteria, five are found in *P. aeruginosa* (types 1, 2, 3, 5, and 6). [76] The secreted molecules (effectors) are proteins that cross the membrane in a folded or unfolded state, [77] exerting toxic effects on host cells or other microorganisms or hampering the host immune response. [76] The composition of secretion systems ranges from only 3 (T1SS) [78] to approximately 25 proteins (T3SS). [76] However, they all share common functional sections, including (i) the energy source, which is usually ATPase, (ii) outer membrane channel, and (iii) other protein sections responsible for substrate recognition, architectural stabilization, and regulation. [77] The mechanism of protein passage can be a two-step process in which the N-terminal signal peptide guides proteins to Tet or Sec complexes, [79] which then translocate proteins across the inner membrane. Afterwards, the proteins are exported across the outer membrane into the extracellular space or bound to the bacterial surface by T2SS and T5SS. [75] Alternatively, in a one-step mechanism, the proteins tagged with the secretion signal are directly delivered into the extracellular space (T1SS) or injected into the host cell cytosol *via* one of the syringe-like injectisomes (T3SS, T6SS). [75] The most important T1SS release proteins are alkaline protease AprA and TesG (T1SS effector protein targeting small GTPases), which impair the host immune response by degrading complement proteins and cytokines [80] and by suppressing neutrophil influx, [81] respectively. T2SS releases various in-periplasm folded enzymes, including the most abundant proteases, elastases LasA and LasB, which degrade host extracellular elastin, important for lung elasticity, or immune system components (immunoglobulins, cytokines) [82] and disrupt epithelial tight junctions; [83] lipase LipC, which affects other virulence factors, such as rhamnolipid production and biofilms; [84] lipase LipA, which influences sigma factor PvdS expression, thereby affecting many important virulence genes, including pyoverdine, which is regulated by PvdS; [85] phospholipases C PlcB, PlcH, and PlcN causing haemolysis, [86] pulmonary surfactant inhibition [87] and inhibition of the ROS response of neutrophils; [86] and alkaline phosphatases PhoA and LapA, which are in-

involved in delivering inorganic phosphate to bacteria. [88] Furthermore, T2SS releases exotoxin A (ExoA) and ADP-ribosyl transferase, which inhibit host protein synthesis by ribosylation of elongation factor-2 (EF-2) [89] and colonization-related adhesin chitin-binding protein CbpD. [90] T3SS is the most important injectosome and releases the toxins ExoU, ExoT, ExoS, and ExoY, which correlate with a severe clinical picture and mortality by causing cell necrosis and disruption of the epithelium, dissemination of bacteria through circulation, and inhibition of the host immune response. [91] T5SS releases LepA protease to modulate the host immune response, [92] EstA esterase is involved in all types of motility activities and biofilm formation, [93] and CdrA adhesin [94] and patatin-like phospholipase A PlpD are involved in host membrane lipid destruction. [95] T6SS has a major role in combating competitor bacteria, such as the host microbiome, by secreting Tse bacterial toxins. [96] Furthermore, the secreted molecules may also have a role in bacterial adaptation to the environment, such as ensuring the availability of enough iron needed for bacterial growth or secreting enzymes that breakdown complex carbon sources. [77] An example is the protein haemophore HasA_p, secreted through T1SS, which binds haem from host haemoglobin and internalizes it back to bacteria through the HasR receptor. [97]

1.2.8. Pyocyanin

Pyocyanin (1-hydroxy-N-methyl phenazine) is a redox-active secondary metabolite that is important for bacterial fitness and virulence. [98] Secreted in the extracellular space by T2SS, it permeates the host membrane, where it accepts electrons from NAD(P)H and reduces oxygen, resulting in superoxide anion and H₂O₂ production. [99] The produced ROS cause oxidative damage to DNA [100] and inhibit metabolically important enzymes, e.g., aconitase involved in the tricarboxylic acid (TCA) cycle [101] or the antioxidant enzyme catalase, [102] components of the cell cycle, [99] which all cause cell lysis and tissue damage. Oxidative stress induces the genes responsible for mucin production in the respiratory tract, which facilitates further colonization, [103] while DNA released upon host cell lysis aids in biofilm formation. [104] A further mode of virulent action of pyocyanin is subverting the host immune response. It was shown that pyocyanin has inhibitory effects on IL-2, which leads to decreases in T-cell proliferation [105] and immunoglobulin secretion. [100] Pyocyanin is also important for bacterial survival in bacterial communities with *E. coli* and *Staphylococcus au-*

reus. [106, 107] It exerts antibacterial activity towards these strains by inhibiting the membrane respiratory chain and ROS production. [107]

1.2.9. Rhamnolipids

Rhamnolipids (RHLs) are secreted polymers in *P. aeruginosa* consisting of mono or di-rhamnose linked to various chain lengths of 3-hydroxy fatty acids. The polymerization reaction is catalysed by two OM transferases (RhlB and RhlC), which use dTDP-L-rhamnose and 3-hydroxyalcanoyl-3-hydroxyalcanoate (HAA) monomers (precursors). [93] Rhamonolipids reduce surface tension, thereby facilitating swarming motility, which is important for colonization. [93] Additional virulence roles are the prevention of macrophage phagocytosis [108] and the prevention of bacterial clearance in the lungs by impairing ciliary movements. [109] RHL also seems to play a role in biofilm architecture stabilization by maintaining fluid channels between macrocolonies. [110]

1.3. Antibiotic resistance in *P. aeruginosa*

Antibiotics exert bactericidal or bacteriostatic effects by impeding essential processes in bacteria. Antibiotics are classified into five classes based on the targeted essential process: inhibitors of cell wall synthesis, nucleic acid synthesis and repair, protein synthesis, cell membrane function, and folate metabolism. [111] β -Lactams destabilize bacterial cell walls by binding to transpeptidases (penicillin-binding proteins), which have a role in cross-linking the cell wall. [111] The quinolones target DNA gyrase and topoisomerase IV, which catalyse the relaxation of supercoiled DNA in transcription and replication processes. [111] Aminoglycosides and tetracyclines bind to 16S rRNA in the 30S ribosome subunit, while macrolides and chloramphenicol bind to 23S rRNA of the 50S ribosomal subunit, disrupting the translation process. [111] Sulfonamides and trimethoprim are inhibitors of folate biosynthetic pathway enzymes (dihydropteroate synthase and reductase, respectively) that indirectly negatively affect nucleic acid biosynthesis, where folate is an important cofactor. [112] Polymyxins destabilize the outer membrane at least partially by binding to LPS. [113]

As an evolutionary response to the presence of different bioactive compounds in the surroundings, bacteria have developed various resistance mechanisms to tolerate these compounds. [114] The overuse and misuse of antibiotics in medicine and animal and plant agriculture have led to their broad distribution, especially in developing countries. [115, 116] An

analogous response of bacteria to toxic compounds from nature is known. The result of man-caused and environmental resistance is the rapid development of pathogenic bacterial strains resistant, tolerant or persistent to currently available antibiotics. Antibiotic tolerance is the transient ability of a bacterial population to survive under a high concentration of bactericidal antibiotics, which is mainly achieved by slowing down metabolic rates. [117] This does not affect the concentration of antibiotic needed to kill bacteria, but prolongs the time of antibiotic treatment. Therefore, the antibiotic tolerance is quantified by the minimum duration for killing (MDK99), which is the time needed to kill 99 % of the bacterial population at concentrations much higher than the MIC (minimal inhibitory concentration). [118] The persistence is referred to the subpopulation of metabolically inactive, nongrowing noninheritable bacterial phenotypes among the population of susceptible cells. [119] Antibiotic tolerance and persistence lead to the development of antibiotic resistance. [118] Antibiotic resistance is defined as the ability of bacteria to grow in the presence of a high concentration of antibiotic, independent of the duration of antibiotic exposure. [118] Precisely, a strain is identified as resistant to a certain antibiotic if the measured MIC, which is a minimal antibiotic concentration needed to stop the bacterial growth, is above the clinical breakpoint, which is the highest allowed concentration of antibiotic in the blood. [118] Antibiotic resistance is an inheritable trait: a resistance gene can be wild-type and inherent to bacteria, can emerge from a beneficial mutation that occurs in a single cell and is preserved in progeny, or the complete gene is received through genetic exchange between different bacterial strains, species or even genera *via* horizontal gene transfer, i.e., plasmid-carried resistance genes. [114] These genes are key players in intrinsic, acquired, and adaptive antibiotic resistance mechanisms.

1.3.1. Intrinsic antibiotic resistance

The genes involved in intrinsic resistance are in the core genome [120] and are therefore heritable, stable, and internal properties of bacteria. *P. aeruginosa* intrinsic resistance includes low outer membrane (OM) permeability, LPS, the expulsion of antibiotics by efflux pumps, and the expression of chromosomal antibiotic-inactivating enzymes. [121] The *P. aeruginosa* membrane is 12-100 times less permeable than the membranes of other gram-negative bacteria, including *E. coli*. [122] The main reason is the relatively low abundance of porins and the low population of open conformations among them, e.g., less than 5 % of the

most abundant porin, OprF, is present in the dimeric open conformation. Hydrophilic antibiotics such as quinolones and β -lactams may cross the membrane only through porins, namely, porin OprD, [123] since the entry of antibiotics is inefficient through porin OprF. [122] Hydrophobic antibiotics such as aminoglycosides and polymyxins are internalized through the “self-promoted uptake” mechanism by binding to lipid A of LPS. [123, 124] Resistance towards gentamicin and polymyxin B is achieved by preventing their binding to LPS by chemical modification of LPS through the addition of a 4-amino-4-deoxy-L-arabinose (L-Ara4N) moiety [125] or by stabilization of LPS through interaction with porin OprH. [126] In addition to preventing antibiotic entry, *P. aeruginosa* expels antibiotics by efflux pumps, of which 12 different resistance nodulation-cell division (RND) efflux pumps are the most relevant. [10, 127] These pumps expel antibiotics from the cytoplasm and periplasmic space and consist of a cytoplasmic membrane proton motor (multidrug efflux, MEX) and OM porin (Opr), which are connected by adaptor proteins in the periplasmic space. [128] *P. aeruginosa* can extrude β -lactams (except imipenem and biapenem), chloramphenicol, fluoroquinolones, lincomycin, macrolides, and tetracyclines through MexAB-OprM; chloramphenicol, erythromycin, fluoroquinolones and tetracycline through MexCD-OprJ; chloramphenicol, fluoroquinolones, tetracycline, trimethoprim, and imipenem through MexEF-OprN; and aminoglycosides, tetracycline, erythromycin, and cefepime through the MexXY-OprM efflux system. [129] The antibiotic-modifying enzymes intrinsic to *P. aeruginosa* are β -lactam-degrading β -lactamases and aminoglycoside-modifying aminoglycoside phosphotransferase, acetyltransferase, and nucleotidyltransferase. [121]

1.3.2. Acquired antibiotic resistance

Acquired resistance includes resistance-enhancing mutations affecting resistance genes or antibiotic targets and the acquisition of new resistance genes *via* mechanisms of horizontal gene transfer, such as conjugation, transduction and transformation. To further reduce the intrinsically low efficacy of antibiotic entry, *P. aeruginosa* downregulates the expression of porin *oprD* or impairs its function by frameshift or premature stop codon mutations, which reinforces carbapenem resistance. [121, 130] Overexpression of efflux pumps is induced by mutations in the genes themselves or the corresponding transcriptional regulators, e.g., mutation in transcriptional regulator gene *nfxB* leads to MexCD–OprJ efflux pump overexpression, increasing the resistance to fluoroquinolones and penem (β -lactam) antibiotics. [121]

Another important strategy is masking antibiotic targets by mutational changes. Mutations in DNA gyrase were observed in chronically infected cystic fibrosis patients and resulted in decreased binding efficacy of fluoroquinolones, reducing susceptibility to this antibiotic. [129, 131] Similarly, mutations in the 30S ribosomal subunit and penicillin-binding proteins increased resistance to aminoglycosides and β -lactams, respectively. [121] In addition to mutations, the acquisition of additional antibiotic-modifying enzymes contributes to multi-drug resistance. The six metallo-beta-lactamases, including imipenemase, are adopted through integrons and plasmids. [121] Furthermore, plasmid-encoded 16S rRNA methylases, probably received from aminoglycoside-producing bacteria, protect ribosomes from the most clinically used aminoglycosides. [132]

1.3.3. Adaptive antibiotic resistance and tolerance

Adaptive resistance is a noninheritable and transient response at the transcriptional and regulatory levels triggered by subinhibitory concentrations of antibiotics, [133] which results in protective phenotypic changes. These changes include transitions to a biofilm lifestyle and the formation of persister cells. [121] Biofilms increase tolerance 1000-fold to some antibiotics in comparison to planktonic cells. [133] Biofilm formation contributes to antibiotic tolerance and resistance through physical, physiological, and genetic mechanisms. Physical tolerance is reflected in hindering the penetration of some antibiotics through their binding to the components of the extracellular matrix of biofilms, such as positively charged tobramycin binding to extracellular DNA and phage particles [134] or sequestration of kanamycin by extracellular glycerophosphorylated cyclic β -(1,3)-glucans. [121] In cystic fibrosis patients, mature biofilms are mucoid and slimy as a consequence of the overproduction of alginate, which protects bacteria from antibiotics. [135] Physiological tolerance is caused by the depletion of antibiotic targets due to the low growth rate and low metabolic activity of bacterial subpopulations in deeper layers of biofilm. [136] Additionally, in these populations of biofilms, the starvation-induced stringent response leads to the overexpression of antioxidant enzymes (catalase and superoxide dismutase), which neutralize the ROS-induced bactericidal activity of some antibiotics. [134] Genetic tolerance is related to the differential expression of specific genes in biofilms in comparison to planktonic cells. This includes *pmr* and *arn* genes whose products modify LPS, leading to decreased aminoglycoside entry, [137] or the *tssC1* gene, which is involved in T6SS and whose deletion can result in increased susceptibil-

ity to tobramycin, gentamicin, and ciprofloxacin. [121] Biofilm resistance relies on mutations in resistance genes that are initiated by nutrient deprivation and stress responses in different biofilm niches. [137] Furthermore, the proximity of cells in biofilms is a favourable circumstance for horizontal gene transfers, including resistance genes. [62] Persister cells account for 1 % of biofilm mass; they are generally considered slow-growing, metabolically dormant cells and are one of the main reasons for chronic infections. [121] The formation of these phenotypes is triggered by environmental stress-induced responses, and reversible dormancy is achieved by toxin-antitoxin systems (TA), such as the recently identified TAsystem, which acts by reducing intracellular NAD⁺ levels. [138]

P. aeruginosa synergically combines different resistance mechanisms against some antibiotics. Fluoroquinolone resistance is achieved by modification of targets and efflux pumps. [139] The entry of carbapenems in the bacteria is decreased by downregulation of *oprD* porin expression, while the remaining intracellular molecules are expelled by efflux pumps or degraded by β -lactamases. [140] Multidrug-resistant (MDR) and extensively drug-resistant (XDR) *P. aeruginosa* emerged as a consequence of compiling different resistance genes, in which megaplasms (>420 kb) significantly contributed to the rapid spread of these genes between adjacent cells. [129]

1.4. Global significance and emerging antimicrobial strategies against *P. aeruginosa*

P. aeruginosa is listed in the ESKAPE “bugs” group, comprising six of the world’s most frequent and problematic MDR bacteria. [141] The Infectious Diseases Society of America (IDSA) pointed out that antimicrobial resistance is a major global threat to human health. [142] In the EU, 33000 deaths per year are reported as a consequence of antibiotic resistance, and this number is growing. [143] The current antibiotic therapy in severe cases of *P. aeruginosa* infections is combinatorial, consisting of at least two different classes of antibiotics: cephalosporins or carbapenems with β -lactamase inhibitors (piperacillin/ tazobactam, ceftolozane/tazobactam, ceftazidime/avibactam, imipenem/relebactam) and aminoglycosides or fluoroquinolones. [144] However, *P. aeruginosa* strains resistant to carbapenems and third generation cephalosporins have already been identified. [145] The only antibiotic active against carbapenem-resistant isolates is cefiderocol, a synthetic β -lactam cephalosporin that was recently approved by the FDA. [133, 146] The improvement in activity was achieved by structural modifications that increased its stability towards β -lactamases and by

introducing an iron-binding catechol group, which facilitated antibiotic entry across OM by siderophore receptor recognition, designating it a “Trojan horse” antibiotic. [133] However, the pace of development of novel antibiotics is generally relatively slow. The economic reasons for this include more demanding governmental approval regulations and favouring the development of drugs for long-term use, which will ensure profit, which is not the case with antibiotics. [114] The scientific reasons include the limited number of targets in bacteria and the exhaustion of potential natural sources, i.e., soil bacteria for the isolation of new antibiotics since the majority of antibiotics present on the market are of natural or seminatural origin. [114] Additionally, high-throughput screening of synthetic compounds was not successful, but this might be improved by including more complex compounds in the screening. [114] Therefore, the increasing concern of the medical community caused by this large disproportion in rates of development of resistance and novel antibiotics resulted in the announcement of a priority list of bacterial species for which the development of new antibiotics is urgently needed. Alongside carbapenem-resistant *Acinetobacter baumannii* and *Enterobacteriaceae*, *P. aeruginosa* was listed in the most critical priority group. [147]

Novel strategies have emerged to overcome this global crisis in antibiotic development. They include bacteriophage therapy, antimicrobial peptides, augmenting host immune response by administration of antibodies or antisera, anti-virulence, and anti-resistance adjuvants. [133]

1.4.1. Anti-resistance therapy

Anti-resistance therapy aims to increase the efficacy of existing antibiotics by adding adjuvant compounds, which will inhibit the target responsible for the resistance to a specific antibiotic. Currently, anti-resistance therapy strategies include OM permeabilizers and inhibitors of β -lactamases, efflux pumps, biofilms, and persister cells, some of which are already in clinical use.

The combination of β -lactam antibiotics and β -lactamase inhibitors is a successful anti-resistance therapy since the β -lactamase inhibitors clavulanic acid, sulbactam, and tazobactam have been widely used in clinical use for a few decades. [129] *P. aeruginosa* possesses AmpC β -lactamases, which hydrolyse cephalosporins and cephamycins and are not inhibited by clavulanate, sulbactam, and tazobactam; extended-spectrum beta-lactamases (ESBL), which hydrolyse oxyimino β -lactams such as cefotaxime, ceftriaxone, ceftazidime, and mon-

obactams; and metallo beta-lactamase enzymes (MBL), which hydrolyse carbapenems. [148] From the novel generation of inhibitors with a broader spectrum of inhibition activity, avibactam and relebactam in combination with meropenem are efficacious against *P. aeruginosa*. [129] Furthermore, additional inhibitors are in development: taniborbactam inhibits serine- β -lactamases and MBL, and in combination with cefepime, it has been evaluated against carbapenem-resistant *P. aeruginosa* in clinical phase III trials; zidebactam inhibits MBL and is in clinical phase I trials. [133]

Outer membrane permeabilization increases antibiotic effectiveness by facilitating their entrance into the bacterial cell. These compounds are mostly cationic and amphiphilic peptides and lipids, including antimicrobial peptides and cholic acid. [142] Natural polyamines have succeeded in increasing *P. aeruginosa* susceptibility to some antibiotics, including β -lactams and chloramphenicol, [142] while the permeabilizer polymyxin B nonapeptide passed clinical phase I. [149] The obstacle in introducing these types of compounds to the market could be toxic effects, which they might cause due to the lack of specificity to prokaryotic cells, e.g., cholic acid and its derivatives, or even by altering the lipid metabolism of eukaryotic cells. [142] However, antimicrobial peptides or even immunomodulatory peptides, which are part of our innate immune system and inhibitors of enzymes involved in LPS biosynthesis, are worth further investigation in this field.

Efflux pump inhibition is an important anti-resistance strategy that could re-establish many currently available poorly effective antibiotics. Moreover, efficient efflux pump inhibitors would decrease antibiotic MIC, reducing the resistance rate and toxicity of some antibiotics. [150] Specific inhibitors can also be used as diagnostic tools to identify resistance mechanisms in clinical strains. [151] There are different strategies to inhibit efflux pumps: preventing the expression of essential pump proteins by blocking regulatory genes or using anti-sense peptide nucleic acids (PNAs), which specifically recognize and block gene expression; hindering the assembly of pump components; designing competitive or non-competitive inhibitors; blocking OM pore; decoupling the proton motive force of a pump and modifying the structure of antibiotic to reduce its affinity to the pump. [150] Recent advances in the field were achieved by identifying the inhibitory activity of the already approved drug nilotinib towards NorA efflux pump in *S. aureus*, demonstrating increased bacterial susceptibility and reduced biofilm formation in combination with ciprofloxacin. [152] In *P. aeruginosa*, the most studied pump inhibitor is the peptidomimetic compound phenylalanine arginyl β -

naphthylamide (PA β N), which competitively inhibits MexAB-OprM, MexCD-OprJ, and MexEF-OprN pumps and which was shown to increase bacterial susceptibility to fluoroquinolones significantly. [153] Unfortunately, PA β N and some other pump inhibitors are shown to be toxic to human cells. [154] To overcome this, the structural modifications of PA β N [155] as well as decreasing the applied concentration of PA β N by combining it with an OM permeabilizer, such as polymyxin B nonapeptide, gave promising results [154]. Additional efflux pump inhibitors active in *P. aeruginosa* include plant alkaloid conessine [156], an inhibitor of MexAB-OprM pump and synthesized peptides [157], and inhibitors of small multidrug resistance (SMR) efflux protein dimerization, were recently identified.

Since biofilm is a virulence and antibiotic resistance determinant, using the anti-virulent drugs which prevent biofilm formation together with antibiotics could significantly potentiate the activity of an antibiotic. There are different strategies to inhibit the formation or stimulate the dispersion of biofilms. A recent approach showing *in vitro* anti-biofilm activity in combination with ciprofloxacin, tobramycin, and colistin is QS inhibitor N-(2-pyrimidinyl) butanamide. [158] Using monoclonal antibodies against biofilm exopolysaccharide Psl was shown to reduce biofilm mass in the presence of neutrophils. [159] Antimicrobial peptide AMP 1018 was shown to be effective in inhibiting biofilm formation but also in causing dispersion of already formed biofilms by degrading ppGpp, which is a signalling molecule included in biofilm formation and stringent response. [133] Similarly, AMP P5 showed antibiofilm and synergic activity in the meropenem treatment of carbapenem-resistant *P. aeruginosa*. [160] Low concentrations of nitric oxide cause dispersion of biofilms *via* activation of phosphodiesterase, which degrades cyclic di-GMP, a secondary messenger involved in biofilm regulation. [129] Another approach to biofilm dispersion in the lungs is achieved by targeting eDNA *via* administration of an aerosol containing recombinant human deoxyribonuclease to cystic fibrosis patients, commercially available as Pulmozyme. [161]

The anti-microbial strategy against persister cells is particularly challenging since targeting essential processes and virulence factors is problematic as these cells are metabolically locked. Remarkably, several compounds already showed some positive effects. Acyldepsipeptide 4 (ADEP4) binds ATP-dependent ClpP protease instead of ATP. [134] This results in non-specific proteolysis leading to massive cell deaths in biofilm. [134] Poly-acetyl-arginyl-glucosamine (PAAG) is shown to successfully eradicate persister cells by bacterial membrane permeabilization, having an anti-inflammatory effect and promoting mucociliary bacterial

clearance. [162] The QS inhibitor (Z)-4-bromo-5-(bromomethylene)-3-methylfuran-2(5H)-one (BF8) was shown to revert tobramycin susceptibility of *P. aeruginosa* persister cells, although the precise mechanism is unknown [163]. The promising approach is the prevention of persister cell formation by targeting TA systems, which was demonstrated by persister cell eradication achieved through blocking MqsR toxin of MqsRA TA system by antisense peptide nucleic acid. [164]

1.4.2. Anti-virulence therapy

It was noticed that besides killing bacteria, some antibiotics additionally exert an anti-virulent effect, e.g., azithromycin possesses the ability to decrease the expression of virulence genes in *P. aeruginosa*. [165] This gave rise to considering a new therapeutic approach, anti-virulence therapy, focusing only on disarming virulent factors responsible for the infection and damaging host tissues without affecting bacterial viability [166]. This therapy is expected to decrease the pace of development of resistance due to less selective pressure. [166] In this regard, an anti-virulence drug should preferably not impair bacterial fitness or growth. [165] An additional advantage of anti-virulence therapy is its selectivity towards pathogens since host-microbiome bacteria do not produce virulence factors. Additionally, a new approach offers a broader collection of possible targets to be explored. [166] From an array of different virulence factors in *P. aeruginosa*, the targeting of QS, adhesion virulence factors, and protein secretion systems were already explored with promising results. Although no compound passed the third clinical phase until now, the approach has potential since anti-virulence drugs against other pathogens, including *C. botulinum*, *C. difficile*, and *Bacillus anthracis*, are already in use. [133]

The idea of simultaneously impairing the expression of several virulence factors by inhibiting their regulatory QS system or c-di-GMP signaling has already given encouraging results. Inhibitors of Las QS system, meta-bromo-thiolactone or 6-gingerol showed an anti-virulence effect in mice and *C. elegans* models and inhibited pyoverdine, pyochelin, and biofilm formation. [133] The impairment in biofilm formation was also achieved by c-di-GMP inhibitor ebselen. [133] The QS inhibitor isolated from natural resources (garlic) is ajoene which targets the Gac/Rsm component of QS. Still, synthetic analogs are further developing to encompass instability, low quantities, and hydrophobicity. [129]

The strategy of blocking protein secretion systems or their effectors is under development by some pharmaceutical companies. To disarm the major injectosom, Microbiotix Pharmaceuticals is developing phenoxy acetamide inhibitors that target the PscF needle of T3SS. [133, 146] Inhibitors against ExoA, which is a T3SS effector [133], and LasB elastase which is a T2SS effector, are identified (AntaBio) [146].

Blocking LptD-mediated transport of LPS across OM, which allows LPS positioning on the bacterial surface, was achieved by the synthetic peptide murepavadin. Strikingly, this peptide showed activity against carbapenem, ceftolozane/tazobactam, and colistin-resistant *P. aeruginosa* strains. Unfortunately, observed renal failures in patients with ventilation-associated pneumonia upon intravenously administrated murepavadin dismissed the clinical phase III study, leaving just the possibility for topical application. [146]

Anti-adhesion therapy aims to prevent the initial phase of infection and biofilm formation by targeting the bacteria-host interactions. This strategy has different approaches, including blocking the biosynthesis of essential adhesins like pili, using antibodies against adhesins, interfering in adhesin-host receptor recognition by using adhesin or receptors analogs, modifying host cell surface receptors, etc. [167] An example of a successful adhesin analogy strategy are the polymeric microbeads functionalized with multivalent adhesion molecule-7 (MAM-7) distributed in many Gram-negative bacteria, which decreased the attachment and spreading of MDR *P. aeruginosa* strain in murine burn wound infection model, without disturbing natural wound healing processes. [168] Similarly, various glycoclusters, synthesized as host receptor analogs of *P. aeruginosa* lectins, LecA and lecB, were shown to destabilize bacterial attachment and, in the case of galactoside and fucoside-functionalized calix[4]arene-based glycoclusters, to significantly prevent lung infection in a murine model. [169] The main disadvantage of this strategy is the presence of many different adhesins with similar roles and sharing epitopes with human proteins. [167]

The potential of already clinically used drugs in showing an additional anti-virulence role is explored by computational screening to accelerate the emergence of anti-virulence drugs. This led to the identification and experimental confirmation of the anti-virulence activity of the drug raloxifene, which decreases pyocyanin production through binding to PhzB2, a protein involved in pyocyanin biosynthesis. [170] Similarly, already approved drugs niclosamide and clofoctol showed QS inhibiting activities. [133]

Any virulence factor might or might not be worth inhibiting. The significance of a certain virulence factor for the infection and the efficacy of the corresponding anti-virulence drug are estimated by the ability to clear infection in an animal model. [142] Therefore, animal experiments have to be included in the earlier phases, which increases the required time and costs. A suitable anti-virulence drug should not elicit bacterial resistance. Although this is the case for most anti-virulence targets/drugs, some exceptions include QS inhibitors, azithromycin, and brominated furanone C-30, which increase the population of more virulent cells, i.e., elicit anti-virulence resistance. [142] Other challenges of anti-virulence therapy are the clearance of disarmed pathogens in immunocompromised patients and often a narrow spectrum of action, which makes prophylaxis difficult. [142] Therefore, in these cases, using anti-virulence drugs as antibiotic adjuvants seems to be a rational option.

1.5. *P. aeruginosa* hydrolytic enzymes and their potential as antimicrobial targets

Hydrolases (EC 3) is one of seven enzyme classes that catalyze the cleavage of different chemical bonds, including C-O, C-N, and C-C bonds, using water molecules. The general mechanism is the nucleophilic attack of activated enzyme amino acid side-chain nucleophilic moiety or enzyme-bound water molecule on the electrophilic atom of the substrate. Nucleophile activation is usually achieved through the abstraction of a proton with a subsequent proton shuttle by adjacent amino acid residues in the active site. According to the moiety responsible for the nucleophile attack, hydrolases are classified into carboxyl, histidine, cysteine, serine, threonine, tyrosine, N-terminal proline, and metallohydrolases. In metallohydrolases, an activated water molecule is the only nucleophile and metal ion/s coordinate the substrate in the correct position. [171] Concerning the type of substrate bond being hydrolyzed, hydrolases contain 13 subclasses, including esterase, glycosylase, peptidase, hydrolase acting on non-peptide C-N bond, hydrolase acting on ether bonds, hydrolase acting on acid anhydrides, hydrolases acting on P-N, C-C, C-P, S-S, C-S, S-N and halide bonds. [172] Accordingly, the hydrolase class includes enzymes hydrolyzing various substrates which belong to all biomacromolecule types - polysaccharides, nucleic acids, proteins, and lipids. It is obvious why hydrolases are represented in all domains of life, considering their importance in the homeostasis of various macromolecules in a cell. [173] However, from the quantitative aspect, ligases are the enzymes enriched in essential bacterial genes, including *P. aeruginosa*, while hydrolases are slightly more represented in non-essential genes. [174] Among non-

essential genes are virulence factors, virulence factor regulators, and antibiotic-resistance genes. Many of them exert their function by hydrolyzing different substrates of the host, environmental (xenobiotics), or bacterial origin.

1.5.1. Esterases

Esterases (EC 3.1) include many sub-subclasses, among them carboxylic-ester hydrolases (EC 3.1.1), thioester hydrolases (EC 3.1.2), phosphoric-monoester hydrolases (phosphatases) (EC 3.1.3), phosphoric-diester hydrolases (EC 3.1.4), exonucleases (EC 3.1.11-16) and endonucleases (EC 3.1.21-31). [172] Bacterial esterases often show substrate promiscuity for esters, thioesters, and phosphoesters. [175, 176]

Carboxylic-ester hydrolases (carboxy hydrolase) have broad substrate specificity and hydrolyze oxo-esters, releasing alcohol and carboxylate. [172] The term esterase typically refers to carboxylesterases (EC 3.1.1.1), which hydrolyze small, partially to completely water-soluble esters with short-chain acylglycerol containing less than ten carbon atoms ($< C_{10}$) [177, 178]. In contrast, the hydrolysis of long-chain acylglycerol esters insoluble in water is catalyzed by true lipases (EC 3.1.1.3). [177] Typically, esterases hydrolyze tributyrin (triglyceride ester with C_4 fatty acid chain) and lipases olive oil (triglyceride ester with C_{16} or C_{18} fatty acid chains). [173]

1.5.2. Lipases

In contrast to esterases, many lipases follow the phenomenon of interfacial activation, which represents a sharp increase in lipase activity when the substrate concentration is high enough to induce micelles formation. The activity increase results from opening the lid-like structure covering the active site upon micelle binding and is reflected in the sigmoidal kinetic curve. [173] Most of the esterases and lipases have an α/β -hydrolase fold comprised of twisted 8-11 stranded β -sheets with flanking α -helices and a canonical GXSXG-pentapeptide signature in the active site, where serine is a catalytic nucleophile. [173] Lipolytic enzymes in bacteria include esterase, lipase, and phospholipase playing general roles in maintaining membrane homeostasis, adaptation, lipid signaling, and virulence. [179] Lipolytic enzymes, including esterase and lipase, are classified into 19 families by phylogenetic position, conserved sequence motifs, and biological functions. [173] One of the 30 most represented outer membrane and vesicular proteins in *P. aeruginosa* is autotransporter-conjugated esterase

EstA with $\alpha/\beta/\alpha$ structural fold, N-terminal positioned active site GDSL motif [93], and strong selectivity towards butyl esters [180]. This esterase is involved in the processing of rhamnolipid (Chapter 1.2), and its virulence role is shown in a rat model. [93] Periplasmic esterase PfeE with α/β hydrolase fold and GX β XXG motif hydrolyzes siderophore enterobactin providing iron, which is vital for cell growth and virulence. [181] Besides their role in virulence, esterases can exert antibiotic resistance roles. Erythromycin esterases capable of cleaving macrolides' macrolactone ring are found in different pathogen species from the *Pseudomonas* genus. [182, 183] Secreted virulence factors, lipases LipA and LipC, (described in chapter 1.2) belong to the family I.1. of lipolytic enzymes, which have an α/β hydrolase fold and conserved calcium-binding pocket. Their folding to the native structure is assisted by steric chaperone LipH, which binds to LipA during or after translocation through OM. [184, 185]

1.5.3. Phospholipases

While lipases hydrolyze hydrophobic neutral triacylglycerols, phospholipases catalyze the hydrolysis of amphiphilic charged glycerophospholipids. Glycerophospholipids are glycerol-3-phosphates esterified at sn-1 and sn-2 glycerol carbon positions with nonpolar fatty acids, and the sn-3 position is a phosphoryl group further esterified with alcohol such as choline, ethanolamine, glycerol, or inositol. [186] Phospholipases that hydrolyze oxo-ester bonds in glycerophospholipids are acyl hydrolases (phospholipases A and B, PLA and PLB), while phospholipases C and D (PLC and PLD), which hydrolyze phospho-ester bonds, belong to phosphodiesterase class which differs from the carboxy hydrolase class.

Phospholipase A1 (EC 3.1.1.32) and phospholipase A2 (EC 3.1.1.4) hydrolyze sn-1 and sn-2 ester bonds, producing 2-acyl-lysophospholipids or 1-acyl-lysophospholipids, respectively, and free fatty acid. [186] The remaining ester bonds in lysophospholipid can be hydrolyzed by lysophospholipases (EC 3.1.1.5), producing glycerophosphoalcohol and carboxylate. [172] All PLA1 have Ser-His-Asp catalytic triad, while PLA2 are more diverse, but the majority have His/Asp catalytic dyad and conserved Ca^{2+} -binding loop and disulfide bridges. [186] Phospholipases B (EC 3.1.1.5) have PLA1 and PLA2 activities. *P. aeruginosa* ExoU, the most detrimental T3SS toxin, expressed by almost 30 % of clinical strains, [187] is a patatin-like phospholipase (PLP) [188]. ExoU has an α/β hydrolase fold with a GxSxG motif and Ser-Asp catalytic dyad responsible for PLA2 and lysophospholipase activities, which are unlocked probably by ubiquitinylation of C-terminus in host cells. [188] This leads to cytotoxicity

caused by hydrolysis of phospholipids in host cell membranes, which result in severe acute lung injury and the possibility of septic shock. [187] Another PLP member is *P. aeruginosa* T5SS effector PlpD which has lipase and phospholipase A1 activity [95]. PlpD has a lipase-specific flexible lid covering the active site; it is secreted in the active form and exerts its virulence role through hydrolysis of different phosphatidylinositols in host cell membranes. [189] T6SS effector TplE has lipase and PLA1 activity and exerts its toxic effect by disrupting the endoplasmic reticulum of a host cell and inducing unfolded protein response which leads to autophagy. [190] The prevention of a similar scenario within the bacteria is achieved by binding antitoxin TlpEi to toxin TlpE. The antimicrobial strategy of disrupting this interaction by the designed peptide was able to induce bacterial death. [191] Besides exerting direct toxic effects, phospholipases can influence bacterial adaptation, virulence, or antibiotic resistance by a more sophisticated approach.

Phospholipases C (PLC) (EC 3.1.4.3) cleave the glycerophosphate bond in phospholipid, releasing 1,2-diacylglycerol and polar phospho-alcohol. [186] PLCs have highly conserved X and Y domains that form a catalytic site and are surrounded by the EF-hand motif, which is a helix-turn-helix and regulatory C2 motif, both binding Ca^{2+} ions. [192] *P. aeruginosa* virulence factor phospholipase C PlcH (see secretion systems, Chapter 1.2) belongs to the acid phosphatase superfamily of PLC, does not require Zn^{2+} cofactor, is expressed and secreted as a heterodimer with its chaperon PlcR2 [193] and prefers phosphatidylcholine and sphingomyelin substrates, but also shows activity with cardiolipin, phosphatidyl-ethanolamine, and phosphatidylglycerol. [192] PlcB is a virulence factor that belongs to the metallophospholipases coordinating three Zn^{2+} in the substrate-binding pocket and hydrolyzes phosphatidylcholine and phosphatidylethanolamine. [192] PlcB is essential for chemotaxis-guided twitching motility towards phospholipids. [192] It has been recently shown that novel intracellular phospholipase C PlcP is a member of the new *P. aeruginosa* conserved lipid remodeling pathway, which replaces membrane phospholipids with glycolipids in the phosphate-depleted environment, such as CF lungs. [194] Apart from contributing to bacterial survival and adaptation, this lipid switch caused increased resistance toward polymyxin B, probably due to decreased binding of positively charged polymyxin to neutral glycolipids. [194]

Phospholipases D, PLD (EC 3.1.4.3) remove the phospholipid headgroup, releasing alcohol and phosphatidic acid. [186] Bacterial PLDs fold into pseudo-dimer, comprised of two homologous domains with β -sandwich fold, forming the active site at the domains' interface.

[192] In *P. aeruginosa*, T6SS secrete phospholipases D PldB and PldA promote the entry of bacteria into non-phagosomal cells by activating the PI3K/Akt pathway. [195] PldA is shown to be prevalent in clinical isolates of severe acute infection and MDR strains. [196]

1.5.4. Acyl-CoA thioesterases

Acyl-CoA thioesterases (AT) are ubiquitous enzymes that hydrolyze thioester bonds and often participate in essential cellular processes such as acyl-CoA turnover, lipid metabolism, membrane synthesis, polyketide, fatty acid, and non-ribosomal peptide antibiotics synthesis, signal transduction, gene transcription, bioluminescence. [197] [198] They are divided into two major families: thioesterase I, which has an α/β -hydrolase fold, and Ser-His-Asp catalytic triad and thioesterase II family, which has a hot-dog fold, the most abundant fold in thioesterase family and Asp-Glu in the active site. [199] The hot-dog fold comprises a five-turn α -helix wrapped with an anti-parallel β -sheet. [197] The majority of thioesterases hydrolyze fatty acyl-coenzyme A (CoA), releasing free fatty acid and CoASH. [200] Other substrates include acyl-acyl carrier proteins (ACPs) and glutathione. [200] In *P. aeruginosa* PchC thioesterase II is shown to have an editing role in the synthesis of antibiotic dihydroaeruginoate (Dha) and siderophore pyochelin. [201] Another *P. aeruginosa* thioesterase PqsE hydrolyzes 2-aminobenzoylacetyl-CoA, which is the intermediate in the biosynthesis of quorum sensing molecules alkyl quinolones, involved in the regulation of many virulence factors, including biofilm. [202] [203]

1.5.5. Phosphatases

Phosphatases catalyze the hydrolysis of phosphoric-monoester bonds releasing alcohol and phosphate. [172] Phosphatase substrates are diverse, including nucleotides, sugars, sugar alcohols, and proteins. [204] Phosphatases are further classified as alkaline, neutral, acid, and protein phosphatases. [204] Most phosphatases require metal cofactor, mostly Mg^{2+} or Mn^{2+} . [204] In bacteria, phosphatases targeting phosphorylated Ser/Thr and Tyr residues in protein substrates, together with their counter partners – kinases, are included in different signaling pathways that regulate bacterial growth, pathogenesis, and response to host factors. [205] In *P. aeruginosa*, Ser/Thr protein phosphatase PppA is involved in T6SS regulation [205], while Tyr protein phosphatase TpbA negatively regulates c-di-GMP production, lead-

ing to decreased biofilm production, increased flagellar-mediated motilities (swimming and swarming) [206] and increased eDNA [207]. His-Asp protein phosphatases, as a member of two-component kinase/phosphatase systems, are included in the regulation of chemotaxis, alginate production, and iron acquisition. [207] Phosphatase CheZ is a component of the intracellular chemotaxis cascade regulating the flagellum direction of rotation. [43] Secreted alkaline phosphatase such as PhoA (see secretion systems, Chapter 1.2) hydrolyze organo-phosphate compounds releasing inorganic phosphate that can be imported into bacteria by specific transporters. [208]

1.5.6. Phosphoric-diester hydrolases

Phosphoric-diester hydrolases (EC 3.1.4) cleave phosphodiester bonds in various substrates, including cyclic nucleotides (cAMP, cGMP), single or double-stranded nucleic acids, and phospholipids. [204] Depending on the substrate specificity, they are subclassified into phosphodiesterase (EC 3.1.4.17) and phospholipase C (EC 3.1.4.3).

All currently known phosphodiesterases require divalent metal ions as a cofactor, mostly Mg^{2+} or Mn^{2+} . [204] Cyclic nucleotide phosphodiesterases class III hydrolyze ubiquitous signaling molecule cAMP in bacteria. [209] They belong to the calcineurin-like metallophosphoesterases superfamily, which has a specific $\beta\alpha\beta\alpha\beta$ calcineurin-like fold and two metal ions coordinated with seven conserved amino acid residues (His, Asp, Asn) and one water molecule, forming an octahedral complex in the centrally positioned active site. [210] In *P. aeruginosa* metallophosphoesterase CpdA hydrolyzes cAMP and therefore contributes to the homeostasis of this messenger, which regulates the expression of many virulence genes, including T4P, T3SS, ExoS, ExoT, and ExoY. [211]

1.5.7. Glycosylases

Glycosylases (EC 3.2) include glycosidases that hydrolyze O- and S-glycoside bonds and enzymes that hydrolyze N-glycosyl bonds, [172] releasing sugar hemiacetal or hemiketal and aglycon alcohol [212]. This diverse enzyme class includes 135 families [212], which may hydrolyze terminal or internal glycosidic bonds (exo- and endoglycosidase, respectively) with or without retention of anomeric C atom configuration by employing a general acid mechanism [213]. Bacterial glycosidases involved in cell wall remodeling include N-acetylglucosaminidase and lysozymes. [212] *P. aeruginosa* cytosolic exoglycosidase *nagZ* is a

single domain TIM-barrel protein with β -N-acetylglucosaminidase activity. [214] In a two-step catalytic mechanism, histidine acts as a general acid/base catalyst, characteristic of glycosidases, and aspartate is a nucleophile that forms a covalent glycosyl-enzyme intermediate. [215] This enzyme is involved in peptidoglycan (PG) recycling, a process that, together with PG *de novo* synthesis, ensures essential cell wall homeostasis during cell growth, division, elongation, and cell wall repair after damage by antibiotics. [216] Moreover, *nagZ* contributes to β -lactam resistance by activating β -lactamase *ampC* expression, achieved *via* *nagZ* product 1,6-anhydromuropeptide binding to AmpC regulator AmpR. [216] The *nagZ* inhibitor cyclophellitol was able to reduce the MIC of tested β -lactams in *P. aeruginosa* clinical strains. [215] *P. aeruginosa* endoglycosidase PslG is composed of a C-terminal β -sandwich domain and N-terminal $(\beta/\alpha)_8$ barrel domain with an N-terminal transmembrane region that resides in the inner membrane and positions the protein in the periplasm. [217] In the centrally positioned active site groove, two glutamate residues act as the acid/base and nucleophiles. [217] PslG hydrolyzes Psl, thereby participating in the biosynthesis of this exopolysaccharide that has a significant role in the adhesion and biofilm formation. [217] When added externally, PslG caused the dispersion of biofilms and therefore is a promising anti-resistance drug. [218] Glycosylases that cleave N-glycoside bonds include enzymes involved in DNA repair, such as uracil DNA glycosylase that recognizes uracil in DNA and initiates base-excision repair. [219] Since the secondary bactericidal mechanism of some antibiotics (aminoglycosides, β -lactams) is the induction of oxidative damage in bacteria, inhibiting enzymes involved in DNA repair is the strategy being considered.

1.5.8. Peptidases

Peptidases (proteases) (EC 3.4) are divided into exopeptidase (aminopeptidase and carboxypeptidase) and endopeptidase. [172] By the amino acid involved in the nucleophilic attack on electrophilic carbon in substrate amide bond, proteases are categorized as serine, cysteine, threonine, aspartic, and metalloprotease. Serine, cysteine, and threonine protease form the tetrahedral covalent acyl-enzyme intermediate, which is subsequently hydrolyzed. [220] The aspartic and metalloprotease form non-covalent tetrahedral intermediate by nucleophilic attack of the activated water molecule. [220] Subsequently, the intermediate is hydrolyzed by acid-base rearrangement of adjacent amino acid residues. Proteases have roles in essential cellular processes, virulence, and antibiotic resistance. Extracellular proteases are

usually monomers with broad substrate specificity and expressed as inactive zymogens to protect bacterial proteins. [221] Most extracellular proteases are virulence factors that assist in bacterial invasion by degrading host tissue proteins (fibronectin, laminin, elastin) or hampering host immune response by degrading defensive proteins (immunoglobulins, complement proteins, cytokines). [220] *P. aeruginosa* secretes virulence factors zinc metalloendopeptidases LasA and LasB (see chapter 1.2), zinc metalloprotease alkaline protease (AprA), serin protease IV, zinc leucine aminopeptidase *Pseudomonas* small protease (PASP), large exoprotease A (LepA), serine endoprotease MucD, and *P. aeruginosa* leucine aminopeptidase (PAAP). [222]

Intracellular proteases are multimers with narrow substrate specificity and a catalytic site hidden deeper into the barrel-like fold. [220] They are often associated with chaperons assisting them in targeting misfolded or unfolded proteins or themselves, partially unfolding the substrate to prepare it for hydrolysis. [221, 223] Intracellular proteases are involved in essential processes such as cell viability, stress response, protein quality control, and virulence and antibiotic resistance factors. [224] *P. aeruginosa* Lon protease is a cytosolic ATP-dependent serine protease with a hexameric ring-like quaternary structure. [225] This enzyme is necessary to establish a full virulent phenotype, including biofilm formation, T3SS assembly, swarming, twitching, and ciprofloxacin resistance. [225] In *P. aeruginosa* cell membranes, periplasmic space and PG layer are distributed over 40 proteases, which have essential roles in PG remodeling, protein secretion, protein quality control, controlling gene expression, etc. [226] The transpeptidase (penicillin-binding protein 3) is involved in the biosynthesis of cell wall PG and is the target of ceftazidime antibiotic. [227] Periplasmic carboxypeptidase CtpA is shown to be critical for the normal function of T3SS. [228]

1.5.9. Hydrolases acting on non-peptide C-N bond

Hydrolases acting on non-peptide C-N bond (EC 3.5) hydrolyze amides, amidines, and other C-N bonds. [172] Amidase is one of the hydrolases involved in the cell wall remodeling by cleaving the amide bond between N-acetylmuramic acid and L-alanine residue. [212] *P. aeruginosa* amidase AmiB has a critical role in cell wall septum formation during cell division, which further causes disturbances in outer membrane integrity and concomitantly increases susceptibility to aminoglycosides and vancomycin. [229] Therefore, inhibitors of AmiB might be used as anti-resistance adjuvants. Another important group of amidases that degrade β -

lactam antibiotics by hydrolyzing amide bonds in the β -lactam ring is β -lactamases (EC 3.5.2.6). By their sequence similarities, they are classified into A, B, C, and D classes. [230] Classes A, C, and D are serine hydrolases, while class B is zinc metallohydrolase. [231]

1.6. Aims of the study

Research of *P. aeruginosa* virulence and antibiotic resistance is of global importance, as the multi-drug resistant clones of this highly virulent nosocomial and opportunistic pathogen have become prevalent worldwide. [232] The further molecular deciphering of biomedically relevant traits of *P. aeruginosa* is challenged since more than 40 % of genes in the genome were not experimentally studied and therefore have an unknown function (genes of unknown function, GUFs). This affects interpreting global transcriptomics and proteomics analyses in which the largest class of identified genes is often GUFs. [233] The main reason for frequent misannotations of GUFs functions in databases is a small number of experimentally characterized genes used for annotations. [234, 235]

One of the most valuable reasons to study GUFs is the suggestion that they represent a promising pool of genes for finding novel drug targets. [236] The *P. aeruginosa* GUFs might include essential genes or important virulence factors with a novel structure, mechanism, or function [237]. Here we aimed to shed light on *P. aeruginosa* GUFs by *in silico* guided experimental characterization of this genomic “dark matter” functions. Since enzymes are the most frequent drug targets [238] and many virulence and antibiotic-resistance factors are hydrolases, the research has been focused on the hydrolytic enzymes.

This thesis aims to identify novel hydrolases among *P. aeruginosa* GUFs and investigate their potential as antimicrobial drug targets. To achieve this, the medium-throughput *in silico* and experimental approaches were developed and followed to:

1. Assign putative biochemical functions to *P. aeruginosa* GUFs by structural homology modeling. These putative functions served as a guide for the experimental characterization of GUFs.
2. Generate expression plasmid suitable for the production of proteins encoded by *P. aeruginosa* GUFs in *E. coli* and *P. aeruginosa*.
3. Create the expression plasmid library of putative hydrolases.
4. Express GUFs-encoding putative hydrolases and determine their biochemical functions.

5. Test virulence phenotypes of newly identified hydrolases.

This comprehensive study of more than 400 of putative hydrolases from *P. aeruginosa* revealed biochemical functions of tenths of novel enzymes. Several of them were shown to be putative virulent factors and biofilm effectors. Additionally, the potential of glycoamidoamine compounds to inhibit lectin LecB, biofilm and adhesion-related virulence factor, was studied in collaboration with Prof. Laura Hartmann (HHU Düsseldorf).

2. Material and methods

2.1. Chemicals

Basic chemicals were purchased from Carl Roth (Karlsruhe, Germany) or Sigma Aldrich/Merck (Taufkirchen, Germany), if not stated differently. The endonucleases Sma I and Afl II (BspTI), T4 DNA ligase, T4 polynucleotide kinase, Shrimp Alkaline phosphatase (rSAP), cut smart buffer, and Gibson cloning master mix were purchased from the New England Biolabs (Ipswich, Massachusetts, United States) and other enzymes used in cloning from Thermofisher Scientific (Waltham, Massachusetts, United States). The phospholipid substrates used in NEFA assay were purchased from Avanti Polar Lipids (Alabaster, United States); α -D-galactose-PAA-biotin and α -D-Galactose-PAA-biotin used in mELLA assay from GlycoTech (Gaithersburg, Maryland, USA).

2.2. *In silico* methods

2.2.1. Databases

Pseudomonas Genome Database (PGD, www.pseudomonas.com) [239] was used to obtain the gene annotations and DNA sequences, while the protein sequences and annotations were retrieved from the Uniprot database (www.uniprot.org). PGD annotations were used to compile the list of genes with human homologs, *P. aeruginosa* PAO1 and PA14 genes with transposon insertion sites, and pathogen-associated genes. The list of virulence factors was composed using the PGD, Virulence factor database (www.mgc.ac.cn/VFs), and Victors virulence factors knowledge database (www.phidias.us/victors). Conserved Domain Database (CDD, www.ncbi.nlm.nih.gov/cdd/) was used to identify protein domains. Multiple protein sequence alignment was performed using a corresponding tool available at the Uniprot database.

2.2.2. Servers

Protein homology/analogy recognition engine (Phyre2)

Phyre2 is an online server for protein structure and function prediction based on the detection of homologs of known 3D structure, i.e., template-based homology modeling or fold recognition [240]. For automated homology modeling of multiple proteins, the amino acid sequences in FASTA format were submitted for the batch processing (normal mode) using Phyre 2 server.

SOSUI server

SOSUI server [241] was used to predict the cellular localization of proteins.

Procheck

The stereochemical parameters, i.e., distributions of the residues in Ramachandran plot, of selected homology models were obtained using the PROCHECK v.3.5 server (<https://servicesn.mbi.ucla.edu/PROCHECK>).

2.2.3. The Basic Local Alignment Search Tool (BLAST)

The simultaneous analysis of hundreds of nucleotide sequences obtained by the Sanger sequencing was performed by searching highly similar sequences in the *P. aeruginosa* PAO1 genome (taxid:208964) using the BLASTN batch tool available at the U.S. National Library of Medicine site (<https://blast.ncbi.nlm.nih.gov/Blast.cgi>). Since the first and last 100 nucleotides of sequencing results are unreliable, the forward and reverse sequencing primers were designed to bind on the plasmid backbone at least 100 bp distant from the gene start and gene end, respectively. To avoid possible mispairings between the plasmid backbone remnants and the *P. aeruginosa* genome sequence, the remaining plasmid backbone sequences were removed from the sequencing results before submission to BLASTN. This was achieved as follows:

1. Conversion of sequencing results from FASTA to tab format using the online tool (<http://sequenceconversion.bugaco.com>)
2. Trimming plasmid backbone sequence, i.e., obtaining only the sequence between expected gene start - Afl II restriction site and gene end - 6xHis tag using text separator feature in Microsoft Excel
3. Conversion of trimmed sequences from tab to FASTA format using the online tool (<http://sequenceconversion.bugaco.com>)

2.2.4. Programs

CloneManager9 (Scientific and Educational Software, USA): Analyses of individual DNA sequences obtained after sequencing; identification of the genes containing the restriction sites; construction of a plasmid map; *in silico* cloning. Image J [242]: Densitometric analysis of dot-blot signals. BioEdit [243]: automated design of the primers for 2137 GUFs; an inspection of the Sanger sequencing chromatograms; determining the percentage of sequence

similarity of two aligned protein sequences. Microsoft Excel: analysis and management of data obtained after the homology modeling, Sanger sequencing, enzyme screening and validation, calculations, and visualizations. Microsoft PowerPoint: Data Visualization. OriginPro (OriginLab Corporation, Northampton, MA, USA): plotting sigmoidal curves; calculation of IC_{50} values; construction of two y-axis diagrams (HPLC chromatogram). Swiss-PdbViewer (<https://spdbv.vital-it.ch>): visualization and superimposition of protein structures and energy minimization of homology models using the GROMOS96 43B1 force field. PyMol software (Schrödinger, L., & DeLano, W. (2020)): the analysis and visualization of homology models.

2.2.5. Design of primers for PCR amplification of GUFs

The primers of the 20 bp annealing region were designed by the use of the BioEdit program after importing the *P. aeruginosa* genomeORF sequences obtained from the PGD database. The GUFs which contained Afl II recognition sequence were identified by the CloneManager9 program. The 5' flanking region of Afl II restriction site (5'CTTAAG3'), following three randomly chosen bases (GAT), recommended for an increasing of the efficiency of Afl II endonuclease activity, was inserted in front of the annealing region of the forward primers. The stop codon was omitted from the reverse primers. Primer sequences (without 5' flanking region) were submitted to the online T_m calculator (www.tmcaculator.neb.com) and the sequences of primer pairs with significantly high T_m differences ($>10-15$ °C) were manually optimized to minimize differences in T_m . Primers with similar T_m values were organized in the same plate for subsequent PCR. Primer sequences are listed in the Table S1.

2.3. DNA methods

2.3.1. Touchdown polymerase chain reaction (TD-PCR)

This method overcomes an imprecise estimation of primer T_m , resulting in the selection of non-optimal annealing conditions. [244] TD-PCR employs successive decreasing of annealing temperatures in the first 10-15 cycles, in which the annealing starts above the estimated primer T_m and finishes at or below the estimated T_m . Mostly, this leads to an increase in the specificity, sensitivity, and yield of PCR, especially with the DNA templates having high G+C content. [244] In this work TD-PCR program [244] was adapted and modified for simultaneous PCR amplification of 94 genes with different T_m in 96-well plates. Instead of primer T_m , annealing temperature (T_a) of primer pairs was considered and maximum (T_a^{\max}), minimum

(T_a^{\min}), and average (T_a^{average}) values for each 96-well plate were calculated. In approximately first 10-15 cycles, the range of temperatures between $T_a^{\max} + 2\text{ }^{\circ}\text{C}$ and $T_a^{\min} - 2\text{ }^{\circ}\text{C}$ was covered with the temperature decrease of $1\text{ }^{\circ}\text{C}$ per cycle, while in the second step of the program slightly lower temperature than the average annealing temperature ($T_a^{\text{average}} - 2\text{ }^{\circ}\text{C}$) was kept constant (Fig. 2). The annealing time was set for each plate, considering the average expected gene size. Primer dilution and pipetting were performed using the 96-channel manual pipetting system PLATEMASTER® (Gilson, Middleton, Wisconsin, USA). The $50\text{ }\mu\text{l}$ PCR reaction containing $1\times\text{HF}$ buffer, 25 ng of *P. aeruginosa* PAO1 genomic DNA, $200\text{ }\mu\text{M}$ of each dNTP, 500 nM of each primer, 1 U Phusion DNA polymerase, 1.5 M betaine, and $5\text{ }\mu\text{g }\mu\text{l}^{-1}$ BSA was incubated in the Biometra TAdvanced thermal cycler (Analytik Jena, Jena, Germany). High-throughput TD-PCR was performed in the 96-well PCR plates (BR781378-50EA, Merck) sealed with the aluminum foil (Art. Nr. 3911256, VWR).

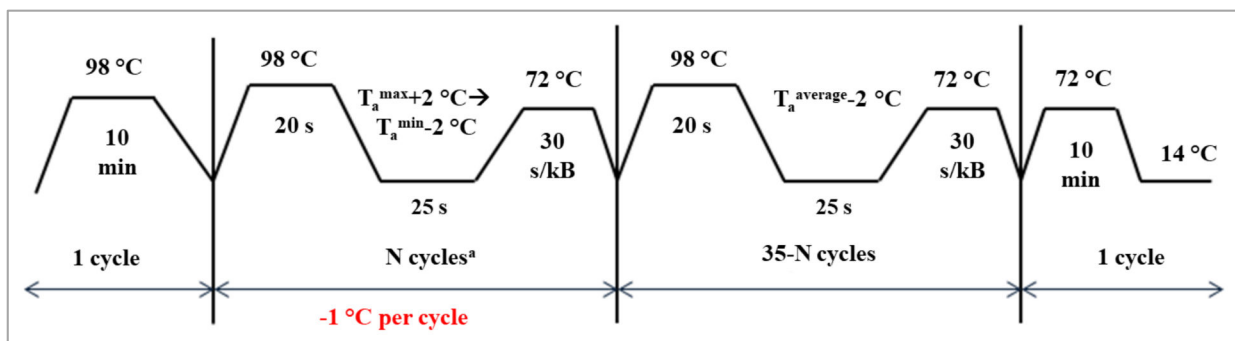


Fig. 2. The modified TD-PCR cycling protocol for the amplification of GUFs in 96-well plate. $N\text{ cycles} = T_a^{\max} - T_a^{\min} + 5$, T_a^{\max} , T_a^{\min} , T_a^{average} represent maximal, minimal, and the average annealing temperature of primer pairs in one 96-well plate.

2.3.2. Trypsin treatment of the PCR products

Phusion DNA polymerase was degraded with trypsin to increase the cloning efficiency [245]. $1\text{ }\mu\text{g}$ of trypsin per 1 U of Phusion DNA polymerase was added to PCR reaction and incubated 40 min at $25\text{ }^{\circ}\text{C}$, followed by the trypsin inactivation for 10 min at $99\text{ }^{\circ}\text{C}$.

2.3.3. Isolation of genomic DNA

Genomic DNA of the *P. aeruginosa* PAO1 was isolated using the Dneasy blood and tissue kit (Qiagen, Hilden) from 40 ml of overnight culture cultivated in LB medium at $37\text{ }^{\circ}\text{C}$, yielding 3 ml $257.7\text{ ng}/\mu\text{l}$ DNA with satisfactory purity ($A_{260}/A_{280} = 2.12$, $A_{260}/A_{230} = 2.18$). The DNA

concentration and purity was measured in the NanoDrop 2000 C spectrophotometer (Thermo Fisher Scientific Germany, Dreiech).

2.3.4. Isolation of plasmid DNA

For the isolation of plasmid DNA from 10-15 ml of the *E. coli* DH5 α cultures, the innuPREP Plasmid Mini Kit (Analytik Jena, Jena) based on alkaline cell lysis and DNA binding to silica-membrane was used according to the manufacturer's recommendations. Centrifugation steps were performed using mikrocentrifuge (Mikro200, Hettich GmbH & Co. KG, Tuttlingen, Germany)

The large scale pGUF plasmid isolation was performed using the NucleoBond™ Xtra Midi kit (Macherey-Nagel™, Düren) following the instructions for the low-copy number plasmids starting from 1 L of overnight *E. coli* DH5 α culture, grown in the TB medium. To minimize the volume of plasmid eluted from the silica columns and to exchange the elution buffer with H₂O, the plasmid was concentrated by isopropanol precipitation. The plasmid DNA was precipitated by the addition of 1/2 volume parts of 7.5 M NH₄OAc and 2 volume parts of isopropanol, followed by the incubation for 2 h at the room temperature. The pellet was obtained by centrifugation for 15 min at 20000 x *g* (Sorvall™ RC 6 Plus Centrifuge, Thermo Scientific, Langerwehe, Germany) and washed with 70 % (v/v) ethanol. After the residual ethanol was removed by evaporation for 15 min under the fume hood, the pellet was dissolved in 3 ml nuclease-free H₂O yielding 210 ng/ μ l DNA.

2.3.5. Purification of DNA

The purification of DNA after PCR amplification and cloning steps was performed using the NucleoSpin Gel and the PCR Clean-up kit (Macherey-Nagel™, Düren) according to the enclosed protocol, except that the DNA was eluted with the nuclease-free H₂O.

Purification after PCR in 96-well plates was done by the modified protocol of the Whatman 96-well PCR cleanup manual for non-kit users and using the 96-channel manual pipetting system PLATEMASTER®. The modifications of the kit include pre-wetting of a binding plate with 20 μ l of nuclease-free H₂O and centrifugation steps were performed at 3320 x *g* for 30 min. The second washing step was introduced, residual ethanol was removed by the incubation at 70 °C for 20 minutes, and DNA was eluted with 40 μ l of nuclease-free water.

2.3.6. Endonuclease hydrolysis and dephosphorylation of pGUF vector

The isolated pGUF plasmid (3 ml) was hydrolyzed with 6000 U of Sma I endonuclease in 1 x cut smart buffer at 25 °C for 16 h. After the complete linearization of pGUF was achieved, as judged by the agarose gel electrophoresis (1 % w/v), the enzyme was heat-inactivated for 15 min at 80 °C. Further hydrolysis and dephosphorylation were achieved by the addition of 6000 U of Afl II, 300 U of shrimp alkaline phosphatase (rSAP), and 67 µl of 10 x cut smart buffer, followed by the incubation at 37 °C for 16 h. The success of hydrolysis was estimated with agarose gel electrophoresis (2 % w/v). The efficiency of dephosphorylation was tested by counting the colonies grown on the tetracycline LB agar plates, after transforming the *E. coli* DH5α with ligation mixture containing 100 ng of hydrolyzed/dephosphorylated pGUF, 1 µl of T4 DNA ligase (2000000 U/ml), and 1 mM ATP in 1 x cut smart buffer. After the inactivation of rSAP and Afl II enzymes by the incubation at 80 °C for 15 min, the hydrolyzed fragments were separated by the ion-exchange chromatography.

2.3.7. Purification of linearized pGUF with the anion exchange chromatography

Large-scale purification of the pGUF hydrolyzed with Afl II and SmaI was achieved using Mono Q™ 5/50 GL column with the chromatography system ÄKTA pure (GE Healthcare, Solingen, Germany), as described previously. [246] The purity of desired fractions (1 ml per well) collected in nuclease-free deep 96-well plates (DWP7323322, VWR) were tested by 2 % (w/v) agarose gel electrophoresis. The fractions containing only linearized pGUF were combined and DNA precipitated with isopropanol as described in Gallet *et al.* (2010) [246]. The pellet was dissolved in nuclease-free H₂O.

2.3.8. Gibson assembly cloning

This Gibson cloning technique [247] allows the assembly of several DNA fragments and was used for the construction of the pGUF vector. The 4772 bp fragment was amplified using linearized pBBR1mcs3 as a template in PCR and *lacI* fragment (1130 bp) was amplified using pET22b vector as a template. The primers (Table S1) used for the amplification of the fragments allowed 22 bp homology regions between three fragments in the correct order. The modified *lacZα* fragment (545 bp) was synthesized by the Eurofins Scientific (Luxembourg). The purified fragments were mixed with the Gibson assembly master mix following the manufacturer's protocol and recommendations.

2.3.9. Endonuclease hydrolysis and phosphorylation of GUFs in 96-well plates

The reaction mixture in each well contained 13 µl purified GUF DNA, 0.5 µl Afl II (20000 U/ml), 0.5 µl T4 Polynucleotide Kinase (10000 U/ml), 0.5 µl 10 x cut-smart buffer, 2.5 µl 10 mM ATP, and 6 µl H₂O. The incubation was performed in the PCR cycler at 37 °C for 10 h, followed by the enzyme inactivation for 20 min at 85 °C.

2.3.10. Ligation in 96-well plates

The reaction mixture contained 10 µl GUF digestion mixture, 1 µl T4 DNA ligase (2000000 U/ml), 1 µl 100 ng/µl linear pGUF (in H₂O), 2 µl 10 mM ATP, 1 µl 10 x cut-smart buffer, and 5 µl H₂O. Incubation was performed in the PCR cycler at 16 °C overnight, followed by 1 h at 25 °C, and inactivation of ligase at 65 °C for 10 min. As a ligation control, Sma I digested pGUF was used.

2.3.11. Agarose gel electrophoresis

Agarose gel electrophoresis was used for the qualitative analysis of DNA samples and the isolation of desired DNA fragments. [248] DNA samples and standard size marker (Gene Ruler 1 kb DNA ladder, Thermo Fisher Scientific) were premixed with 5 x DNA sample dye (100 mM Na₂EDTA, 43 % (v/v) glycerol, 0.5 % (w/v) bromphenol blue) and separated in 0.5-2 % (w/v) agarose gel containing 0.008 % (v/v) of Midori green advance dye (NipponGenetics, Düren, Germany) in 0.5 x TBE buffer (44.5 mM TRIS, 44.5 mM boric acid, 1 mM EDTA, pH 8) by applying 130 V for 30 minutes in the Mini-Sub® Cell GT aperture (BioRad GmbH, Munich, Germany) system. The image was recorded under UV light using the Gel iX Imager (Intas Science Imaging Instruments GmbH, Göttingen, Germany).

2.3.12. Colony PCR

Colony PCR was used to estimate if a colony carried a positive construct. A colony was picked with a sterile toothpick and swirled a few times in 20 µl PCR reaction mixture containing 1xHF buffer (ThermoFisher Scientific, Massachusetts, United States), 200 µM of each dNTP, 500 nM of each primer, and 0.4 U of Phusion DNA polymerase. The same colony was used to inoculate enumerated square of LB agar plate or a liquid medium culture for later sequencing analysis. For analysis of pGUF constructs, the primers which bind to the regions flanking *lacZα* gene (FP_*lacZα*, RP_*lacZα*, Table 6) were used under the following conditions: 1 cycle,

98 °C, 10 min; 35 cycles of 98 °C for 30 s, 60 °C for 30 s and 72 °C for 80 s; and final extension at 72 °C for 10 min. After PCR was completed, 6 µl of each sample was analyzed by the electrophoresis using 1 % (w/v) agarose gel.

2.3.13. DNA sequencing

After transformation of the *E. coli* DH5α with ligation mixtures, a single colony for each GUF was used to inoculate 200 µl of agar medium with 10 µg/ml tetracycline in a 96-well plate. The isolation of pGUF constructs and subsequent Sanger sequencing were performed by MTP premium run service at the LGC Genomics Biosearch Technologies (Berlin, Germany). Used primers for forward and reverse sequencing are listed in the Table S1.

2.4. Cultivation and manipulation of bacteria

2.4.1. Used media, bacterial strains, and plasmids

Media and solutions were sterilized by autoclaving at 121 °C, 200 kPa for 20 min, with the exception of glucose, lactose, and isopropyl β-d-1-thiogalactopyranoside (IPTG) solutions, which were sterilized by filtration using filters with 0.2 µm pore size.

LB (Lysogeny Broth) medium [249]: 10 g/l tryptone, 5 g/l yeast extract, 10 g/l NaCl, pH 7 (as premixed powder from Roth).

LB agar medium: LB medium with 1.5 % (w/v) agar.

Super optimal broth with catabolite repression (SOC): 20 g/l tryptone, 5 g/l yeast extract, 10 mM NaCl, 2.5 mM KCl, 10 mM MgCl₂, 10 mM MgSO₄, 20 mM glucose.

Terrific broth (TB) medium: 900 ml solution 1 (20 g/l tryptone, 24 g/l yeast extract, 4 g/l glycerol) mixed with 100 ml solution 2 (0.17 M KH₂PO₄, 0.72 M K₂HPO₄).

Autoinduction (AI) medium: After autoclaving 960 ml solution containing 6 g/l Na₂HPO₄, 3 g/l KH₂PO₄, 20 g/l tryptone, and 5 g/l yeast extract, 5 ml 10 % glucose (w/v), 25 ml 8 % lactose (w/v) and 10 ml 60 % glycerol (w/v) were added.

Table 1. Used bacterial strains. Tn stands for transposon mutants.

Strain	Genotype	Application
<i>E. coli</i> DH5 α [250]	F ⁻ ϕ 80 <i>lacZ</i> Δ M15 Δ (<i>lacZ</i> YA- <i>argF</i>)U169 <i>recA1 endA1 hsdR17</i> (r _K ⁻ , m _K ⁺) <i>gal</i> ⁻ <i>phoA supE44</i> λ ⁻ <i>thi-1 gyrA96 relA1</i>	cloning, plasmid isolation
<i>E. coli</i> BL21(DE3) [251]	F ⁻ <i>ompT hsdS_B</i> (r _B ⁻ , m _B ⁻) <i>gal dcm</i> (DE3)	gene expression
<i>E. coli</i> C43(DE3) [252]	F ⁻ <i>ompT gal dcm hsdS_B</i> (r _B ⁻ m _B ⁻)(DE3)	gene expression
<i>P. aeruginosa</i> PA01 [253]	Wild-type	gene expression, gDNA isolation
PW4146 [254]	Tn_PA1784	virulence assay
PW1521 [254]	Tn_PA0285	virulence assay
PW1591 [254]	Tn_PA0319	biofilm assay
PW1887 [254]	Tn_PA0484	biofilm assay
PW1915 [254]	Tn_PA0497	biofilm assay
PW1917 [254]	Tn_PA0498	biofilm assay
PW2141 [254]	Tn_PA0627	biofilm assay
PW2506 [254]	Tn_PA0829	biofilm assay
PW3155 [254]	Tn_PA1193	biofilm assay
PW3192 [254]	Tn_PA1214	biofilm assay
PW3467 [254]	Tn_PA1356	biofilm assay
PW4340 [254]	Tn_PA1906	biofilm assay
PW4563 [254]	Tn_PA2067	biofilm assay
PW4573 [254]	Tn_PA2074	biofilm assay
PW4626 [254]	Tn_PA2106	biofilm assay
PW5074 [254]	Tn_PA2419	biofilm assay
PW5513 [254]	Tn_PA2693	biofilm assay
PW5575 [254]	Tn_PA2729	biofilm assay
PW6159 [254]	Tn_PA3074	biofilm assay
PW6521 [254]	Tn_PA3288	biofilm assay
PW6956 [254]	Tn_PA3518	biofilm assay
PW7139 [254]	Tn_PA3614	biofilm assay
PW7141 [254]	Tn_PA3615	biofilm assay
PW7346 [254]	Tn_PA3750	biofilm assay
PW7409 [254]	Tn_PA3785	biofilm assay
PW9359 [254]	Tn_PA4968	biofilm assay
PW9457 [254]	Tn_PA5033	biofilm assay
PW9539 [254]	Tn_PA5088	biofilm assay
PW9710 [254]	Tn_PA5178	biofilm assay
PW10104 [254]	Tn_PA5396	biofilm assay
PW10190 [254]	Tn_PA5441	biofilm assay

Table 2. Used plasmids.

Name	Genotype	Literature
pET-22b (+)	ColE1 Ampr lacIq PT7	Novagen (Merck)
pBBR1MCS-3	Tcr lacZα Plac pBBR1 Rep pBBR1 oriV	[255]
pGUF	Tcr lacZα* lacI Plac Pt7 pBBR1 Rep pBBR1 oriV Afl II 6xHis t7term	this study
pGUF-plaf	pa2949 gene inserted in Afl II / SmaI of pGUF	this study
pGUF-pa2146	pa2146 gene inserted in Afl II / SmaI of pGUF	this study
pGUF-pa2501	pa2501 gene inserted in Afl II / SmaI of pGUF	this study
pGUF-pa1478	pa1478 gene inserted in Afl II / SmaI of pGUF	this study
pGUF-pa4940	pa4940 gene inserted in Afl II / SmaI of pGUF	this study
pGUF-pa3501	pa3501 gene inserted in Afl II / SmaI of pGUF	this study
pGUF-pa0722	pa0722 gene inserted in Afl II / SmaI of pGUF	this study
pGUF-pa2737	pa2737 gene inserted in Afl II / SmaI of pGUF	this study
pGUF-pa1508	pa1508 gene inserted in Afl II / SmaI of pGUF	this study
pGUF-pa2182	pa2182 gene inserted in Afl II / SmaI of pGUF	this study
pGUF-pa0954	pa0954 gene inserted in Afl II / SmaI of pGUF	this study
pGUF-pa0466	pa0466 gene inserted in Afl II / SmaI of pGUF	this study
pGUF-pa3390	pa3390 gene inserted in Afl II / SmaI of pGUF	this study
pGUF-pa2038	pa2038 gene inserted in Afl II / SmaI of pGUF	this study
pGUF-pa2759	pa2759 gene inserted in Afl II / SmaI of pGUF	this study
pGUF-pa3224	pa3224 gene inserted in Afl II / SmaI of pGUF	this study
pGUF-pa0939	pa0939 gene inserted in Afl II / SmaI of pGUF	this study
pGUF-pa1506	pa1506 gene inserted in Afl II / SmaI of pGUF	this study
pGUF-pa0565	pa0565 gene inserted in Afl II / SmaI of pGUF	this study
pGUF-pa1917	pa1917 gene inserted in Afl II / SmaI of pGUF	this study
pGUF-pa3664	pa3664 gene inserted in Afl II / SmaI of pGUF	this study
pGUF-pa5303	pa5303 gene inserted in Afl II / SmaI of pGUF	this study
pGUF-pa1966	pa1966 gene inserted in Afl II / SmaI of pGUF	this study
pGUF-pa1095	pa1095 gene inserted in Afl II / SmaI of pGUF	this study
pGUF-pa1518	pa1518 gene inserted in Afl II / SmaI of pGUF	this study
pGUF-pa5339	pa5339 gene inserted in Afl II / SmaI of pGUF	this study
pGUF-pa3869	pa3869 gene inserted in Afl II / SmaI of pGUF	this study
pGUF-pa2358	pa2358 gene inserted in Afl II / SmaI of pGUF	this study
pGUF-pa3786	pa3786 gene inserted in Afl II / SmaI of pGUF	this study
pGUF-pa5202	pa5202 gene inserted in Afl II / SmaI of pGUF	this study
pGUF-pa5347	pa5347 gene inserted in Afl II / SmaI of pGUF	this study
pGUF-pa2375	pa2375 gene inserted in Afl II / SmaI of pGUF	this study
pGUF-pa4471	pa4471 gene inserted in Afl II / SmaI of pGUF	this study
pGUF-pa5144	pa5144 gene inserted in Afl II / SmaI of pGUF	this study
pGUF-pa0474	pa0474 gene inserted in Afl II / SmaI of pGUF	this study
pGUF-pa0925	pa0925 gene inserted in Afl II / SmaI of pGUF	this study
pGUF-pa0957	pa0957 gene inserted in Afl II / SmaI of pGUF	this study
pGUF-pa3289	pa3289 gene inserted in Afl II / SmaI of pGUF	this study
pGUF-pa4325	pa4325 gene inserted in Afl II / SmaI of pGUF	this study
pGUF-pa5392	pa5392 gene inserted in Afl II / SmaI of pGUF	this study
pGUF-pa1870	pa1870 gene inserted in Afl II / SmaI of pGUF	this study
pGUF-pa3332	pa3332 gene inserted in Afl II / SmaI of pGUF	this study

pGUF-pa2120	pa2120 gene inserted in Afl II / SmaI of pGUF	this study
pGUF-pa1428	pa1428 gene inserted in Afl II / SmaI of pGUF	this study
pGUF-pa0404	pa0404 gene inserted in Afl II / SmaI of pGUF	this study
pGUF-pa4767	pa4767 gene inserted in Afl II / SmaI of pGUF	this study
pGUF-pa5196	pa5196 gene inserted in Afl II / SmaI of pGUF	this study
pGUF-pa0315	pa0315 gene inserted in Afl II / SmaI of pGUF	this study
pGUF-pa1835	pa1835 gene inserted in Afl II / SmaI of pGUF	this study
pGUF-pa3017	pa3017 gene inserted in Afl II / SmaI of pGUF	this study
pGUF-pa3180	pa3180 gene inserted in Afl II / SmaI of pGUF	this study
pGUF-pa5079	pa5079 gene inserted in Afl II / SmaI of pGUF	this study
pGUF-pa0481	pa0481 gene inserted in Afl II / SmaI of pGUF	this study
pGUF-pa0968	pa0968 gene inserted in Afl II / SmaI of pGUF	this study
pGUF-pa1594	pa1594 gene inserted in Afl II / SmaI of pGUF	this study
pGUF-pa2538	pa2538 gene inserted in Afl II / SmaI of pGUF	this study
pGUF-pa3320	pa3320 gene inserted in Afl II / SmaI of pGUF	this study
pGUF-pa2102	pa2102 gene inserted in Afl II / SmaI of pGUF	this study
pGUF-pa3470	pa3470 gene inserted in Afl II / SmaI of pGUF	this study
pGUF-pa4746	pa4746 gene inserted in Afl II / SmaI of pGUF	this study
pGUF-pa5329	pa5329 gene inserted in Afl II / SmaI of pGUF	this study
pGUF-pa1788	pa1788 gene inserted in Afl II / SmaI of pGUF	this study
pGUF-pa4387	pa4387 gene inserted in Afl II / SmaI of pGUF	this study
pGUF-pa4948	pa4948 gene inserted in Afl II / SmaI of pGUF	this study
pGUF-pa5481	pa5481 gene inserted in Afl II / SmaI of pGUF	this study
pGUF-pa2625	pa2625 gene inserted in Afl II / SmaI of pGUF	this study
pGUF-pa5395	pa5395 gene inserted in Afl II / SmaI of pGUF	this study
pGUF-pa1206	pa1206 gene inserted in Afl II / SmaI of pGUF	this study
pGUF-pa1593	pa1593 gene inserted in Afl II / SmaI of pGUF	this study
pGUF-pa4360	pa4360 gene inserted in Afl II / SmaI of pGUF	this study
pGUF-pa1357	pa1357 gene inserted in Afl II / SmaI of pGUF	this study
pGUF-pa3785	pa3785 gene inserted in Afl II / SmaI of pGUF	this study
pGUF-pa1289	pa1289 gene inserted in Afl II / SmaI of pGUF	this study
pGUF-pa3259	pa3259 gene inserted in Afl II / SmaI of pGUF	this study
pGUF-pa2768	pa2768 gene inserted in Afl II / SmaI of pGUF	this study
pGUF-pa2822	pa2822 gene inserted in Afl II / SmaI of pGUF	this study
pGUF-pa3856	pa3856 gene inserted in Afl II / SmaI of pGUF	this study
pGUF-pa3982	pa3982 gene inserted in Afl II / SmaI of pGUF	this study
pGUF-pa0560	pa0560 gene inserted in Afl II / SmaI of pGUF	this study
pGUF-pa1040	pa1040 gene inserted in Afl II / SmaI of pGUF	this study
pGUF-pa1753	pa1753 gene inserted in Afl II / SmaI of pGUF	this study
pGUF-pa1841	pa1841 gene inserted in Afl II / SmaI of pGUF	this study
pGUF-pa2693	pa2693 gene inserted in Afl II / SmaI of pGUF	this study
pGUF-pa3756	pa3756 gene inserted in Afl II / SmaI of pGUF	this study
pGUF-pa3288	pa3288 gene inserted in Afl II / SmaI of pGUF	this study
pGUF-pa3951	pa3951 gene inserted in Afl II / SmaI of pGUF	this study
pGUF-pa0055	pa0055 gene inserted in Afl II / SmaI of pGUF	this study
pGUF-pa1746	pa1746 gene inserted in Afl II / SmaI of pGUF	this study
pGUF-pa3618	pa3618 gene inserted in Afl II / SmaI of pGUF	this study

pGUF-pa5551	pa5551 gene inserted in Afl II / SmaI of pGUF	this study
pGUF-pa0484	pa0484 gene inserted in Afl II / SmaI of pGUF	this study
pGUF-pa3911	pa3911 gene inserted in Afl II / SmaI of pGUF	this study
pGUF-pa0145	pa0145 gene inserted in Afl II / SmaI of pGUF	this study
pGUF-pa0824	pa0824 gene inserted in Afl II / SmaI of pGUF	this study
pGUF-pa2750	pa2750 gene inserted in Afl II / SmaI of pGUF	this study
pGUF-pa1062	pa1062 gene inserted in Afl II / SmaI of pGUF	this study
pGUF-pa3693	pa3693 gene inserted in Afl II / SmaI of pGUF	this study
pGUF-pa2464	pa2464 gene inserted in Afl II / SmaI of pGUF	this study
pGUF-pa4965	pa4965 gene inserted in Afl II / SmaI of pGUF	this study
pGUF-pa1885	pa1885 gene inserted in Afl II / SmaI of pGUF	this study
pGUF-pa0006	pa0006 gene inserted in Afl II / SmaI of pGUF	this study
pGUF-pa1906	pa1906 gene inserted in Afl II / SmaI of pGUF	this study
pGUF-pa4841	pa4841 gene inserted in Afl II / SmaI of pGUF	this study
pGUF-pa0449	pa0449 gene inserted in Afl II / SmaI of pGUF	this study
pGUF-pa1536	pa1536 gene inserted in Afl II / SmaI of pGUF	this study
pGUF-pa1550	pa1550 gene inserted in Afl II / SmaI of pGUF	this study
pGUF-pa4458	pa4458 gene inserted in Afl II / SmaI of pGUF	this study
pGUF-pa4620	pa4620 gene inserted in Afl II / SmaI of pGUF	this study
pGUF-pa3846	pa3846 gene inserted in Afl II / SmaI of pGUF	this study
pGUF-pa2141	pa2141 gene inserted in Afl II / SmaI of pGUF	this study
pGUF-pa3978	pa3978 gene inserted in Afl II / SmaI of pGUF	this study
pGUF-pa0671	pa0671 gene inserted in Afl II / SmaI of pGUF	this study
pGUF-pa1575	pa1575 gene inserted in Afl II / SmaI of pGUF	this study
pGUF-pa4612	pa4612 gene inserted in Afl II / SmaI of pGUF	this study
pGUF-pa0107	pa0107 gene inserted in Afl II / SmaI of pGUF	this study
pGUF-pa0431	pa0431 gene inserted in Afl II / SmaI of pGUF	this study
pGUF-pa2189	pa2189 gene inserted in Afl II / SmaI of pGUF	this study
pGUF-pa1009	pa1009 gene inserted in Afl II / SmaI of pGUF	this study
pGUF-pa1675	pa1675 gene inserted in Afl II / SmaI of pGUF	this study
pGUF-pa2331	pa2331 gene inserted in Afl II / SmaI of pGUF	this study
pGUF-pa5176	pa5176 gene inserted in Afl II / SmaI of pGUF	this study
pGUF-pa5519	pa5519 gene inserted in Afl II / SmaI of pGUF	this study
pGUF-pa0581	pa0581 gene inserted in Afl II / SmaI of pGUF	this study
pGUF-pa4118	pa4118 gene inserted in Afl II / SmaI of pGUF	this study
pGUF-pa2134	pa2134 gene inserted in Afl II / SmaI of pGUF	this study
pGUF-pa2372	pa2372 gene inserted in Afl II / SmaI of pGUF	this study
pGUF-pa5123	pa5123 gene inserted in Afl II / SmaI of pGUF	this study
pGUF-pa1878	pa1878 gene inserted in Afl II / SmaI of pGUF	this study
pGUF-pa2972	pa2972 gene inserted in Afl II / SmaI of pGUF	this study
pGUF-pa3255	pa3255 gene inserted in Afl II / SmaI of pGUF	this study
pGUF-pa3953	pa3953 gene inserted in Afl II / SmaI of pGUF	this study
pGUF-pa1280	pa1280 gene inserted in Afl II / SmaI of pGUF	this study
pGUF-pa4336	pa4336 gene inserted in Afl II / SmaI of pGUF	this study
pGUF-pa4639	pa4639 gene inserted in Afl II / SmaI of pGUF	this study
pGUF-pa4923	pa4923 gene inserted in Afl II / SmaI of pGUF	this study
pGUF-pa0168	pa0168 gene inserted in Afl II / SmaI of pGUF	this study

pGUF-pa0387	pa0387 gene inserted in Afl II / SmaI of pGUF	this study
pGUF-pa0370	pa0370 gene inserted in Afl II / SmaI of pGUF	this study
pGUF-pa1573	pa1573 gene inserted in Afl II / SmaI of pGUF	this study
pGUF-pa3941	pa3941 gene inserted in Afl II / SmaI of pGUF	this study
pGUF-pa0174	pa0174 gene inserted in Afl II / SmaI of pGUF	this study
pGUF-pa2459	pa2459 gene inserted in Afl II / SmaI of pGUF	this study
pGUF-pa4478	pa4478 gene inserted in Afl II / SmaI of pGUF	this study
pGUF-pa1219	pa1219 gene inserted in Afl II / SmaI of pGUF	this study
pGUF-pa1198	pa1198 gene inserted in Afl II / SmaI of pGUF	this study
pGUF-pa1202	pa1202 gene inserted in Afl II / SmaI of pGUF	this study
pGUF-pa4833	pa4833 gene inserted in Afl II / SmaI of pGUF	this study
pGUF-pa5330	pa5330 gene inserted in Afl II / SmaI of pGUF	this study
pGUF-pa2632	pa2632 gene inserted in Afl II / SmaI of pGUF	this study
pGUF-pa4968	pa4968 gene inserted in Afl II / SmaI of pGUF	this study
pGUF-pa0981	pa0981 gene inserted in Afl II / SmaI of pGUF	this study
pGUF-pa1111	pa1111 gene inserted in Afl II / SmaI of pGUF	this study
pGUF-pa5547	pa5547 gene inserted in Afl II / SmaI of pGUF	this study
pGUF-pa0144	pa0144 gene inserted in Afl II / SmaI of pGUF	this study
pGUF-pa1495	pa1495 gene inserted in Afl II / SmaI of pGUF	this study
pGUF-pa0629	pa0629 gene inserted in Afl II / SmaI of pGUF	this study
pGUF-pa0959	pa0959 gene inserted in Afl II / SmaI of pGUF	this study
pGUF-pa4440	pa4440 gene inserted in Afl II / SmaI of pGUF	this study
pGUF-pa2498	pa2498 gene inserted in Afl II / SmaI of pGUF	this study
pGUF-pa1211	pa1211 gene inserted in Afl II / SmaI of pGUF	this study
pGUF-pa0826	pa0826 gene inserted in Afl II / SmaI of pGUF	this study
pGUF-pa0990	pa0990 gene inserted in Afl II / SmaI of pGUF	this study
pGUF-pa0741	pa0741 gene inserted in Afl II / SmaI of pGUF	this study
pGUF-pa0832	pa0832 gene inserted in Afl II / SmaI of pGUF	this study
pGUF-pa4017	pa4017 gene inserted in Afl II / SmaI of pGUF	this study
pGUF-pa5086	pa5086 gene inserted in Afl II / SmaI of pGUF	this study
pGUF-pa5414	pa5414 gene inserted in Afl II / SmaI of pGUF	this study
pGUF-pa5534	pa5534 gene inserted in Afl II / SmaI of pGUF	this study
pGUF-pa2941	pa2941 gene inserted in Afl II / SmaI of pGUF	this study
pGUF-pa4048	pa4048 gene inserted in Afl II / SmaI of pGUF	this study
pGUF-pa0013	pa0013 gene inserted in Afl II / SmaI of pGUF	this study
pGUF-pa1143	pa1143 gene inserted in Afl II / SmaI of pGUF	this study
pGUF-pa1274	pa1274 gene inserted in Afl II / SmaI of pGUF	this study
pGUF-pa3955	pa3955 gene inserted in Afl II / SmaI of pGUF	this study
pGUF-pa4121	pa4121 gene inserted in Afl II / SmaI of pGUF	this study
pGUF-pa1090	pa1090 gene inserted in Afl II / SmaI of pGUF	this study
pGUF-pa0065	pa0065 gene inserted in Afl II / SmaI of pGUF	this study
pGUF-pa0318	pa0318 gene inserted in Afl II / SmaI of pGUF	this study
pGUF-pa5177	pa5177 gene inserted in Afl II / SmaI of pGUF	this study
pGUF-pa2067	pa2067 gene inserted in Afl II / SmaI of pGUF	this study
pGUF-pa5245	pa5245 gene inserted in Afl II / SmaI of pGUF	this study
pGUF-pa1167	pa1167 gene inserted in Afl II / SmaI of pGUF	this study
pGUF-pa1193	pa1193 gene inserted in Afl II / SmaI of pGUF	this study

pGUF-pa2230	pa2230 gene inserted in Afl II / SmaI of pGUF	this study
pGUF-pa2814	pa2814 gene inserted in Afl II / SmaI of pGUF	this study
pGUF-pa0976	pa0976 gene inserted in Afl II / SmaI of pGUF	this study
pGUF-pa3564	pa3564 gene inserted in Afl II / SmaI of pGUF	this study
pGUF-pa2419	pa2419 gene inserted in Afl II / SmaI of pGUF	this study
pGUF-pa2698	pa2698 gene inserted in Afl II / SmaI of pGUF	this study
pGUF-pa3172	pa3172 gene inserted in Afl II / SmaI of pGUF	this study
pGUF-pa4379	pa4379 gene inserted in Afl II / SmaI of pGUF	this study
pGUF-pa4532	pa4532 gene inserted in Afl II / SmaI of pGUF	this study
pGUF-pa1894	pa1894 gene inserted in Afl II / SmaI of pGUF	this study
pGUF-pa2974	pa2974 gene inserted in Afl II / SmaI of pGUF	this study
pGUF-pa3727	pa3727 gene inserted in Afl II / SmaI of pGUF	this study
pGUF-pa3681	pa3681 gene inserted in Afl II / SmaI of pGUF	this study
pGUF-pa3731	pa3731 gene inserted in Afl II / SmaI of pGUF	this study
pGUF-pa5052	pa5052 gene inserted in Afl II / SmaI of pGUF	this study
pGUF-pa0310	pa0310 gene inserted in Afl II / SmaI of pGUF	this study
pGUF-pa1210	pa1210 gene inserted in Afl II / SmaI of pGUF	this study
pGUF-pa5281	pa5281 gene inserted in Afl II / SmaI of pGUF	this study
pGUF-pa1371	pa1371 gene inserted in Afl II / SmaI of pGUF	this study
pGUF-pa4679	pa4679 gene inserted in Afl II / SmaI of pGUF	this study
pGUF-pa0947	pa0947 gene inserted in Afl II / SmaI of pGUF	this study
pGUF-pa1935	pa1935 gene inserted in Afl II / SmaI of pGUF	this study
pGUF-pa4635	pa4635 gene inserted in Afl II / SmaI of pGUF	this study
pGUF-pa1831	pa1831 gene inserted in Afl II / SmaI of pGUF	this study
pGUF-pa2111	pa2111 gene inserted in Afl II / SmaI of pGUF	this study
pGUF-pa4010	pa4010 gene inserted in Afl II / SmaI of pGUF	this study
pGUF-pa1792	pa1792 gene inserted in Afl II / SmaI of pGUF	this study
pGUF-pa4802	pa4802 gene inserted in Afl II / SmaI of pGUF	this study
pGUF-pa1597	pa1597 gene inserted in Afl II / SmaI of pGUF	this study
pGUF-pa1415	pa1415 gene inserted in Afl II / SmaI of pGUF	this study
pGUF-pa1559	pa1559 gene inserted in Afl II / SmaI of pGUF	this study
pGUF-pa1733	pa1733 gene inserted in Afl II / SmaI of pGUF	this study
pGUF-pa2106	pa2106 gene inserted in Afl II / SmaI of pGUF	this study
pGUF-pa0731	pa0731 gene inserted in Afl II / SmaI of pGUF	this study
pGUF-pa2156	pa2156 gene inserted in Afl II / SmaI of pGUF	this study
pGUF-pa4317	pa4317 gene inserted in Afl II / SmaI of pGUF	this study
pGUF-pa2803	pa2803 gene inserted in Afl II / SmaI of pGUF	this study
pGUF-pa5520	pa5520 gene inserted in Afl II / SmaI of pGUF	this study
pGUF-pa4972	pa4972 gene inserted in Afl II / SmaI of pGUF	this study
pGUF-pa0309	pa0309 gene inserted in Afl II / SmaI of pGUF	this study
pGUF-pa0492	pa0492 gene inserted in Afl II / SmaI of pGUF	this study
pGUF-pa1012	pa1012 gene inserted in Afl II / SmaI of pGUF	this study
pGUF-pa5532	pa5532 gene inserted in Afl II / SmaI of pGUF	this study
pGUF-pa2411	pa2411 gene inserted in Afl II / SmaI of pGUF	this study
pGUF-pa5028	pa5028 gene inserted in Afl II / SmaI of pGUF	this study
pGUF-pa2872	pa2872 gene inserted in Afl II / SmaI of pGUF	this study
pGUF-pa1307	pa1307 gene inserted in Afl II / SmaI of pGUF	this study

pGUF-pa5135	pa5135 gene inserted in Afl II / SmaI of pGUF	this study
pGUF-pa2959	pa2959 gene inserted in Afl II / SmaI of pGUF	this study
pGUF-pa4824	pa4824 gene inserted in Afl II / SmaI of pGUF	this study
pGUF-pa4699	pa4699 gene inserted in Afl II / SmaI of pGUF	this study
pGUF-pa0862	pa0862 gene inserted in Afl II / SmaI of pGUF	this study
pGUF-pa1501	pa1501 gene inserted in Afl II / SmaI of pGUF	this study
pGUF-pa3680	pa3680 gene inserted in Afl II / SmaI of pGUF	this study
pGUF-pa0642	pa0642 gene inserted in Afl II / SmaI of pGUF	this study
pGUF-pa1166	pa1166 gene inserted in Afl II / SmaI of pGUF	this study
pGUF-pa3797	pa3797 gene inserted in Afl II / SmaI of pGUF	this study
pGUF-pa4382	pa4382 gene inserted in Afl II / SmaI of pGUF	this study
pGUF-pa0480	pa0480 gene inserted in Afl II / SmaI of pGUF	this study
pGUF-pa2871	pa2871 gene inserted in Afl II / SmaI of pGUF	this study
pGUF-pa4045	pa4045 gene inserted in Afl II / SmaI of pGUF	this study
pGUF-pa1732	pa1732 gene inserted in Afl II / SmaI of pGUF	this study
pGUF-pa3127	pa3127 gene inserted in Afl II / SmaI of pGUF	this study
pGUF-pa3505	pa3505 gene inserted in Afl II / SmaI of pGUF	this study
pGUF-pa5194	pa5194 gene inserted in Afl II / SmaI of pGUF	this study
pGUF-pa3251	pa3251 gene inserted in Afl II / SmaI of pGUF	this study
pGUF-pa2074	pa2074 gene inserted in Afl II / SmaI of pGUF	this study
pGUF-pa3419	pa3419 gene inserted in Afl II / SmaI of pGUF	this study
pGUF-pa0735	pa0735 gene inserted in Afl II / SmaI of pGUF	this study
pGUF-pa3293	pa3293 gene inserted in Afl II / SmaI of pGUF	this study
pGUF-pa3598	pa3598 gene inserted in Afl II / SmaI of pGUF	this study
pGUF-pa4516	pa4516 gene inserted in Afl II / SmaI of pGUF	this study
pGUF-pa4632	pa4632 gene inserted in Afl II / SmaI of pGUF	this study
pGUF-pa0356	pa0356 gene inserted in Afl II / SmaI of pGUF	this study
pGUF-pa0878	pa0878 gene inserted in Afl II / SmaI of pGUF	this study
pGUF-pa0539	pa0539 gene inserted in Afl II / SmaI of pGUF	this study
pGUF-pa0935	pa0935 gene inserted in Afl II / SmaI of pGUF	this study
pGUF-pa4106	pa4106 gene inserted in Afl II / SmaI of pGUF	this study
pGUF-pa1140	pa1140 gene inserted in Afl II / SmaI of pGUF	this study
pGUF-pa1291	pa1291 gene inserted in Afl II / SmaI of pGUF	this study
pGUF-pa0987	pa0987 gene inserted in Afl II / SmaI of pGUF	this study
pGUF-pa2707	pa2707 gene inserted in Afl II / SmaI of pGUF	this study
pGUF-pa1539	pa1539 gene inserted in Afl II / SmaI of pGUF	this study
pGUF-pa3283	pa3283 gene inserted in Afl II / SmaI of pGUF	this study
pGUF-pa0469	pa0469 gene inserted in Afl II / SmaI of pGUF	this study
pGUF-pa3132	pa3132 gene inserted in Afl II / SmaI of pGUF	this study
pGUF-pa3240	pa3240 gene inserted in Afl II / SmaI of pGUF	this study
pGUF-pa4788	pa4788 gene inserted in Afl II / SmaI of pGUF	this study
pGUF-pa2418	pa2418 gene inserted in Afl II / SmaI of pGUF	this study
pGUF-pa4465	pa4465 gene inserted in Afl II / SmaI of pGUF	this study
pGUF-pa2745	pa2745 gene inserted in Afl II / SmaI of pGUF	this study
pGUF-pa4872	pa4872 gene inserted in Afl II / SmaI of pGUF	this study
pGUF-pa1018	pa1018 gene inserted in Afl II / SmaI of pGUF	this study
pGUF-pa2915	pa2915 gene inserted in Afl II / SmaI of pGUF	this study

pGUF-pa3037	pa3037 gene inserted in Afl II / SmaI of pGUF	this study
pGUF-pa4200	pa4200 gene inserted in Afl II / SmaI of pGUF	this study
pGUF-pa1688	pa1688 gene inserted in Afl II / SmaI of pGUF	this study
pGUF-pa5087	pa5087 gene inserted in Afl II / SmaI of pGUF	this study
pGUF-pa1135	pa1135 gene inserted in Afl II / SmaI of pGUF	this study
pGUF-pa3323	pa3323 gene inserted in Afl II / SmaI of pGUF	this study
pGUF-pa5488	pa5488 gene inserted in Afl II / SmaI of pGUF	this study
pGUF-pa5513	pa5513 gene inserted in Afl II / SmaI of pGUF	this study
pGUF-pa5088	pa5088 gene inserted in Afl II / SmaI of pGUF	this study
pGUF-pa1239	pa1239 gene inserted in Afl II / SmaI of pGUF	this study
pGUF-pa4069	pa4069 gene inserted in Afl II / SmaI of pGUF	this study
pGUF-pa0057	pa0057 gene inserted in Afl II / SmaI of pGUF	this study
pGUF-pa3200	pa3200 gene inserted in Afl II / SmaI of pGUF	this study
pGUF-pa2823	pa2823 gene inserted in Afl II / SmaI of pGUF	this study
pGUF-pa3623	pa3623 gene inserted in Afl II / SmaI of pGUF	this study
pGUF-pa4717	pa4717 gene inserted in Afl II / SmaI of pGUF	this study
pGUF-pa0485	pa0485 gene inserted in Afl II / SmaI of pGUF	this study
pGUF-pa3429	pa3429 gene inserted in Afl II / SmaI of pGUF	this study
pGUF-pa3772	pa3772 gene inserted in Afl II / SmaI of pGUF	this study
pGUF-pa5539	pa5539 gene inserted in Afl II / SmaI of pGUF	this study
pGUF-pa3886	pa3886 gene inserted in Afl II / SmaI of pGUF	this study
pGUF-pa2086	pa2086 gene inserted in Afl II / SmaI of pGUF	this study
pGUF-pa1231	pa1231 gene inserted in Afl II / SmaI of pGUF	this study
pGUF-pa2474	pa2474 gene inserted in Afl II / SmaI of pGUF	this study
pGUF-pa2689	pa2689 gene inserted in Afl II / SmaI of pGUF	this study
pGUF-pa2875	pa2875 gene inserted in Afl II / SmaI of pGUF	this study
pGUF-pa4656	pa4656 gene inserted in Afl II / SmaI of pGUF	this study
pGUF-pa0100	pa0100 gene inserted in Afl II / SmaI of pGUF	this study
pGUF-pa2421	pa2421 gene inserted in Afl II / SmaI of pGUF	this study
pGUF-pa4404	pa4404 gene inserted in Afl II / SmaI of pGUF	this study
pGUF-pa1517	pa1517 gene inserted in Afl II / SmaI of pGUF	this study
pGUF-pa2017	pa2017 gene inserted in Afl II / SmaI of pGUF	this study
pGUF-pa4908	pa4908 gene inserted in Afl II / SmaI of pGUF	this study
pGUF-pa3071	pa3071 gene inserted in Afl II / SmaI of pGUF	this study
pGUF-pa0829	pa0829 gene inserted in Afl II / SmaI of pGUF	this study
pGUF-pa2599	pa2599 gene inserted in Afl II / SmaI of pGUF	this study
pGUF-pa1205	pa1205 gene inserted in Afl II / SmaI of pGUF	this study
pGUF-pa0468	pa0468 gene inserted in Afl II / SmaI of pGUF	this study
pGUF-pa3301	pa3301 gene inserted in Afl II / SmaI of pGUF	this study
pGUF-pa0955	pa0955 gene inserted in Afl II / SmaI of pGUF	this study
pGUF-pa2595	pa2595 gene inserted in Afl II / SmaI of pGUF	this study
pGUF-pa1213	pa1213 gene inserted in Afl II / SmaI of pGUF	this study
pGUF-pa2211	pa2211 gene inserted in Afl II / SmaI of pGUF	this study
pGUF-pa2440	pa2440 gene inserted in Afl II / SmaI of pGUF	this study
pGUF-pa4437	pa4437 gene inserted in Afl II / SmaI of pGUF	this study
pGUF-pa2293	pa2293 gene inserted in Afl II / SmaI of pGUF	this study
pGUF-pa0543	pa0543 gene inserted in Afl II / SmaI of pGUF	this study

pGUF-pa3445	pa3445 gene inserted in Afl II / SmaI of pGUF	this study
pGUF-pa2610	pa2610 gene inserted in Afl II / SmaI of pGUF	this study
pGUF-pa0496	pa0496 gene inserted in Afl II / SmaI of pGUF	this study
pGUF-pa5396	pa5396 gene inserted in Afl II / SmaI of pGUF	this study
pGUF-pa1680	pa1680 gene inserted in Afl II / SmaI of pGUF	this study
pGUF-pa4657	pa4657 gene inserted in Afl II / SmaI of pGUF	this study
pGUF-pa0360	pa0360 gene inserted in Afl II / SmaI of pGUF	this study
pGUF-pa3518	pa3518 gene inserted in Afl II / SmaI of pGUF	this study
pGUF-pa0319	pa0319 gene inserted in Afl II / SmaI of pGUF	this study
pGUF-pa0368	pa0368 gene inserted in Afl II / SmaI of pGUF	this study
pGUF-pa3449	pa3449 gene inserted in Afl II / SmaI of pGUF	this study
pGUF-pa0498	pa0498 gene inserted in Afl II / SmaI of pGUF	this study
pGUF-pa3513	pa3513 gene inserted in Afl II / SmaI of pGUF	this study
pGUF-pa3619	pa3619 gene inserted in Afl II / SmaI of pGUF	this study
pGUF-pa4040	pa4040 gene inserted in Afl II / SmaI of pGUF	this study
pGUF-pa4322	pa4322 gene inserted in Afl II / SmaI of pGUF	this study
pGUF-pa3868	pa3868 gene inserted in Afl II / SmaI of pGUF	this study
pGUF-pa1186	pa1186 gene inserted in Afl II / SmaI of pGUF	this study
pGUF-pa3500	pa3500 gene inserted in Afl II / SmaI of pGUF	this study
pGUF-pa0308	pa0308 gene inserted in Afl II / SmaI of pGUF	this study
pGUF-pa2223	pa2223 gene inserted in Afl II / SmaI of pGUF	this study
pGUF-pa4952	pa4952 gene inserted in Afl II / SmaI of pGUF	this study
pGUF-pa2309	pa2309 gene inserted in Afl II / SmaI of pGUF	this study
pGUF-pa3073	pa3073 gene inserted in Afl II / SmaI of pGUF	this study
pGUF-pa3981	pa3981 gene inserted in Afl II / SmaI of pGUF	this study
pGUF-pa1763	pa1763 gene inserted in Afl II / SmaI of pGUF	this study
pGUF-pa4631	pa4631 gene inserted in Afl II / SmaI of pGUF	this study
pGUF-pa2993	pa2993 gene inserted in Afl II / SmaI of pGUF	this study
pGUF-pa1605	pa1605 gene inserted in Afl II / SmaI of pGUF	this study
pGUF-pa3492	pa3492 gene inserted in Afl II / SmaI of pGUF	this study
pGUF-pa1640	pa1640 gene inserted in Afl II / SmaI of pGUF	this study
pGUF-pa3519	pa3519 gene inserted in Afl II / SmaI of pGUF	this study
pGUF-pa2581	pa2581 gene inserted in Afl II / SmaI of pGUF	this study
pGUF-pa0732	pa0732 gene inserted in Afl II / SmaI of pGUF	this study
pGUF-pa0069	pa0069 gene inserted in Afl II / SmaI of pGUF	this study
pGUF-pa4362	pa4362 gene inserted in Afl II / SmaI of pGUF	this study
pGUF-pa0599	pa0599 gene inserted in Afl II / SmaI of pGUF	this study
pGUF-pa2330	pa2330 gene inserted in Afl II / SmaI of pGUF	this study
pGUF-pa3615	pa3615 gene inserted in Afl II / SmaI of pGUF	this study
pGUF-pa3076	pa3076 gene inserted in Afl II / SmaI of pGUF	this study
pGUF-pa2660	pa2660 gene inserted in Afl II / SmaI of pGUF	this study
pGUF-pa3969	pa3969 gene inserted in Afl II / SmaI of pGUF	this study
pGUF-pa3481	pa3481 gene inserted in Afl II / SmaI of pGUF	this study
pGUF-pa4438	pa4438 gene inserted in Afl II / SmaI of pGUF	this study
pGUF-pa3080	pa3080 gene inserted in Afl II / SmaI of pGUF	this study
pGUF-pa4673	pa4673 gene inserted in Afl II / SmaI of pGUF	this study
pGUF-pa2218	pa2218 gene inserted in Afl II / SmaI of pGUF	this study

pGUF-pa1356	pa1356 gene inserted in Afl II / SmaI of pGUF	this study
pGUF-pa0891	pa0891 gene inserted in Afl II / SmaI of pGUF	this study
pGUF-pa3093	pa3093 gene inserted in Afl II / SmaI of pGUF	this study
pGUF-pa3230	pa3230 gene inserted in Afl II / SmaI of pGUF	this study
pGUF-pa2831	pa2831 gene inserted in Afl II / SmaI of pGUF	this study
pGUF-pa2958	pa2958 gene inserted in Afl II / SmaI of pGUF	this study
pGUF-pa3400	pa3400 gene inserted in Afl II / SmaI of pGUF	this study
pGUF-pa1112	pa1112 gene inserted in Afl II / SmaI of pGUF	this study
pGUF-pa5390	pa5390 gene inserted in Afl II / SmaI of pGUF	this study
pGUF-pa3374	pa3374 gene inserted in Afl II / SmaI of pGUF	this study
pGUF-pa2630	pa2630 gene inserted in Afl II / SmaI of pGUF	this study
pGUF-pa2315	pa2315 gene inserted in Afl II / SmaI of pGUF	this study
pGUF-pa1047	pa1047 gene inserted in Afl II / SmaI of pGUF	this study
pGUF-pa2705	pa2705 gene inserted in Afl II / SmaI of pGUF	this study
pGUF-pa1188	pa1188 gene inserted in Afl II / SmaI of pGUF	this study
pGUF-pa2662	pa2662 gene inserted in Afl II / SmaI of pGUF	this study
pGUF-pa2328	pa2328 gene inserted in Afl II / SmaI of pGUF	this study
pGUF-pa5535	pa5535 gene inserted in Afl II / SmaI of pGUF	this study
pGUF-pa2221	pa2221 gene inserted in Afl II / SmaI of pGUF	this study
pGUF-pa2691	pa2691 gene inserted in Afl II / SmaI of pGUF	this study
pGUF-pa3734	pa3734 gene inserted in Afl II / SmaI of pGUF	this study
pGUF-pa2228	pa2228 gene inserted in Afl II / SmaI of pGUF	this study
pGUF-pa4344	pa4344 gene inserted in Afl II / SmaI of pGUF	this study
pGUF-pa0446	pa0446 gene inserted in Afl II / SmaI of pGUF	this study
pGUF-pa4008	pa4008 gene inserted in Afl II / SmaI of pGUF	this study
pGUF-pa2346	pa2346 gene inserted in Afl II / SmaI of pGUF	this study
pGUF-pa2325	pa2325 gene inserted in Afl II / SmaI of pGUF	this study
pGUF-pa1488	pa1488 gene inserted in Afl II / SmaI of pGUF	this study
pGUF-pa2682	pa2682 gene inserted in Afl II / SmaI of pGUF	this study
pGUF-pa1450	pa1450 gene inserted in Afl II / SmaI of pGUF	this study
pGUF-pa4065	pa4065 gene inserted in Afl II / SmaI of pGUF	this study
pGUF-pa0587	pa0587 gene inserted in Afl II / SmaI of pGUF	this study
pGUF-pa0333	pa0333 gene inserted in Afl II / SmaI of pGUF	this study
pGUF-pa0726	pa0726 gene inserted in Afl II / SmaI of pGUF	this study
pGUF-pa1513	pa1513 gene inserted in Afl II / SmaI of pGUF	this study
pGUF-pa2091	pa2091 gene inserted in Afl II / SmaI of pGUF	this study
pGUF-pa4011	pa4011 gene inserted in Afl II / SmaI of pGUF	this study
pGUF-pa4186	pa4186 gene inserted in Afl II / SmaI of pGUF	this study
pGUF-pa2530	pa2530 gene inserted in Afl II / SmaI of pGUF	this study
pGUF-pa2613	pa2613 gene inserted in Afl II / SmaI of pGUF	this study
pGUF-pa3464	pa3464 gene inserted in Afl II / SmaI of pGUF	this study
pGUF-pa0451	pa0451 gene inserted in Afl II / SmaI of pGUF	this study
pGUF-pa1791	pa1791 gene inserted in Afl II / SmaI of pGUF	this study
pGUF-pa2927	pa2927 gene inserted in Afl II / SmaI of pGUF	this study
pGUF-pa3170	pa3170 gene inserted in Afl II / SmaI of pGUF	this study
pGUF-pa1451	pa1451 gene inserted in Afl II / SmaI of pGUF	this study
pGUF-pa0142	pa0142 gene inserted in Afl II / SmaI of pGUF	this study

pGUF-pa2729	pa2729 gene inserted in Afl II / SmaI of pGUF	this study
pGUF-pa3238	pa3238 gene inserted in Afl II / SmaI of pGUF	this study
pGUF-pa5106	pa5106 gene inserted in Afl II / SmaI of pGUF	this study
pGUF-pa5209	pa5209 gene inserted in Afl II / SmaI of pGUF	this study
pGUF-pa1416	pa1416 gene inserted in Afl II / SmaI of pGUF	this study
pGUF-pa4115	pa4115 gene inserted in Afl II / SmaI of pGUF	this study
pGUF-pa3919	pa3919 gene inserted in Afl II / SmaI of pGUF	this study
pGUF-pa5113	pa5113 gene inserted in Afl II / SmaI of pGUF	this study
pGUF-pa1567	pa1567 gene inserted in Afl II / SmaI of pGUF	this study
pGUF-pa1918	pa1918 gene inserted in Afl II / SmaI of pGUF	this study
pGUF-pa3614	pa3614 gene inserted in Afl II / SmaI of pGUF	this study
pGUF-pa3424	pa3424 gene inserted in Afl II / SmaI of pGUF	this study
pGUF-pa1888	pa1888 gene inserted in Afl II / SmaI of pGUF	this study
pGUF-pa4371	pa4371 gene inserted in Afl II / SmaI of pGUF	this study
pGUF-pa2529	pa2529 gene inserted in Afl II / SmaI of pGUF	this study
pGUF-pa4474	pa4474 gene inserted in Afl II / SmaI of pGUF	this study
pGUF-pa2283	pa2283 gene inserted in Afl II / SmaI of pGUF	this study
pGUF-pa4958	pa4958 gene inserted in Afl II / SmaI of pGUF	this study
pGUF-pa5136	pa5136 gene inserted in Afl II / SmaI of pGUF	this study
pGUF-pa0371	pa0371 gene inserted in Afl II / SmaI of pGUF	this study
pGUF-pa4308	pa4308 gene inserted in Afl II / SmaI of pGUF	this study
pGUF-pa5290	pa5290 gene inserted in Afl II / SmaI of pGUF	this study
pGUF-pa4961	pa4961 gene inserted in Afl II / SmaI of pGUF	this study
pGUF-pa1915	pa1915 gene inserted in Afl II / SmaI of pGUF	this study
pGUF-pa5310	pa5310 gene inserted in Afl II / SmaI of pGUF	this study
pGUF-pa1214	pa1214 gene inserted in Afl II / SmaI of pGUF	this study
pGUF-pa1764	pa1764 gene inserted in Afl II / SmaI of pGUF	this study
pGUF-pa0049	pa0049 gene inserted in Afl II / SmaI of pGUF	this study
pGUF-pa2075	pa2075 gene inserted in Afl II / SmaI of pGUF	this study
pGUF-pa1865	pa1865 gene inserted in Afl II / SmaI of pGUF	this study
pGUF-pa1972	pa1972 gene inserted in Afl II / SmaI of pGUF	this study
pGUF-pa0007	pa0007 gene inserted in Afl II / SmaI of pGUF	this study
pGUF-pa3716	pa3716 gene inserted in Afl II / SmaI of pGUF	this study
pGUF-pa4163	pa4163 gene inserted in Afl II / SmaI of pGUF	this study
pGUF-pa5567	pa5567 gene inserted in Afl II / SmaI of pGUF	this study
pGUF-pa3074	pa3074 gene inserted in Afl II / SmaI of pGUF	this study
pGUF-pa3233	pa3233 gene inserted in Afl II / SmaI of pGUF	this study
pGUF-pa4517	pa4517 gene inserted in Afl II / SmaI of pGUF	this study
pGUF-pa1383	pa1383 gene inserted in Afl II / SmaI of pGUF	this study
pGUF-pa1797	pa1797 gene inserted in Afl II / SmaI of pGUF	this study
pGUF-pa3670	pa3670 gene inserted in Afl II / SmaI of pGUF	this study
pGUF-pa2044	pa2044 gene inserted in Afl II / SmaI of pGUF	this study
pGUF-pa3923	pa3923 gene inserted in Afl II / SmaI of pGUF	this study
pGUF-pa1433	pa1433 gene inserted in Afl II / SmaI of pGUF	this study
pGUF-pa0391	pa0391 gene inserted in Afl II / SmaI of pGUF	this study
pGUF-pa4929	pa4929 gene inserted in Afl II / SmaI of pGUF	this study
pGUF-pa1689	pa1689 gene inserted in Afl II / SmaI of pGUF	this study

pGUF-pa1046	pa1046 gene inserted in Afl II / SmaI of pGUF	this study
pGUF-pa1115	pa1115 gene inserted in Afl II / SmaI of pGUF	this study
pGUF-pa2072	pa2072 gene inserted in Afl II / SmaI of pGUF	this study
pGUF-pa0788	pa0788 gene inserted in Afl II / SmaI of pGUF	this study
pGUF-pa4060	pa4060 gene inserted in Afl II / SmaI of pGUF	R. Oben B.Sc thesis*
pGUF-pa4789	pa4789 gene inserted in Afl II / SmaI of pGUF	R. Oben B.Sc thesis*
pGUF-pa3762	pa3762 gene inserted in Afl II / SmaI of pGUF	R. Oben B.Sc thesis*
pGUF-pa0573	pa0573 gene inserted in Afl II / SmaI of pGUF	R. Oben B.Sc thesis*
pGUF-pa3046	pa3046 gene inserted in Afl II / SmaI of pGUF	R. Oben B.Sc thesis*
pGUF-pa1568	pa1568 gene inserted in Afl II / SmaI of pGUF	R. Oben B.Sc thesis*
pGUF-pa0630	pa0630 gene inserted in Afl II / SmaI of pGUF	R. Oben B.Sc thesis*
pGUF-pa1842	pa1842 gene inserted in Afl II / SmaI of pGUF	R. Oben B.Sc thesis*
pGUF-pa3674	pa3674 gene inserted in Afl II / SmaI of pGUF	R. Oben B.Sc thesis*
pGUF-pa0988	pa0988 gene inserted in Afl II / SmaI of pGUF	R. Oben B.Sc thesis*
pGUF-pa2801	pa2801 gene inserted in Afl II / SmaI of pGUF	R. Oben B.Sc thesis*
pGUF-pa5371	pa5371 gene inserted in Afl II / SmaI of pGUF	R. Oben B.Sc thesis*
pGUF-pa0868	pa0868 gene inserted in Afl II / SmaI of pGUF	R. Oben B.Sc thesis*
pGUF-pa4093	pa4093 gene inserted in Afl II / SmaI of pGUF	R. Oben B.Sc thesis*
pGUF-pa5130	pa5130 gene inserted in Afl II / SmaI of pGUF	R. Oben B.Sc thesis*
pGUF-pa2756	pa2756 gene inserted in Afl II / SmaI of pGUF	R. Oben B.Sc thesis*
pGUF-pa3499	pa3499 gene inserted in Afl II / SmaI of pGUF	R. Oben B.Sc thesis*
pGUF-pa3130	pa3130 gene inserted in Afl II / SmaI of pGUF	R. Oben B.Sc thesis*
pGUF-pa2833	pa2833 gene inserted in Afl II / SmaI of pGUF	R. Oben B.Sc thesis*
pGUF-pa1616	pa1616 gene inserted in Afl II / SmaI of pGUF	R. Oben B.Sc thesis*
pGUF-pa0351	pa0351 gene inserted in Afl II / SmaI of pGUF	R. Oben B.Sc thesis*
pGUF-pa1035	pa1035 gene inserted in Afl II / SmaI of pGUF	R. Oben B.Sc thesis*
pGUF-pa0127	pa0127 gene inserted in Afl II / SmaI of pGUF	R. Oben B.Sc thesis*
pGUF-pa0457	pa0457 gene inserted in Afl II / SmaI of pGUF	R. Oben B.Sc thesis*
pGUF-pa1768	pa1768 gene inserted in Afl II / SmaI of pGUF	R. Oben B.Sc thesis*
pGUF-pa3726	pa3726 gene inserted in Afl II / SmaI of pGUF	R. Oben B.Sc thesis*
pGUF-pa2301	pa2301 gene inserted in Afl II / SmaI of pGUF	R. Oben B.Sc thesis*
pGUF-pa3066	pa3066 gene inserted in Afl II / SmaI of pGUF	R. Oben B.Sc thesis*
pGUF-pa4012	pa4012 gene inserted in Afl II / SmaI of pGUF	R. Oben B.Sc thesis*
pGUF-pa3472	pa3472 gene inserted in Afl II / SmaI of pGUF	R. Oben B.Sc thesis*
pGUF-pa1089	pa1089 gene inserted in Afl II / SmaI of pGUF	R. Oben B.Sc thesis*
pGUF-pa4535	pa4535 gene inserted in Afl II / SmaI of pGUF	R. Oben B.Sc thesis*
pGUF-pa1558	pa1558 gene inserted in Afl II / SmaI of pGUF	R. Oben B.Sc thesis*
pGUF-pa2222	pa2222 gene inserted in Afl II / SmaI of pGUF	R. Oben B.Sc thesis*
pGUF-pa0335	pa0335 gene inserted in Afl II / SmaI of pGUF	R. Oben B.Sc thesis*
pGUF-pa0562	pa0562 gene inserted in Afl II / SmaI of pGUF	R. Oben B.Sc thesis*
pGUF-pa5391	pa5391 gene inserted in Afl II / SmaI of pGUF	R. Oben B.Sc thesis*
pGUF-pa4510	pa4510 gene inserted in Afl II / SmaI of pGUF	R. Oben B.Sc thesis*
pGUF-pa1784	pa1784 gene inserted in Afl II / SmaI of pGUF	R. Oben B.Sc thesis*
pGUF-pa2764	pa2764 gene inserted in Afl II / SmaI of pGUF	R. Oben B.Sc thesis*
pGUF-pa0462	pa0462 gene inserted in Afl II / SmaI of pGUF	R. Oben B.Sc thesis*
pGUF-pa0544	pa0544 gene inserted in Afl II / SmaI of pGUF	R. Oben B.Sc thesis*
pGUF-pa4445	pa4445 gene inserted in Afl II / SmaI of pGUF	R. Oben B.Sc thesis*

pGUF-pa1762	pa1762 gene inserted in Afl II / SmaI of pGUF	R. Oben B.Sc thesis*
pGUF-pa1195	pa1195 gene inserted in Afl II / SmaI of pGUF	R. Oben B.Sc thesis*
pGUF-pa1813	pa1813 gene inserted in Afl II / SmaI of pGUF	R. Oben B.Sc thesis*
pGUF-pa4122	pa4122 gene inserted in Afl II / SmaI of pGUF	R. Oben B.Sc thesis*
pGUF-pa1621	pa1621 gene inserted in Afl II / SmaI of pGUF	R. Oben B.Sc thesis*
pGUF-pa1938	pa1938 gene inserted in Afl II / SmaI of pGUF	R. Oben B.Sc thesis*
pGUF-pa3226	pa3226 gene inserted in Afl II / SmaI of pGUF	R. Oben B.Sc thesis*
pGUF-pa4030	pa4030 gene inserted in Afl II / SmaI of pGUF	R. Oben B.Sc thesis*
pGUF-pa3787	pa3787 gene inserted in Afl II / SmaI of pGUF	R. Oben B.Sc thesis*
pGUF-pa5343	pa5343 gene inserted in Afl II / SmaI of pGUF	R. Oben B.Sc thesis*
pGUF-pa0495	pa0495 gene inserted in Afl II / SmaI of pGUF	R. Oben B.Sc thesis*
pGUF-pa1638	pa1638 gene inserted in Afl II / SmaI of pGUF	R. Oben B.Sc thesis*
pGUF-pa3070	pa3070 gene inserted in Afl II / SmaI of pGUF	R. Oben B.Sc thesis*
pGUF-pa3586	pa3586 gene inserted in Afl II / SmaI of pGUF	R. Oben B.Sc thesis*
pGUF-pa4604	pa4604 gene inserted in Afl II / SmaI of pGUF	R. Oben B.Sc thesis*
pGUF-pa1293	pa1293 gene inserted in Afl II / SmaI of pGUF	R. Oben B.Sc thesis*
pGUF-pa4372	pa4372 gene inserted in Afl II / SmaI of pGUF	R. Oben B.Sc thesis*
pGUF-pa3515	pa3515 gene inserted in Afl II / SmaI of pGUF	R. Oben B.Sc thesis*
pGUF-pa2172	pa2172 gene inserted in Afl II / SmaI of pGUF	R. Oben B.Sc thesis*
pGUF-pa2695	pa2695 gene inserted in Afl II / SmaI of pGUF	R. Oben B.Sc thesis*
pGUF-pa0667	pa0667 gene inserted in Afl II / SmaI of pGUF	R. Oben B.Sc thesis*
pGUF-pa1730	pa1730 gene inserted in Afl II / SmaI of pGUF	R. Oben B.Sc thesis*
pGUF-pa2448	pa2448 gene inserted in Afl II / SmaI of pGUF	R. Oben B.Sc thesis*
pGUF-pa4782	pa4782 gene inserted in Afl II / SmaI of pGUF	D. Lorenz B.Sc thesis*
pGUF-pa2485	pa2485 gene inserted in Afl II / SmaI of pGUF	D. Lorenz B.Sc thesis*
pGUF-pa3502	pa3502 gene inserted in Afl II / SmaI of pGUF	D. Lorenz B.Sc thesis*
pGUF-pa0589	pa0589 gene inserted in Afl II / SmaI of pGUF	D. Lorenz B.Sc thesis*
pGUF-pa2898	pa2898 gene inserted in Afl II / SmaI of pGUF	D. Lorenz B.Sc thesis*
pGUF-pa1969	pa1969 gene inserted in Afl II / SmaI of pGUF	D. Lorenz B.Sc thesis*
pGUF-pa2769	pa2769 gene inserted in Afl II / SmaI of pGUF	D. Lorenz B.Sc thesis*
pGUF-pa3741	pa3741 gene inserted in Afl II / SmaI of pGUF	D. Lorenz B.Sc thesis*
pGUF-pa0061	pa0061 gene inserted in Afl II / SmaI of pGUF	D. Lorenz B.Sc thesis*
pGUF-pa2860	pa2860 gene inserted in Afl II / SmaI of pGUF	D. Lorenz B.Sc thesis*
pGUF-pa0822	pa0822 gene inserted in Afl II / SmaI of pGUF	D. Lorenz B.Sc thesis*
pGUF-pa5026	pa5026 gene inserted in Afl II / SmaI of pGUF	D. Lorenz B.Sc thesis*
pGUF-pa4015	pa4015 gene inserted in Afl II / SmaI of pGUF	D. Lorenz B.Sc thesis*
pGUF-pa5246	pa5246 gene inserted in Afl II / SmaI of pGUF	D. Lorenz B.Sc thesis*
pGUF-pa5222	pa5222 gene inserted in Afl II / SmaI of pGUF	D. Lorenz B.Sc thesis*
pGUF-pa4643	pa4643 gene inserted in Afl II / SmaI of pGUF	D. Lorenz B.Sc thesis*
pGUF-pa1189	pa1189 gene inserted in Afl II / SmaI of pGUF	D. Lorenz B.Sc thesis*
pGUF-pa0800	pa0800 gene inserted in Afl II / SmaI of pGUF	D. Lorenz B.Sc thesis*
pGUF-pa1154	pa1154 gene inserted in Afl II / SmaI of pGUF	D. Lorenz B.Sc thesis*
pGUF-pa4830	pa4830 gene inserted in Afl II / SmaI of pGUF	D. Lorenz B.Sc thesis*
pGUF-pa2636	pa2636 gene inserted in Afl II / SmaI of pGUF	D. Lorenz B.Sc thesis*
pGUF-pa0989	pa0989 gene inserted in Afl II / SmaI of pGUF	D. Lorenz B.Sc thesis*
pGUF-pa0201	pa0201 gene inserted in Afl II / SmaI of pGUF	D. Lorenz B.Sc thesis*
pGUF-pa3414	pa3414 gene inserted in Afl II / SmaI of pGUF	D. Lorenz B.Sc thesis*

pGUF-pa1677	pa1677 gene inserted in Afl II / SmaI of pGUF	D. Lorenz B.Sc thesis*
pGUF-pa2451	pa2451 gene inserted in Afl II / SmaI of pGUF	D. Lorenz B.Sc thesis*
pGUF-pa1639	pa1639 gene inserted in Afl II / SmaI of pGUF	D. Lorenz B.Sc thesis*
pGUF-pa3069	pa3069 gene inserted in Afl II / SmaI of pGUF	D. Lorenz B.Sc thesis*
pGUF-pa3379	pa3379 gene inserted in Afl II / SmaI of pGUF	D. Lorenz B.Sc thesis*
pGUF-pa3110	pa3110 gene inserted in Afl II / SmaI of pGUF	D. Lorenz B.Sc thesis*
pGUF-pa1118	pa1118 gene inserted in Afl II / SmaI of pGUF	D. Lorenz B.Sc thesis*
pGUF-pa2471	pa2471 gene inserted in Afl II / SmaI of pGUF	D. Lorenz B.Sc thesis*
pGUF-pa4278	pa4278 gene inserted in Afl II / SmaI of pGUF	D. Lorenz B.Sc thesis*
pGUF-pa1434	pa1434 gene inserted in Afl II / SmaI of pGUF	D. Lorenz B.Sc thesis*
pGUF-pa4543	pa4543 gene inserted in Afl II / SmaI of pGUF	D. Lorenz B.Sc thesis*
pGUF-pa3750	pa3750 gene inserted in Afl II / SmaI of pGUF	D. Lorenz B.Sc thesis*
pGUF-pa1030	pa1030 gene inserted in Afl II / SmaI of pGUF	D. Lorenz B.Sc thesis*
pGUF-pa4312	pa4312 gene inserted in Afl II / SmaI of pGUF	D. Lorenz B.Sc thesis*
pGUF-pa2168	pa2168 gene inserted in Afl II / SmaI of pGUF	D. Lorenz B.Sc thesis*
pGUF-pa5180	pa5180 gene inserted in Afl II / SmaI of pGUF	D. Lorenz B.Sc thesis*
pGUF-pa1622	pa1622 gene inserted in Afl II / SmaI of pGUF	D. Lorenz B.Sc thesis*
pGUF-pa3509	pa3509 gene inserted in Afl II / SmaI of pGUF	D. Lorenz B.Sc thesis*
pGUF-pa3912	pa3912 gene inserted in Afl II / SmaI of pGUF	D. Lorenz B.Sc thesis*
pGUF-pa3994	pa3994 gene inserted in Afl II / SmaI of pGUF	D. Lorenz B.Sc thesis*
pGUF-pa2661	pa2661 gene inserted in Afl II / SmaI of pGUF	D. Lorenz B.Sc thesis*
pGUF-pa5363	pa5363 gene inserted in Afl II / SmaI of pGUF	D. Lorenz B.Sc thesis*
pGUF-pa3695	pa3695 gene inserted in Afl II / SmaI of pGUF	D. Lorenz B.Sc thesis*
pGUF-pa2452	pa2452 gene inserted in Afl II / SmaI of pGUF	D. Lorenz B.Sc thesis*
pGUF-pa4509	pa4509 gene inserted in Afl II / SmaI of pGUF	D. Lorenz B.Sc thesis*
pGUF-pa1209	pa1209 gene inserted in Afl II / SmaI of pGUF	D. Lorenz B.Sc thesis*
pGUF-pa0858	pa0858 gene inserted in Afl II / SmaI of pGUF	D. Lorenz B.Sc thesis*
pGUF-pa3087	pa3087 gene inserted in Afl II / SmaI of pGUF	D. Lorenz B.Sc thesis*
pGUF-pa0064	pa0064 gene inserted in Afl II / SmaI of pGUF	D. Lorenz B.Sc thesis*
pGUF-pa4391	pa4391 gene inserted in Afl II / SmaI of pGUF	D. Lorenz B.Sc thesis*
pGUF-pa2793	pa2793 gene inserted in Afl II / SmaI of pGUF	D. Lorenz B.Sc thesis*
pGUF-pa2549	pa2549 gene inserted in Afl II / SmaI of pGUF	D. Lorenz B.Sc thesis*
pGUF-pa3958	pa3958 gene inserted in Afl II / SmaI of pGUF	D. Lorenz B.Sc thesis*
pGUF-pa0099	pa0099 gene inserted in Afl II / SmaI of pGUF	D. Lorenz B.Sc thesis*
pGUF-pa2922	pa2922 gene inserted in Afl II / SmaI of pGUF	D. Lorenz B.Sc thesis*
pGUF-pa3241	pa3241 gene inserted in Afl II / SmaI of pGUF	D. Lorenz B.Sc thesis*
pGUF-pa3401	pa3401 gene inserted in Afl II / SmaI of pGUF	D. Lorenz B.Sc thesis*
pGUF-pa3461	pa3461 gene inserted in Afl II / SmaI of pGUF	D. Lorenz B.Sc thesis*
pGUF-pa0097	pa0097 gene inserted in Afl II / SmaI of pGUF	D. Lorenz B.Sc thesis*
pGUF-pa4677	pa4677 gene inserted in Afl II / SmaI of pGUF	D. Lorenz B.Sc thesis*
pGUF-pa5133	pa5133 gene inserted in Afl II / SmaI of pGUF	D. Lorenz B.Sc thesis*
pGUF-pa3043	pa3043 gene inserted in Afl II / SmaI of pGUF	D. Lorenz B.Sc thesis*
pGUF-pa2004	pa2004 gene inserted in Afl II / SmaI of pGUF	D. Lorenz B.Sc thesis*
pGUF-pa4701	pa4701 gene inserted in Afl II / SmaI of pGUF	D. Lorenz B.Sc thesis*
pGUF-pa3310	pa3310 gene inserted in Afl II / SmaI of pGUF	D. Lorenz B.Sc thesis*
pGUF-pa2567	pa2567 gene inserted in Afl II / SmaI of pGUF	D. Lorenz B.Sc thesis*
pGUF-pa0454	pa0454 gene inserted in Afl II / SmaI of pGUF	D. Lorenz B.Sc thesis*

pGUF-pa2984	pa2984 gene inserted in Afl II / SmaI of pGUF	D. Lorenz B.Sc thesis*
-------------	---	------------------------

*The constructs were generated by Diana Lorenz (B.Sc thesis, HHU Düsseldorf, 2020) and Rolland Oben (B.Sc. thesis, HHU Düsseldorf, 2019) under my supervision.

2.4.2. Cultivation of bacteria

Bacteria were cultivated in a liquid medium occupying 1/10 of the volume of the Erlenmeyer flasks at 37 °C and 150 rpm in the rotational incubation shaker (3033, GFLProfiLab24 GmbH, Berlin, Germany). Medium-throughput cultivation of bacteria was performed in 0.6 or 1 ml of medium in DWP (Art. Nr. 7323325, VWR, Pennsylvania, USA) sealed with the sterile air-permeable foil (Art. Nr. 3911262, VWR, Pennsylvania, USA) at 37 °C and 1000 rpm in the plate incubation shaker (TiMix control, Edmund Bühler GmbH, Bodelshausen, Germany). Single colonies on LB agar plates were obtained following the streak-plating method of mechanical dilution using an inoculation loop (eza). [256] The plates were prepared by pouring liquid LB agar medium at 60 °C into Petri dishes, followed by cooling at room temperature until agar solidifies. After transformation with ligation mixture or Gibson cloning mixture, bacteria were spread on LB agar Petri dish using glass beads to obtain single clones. After transformation of bacteria in 96-well MTP (microtiter plates), 5-10 beads were added to 60 mm x 15 mm Petri dishes using an autoclaved metal spoon, bacterial suspension was spread and plates were placed in a hermetically closed plastic box to avoid the evaporation during incubation in an agar-up position at 37 °C for 16 h in the incubator (Certomat HK, Sartorius, Göttingen, Germany). Inoculation of overnight liquid cultures was achieved using cryocultures or picking single colonies from the agar plate by a toothpick. The medium was supplemented with the corresponding antibiotic to maintain the plasmid in bacterial cells. In the case of pGUF and pBBR1mcs3 plasmids, the concentration of tetracycline in the medium was 10 µg/ml for the *E. coli* cultures and 100 µg/ml for the *P. aeruginosa*. A stock solution of tetracycline (50 mg/ml) was prepared in 70 % (v/v) ethanol, protected from the light and stored at - 20 °C.

The estimation of bacteria biomass in liquid cultures was achieved by measuring optical density (OD), which represents a logarithmic measurement of the ratio of light transmitted by bacterial cells; $OD = \log_{10} I_0/I_1$, where I_0 is the intensity of visible light incident and I_1 is the intensity of light transmitted. [257] The OD was measured at 580 nm in a Genesys™ 10S UV/Vis spectrophotometer (Thermo Fisher, Dreieich, Germany).

2.4.3. Storage of bacteria

Overnight LB cultures of *E. coli* and *P. aeruginosa* were stored at - 80 °C in the cryo-tubes or 96-DWP in a medium containing 30 % (v/v) of glycerol or 7 % (v/v) of DMSO as cryo-protectants.

2.4.4. Preparation of chemically competent *E. coli*

The bacteria were transformed by modification of the previous procedure. [258] The LB medium (600 ml) was inoculated to OD₅₈₀ of 0.05 with fresh overnight *E. coli* culture and cultivated at 37 °C 150 rpm. When OD₅₈₀ reached 0.4 - 0.6, the cells were harvested by centrifugation 10 min at 3000 x g 4 °C (Sorvall™ RC 6 Plus Centrifuge, Thermo Scientific, Langerwehe, Germany). The cell pellet was suspended in 300 ml of cold transformation buffer (100 mM CaCl₂, 50 mM RbCl, 40 mM MnCl₂) and stored 1 h on ice. After the second centrifugation, the cells were finally suspended in 15 ml of transformation buffer and 4.5 ml of 86 % glycerol (v/v), aliquoted in sterile falcons (for MTP transformation) or Eppendorf tubes and stored at - 80 °C. The potential contamination was tested by the cultivation of competent cells in a 2 ml LB medium containing the respective antibiotic.

2.4.5. Preparation of chemically competent *P. aeruginosa* PA01

The transformation was performed similarly as described in the work of Riley et al. (2013). [259] *P. aeruginosa* PA01 cells were harvested from 600 ml LB culture at OD₅₈₀ 0.4 - 0.6 by centrifugation 3000 x g at 4 °C. The cells were suspended in 500 ml of transformation buffer (150 mM MgCl₂), incubated 5 min on ice, centrifuged 10 min at 3000 x g at 4 °C, followed by the re-suspension in 300 ml transformation buffer, 20 min incubation, and centrifugation (10 min at 3000 x g and 4 °C). Finally, the cell pellet was suspended in 30 ml transformation buffer and 9 ml 86 % glycerol (v/v), incubated at 4 °C overnight, aliquoted, and stored at - 80 °C.

2.4.6. Chemical transformation of bacteria

Transformation of *E. coli* and *P. aeruginosa* was performed by mixing 50 - 100 ng DNA (1-2 µl of plasmid or 10 µl of ligation mixture) with 30 µl competent cells. After 20 min incubation on ice, heat shock was done at 42 °C for 2 min. The cells were recovered by short incubation on ice and the addition of 100 µl (in MTP: non-treated BRAND plates 7352024 VWR) or 500

μl (in Eppendorf tubes) SOC medium pre-warmed at 37 °C. The antibiotic resistance gene was expressed during bacterial cultivation at 37 °C with the agitation of 1000 rpm for MTP covered with air-permeable foil in plate shaker (TiMix control, Edmund Bühler GmbH, Bodelshausen, Germany) or 150 - 200 rpm for Eppendorf tubes (Shaker 3033, GFL) for sufficient amount of time (for tetracycline 2.5 h, ampicillin 45 min). After incubation, the total amount of cells was used to inoculate LB agar Petri dishes or liquid cultures containing the appropriate antibiotic.

2.5. Protein methods

2.5.1. Protein expression in *E. coli*

For validation of the pGUF plasmid expression elements, the *E. coli* BL21(DE3) was transformed with pGUF and pGUF-*plaf* and cultivated in 10 ml of AI medium in Erlenmeyer flasks during 20 h at 37 °C and 150 rpm.

E. coli BL21(DE3) and *E. coli* C43(DE3) were transformed with 1-2 μl of purified pGUF-*guf* constructs and cultivated (shaking at 1000 rpm, 37 °C, 16 h) in DWP containing 0.6 ml LB and 10 μg/ml tetracycline to express PUFs for enzyme screening. From each overnight culture, 100 μl and 10 μl was used to inoculate new DWP containing 900 μl of TB or 990 μl AI medium per well, respectively. Expression in DWPs with TB was induced at OD₅₈₀ 0.5 - 0.8 with 1 mM IPTG followed by the incubation for 4 h at 37 °C 1000 rpm, while expression in AI DWPs was performed during 24 h at 37 °C and 1000 rpm. The cell pellets from all 4 DWPs (2 cell types and 2 different media) were harvested by centrifugation (3320 x g 20 min 4 °C), combined in one plate, and stored at - 20 °C.

For validation of enzyme screening results, the expression was performed in Erlenmeyer flask or DWP in which each sample was surrounded by 4 empty wells. *E. coli* BL21(DE3) was transformed with selected constructs in Eppendorf tubes and used to inoculate 5 ml of LB medium in Erlenmeyer flask or 0.6 ml of LB medium in DWP. After overnight incubation at 37 °C, the culture was used to inoculate 5 ml of AI in Erlenmeyer flask to OD₅₈₀ 0.1 or 1 ml of AI (MagicMedia™ Thermo Fisher Scientific) in DWP. AI culture was grown for 24 h at 37 °C in Erlenmeyer flask agitated at 150 rpm or in DWP agitated at 1000 rpm. Cells were harvested by centrifugation (3320 x g, 20 min, 4 °C). For the proteins expressed in the Erlenmeyer flask, OD₅₈₀ of cell lysates was measured in the cuvette and set to 2, while for the proteins expressed in DWP, the OD₅₈₀ was measured in 96-well MTP, and the activities were normalized

to OD₅₈₀ values. The measured activities of tested pGUF-*guf* constructs and pGUF empty vector control were compared by a two-sample t-test with different variances (type 3 t-test), except for the validation of phospholipase A2 activities of pGUF-*pa2660* and pGUF-*pa0484* (type 2 t-test).

2.5.2. Protein expression in *P. aeruginosa*

For validation of the pGUF plasmid, overnight cultures of *P. aeruginosa* PA01 transformed with pGUF and pGUF-*plaf* were grown in 25 ml of AI medium in Erlenmeyer flasks for 36 h at 37 °C and agitated at 150 rpm.

2.5.3. Preparation of bacterial cell lysates

Combined cell pellets containing expressed proteins were suspended in 300 µl of cold 100 mM Tris-HCl pH 8. The average OD₅₈₀ of the plate was estimated based on OD₅₈₀ values of 5-10 randomly chosen samples and used to prepare cell lysates with desired OD₅₈₀. Cell lysates were prepared in DWP for enzyme screening measurements by diluting the cell suspension with 800 µl of cold 100 mM Tris-HCl pH 8 with 0.2 % (v/v) Triton X-100 to OD₅₈₀ ≈ 2. From this plate, 25 µl of cell lysate was aliquoted in 96-MTPs and the plates were stored at - 20 °C. Suspending and pipetting steps were performed using the 96-channel manual pipetting system PLATEMASTER® and the plates were kept on ice. In 96-well MTP, OD₅₈₀ was measured using the plate reader (SpectraMax i3x, Molecular Devices, San Jose, California, United States) from 50 µl of cell lysate and used to normalize the enzyme activities in the screening. Before measuring the enzyme activity, the cell lysates were thawed on the ice and frozen at - 20 °C two times.

For the dot-blot and Western blot analysis, the corresponding amount of cell suspension was transferred into 96-well MTP and the cells were harvested by the centrifugation (15 min, 3320 x g, 4 °C). The pellet was suspended in 100 mM Tris pH 8 with 8 M urea, 1 % Triton X-100 and 5 mM 2-carboxyethylphosphin-hydrochlorid (TCEP, Sigma Aldrich) to the final OD₅₈₀ of 5 and 15, for dot-blot and Western blot, respectively. After the addition of SDS sample buffer (end concentration: 50 mM Tris, pH 6.8, 2 % (w/v) SDS, 5 % (v/v) glycerol, 0.015 % (w/v) bromophenol blue, 200 mM 2-mercaptoethanol), the samples were incubated for 5 min at 95 °C with shaking.

2.5.4. Dot-blot

Proteins from total cell extracts were adsorbed on the membrane and immunologically detected to estimate PUFs expression rate in DWP. The procedure was similar as described by Putra *et al.* (2014) [260]. Nitrocellulose membrane (pore size 0.2 μm , Amersham, UK) was placed on the two sheets of Whatman paper; 4 μl of cell lysates $\text{OD}_{580\text{nm}} = 5$ were carefully spotted using the 96-channel manual pipetting system PLATEMASTER®; and the membrane was dried entirely at the room temperature. After 10 min of incubation in TBST buffer (0.1 % Tween 20 (v/v), 20 mM Tris, 150 mM NaCl, pH 7.5), bromophenol blue was washed out from the samples. The membrane was stained in 0.1 % (w/v) PonceauS stain (Merck, USA) in 5 % acetic acid to estimate the success of protein adsorption and ensure the loading control. The image was recorded in the Intas Advanced Fluorescence Imager (Intas Science Imaging, Göttingen, Germany). After destaining in TBST buffer, the membrane was blocked for 1 h in 5 % (w/v) non-fat milk in TBST, followed by the incubation in 1:3500 anti-C-6xHis HRP conjugate (Invitrogen, Massachusetts, United States) in TBST during 1 h at the room temperature or overnight at 4 °C. After washing 3 x 10 min in TBST, the membrane was incubated with enhanced chemiluminescent reagent (SuperSignal West Atto Thermo Scientific™ Pierce ECL, Massachusetts, USA) for 1 min, covered with the plastic foil, and the luminescence signal was recorded in the INTAS device.

2.5.5. SDS-polyacrylamide gel electrophoresis (SDS-PAGE)

The protein samples were analyzed in discontinuous polyacrylamide gel electrophoretic system developed by U. Laemmli (1970) [261], in which proteins were separated according to the differences in their molecular masses and compared to the molecular weight standard (PageRuler prestained protein ladder, 10-180 kDa, Thermo Fisher Scientific). The procedure was similar as described by Sambrook *et al.* (2006). [262] The polyacrylamide resolving (12 or 14 %) and stacking (5 %) gels of 0.75 or 1 mm thickness were composed, as shown in Table 3. After casting resolving gel, 200 μl of 70 % (v/v) ethanol was added to align the surface of the gel and reinforce the polymerization process by depleting oxygen at the interface. The samples were prepared in 1 x SDS sample buffer. Electrophoresis was performed using the mini Protean 3 system (BioRad GmbH, Munich) in 1 x SDS running buffer (250 mM glycine, 25 mM TRIS, 3.5 mM sodium dodecyl sulfate) at 100 V for 15 min and 200 V for 45 min using the electrophoresis power supply EPS 601 (GE Healthcare, Illinois, USA). The visualization and

fixation of proteins in the gel was achieved by the overnight incubation with shaking in Coomassie Brilliant Blue staining solution (10 % (w/v) ammonium sulfate, 0.12 % (w/v) Coomassie Brilliant Blue R-250, 1.2 % (v/v) phosphoric acid, and 20 % (v/v) methanol).

Table 3. Composition of SDS-polyacrylamide gels.

Components	Gel percentage		
	5 %	12 %	14 %
30 % acrylamide ^a	0.83 ml	4.0 ml	4.67 ml
Tris-HCl (1.5 M, pH = 8.8)	1.25 ml ^b	2.5 ml	2.5 ml
H ₂ O	2.77 ml	3.35 ml	2.68 ml
SDS 10 % (w/v)	50 µl	100 µl	100 µl
APS 10 % (w/v)	50 µl	100 µl	100 µl
TEMED	10 µl	10 µl	10 µl

^a Mix of 29 % (w/v) acrylamide and 1 % (w/v) N,N'-methylene-bisacrylamide ^bStacking gel (5 %) was prepared with 0.5 M Tris-HCl (pH = 6.8)

2.5.6. Western blot

Proteins were transferred from gels on the polyvinylidene difluoride (PVDF) membrane (0.2 µm) following the Western blotting procedure to enable the immunodetection of specific proteins after SDS-PAGE separation. [263] The PVDF membrane was activated in methanol for 2 min and washed in water. Before transfer, the membrane and the gels were equilibrated for 10 min in Dunn Carbonate transfer buffer (10 mM NaHCO₃, 3 mM Na₂CO₃, pH 9.9 with 20 % (v/v) methanol). The protein transfer was carried out in the Mini Trans-Blot Electrophoretic Transfer Cell (BioRad GmbH, Munich) in Dunn Carbonate buffer for 15 min at 150 mA and 30 min at 300 mA. The efficiency of the transfer was inspected by staining with 0.1 % (w/v) PonceauS. After short incubation in TBST buffer, the membrane was blocked for 1 h in 5 % (w/v) non-fat milk in TBST, incubated in 1:5000 anti-C-6xHis HRP conjugate antibody (Invitrogen, Massachusetts, USA) during 1 h at the room temperature or overnight at 4 °C. After washing 3 x 10 min with TBST buffer, the ECL substrate (SuperSignal West Pico Plus, Pierce ECL, Massachusetts, USA) was added, and the chemiluminescence signal was detected using the Intas Advanced Fluorescence Imager.

2.6. Enzyme assays

All enzyme activities were measured by detecting colorimetric reaction product in 96-MTP using the plate reader (SpectraMax i3x, Molecular Devices, San Jose, California, USA).

2.6.1. Esterase activity assay

The assay was performed similarly as described previously. [264] The substrate was prepared by diluting 20 mM stock of *p*-nitrophenyl butyrate (*p*-NPB) dissolved in isopropanol with 100 mM potassium phosphate buffer pH 7.5 to 1 mM *p*-NPB. After a short incubation at 37 °C, 175 µl of the substrate was added with the multichannel pipette to 25 µl of cell lysates, and the absorbance at 410 nm was recorded during 30 min. The positive control was phospholipase PlaF produced from pGUF-*plaf* construct in *E. coli* BL21(DE3)/*E. coli* C43(DE3) cell lysates.

2.6.2. Lipase activity assay

The assay was performed similarly as described previously. [264] The substrate was prepared by diluting 20 mM stock of *p*-nitrophenyl decanoate (*p*-NPdec) dissolved in isopropanol with 100 mM potassium phosphate buffer pH 7.5 to 1 mM *p*-NPdec. After a short incubation at 37 °C, 175 µl of the substrate was added with a multichannel pipette to 25 µl of cell lysates, and the absorbance at 410 nm was recorded during 30 min. The positive control was PlaF produced from pGUF-*plaf* construct in *E. coli* BL21(DE3)/*E. coli* C43(DE3) cell lysates.

2.6.3. Phosphatase activity assay

The assay was performed similarly as described by Kuznetsova et al. (2005). [265] The substrate was prepared by diluting 20 mM stock of *p*-nitrophenyl phosphate (pNPP) in 20 mM Tris pH 7.5 with 5 mM MgCl₂ to 4 mM pNPP. After a short incubation at 37 °C, 175 µl of the substrate was added with a multichannel pipette to 25 µl of cell lysates, and the absorbance at 410 nm was recorded during 30 min. The positive control was FastAP™ thermosensitive alkaline phosphatase (Thermo Fisher).

2.6.4. Phosphodiesterase activity assay

The assay was performed similarly as described by Kuznetsova et al. (2005). [265] The substrate was prepared by diluting 16.6 mM stock of bis-*p*-nitrophenyl phosphate (bis-*p*-NPP) in 50 mM Tris pH 8 with 5 mM MgCl₂ to 0.83 mM bis-*p*-NPP. After a short incubation at 37 °C, 175 µl of the substrate was added with a multichannel pipette to 25 µl of cell lysates, and the absorbance at 410 nm was recorded during 30 min.

2.6.5. Phospholipase C activity assay

The assay was performed similarly as described by Kurioka et al. (1976). [266] The substrate was prepared by diluting 20 mM stock of *p*-nitrophenyl phosphorylcholine (*p*-NPPC) in 167 mM Tris buffer pH 7.5 with 40 % sorbitol and 1 μ M ZnCl₂ to 1 mM pNPPC. After a short incubation at 37 °C, 175 μ l of the substrate was added with a multichannel pipette to 25 μ l of cell lysates, and the absorbance at 410 nm was recorded during 30 min. The positive control was phospholipase C from *Bacillus cereus* (Sigma Aldrich).

2.6.6. Protease activity assay

The assay was performed similarly as described by Kuznetsova et al. (2005). [265] The substrate stock was prepared by dissolving α -benzoyl-L-arginine-*p*-nitroanilid (BA-*p*-NA) and L-leucine-*p*-nitroanilide (Leu-*p*-NA) in the reaction buffer 100 mM Tris pH 8.1 mM CaCl₂, 1 mM ZnCl₂ with 20 % (v/v) dimethyl sulfoxide (DMSO). After a short incubation at 37 °C, 175 μ l of 1 mM BA-*p*-NA and 1 mM Leu-*p*-NA was added with a multichannel pipette to 25 μ l of cell lysates, and the absorbance at 410 nm was recorded during 30 min. The positive control was trypsin (Sigma Aldrich).

2.6.7. Glucosidase activity assay

The assay was performed following the quality control test procedure of α -glucosidase substrate, *p*-nitrophenyl α -D-glucoside, from Sigma Aldrich (Missouri, USA). The substrate was prepared by mixing 2 ml of substrate stock (20 mM *p*-nitrophenyl- β -D-glucopyranosid and *p*-nitrophenyl- α -D-glucopyranosid in water) with 200 μ l freshly prepared 10 mM glutathione and 17.6 ml 100 mM potassium phosphate buffer pH 7.5. After a short incubation at 37 °C, 175 μ l of the substrate was added to 25 μ l of cell lysates, and the absorbance at 410 nm was recorded during 30 min.

2.6.8. Thioesterase activity assay

The assay was performed similarly as described by Kovačić et al. (2013). [175] In 25 μ l of cell lysates, 10 μ l of freshly prepared 10 mM 5,5-dithio-bis-(2-nitrobenzoic acid) (DTNB) was added, followed by the addition of 150 μ l of 40 μ M acetyl-CoA and 40 μ M palmitoyl-CoA in 50 mM Tris-HCl pH 7.5 with 0.2 M KCl. The principle is that coenzyme A released by thi-

oesterase activity reacts with the DTNB yielding the 5-thio-2-nitrobenzoate, whose absorbance at 412 nm was recorded during 30 min.

2.6.9. Phospholipase and lipase assay using non-esterified fatty acid (NEFA) kit

The Wako NEFA-HR(2) assay (FUJIFILM Wako Chemicals Europe GmbH, Neuss, Germany) allows quantitative determination of non-esterified fatty acids *via* three coupled enzyme reactions (acyl-CoA synthetase, acyl-CoA oxidase and peroxidase), finally yielding blue-purple pigment. This assay was used to detect phospholipase A and lipase activity, similarly as described previously [264]. Lipase substrate was 268 mM glyceryl tridecanoate, while phospholipase A substrate consisted of 89.33 mM 1,2-dipalmitoyl-sn-glycero-3-phosphocholine (16:0 PC), 89.33 mM 1,2-dipalmitoyl-sn-glycero-3-phosphoethanolamine (16:0 PE) and 89.33 mM 1,2-dipalmitoyl-sn-glycero-3-phospho-(1'-rac-glycerol) (16:0 PG), dissolved in the reaction buffer Tris-HCl pH 7.5 with 1 % (v/v) Triton X-100. The substrates were diluted 20 times with the reaction buffer and ultrasonicated 3x20 s before use. In 96-well MTP 10 µl of cell lysates OD₅₈₀ = 0.4 were mixed with 10 µl of the substrate, covered with the parafilm to avoid evaporation, and incubated for 24 h at 37 °C 150 rpm. After a short centrifugation, 100 µl buffer R1 and 50 µl buffer R2 were added, and the absorbance was measured in a spectrophotometer following the supplier's instructions.

2.6.10. Phospholipase A2 assay

In validation of phospholipase A activities, the sPLA2 assay Kit from Cayman Chemical (Michigan, USA) was used following the supplier's instructions.

2.7. Modified enzyme-linked lectin assay (mELLA)

Testing the binding potential of fucosylated glycooligomers on lectin LecB was performed as described by Bücher et al. (2018). [267]

2.8. Biological assays

2.8.1. Biofilm formation assay

This assay allows the quantification of an early-phase biofilm formed on the walls and/or bottom of a microtiter plate under static conditions. The procedure was similar as described by O'Toole et al. (2011). [268] Transposon mutant and PA01 wild-type strains were plated on the LB agar plate and 7-8 colonies of each strain were used to inoculate 100 µl of LB medium in 96-well MTP. The cultivation was performed for 16 h at 37 °C under the static conditions in a hermetically closed plastic box with water-saturated air to prevent drying. After cultivation, OD₅₈₀ was measured, followed by washing the wells with distilled water to remove the non-attached cells. After drying at 37 °C, the attached cells were stained by the incubation with 125 µl of a 0.1 % crystal violet (w/v) solution for 15 min at the room temperature. After removing the excess of crystal violet by washing with distilled water and subsequent drying, 125 µL of 30 % acetic acid (v/v) was added, and the absorbance at 550 nm was recorded. Testing the inhibitory potential of the fucosylated glycooligomers on biofilm formation was performed as described by Bücher *et al.*(2018). [267]

2.8.2. *Galleria mellonella* virulence assay

The experiment was carried out in cooperation with Prof. Dr. Susanne Häußler and Dr. Sebastian Felgner at the Helmholtz Center for Infection Research at the Institute for Molecular Bacteriology in Braunschweig, as described by Koch *et al.* (2014). [269] The caterpillar larvae (wax worm) *G. mellonella* was used as an infection model to test *P. aeruginosa* transposon mutants. *G. mellonella* larvae (Fauna Topics GmbH, Marbach am Neckar, Germany) were sorted according to the size and split into groups of ten in Petri dishes. To limit the movement of larvae during the application of bacteria, they were stored at 8 °C for 60 min. *P. aeruginosa* PA01 and *P. aeruginosa* transposon mutant strains were grown overnight and subcultured 3 h in liquid LB media at 37 °C. The bacteria were washed twice with PBS and adjusted to OD₅₈₀ = 0.055, which equals 5×10⁵ bacteria per 10 µl. This suspension was diluted with PBS to the infection dose of 500 bacteria per 10 µl, which were injected. For injection, the larvae were hyperextended, and the bacterial suspension was injected into the first segment behind the last abdominal foot and stored at 30 °C. Hereby, PBS (138 mM NaCl, 2.67 mM KCl, 8 mM Na₂HPO₄, 1.5 mM KH₂PO₄, pH 7.4) injections were used as an infection

control and untreated larvae as viability control. After the injection, the larvae were incubated at 30 °C and monitored for the survival.

3. Results

3.1. Bioinformatic analysis of *P. aeruginosa* genes of unknown function (GUFs)

3.1.1. Identification of *P. aeruginosa* GUFs

The list of *P. aeruginosa* GUFs was compiled based on the functional confidence rating for all 5714 proteins encoded by *P. aeruginosa* PA01 genes. According to the PGD, 2103 genes were annotated with functional class IV (the lowest confidence), including 636 conserved hypothetical genes, which are homologs of previously reported genes of unknown function, 1463 hypothetical genes having no similarity to other genes, and additional four genes (PA0964, PA3862, PA3863, PA3864) with experimentally confirmed functions, which were eliminated from our list of selected GUFs. To increase the chance of identifying novel virulence factors with hydrolytic activities, 40 genes of functional class III, whose putative hydrolytic activity was proposed based on the presence of conserved amino acid motif, structural feature, or limited sequence similarity to an experimentally studied gene, were added to the final list. Finally, 2138 GUFs were identified as a subject of research in this thesis (Fig. 3).

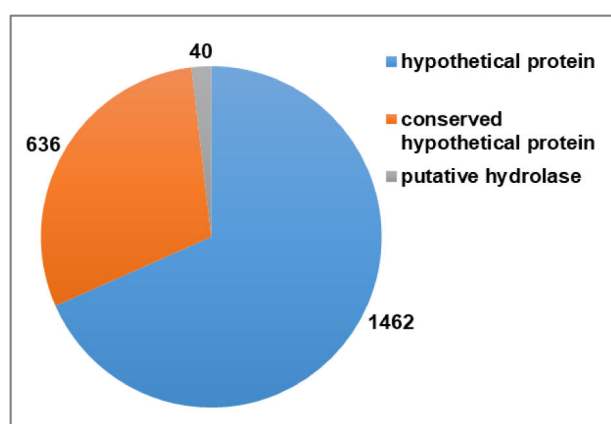


Fig. 3. *P. aeruginosa* genes of unknown function. *P. aeruginosa* GUFs include 2098 genes with functional class IV (hypothetical and conserved hypothetical) and 40 genes of functional class III with putative hydrolase functions. According to the Pseudomonas Genome Database, the genes with functional confidence IV are homologs of previously reported genes of unknown function (conserved hypothetical), or have no similarity to any previously reported sequences (hypothetical), while the function of class III genes is proposed based on the presence of conserved amino acid motif, structural feature or limited sequence similarity to an experimentally studied gene. Gene identifiers of PUFs with here predicted functions are provided in the PaPUF database at www.iet.uni-duesseldorf.de/arbeitsgruppen/bacterial-enzymology.

3.1.2. Comparative genomic analysis of *P. aeruginosa* GUFs

The first step of *in silico* characterization of *P. aeruginosa* GUFs was to examine their sequence homology to other relevant genes to explore the potential of this pool of genes as putative antibiotic and anti-virulence drug targets. Therefore, the genomics mining of PGD annotations and literature was performed to find GUFs having homologs among genes conserved in other pathogenic bacteria, virulence factors, and human genes and to identify essential genes.

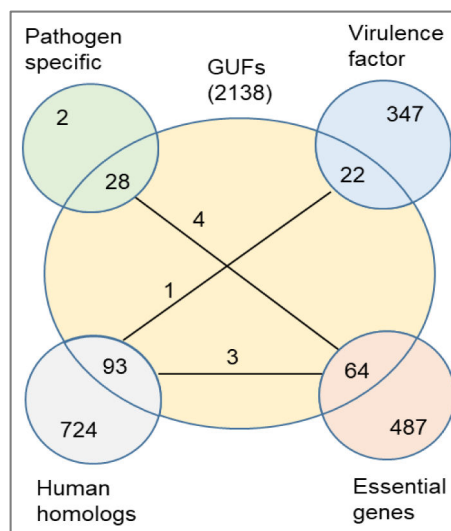


Fig. 4. Pathogen-specific, essential, virulence factors, and genes with human homologs among GUFs. The figure is obtained by overlapping 2138 GUFs identifiers with 30 *P. aeruginosa* genes having homologs only in pathogenic strains (pathogen-specific), 369 *P. aeruginosa* genes with experimentally determined or homology-inferred virulence roles, 817 *P. aeruginosa* genes having homologs in humans and 551 *P. aeruginosa* genes with the essential roles. The numbers in crossing sections indicate the number of GUFs belonging to one of four designated gene groups, while the numbers on lines indicate the number of mutual GUFs among two linked groups. Gene identifiers of PUFs with here predicted functions are provided in the PaPUF database at www.iet.uni-duesseldorf.de/arbeitsgruppen/bacterial-enzymology.

In *P. aeruginosa*, 30 genes were previously identified that had BLAST hits (E-value cut-off of 10^{-7}) only to proteins in pathogenic strains [270], and as many as 28 of them belong to GUFs (Fig. 4).

The list of 369 virulence factors includes *P. aeruginosa* genes whose roles in virulence were experimentally proven by studying respective mutant strains and the genes whose virulence role was inferred from the sequence similarity with virulence factors from other pathogens. [271] Overlapping this list with GUFs resulted in 22 genes from which 13 genes were previously linked to virulence-related processes by studying their functions during infection

of model host organisms (e.g. *Caenorhabditis elegans*, *Drosophila melanogaster*, or *Rattus norvegicus*) and an additional 5 genes were related to common virulence traits (flagella-mediated motility, pyoverdine-mediated iron uptake, type VI secretion of toxins) (Fig. 4) and Table S3 in the accompanying publication [272].

The essentiality was attributed to 64 GUFs based on the experimental finding that mutation of the respective gene leads to cell death [273]. Among them, four (PA0442, PA0977, PA1369, PA2139) are also conserved in pathogens and, therefore, they are particularly promising drug targets (Fig. 4). The majority (2045 GUFs) fulfill important selectivity criterium since they do not share homology with human genes (Fig 4).

Conclusively, genomics mining revealed 106 GUFs as a priority group for investigating novel drug targets based on their essential or virulence-related role in bacteria, the existence of homologs among pathogen-specific genes, and the absence of human homologs.

3.1.3. *In silico* assignment of putative biochemical and biological functions to *P. aeruginosa* PUFs

The second approach for prioritizing GUFs to identify novel virulence and pathogenesis-relevant genes was predicting their biochemical functions. Moreover, *in silico* assignment of putative biochemical functions allows bioinformatically-guided characterization of GUFs in high-throughput experiments. The putative functions were assigned using 3D structural homology modeling by the Phyre2 server. [274] The protein sequences of 2137 GUFs (PA2462 with a size of 573.2 kDa was too large for homology modeling) were obtained from the Uniprot database and submitted for the batch mode of homology modeling. The outcome for every submitted protein sequence (query) was 20 structural models, each built with a different template protein structure. Homology models are characterized by confidence, which is the probability that the match between a query and a template is a true homology [275], sequence identity for query and template alignment [275], and the range of query protein covered with the template. Overall, homology modeling for 2137 PUFs was successful since the majority of PUFs (70 %) were modeled with confidences higher than 90 % (Fig. 5-B), despite nearly 65 % of modeled proteins having low sequence identities (below 20 %) (Fig. 5-A).

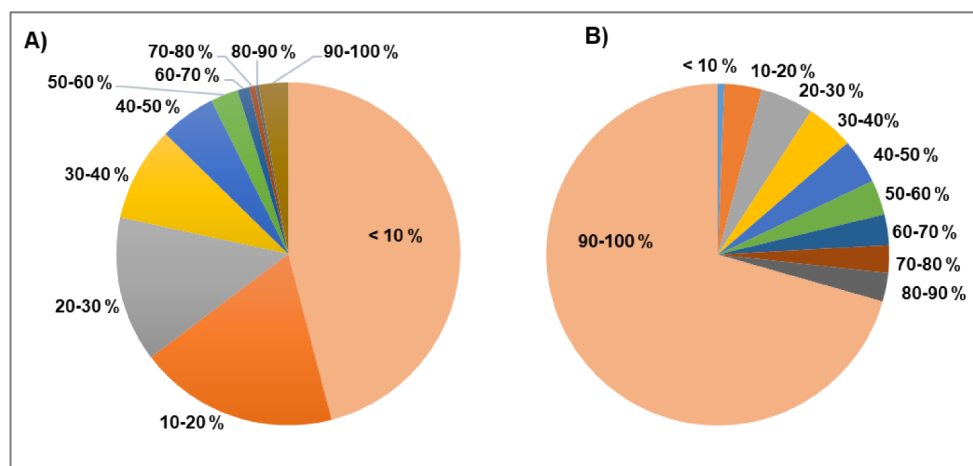


Fig. 5. Pie charts showing success of homology modeling of 2137 *P. aeruginosa* PUFs using the Phyre2 server.

A) Distribution of number of *P. aeruginosa* PUFs modelled with 0-100 % of sequence identity to the template. **B)** Distribution of number of *P. aeruginosa* PUFs modelled with 0-100 % of confidence. Only the highest confidence score of each PUF (the first out of 20 templates) was considered in the analysis. Different colours reflect the proportion of number of modelled genes and are selected arbitrary.

To assign putative biochemical functions, the reliable models were selected by automatically analyzing confidence and the size of the query that is modeled. The minimum value for confidence was set to 75 %. The minimum query size was 50 amino acids for queries modeled with templates having a ligand-binding function and 100 amino acids for enzymes and transporters. After filtering homology modeling results using these cut-off values for the first ten templates per query, textual mining of PDB names of templates used to obtain reliable models was performed (Fig. 6).

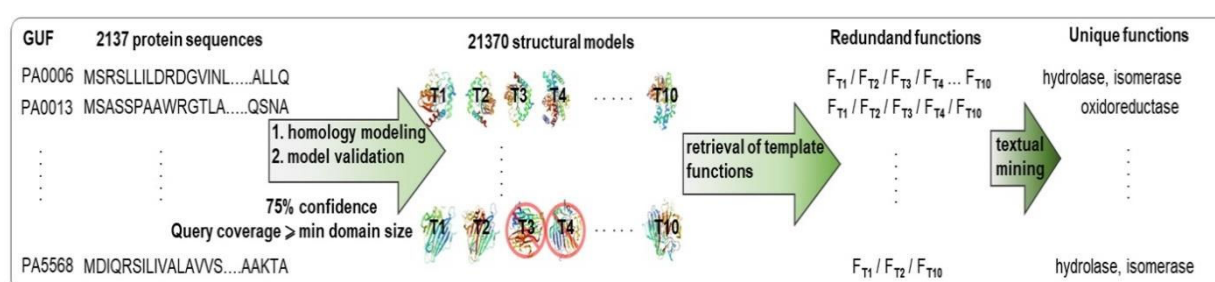


Fig. 6. Pipeline for automatic analysis of results obtained after homology modeling of 2137 PUFs with Phyre2 server. The figure was adopted from Babic & Kovacic (2021) [272] and modified. Protein sequences of 2137 *P. aeruginosa* GUFs were obtained from the UniProt database and submitted for homology modeling using a batch mode of Phyre2 server. For each PUF, 20 models were obtained, ranked by the confidence score and alignment coverage. The reliable models were selected using cut-off criteria for the first ten templates for each PUF: the confidence of homology modeling has to be $\geq 75\%$, and the size of the query aligned to template ≥ 100 residues for transporters and enzymes and ≥ 50 residues for binding proteins. The functional annotations (PDB header and PDB molecule fields) of templates used to obtain a reliable model were automatically

analyzed by searching the keywords listed in Table 4 and transferred to the corresponding PUF. Redundant template functions were removed to obtain a list of unique functions representing putative functions of PUFs.

Textual mining of corresponding templates using the keywords listed in Table 4 was focused on three important biochemical functions: enzymatic activity, ligand binding, and transport function. The keywords represent non-redundant functional annotations of templates, which were used to obtain reliable models in homology modeling and had enzyme, ligand-binding, and transport functions.

Table 4: Keywords used for textual mining of templates used to build reliable structural models (confidence $\geq 75\%$ and the size of the query aligned to template ≥ 100 residues for transporters and enzymes and ≥ 50 residues for binding proteins) by Phyre2 homology modeling. The table is adopted from Babic & Kovacic (2021) [272].

Hydrolase	Transferase	Oxidoreductase	Ligase	Lyase	Isomerase
hydrolase	*transferase*	*oxidoreductase*	*ligase*	*lyase*	*isomerase*
cellulase	*kinase*	*hydroxylase*	*synthetase*	*aldolase*	*epimerase*
glucosidase	*phosphorylase*	*reductase*	*synthase*	*fumarase*	*mutase*
gtpase	*transaldolase*	*oxidase*		*cyclase*	*racemase*
atpase	*transglutaminase*	*oxido-reductase*		*dehydrochlorinase*	
peptide release	*polymerase*	*flavoenzyme*			
peptidase	*thiolase*	*hydrogenase*			
nuclease		*oxygenase*			
dnase		*cytochrom*			
rnase					
phosphatase					
amylase					
amidase					
esterase					
protease					
proteinase					
helicase					
leishmanolysin					
hydrolytic enzyme					
lipase					
phospholipase					
Binding				Transporter	
Nucleic acids	Lipid	Sugar	Nucleotide		
dna	*lipid*	*cellulose*	*atp*	*porin*	*export*
rna	*fatty acid*	*carbohydrat*	*amp*	*channel*	*import*
nucleic		*peptidoglycan*	*nucleot*	*efflux*	*uptake*
		lectin	*fmn*	*pump*	*permease*

		sugar		*transporter*	*anti/sim/port er*
		maltose			

* indicates any character

Applying the procedure shown in Fig. 6 and analyzing the keywords from Table 4 for 21370 templates obtained from homology modeling of 2137 PUFs resulted in the prediction of the enzyme, ligand binding, and transport functions to 1267 (59 %) of PUFs, with more than 1000 proteins with putative enzyme functions (Fig. 7-A). In many cases, there was more than one reliable template per query (Fig. 7-B). Three hundred and five PUFs have two and 45 three of the functions analyzed here, and the most extensive overlap is between enzymes and ligand-binding proteins. Combining homology modeling with results of comparative genomics (Fig. 4) allowed assigning putative biochemical functions to 35 essential and ten virulence-related PUFs, among which the majority were putative enzymes (Fig. 7-C).

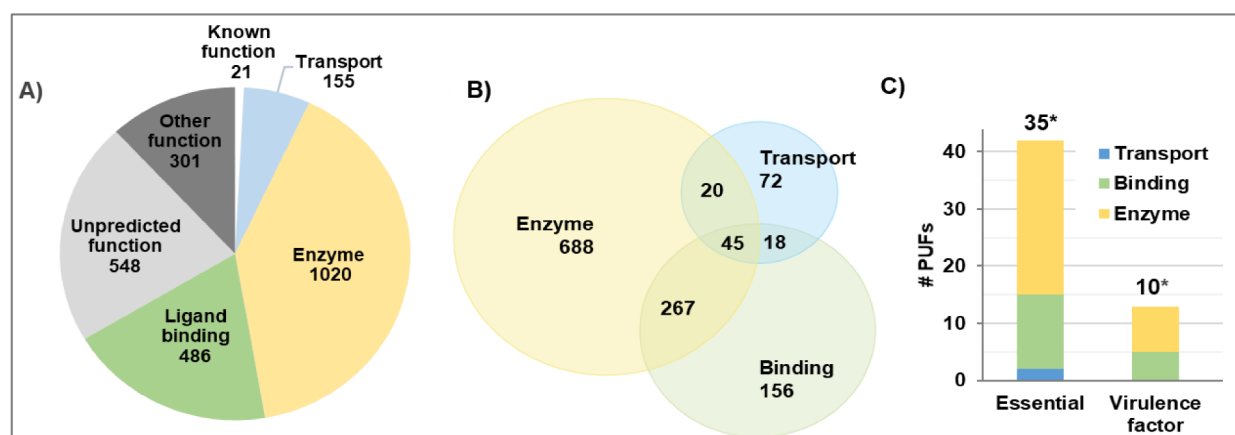


Fig. 7. Predicted biochemical functions for *P. aeruginosa* PUFs by Phyre2 homology modeling. (A) The number of genes with putative enzyme, ligand-binding, and transporter functions (T1-T10, confidence ≥ 75 %, length of query aligned to template ≥ 50 amino acids for ligand binding or 100 amino acids for enzymes and transport). PUFs with unpredicted functions had confidence < 75 %, while PUFs with known functions had sequence identities > 93 %. (B) Venn diagram of PUFs with enzyme, ligand binding, and transport functions. The diagram was generated using bioinformatics.psb.ugent.be/webtools/Venn/. (C) Distribution of essential and virulence factors among PUFs with the predicted enzyme, ligand binding, or transport functions having 35 unique essential and ten unique virulence genes. Gene identifiers of PUFs with here predicted functions are provided in the PaPUF database at www.iet.uni-duesseldorf.de/arbeitsgruppen/bacterial-enzymology.

Using text mining, further classification of putative enzymes revealed hydrolases as the most abundant class, followed by transferases and oxidoreductases (Fig. 8-A). The nucleic acids

binding proteins and transporters were the most abundant among ligand binding and transport functions, respectively (Fig. 8-B and Fig. 8-C). The representative models from all three biochemical functional classes are shown in Fig. 8 D-F. [272]

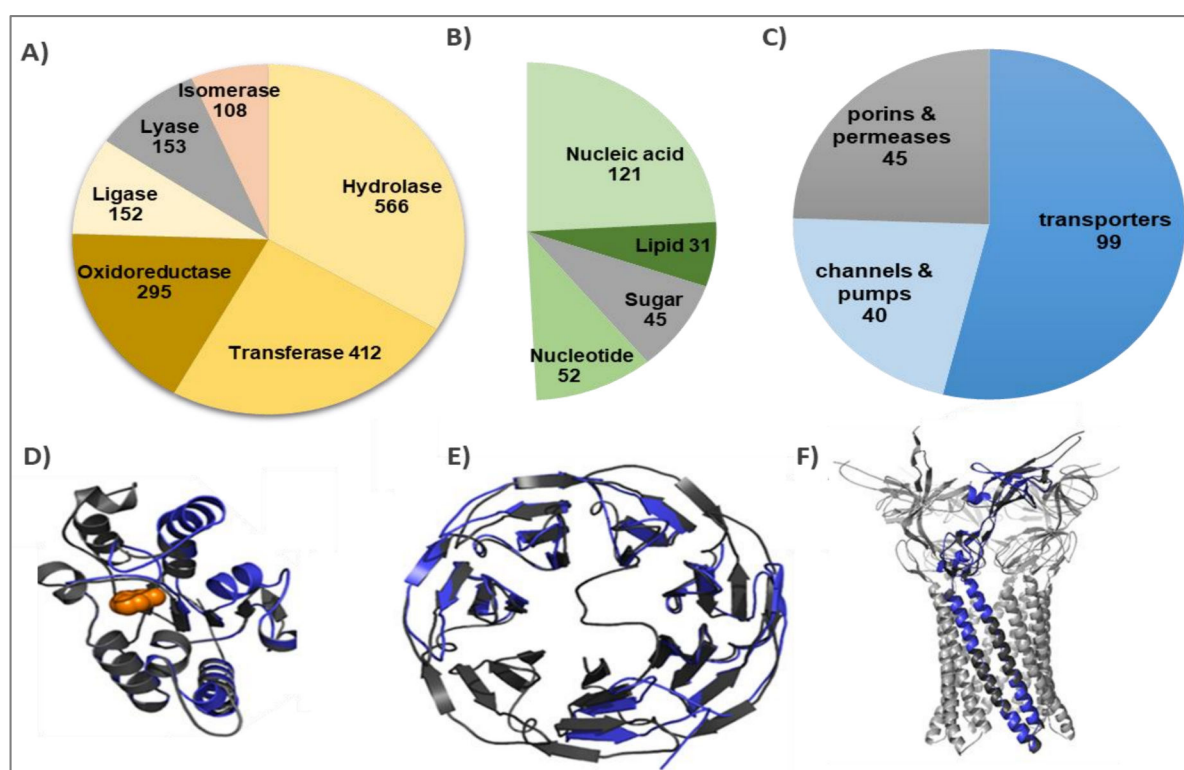


Fig. 8. Subclassification of predicted biochemical functions by Phyre2 homology modeling and superimposition of 3D structures of model and corresponding template for three selected PUFs. A) Distribution of enzyme classes among PUFs with putative enzyme function. **B)** Distribution of ligands in putative ligand-binding proteins. **C)** Distribution of PUFs with predicted transport functions. **D)** Superimposition of a homology model of putative uracil-DNA glycosylase PA4679 with the *T. thermophiles* UGD of [272] (PDB ID 1UI0, chain A, 98.5 % conf., 19 % seq. id., rmsd_{ca} = 0.62 Å, 61 % coverage, 0.9 % disall. res.). The uracil molecule bound to the active site groove of TtUGD is shown as an orange space model. **E)** Superimposition of a homology model of putative lectin PA5033 with the *A. aegerita* lectin [272] (PDB ID 4TQJ, chain A, 88.4 % conf., 19 % seq. id., 1.11 Å rmsd_{ca}, 92 % coverage, 1.3 % of disall. res.) **F)** Superimposition of a homology model of putative antibiotic efflux pump protein PA3304 with the *E. coli* MacA [272] (PDB ID 3FPP, chain A, 99 % conf., 23 % seq. id., 0.56 Å rmsd_{ca}, 81 % coverage, 1.9 % disall. res.). PA3304 is superimposed to one of six MacA protomers, which form a barrel-like functional protein. A homology model is indicated in blue and the corresponding template grey. rmsd_{ca} - root-mean-square deviation of atomic positions; disall. res. - residues found in disallowed regions of Ramachandran plot. The protein structures were visualized using the Pymol software (<http://www.pymol.org>). The list of genes is available in the PaPUF database at www.iet.uni-duesseldorf.de/arbeitsgruppen/bacterial-enzymology. Figures D-F are adopted from Babic & Kovacic (2021). [272]

Additional to analyzing biochemical functions, the potential of identifying PUFs with pathology and virulence-related biological functions was also explored. The text search of functional annotations of reliable templates using keywords that correspond to biological functions of known virulence factors and antibiotic-resistant genes (Table 5) revealed 94 PUFs with a putative role in signaling, 48 PUFs involved in drug resistance, and 33 putative toxins (Fig. 9).

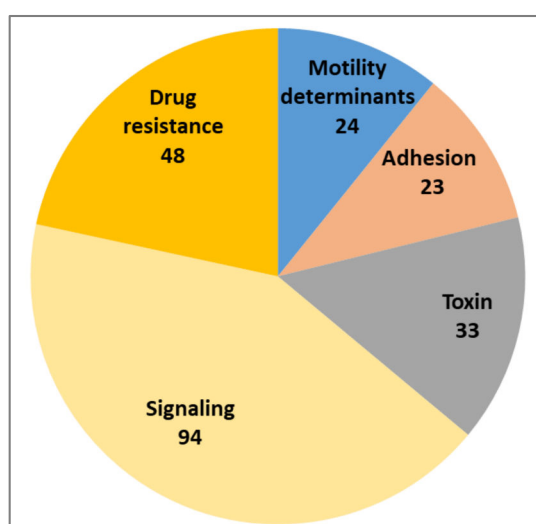


Fig. 9. Predicted virulence-related biological functions for *P. aeruginosa* proteins of unknown function. The numbers in pie diagram represent the number of PUFs for which at least one of ten reliable templates (confidence $\geq 75\%$ and the length of query aligned to template ≥ 100 AA) contained in the PDB titles corresponding keywords listed in Table S5. Total 2137 PUFs were analysed.

Table 5: Keywords used for textual mining of templates with virulence and antibiotic resistance-related functions.

Drug resistance	Signaling	Motility determinants
penicillin degrading enzyme	*chemotaxis*	*pili*
cephalosporin degrading enzyme	*homoserine lactone*	*twitching*
phenazine biosynthesis	*signaling protein*	*motility*
Adhesion	Toxin	*flagella*
alginate biosynthesis	*toxin*	*fimbrial*
adhesion	*hemagglutinin*	
	hemolysin	

* indicates any character

3.2. Novel expression vector pGUF enables functional protein expression in *E. coli* and *P. aeruginosa*

3.2.1. Novel expression plasmid pGUF is constructed by the Gibson cloning

For the generation of *P. aeruginosa* GUF expression plasmid library, a novel pGUF vector was constructed to enable inducible gene expression in *E. coli* and *P. aeruginosa*. The plasmid was assembled from three fragments: the fragment of pBBR1mcs-3 [276] backbone containing tetracycline resistance gene and pMB1 origin of replication, the fragment of *LacI* repressor gene with its promoter from pETb22b(+) vector (Novagen (Merck)) and the fragment containing modified *lacZα* gene (*lacZα**) from the pBBR1mcs-3 vector. The first two fragments were amplified by PCR using respective plasmids as templates, while the third fragment was designed *in silico* and synthesized by Eurofins Genomics (Louisville, KY, USA) (Fig. 10-A). All fragments contained terminal 20 bp homology regions required for assembling by the Gibson cloning [247].

The *lacZα** fragment was designed by modifying multiple cloning site (MCS) in *lacZα* gene from pBBR1mcs-3 and adding flanking regions upstream and downstream from the *lacZα** gene. The region of MCS containing the *Sma*I restriction site and T-7 promoter was deleted from the sequence of the *lacZα* gene (Fig. 10-B). To achieve this without disrupting the *LacZα* fragment's functionality, the MCS region within *lacZα* had to be precisely identified. Therefore, the alignment of protein sequences of *lacZα* and native *LacZ* protein from *E. coli* was performed (Fig. 10-B). The regions of *LacZα* that were conserved in native *LacZ* represent important functional segments, while the region in the middle (labeled in purple), which was not aligned, represents the MCS and could be shortened in *lacZα** (Fig. 10-B). As depicted in the plasmid map of assembled vector, the region upstream of the *lacZα** gene contained *lac* promoter with operator, T7-promoter, ribosome binding site (RBS), and *Afl* II restriction site for cloning GUFs (Fig. 10-C). The positioning of the *Afl* II restriction site before the start codon of the *lacZα** is important to prevent the fusion of amino acids from *LacZα* with a cloned gene. [277] The region downstream from the *lacZα** gene contained a newly inserted *Sma* I restriction site with 6xHis-tag and the stop codon, followed by the T7-terminator (Fig. 10-C).

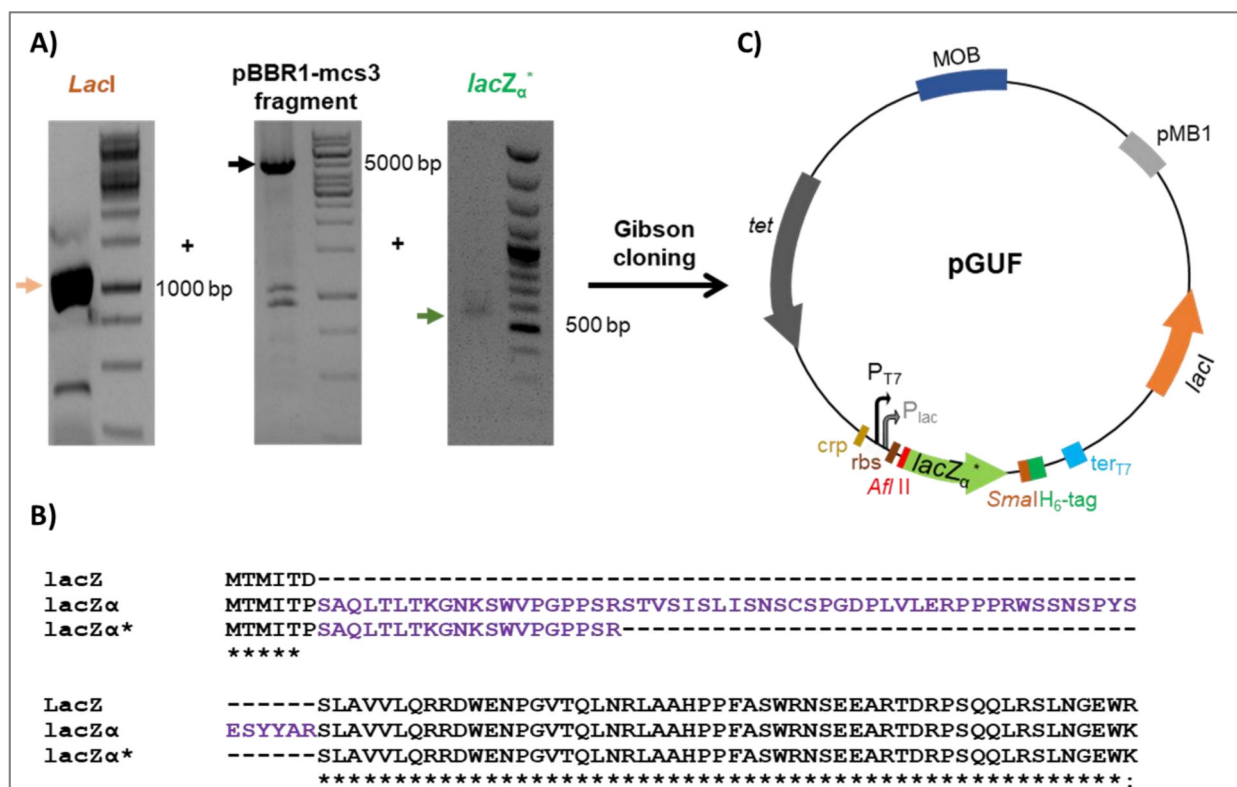


Fig. 10. Design and construction of pGUF vector. **A)** Agarose gel (1 % w/v) electrophoresis of PCR amplified fragments used to construct pGUF vector. Bands labeled with the arrows were cut from the gel, purified and mixed with Gibson master mix. **B)** Multiple amino acid sequence alignment between wild-type LacZ protein from *E. coli*, lacZ α protein from pBBR1mcs3 vector and lacZ α^* from pGUF vector was performed using Clustal W omega online tool. Purple amino acids belong to MCS. The protein sequence of LacZ was obtained from the EcoliWiki page, while the protein sequence of lacZ α was obtained by converting the DNA sequence from the pBBR1mcs-3 plasmid map using Expasy online tool. **C)** Plasmid map of pGUF vector. tet - tetracycline resistance gene; crp - cAMP receptor protein binding site; P_{lac}, P_{T7} - lac and T7 promoters; rbs - ribosome binding site; ter_{T7} - T7 terminator; lacI - lac repressor; pMB1 - ori; MOB - mobilization gene. For *in silico* design of lacZ α^* fragment, P_{T7} and ter_{T7} sequences were obtained from pETb22 vector and crp, P_{lac}, rbs sequences were obtained from the pBBR1mcs-3 vector.

Verification of the pGUF vector isolated from *E. coli* DH5 α was demonstrated by the pattern of fragments obtained after Afl II and Mlu I endonuclease hydrolysis and the successful PCR amplification of *lacI* using specific primers (Table S1) and pGUF as a template (Figs. 11-A and B). Finally, the pGUF sequence was confirmed by multiple Sanger sequencing reactions with respective primers (Table S1). The sequence alignments between obtained sequencing results and pGUF reference covered the complete length of the plasmid backbone with > 99.8 % of sequence identity (Table 6).

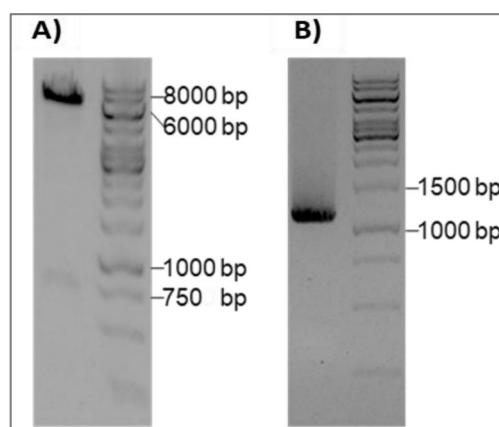


Fig. 11. Verification of pGUF sequence. A) AflII/MluI pGUF hydrolysis fragments (5595 bp and 763 bp) separated on 1 % (w/v) agarose gel. B) Agarose gel electrophoresis (1 %) of PCR-amplified *lacI* using *lacI* specific primers and pGUF as a template.

Table 6. Sequence alignments of pGUF backbone and walking primer Sanger sequencing results.

Sequencing primer	Range of pGUF aligned [bp]	Sequence identity [%]
P7_pGUF	1-877	99,9
P6_pGUF	556-1672	100
P5_pGUF	1590-2684	100
P13_pGUF	2459-3440	99,9
P10_pGUF	3259-4350	99,9
P9_pGUF	4127-5236	99,8
P1_pGUF	5196-6350	99,8
P8_pGUF	5956-6358	100

3.2.2. Validation of the cloning strategy and pGUF functionality

The pGUF-*guf* expression plasmid library was generated following the restriction/ligation cloning strategy illustrated in Fig. 12-A. The gene of interest was hydrolyzed with Afl II endonuclease, and the gene terminus, which was not hydrolyzed with Afl II, was phosphorylated. Such a gene was inserted into the pGUF vector after the excision of the *lacZa** gene with Afl II/Sma I endonucleases and dephosphorylation of the plasmid to prevent the formation of religates. For pGUF validation, *plaF* (*pa2949*) gene encoding esterase/phospholipase A PlaF [278] [279] was successfully cloned as demonstrated by restriction enzyme hydrolysis (Fig 12-B) and later confirmed by the Sanger sequencing.

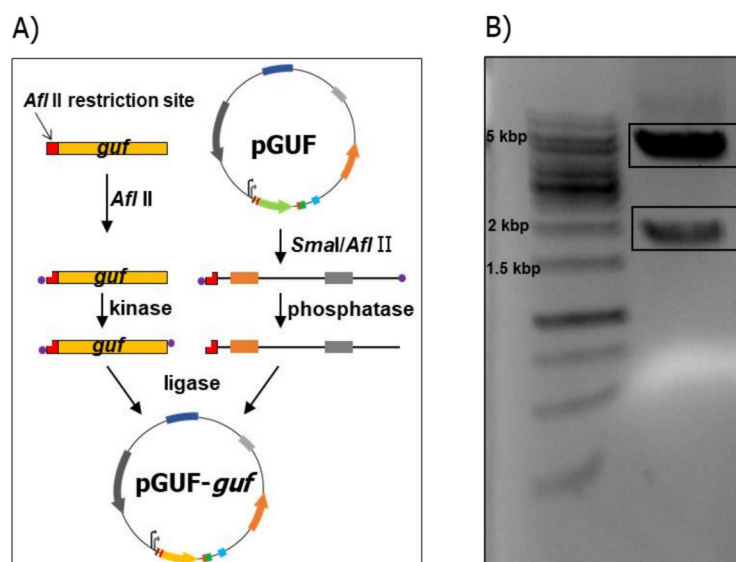


Fig. 12. Cloning strategy for the generation of pGUF constructs. A) Cloning strategy scheme. Purple dots represent the phosphate groups. **B)** Separation of Nco I/Nhe I hydrolysis fragments of pGUF-*plaf* (5272 bp and 1778 bp) on 1 % (w/v) agarose gel.

To verify the functionality of pGUF expression elements and the presence of a 6xHis tag on the C-terminus of a produced protein, recombinant PlaF was expressed in *E. coli* BL21(DE3) and *P. aeruginosa* PA01 strains using pGUF-*plaf* vector. Significantly higher esterase activity measured in *E. coli* BL21(DE3) and *P. aeruginosa* PA01 strains carrying pGUF-*plaf* vector compared to pGUF empty vector strains indicated the production of active phospholipase PlaF (Fig. 13-A and B). Furthermore, the presence of recombinant PlaFH₆ was confirmed by Western blot using an anti-C-6xHis antibody (Fig. 13-C). Finally, the pGUF lacZα* selectable marker functionality was validated on a white-blue selection medium (Fig. 13-D).

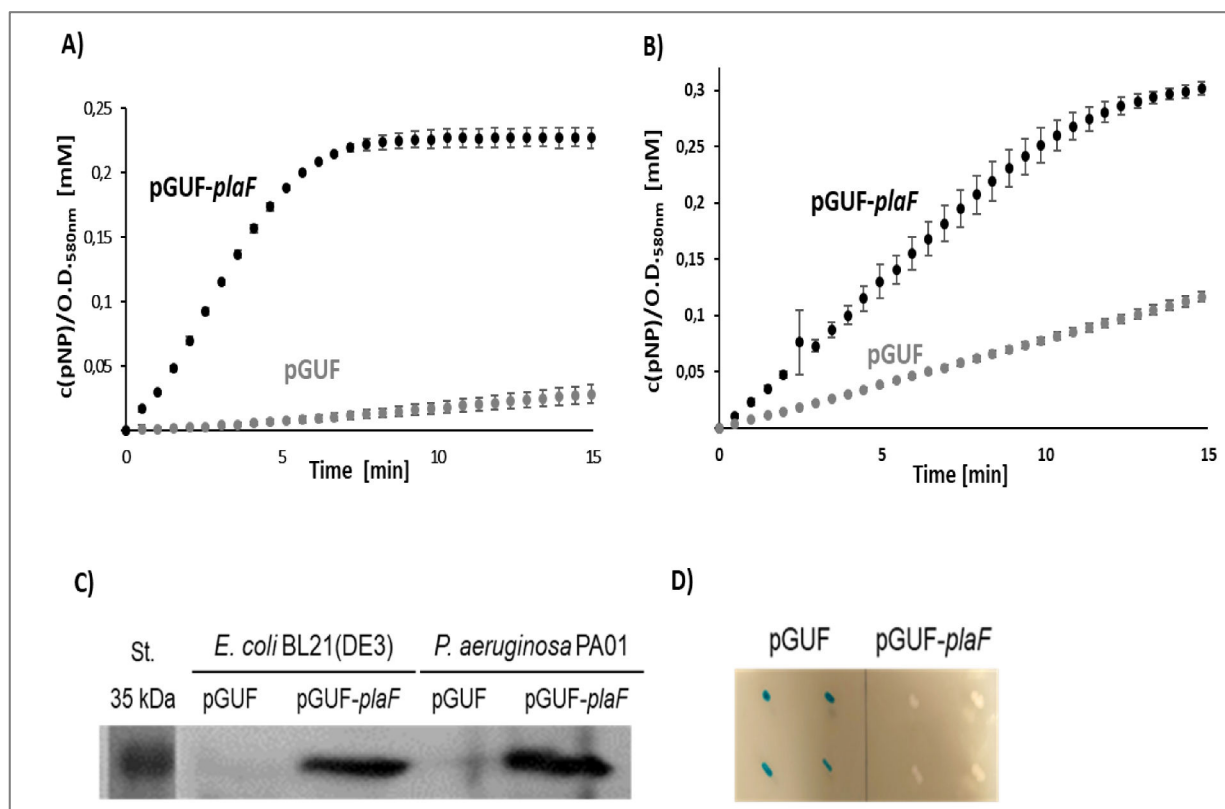


Fig. 13. Validation of pGUF-plaF expression vector in *E. coli* and *P. aeruginosa*. **A)** Esterase activity of recombinant PlaF expressed from pGUF-plaF vector in *E. coli* BL21(DE3). The esterase assay was performed using 25 μ l of cell lysates OD₅₈₀=2 and 175 μ l of 1 mM pNPB substrate in three technical replicates and the increase of A_{410nm} was recorded at 37 °C. **B)** Esterase activity of recombinant PlaF expressed from the pGUF-plaF vector in *P. aeruginosa* PA01. The esterase assay was performed using 25 μ l of cell lysates OD₅₈₀ = 2 and 175 μ l of 1 mM pNPB substrate in three technical replicates and the increase of A_{410nm} was recorded at 37 °C. **C)** Western blot signals of PlaFH6 (34.8 kDa) expression from the pGUF-plaF construct in *E. coli* BL21(DE3) and *P. aeruginosa* PA01 in 15 ml of AI medium 24 h at 37 °C. 15 μ l of cell lysates with OD₅₈₀ = 20 were loaded on 12 % gel and PlaFH₆ was detected with 1:5000 anti-C-6xHis HRP conjugate. **D)** *E. coli* DH5α colonies containing pGUF or pGUF-plaF vector grown on white-blue selection media.

The applied cloning strategy resulted in the generation of the pGUF-plaF expression plasmid, which showed functionality for recombinant protein expression and blue/white selection.

3.3. Development of medium-throughput cloning pipeline and generation of the expression plasmid library

3.3.1. Optimization of medium-throughput cloning

After the cloning strategy was verified with PlaF, the success of every cloning step was tested and optimized under a high-throughput setup in 96-well PCR plates.

Various conditions were tested using four genes of different lengths and GC contents (PA0053, 255 bp, 59 % GC; PA0308, 1020 bp, 69.5 % GC; PA2632, 621 bp, 68 % GC; PA2540, 1761 bp, 69 % GC) to improve the specificity and yield of TD-PCR amplification of GUFs. These conditions included the use of different a) PCR additives (DMSO, betaine, and BSA), b) amounts of template (10, 15, and 20 ng of genomic DNA per reaction), c) Pfu and Phusion DNA polymerases, d) the length of primers (18, 20 and 22 bp) and e) the primer melting temperatures (T_m) calculated with Clone Manager and New England Biolab. Generally, higher specificity was achieved using Biolab calculator T_m values and 1.5 M betaine compared to 5 % (v/v) DMSO, while the addition of BSA enhanced the effect of both additives (K. Wolf 2019). In addition, a higher yield was observed with 20 ng of template and Phusion compared to Pfu DNA polymerase (data not shown). Finally, the better performance of the applied optimization protocol was demonstrated by performing PCR under modified and starting (standard) conditions for each of the four tested genes. The results showed increased yield and specificity for all genes (Fig. 14-A).

To improve the efficiency of the following steps in cloning, similar to cloning DNA fragments amplified by Taq DNA polymerase [245], after PCR reaction, detachment of Phusion polymerase from amplified genes was achieved by trypsin proteolysis. The absence of PCR product (PA2632) in the reaction mixture, which was incubated with trypsin before running the cycling program, showed that the applied amount of trypsin and proteolysis conditions led to Phusion inactivation (Fig 14-B). Subsequently, trypsin was inactivated entirely by incubation at 99 °C for 10 min, as confirmed by the absence of residual proteolytic activity measured with N α -benzoyl-L-arginine 4-nitroanilide substrate (Fig 14-C).

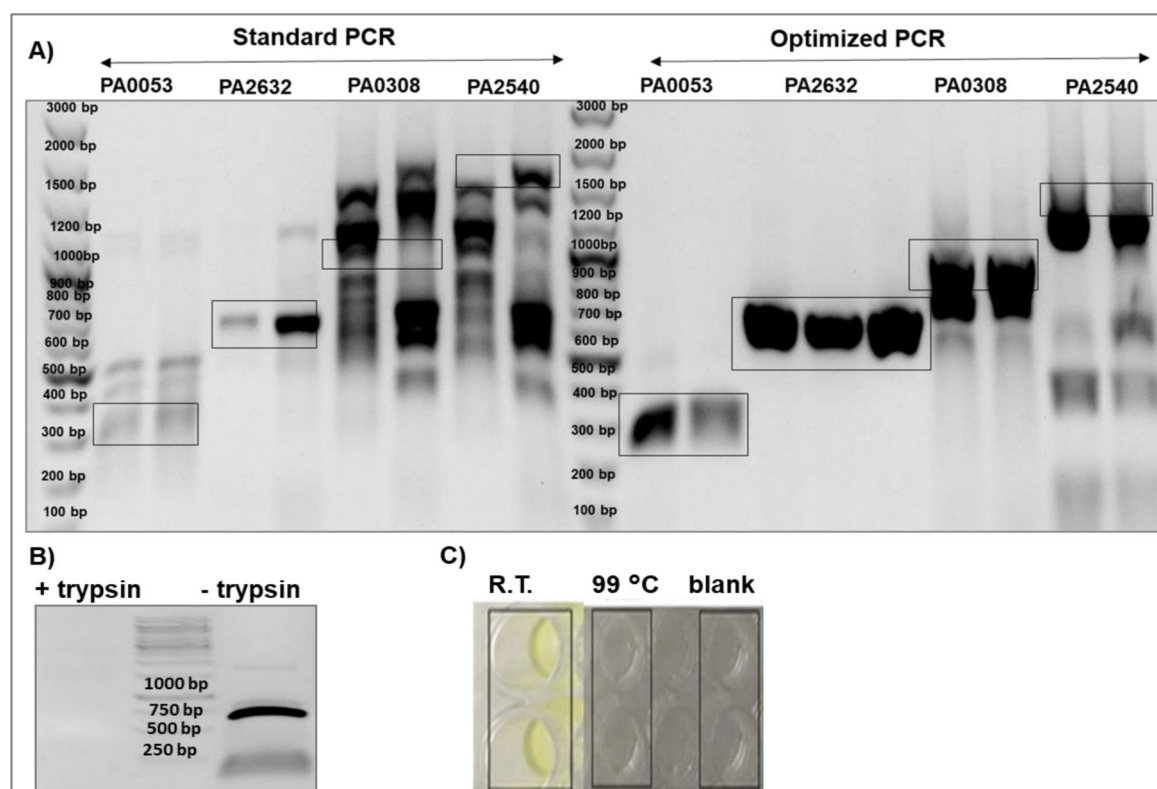


Fig. 14. Optimization of TD-PCR conditions for GUFs amplification in 96-well plates. **A)** Optimized PCR was performed by applying a touch-down cycling program and 1.5 M betaine and 5 $\mu\text{g}/\mu\text{L}$ BSA as additives. The annealing step in the cycling program consisted of 15 cycles with 1 $^{\circ}\text{C}$ temperature decrement per cycle starting from the highest annealing temperature among 4 genes plus 2 $^{\circ}\text{C}$ and 18 cycles during which the average annealing temperature minus 2 $^{\circ}\text{C}$ was set constant. In standard PCR, the average annealing temperature of primer pairs for 4 genes was kept constant during all 33 cycles of the annealing step and the additives were omitted from the PCR mixture. In both experiments, 20 bp long primers and 25 ng of gDNA were used with Phusion DNA polymerase. **B)** 1 % (w/v) agarose gel electrophoresis of PCR amplification product of PA2632 gene (627 bp) after pre-incubation with 1 μg of trypsin 40 min at R.T. and without previous addition of trypsin. **C)** Trypsin activity after the incubation of 20 μL PCR mixture containing 0.02 $\mu\text{g}/\mu\text{L}$ trypsin with 175 μL of α -benzoyl-L-arginine 4-nitroanilide (1 mM in 100 mM Tris buffer pH 8, 1 mM CaCl_2 , 1 mM ZnCl_2 with 20 % (v/v) DMSO) substrate. PCR mixture was 10 min incubated at R.T. or 99 $^{\circ}\text{C}$ before the assay.

The influence of different ligation conditions (16 h at 16 $^{\circ}\text{C}$ or 2 h at 25 $^{\circ}\text{C}$) on the cloning success was estimated to optimize the ligation step. Therefore, ten randomly chosen colonies from two agar plates, obtained after transforming ligation mixtures of the PA2632 gene, which differed only in ligation conditions, were analyzed. As a result, a higher ratio of positive clones was observed when ligation was performed for 16 h at 16 $^{\circ}\text{C}$ (90 % of positive clones) in comparison to ligation during 2 h at 25 $^{\circ}\text{C}$ (60 % of positive clones) as judged by colony PCR (data not shown).

Finally, the chemical transformation of *E. coli* DH5 α in 96-well MTP was optimized to the number of competent cells, growth medium (SOC and LB), and shaking speed. The highest transformation efficiency tested with pGUF (7.8×10^3 CFU/ μ g (DNA)) was achieved using 30 μ l of 2-fold concentrated competent cells, 100 μ l SOC medium, and agitation at 1000 rpm.

3.3.2. Generation of the expression plasmid library

The scheme of optimized medium-throughput cloning pipeline performed in 96-well PCR plates is depicted in Fig. 15. After the TD-PCR amplification, GUFs were purified using silica-filled 96-well plates and eluted in water to avoid the potential inhibition of enzymes used in the following cloning steps by some components of the PCR reaction mixture. Hence, T4 polynucleotide kinase shows 50 % and 75 % activity decrease, respectively, in the presence of 7 mM phosphate or ammonium salts, as reported by the manufacturer New England Biolabs (Massachusetts, USA). Further purification steps between endonuclease hydrolysis, phosphorylation, and ligation reactions were avoided using the universal cut-smart buffer (New England Biolabs, Massachusetts, USA), ensuring the maximal activity of Afl II endonuclease, T4 polynucleotide kinase, and T4 DNA ligase. Moreover, the hydrolysis and phosphorylation of GUFs were performed simultaneously since the corresponding enzymes have the same optimal temperature. The control of each step in cloning is essential; therefore, positive controls for restriction digestion - *pa2037* gene containing Afl II restriction site, ligation - linear pGUF hydrolyzed with Sma I endonuclease, and transformation - pGUF plasmid, were used. Using a developed cloning pipeline, 7-10 days, on average, were sufficient to complete the cloning of two 96-well plates, followed by sequencing and plasmids isolation.

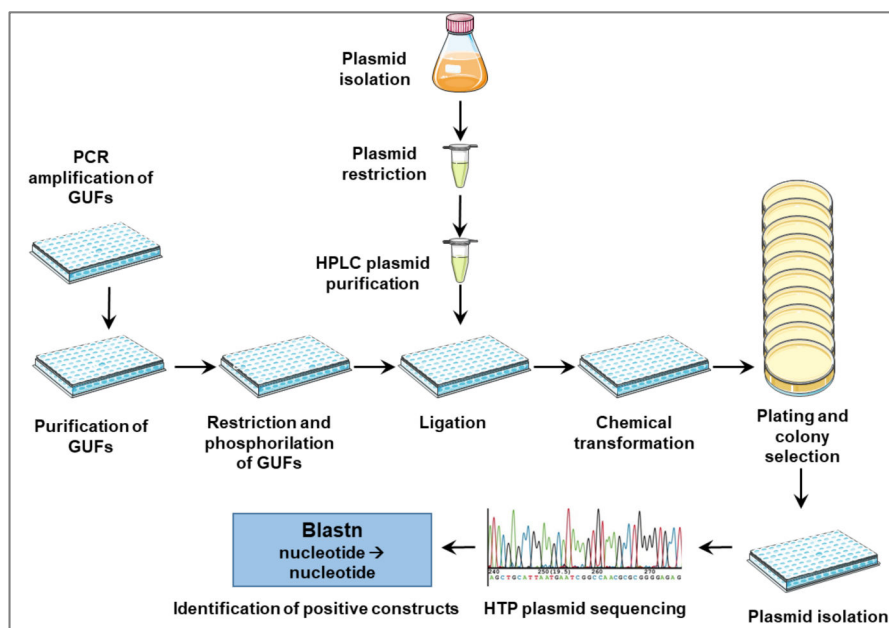


Fig. 15. Scheme of cloning pipeline in 96-well plates. For details, see the text in chapter 3.2.1. Plasmid isolation and Sanger sequencing were performed by LGC Genomics (Berlin, Germany).

3.3.3. Preparing linear pGUF vector for the library construction

To obtain a sufficient amount of high-quality linearized pGUF vector, plasmid isolation, endonuclease hydrolysis, and purification was scaled up. The amount of 0.63 mg of plasmid was isolated from 1 L of *E. coli* DH5 α culture using silica-columns from NucleoBond™ Xtra Midi kit (Macherey-Nagel, Düren) and subsequently precipitated with isopropanol. The total amount of the plasmid was hydrolyzed by Afl II and SmaI endonucleases, followed by dephosphorylation, which was included to minimize the plasmid backbone religation. Dephosphorylation was repeated until the number of colonies obtained after ligation of linearized pGUF (100 ng) was less than 5 per plate. To obtain a linear pGUF fragment (6104 bp), free from the small DNA fragment (254 bp) and buffer components, anion exchange chromatography on a column with an ÄCTA system was performed.

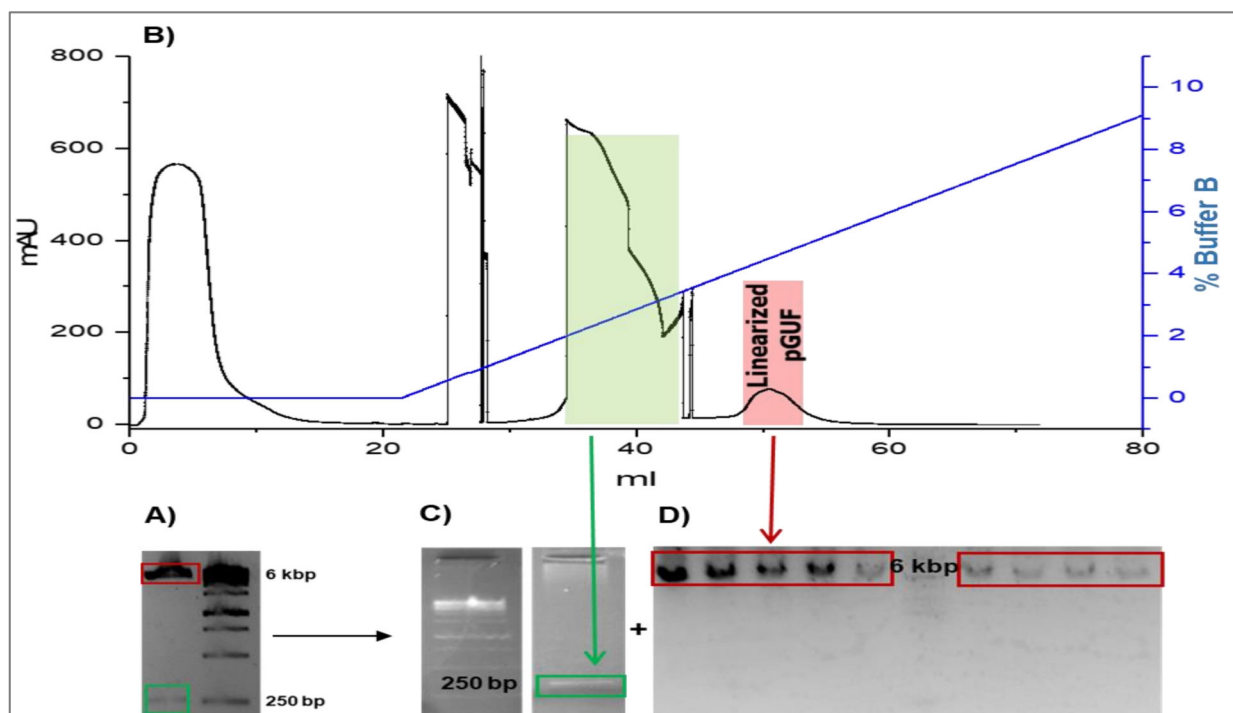


Fig. 16. Large-scale purification of linear pGUF plasmid by Mono Q™ anion exchange chromatography. **A)** Analysis of Afl II/ Sma I hydrolysis fragments of pGUF on 2 % (w/v) agarose electrophoresis gel before the chromatographic purification. **B)** Chromatogram obtained by monitoring A_{254nm} after loading 3 ml of Afl II/ Sma I digested plasmid on Mono Q™ 5/50 GL column (2 ml dead volume). Elution of DNA fragments was achieved by applying 64 ml of NaCl gradient from 700 mM NaCl (0 % buffer B) to 900 mM NaCl (10 % buffer B) at 0.15 ml/min. A gas bubble in the system covers the signal eluted with small concentration of NaCl (green). **C)** Electrophoresis of elution fraction on 2 % agarose gel. One fraction from the signal indicated green showed an isolated 254 bp pGUF hydrolysis fragment. **D)** Electrophoresis (1 % agarose gel) of elution fractions corresponding to signal indicated red showed linearized pGUF hydrolysis fragment. The purification was performed using ÄKTA pure (GE Healthcare, Solingen, Germany).

As shown in Fig. 16, a linearized pGUF vector (6104 bp fragment) was successfully separated from a small lacZ α^* -containing fragment (254 bp) and enzymes from reaction mixtures (first signal in the chromatogram) by anion exchange chromatographic procedure. [246] The fractions corresponding to the 6104 bp DNA fragment signal were collected, precipitated by isopropanol, and suspended in H₂O. This way, 100 μ g of pure linearized pGUF was obtained, sufficient for 1000 ligation reactions.

3.3.4. Medium-throughput TD-PCR amplification of GUFs

The primers for 798 genes (Table S1) were arranged in nine 96-well plates to group genes encoding proteins with similar putative biochemical functions and annealing temperatures.

The average annealing temperature (obtained from the Biolab calculator) and gene length were used for each plate to set the touch-down PCR program parameters. After PCR Phusion DNA polymerase was inactivated, and the specificity and yield of PCR in each plate were estimated by the agarose gel electrophoresis of up to 20 randomly chosen samples from each plate (Fig. 17).

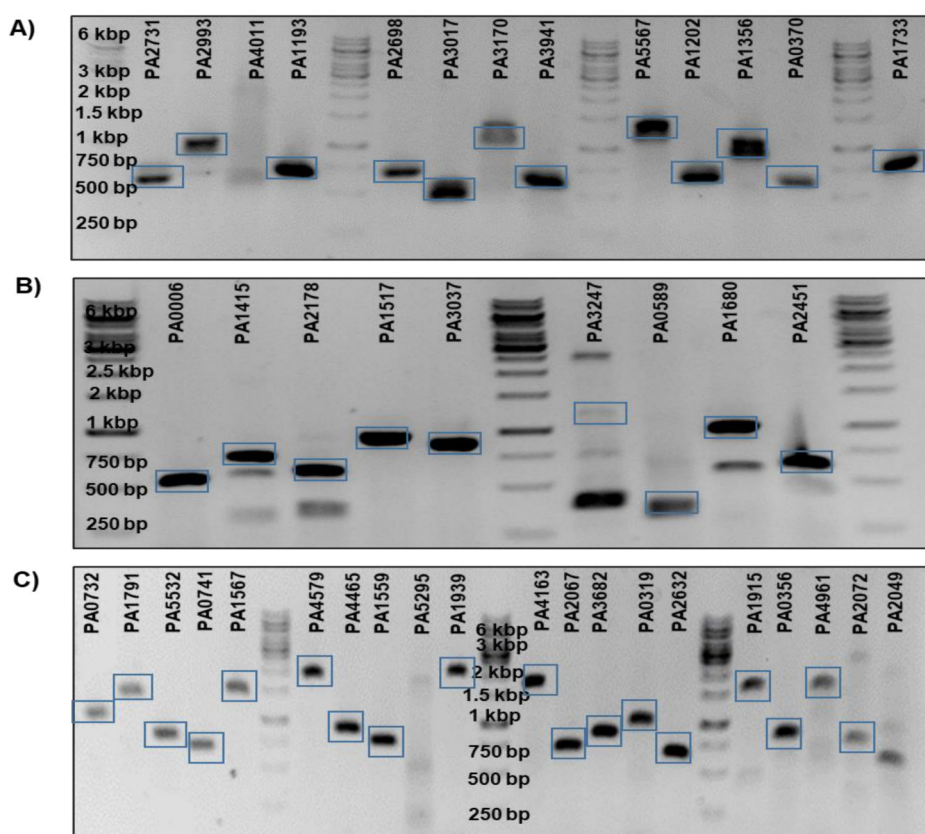


Fig. 17. Agarose gel electrophoresis of GUFs amplified by optimized TD-PCR in 96-well PCR plate. After TD-PCR, 5 μ l of randomly selected samples from plate3 **(A)** plate 5 **(B)** plates 8 and 9 **(C)** were analyzed by electrophoresis on 1 % (w/v) agarose gel. The signals at the expected gene sizes are labeled with the squares. The agarose gel electrophoresis of amplified genes from plates 4 and 7 are shown by R. Oben (HHU Düsseldorf, B.Sc. Thesis, 2019) and D. Lorenz (HHU Düsseldorf, B.Sc. Thesis, 2020), respectively. The lengths of genes are listed in Table S1.

Based on the agarose gel electrophoretic analysis of 42 TD-PCR amplified genes, the success rate of the first step of high-throughput cloning pipeline was estimated to be 93 % (correct bend present) with 80 % specificity (only correct bend present).

3.3.5. Identification of positive pGUF constructs

After chemical transformation and inoculation on LB agar Petri dishes, single colonies were selected to inoculate a 96-well plate containing LB agar medium. These plates were submitted to the LGC Genomics for plasmid isolation and Sanger sequencing. The sequencing results were analyzed in batch sequence alignments against the *P. aeruginosa* genome. The additional colonies were analyzed by colony PCR or restriction digestion of isolated plasmids to increase the chance of finding the positive clones for the genes whose first colony did not contain a positive construct (Fig. 18).

The following criteria were set and analyzed automatically with Microsoft Excel to identify the positive constructs after BLASTN sequence alignments of sequencing results against *P. aeruginosa* genome:

- The difference between the corresponding starting chromosomal coordinate of the expected gene and the starting chromosomal coordinate of the aligned region must be 0 for forward sequencing or 3 nucleotides (because the stop codon is removed from the gene sequence) for reverse sequencing. This confirms that a) the expected gene exactly matches the aligned gene in the genome, b) that the alignment started from the start or the end of the gene, in case of forward or reverse sequencing, respectively, and c) that the gene is inserted into a plasmid in the correct orientation in respect to the promoters.
- Since the reliable sequence of Sanger sequencing result has a length usually between 800 and 1000 nucleotides, the alignment coverages (the ratio of alignment length to reference and the gene length) were separately considered for genes with different lengths. The genes < 1000 bp should have a minimum of 80 % of alignment coverage, while the alignment length for the genes ≥ 1000 bp must be ≥ 800 bp. The genes ≥ 1000 bp whose alignment coverage in forward sequencing was lower than 99 % were additionally sequenced from the opposite side (Table S3).
- The mismatches and gaps (insertions and deletions) that were observed in the first and last 50-100 bp of the alignment in many cases represented the unreliable signal in the sequencing chromatogram (Fig. 19). Therefore, genes < 1000 bp containing ≤ 5 mismatches and/or gaps and the genes ≥ 1000 bp with ≤ 9 mismatches and/or gaps were considered positive.

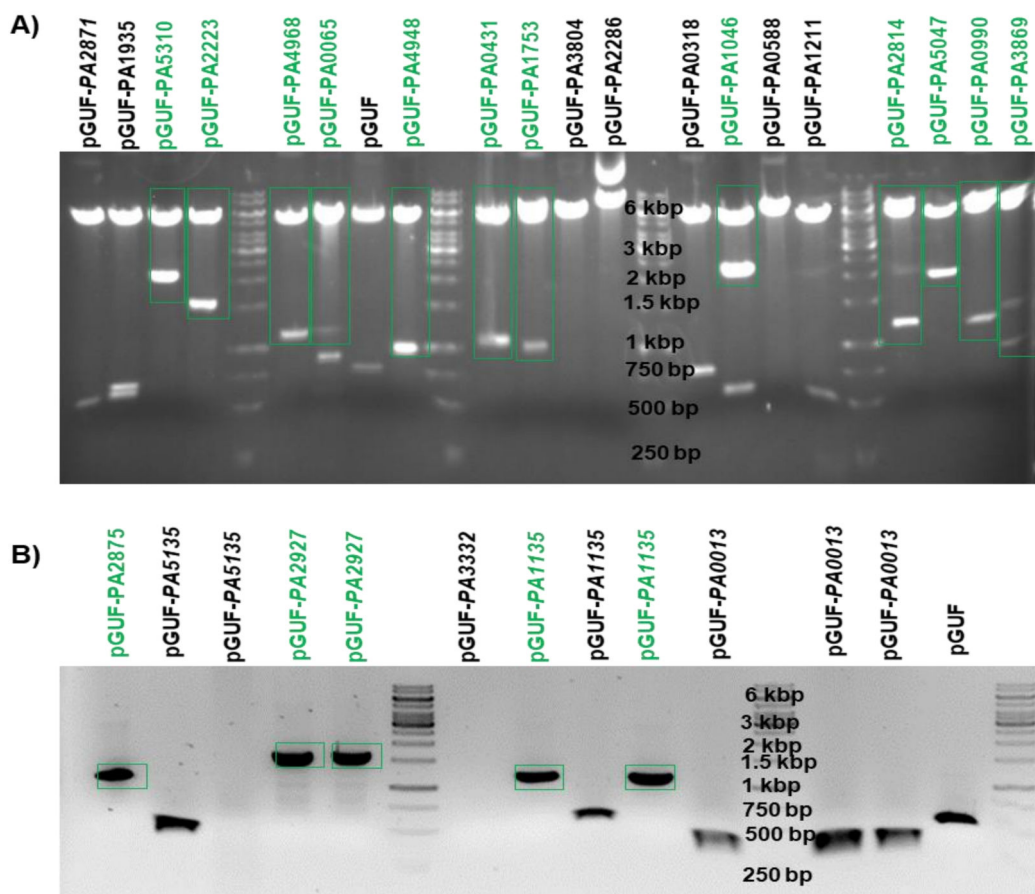


Fig. 18. Screening of positive clones. (A) Restriction digestion analysis of Afl II/ Mlu I hydrolysis fragments of isolated plasmids separated on 1 % (w/v) agarose electrophoresis gel. The constructs showing expected DNA fragments (5595 bp fragment and a fragment containing the corresponding gene with an additional 511 bp of plasmid backbone) are colored green. The positive hydrolysis control was pGUF, which revealed 5595 bp and 763 bp fragments. **(B)** Colony PCR products on 1 % (w/v) agarose electrophoresis gel. Colonies showing expected PCR product size (gene length and additional 278 bp of plasmid backbone) are colored green. Positive PCR control was a colony with pGUF showing an expected 545 bp fragment containing *lacZa** gene. The lengths of tested genes are listed in Table S1.

The majority of the mutations in terminal parts of sequencing results appeared due to partial or complete overlapping of adjacent signals in the chromatogram. In Fig. 19-A, the adenine (A) insertion at position 1102 in the sequencing result of gene *pa4604* was because the signal of adjacent A (1103) was very broad. In contrast, in Fig. 19-B the signal of A at position 994 was not detected in the sequencing result of the *pa3734* gene, resulting in misleading deletion. In Fig. 19-C the chromatogram signal of G at position 946 was not identified due to overlapping with adjacent A (947), which resulted in a false G→A mismatch.

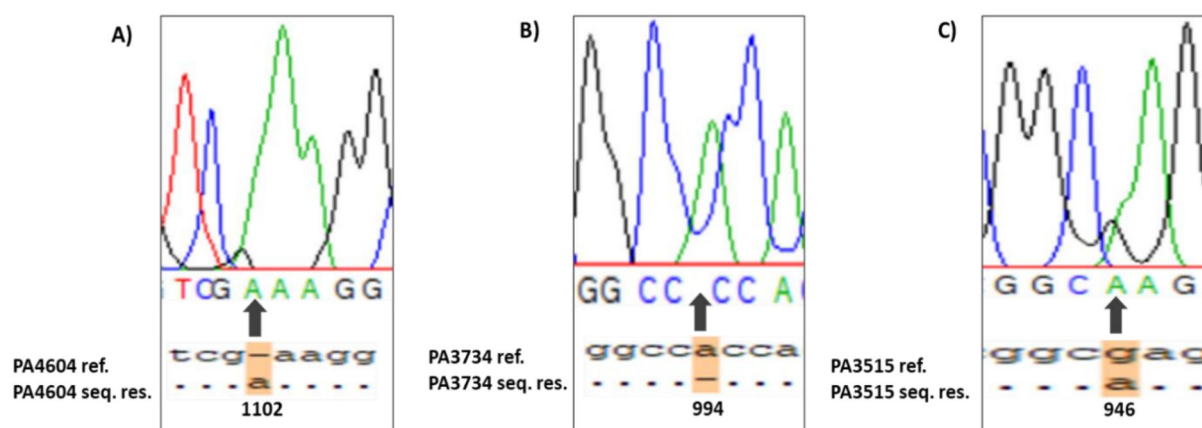


Figure 19. Sequencing results indicate that mismatches and gaps often arose as the consequence of unreliable signals in the sequencing chromatogram. A) The sequence alignment of the *pa4604* gene (reference) and the sequencing result (seq. res.) around a gap at position 1102. The sequencing chromatogram shows the absence of adenosine (A) at position 1102. **B)** The sequence alignment between the *pa3734* gene (reference) and respective sequencing results around the gap at position 994. The sequencing chromatogram shows adenosine (A) at position 994. **C)** The sequence alignment between the *pa3515* gene (reference) and the respective sequencing result around position 946. The sequencing chromatogram shows guanosine (G) at position 946.

Following the above-described criteria, the sequencing results of plasmids isolated after cloning 798 genes were automatically analyzed, which resulted in the identification of positive constructs for 606 genes sequenced with a forward primer (Table S1), and the expression plasmid library data are shown in Table S2. Among them, 95 genes larger than 1000 bp positive were sequenced from the opposite direction using a reverse primer (Table S1), and the results are shown in Table S3.

Table 7. Summarized sequencing data for pGUF-*guf* expression plasmids containing genes < 1000 bp.

Accepted genes < 1000 bp	443
Average gene length	642 bp
Complete genes	425 (96 %)
Perfect match	380 (86 %)
Mismatches ≤ 2; gaps = 0	36 (8 %)
Mismatches = 0; gaps ≤ 2	16 (4 %)
Mismatches ≤ 5; gaps ≤ 2	13 (3 %)
Mistake rate	0.04 %

Accepted genes were those used in further expression and enzyme screening experiments. Complete genes are those which were full-length sequenced. The perfect matches were genes that had no mistakes in the sequenced region. The mistake rate represents the total number of mismatches and gaps relative to the number of nucleotides in alignments of all genes. In brackets are percentages related to accepted genes.

Table 8. Summarized sequencing data for pGUF-*guf* expression plasmids containing genes ≥ 1000 bp.

Accepted genes ≥ 1000 bp	163
Average gene length	1343 bp
Complete genes	105 (64 %)
Perfect match	43 (26 %)
Mismatches ≤ 8 ; gaps = 0	43 (26 %)
Mismatches = 0; gaps ≤ 5	15 (9 %)
Mismatches ≤ 9 ; gaps ≤ 5	64 (38 %)
Mistake rate	0.3 %

Accepted genes were those used in further expression and enzyme screening experiments. Complete genes are those which were full-length sequenced. The perfect matches were genes that had no mistakes in the sequenced region. The mistake rate represents the total number of mismatches and gaps relative to the number of nucleotides in alignments of all genes. In brackets are percentages related to accepted genes.

Accepted genes < 1000 bp had a minimum of 80 % of alignment coverage and ≤ 5 mismatches and/or gaps. Among them, complete genes had ≥ 99 % alignment coverage, while genes with a perfect match to reference had 100 % of sequence identity (no mismatches and gaps). Accepted genes ≥ 1000 bp had a minimum alignment length of 800 bp and ≤ 9 mismatches and/or gaps. Among them, complete genes included those which had ≥ 99 % of alignment coverage (23 genes) and the genes whose sum of alignment lengths with forward and reverse primer was higher or equal to the expected gene size (82 genes).

The pGUF-*guf* expression plasmid library comprises 606 constructs, including 429 putative hydrolases. Among 606 GUFs, 530 had the whole gene length sequenced (complete genes), and 423 of them had a perfect alignment (100 % sequence identity) to the reference gene. As expected, the success of cloning (and/or sequencing) of genes longer than 1000 bp was lower than for the shorter genes, which can be seen in lower percentages of completed genes and perfect matches and higher mistake rates (Tables 7 and 8). The pGUF expression plasmid library, comprising of 606 GUFs in total, includes 429 putative hydrolases, which were used in expression and enzyme screening experiments.

3.4. Screening of hydrolase activities

3.4.1. Expression of putative hydrolases

The 429 pGUF-*guf* constructs containing genes encoded putative hydrolases (listed in the PaPUF database) were organized in six 96-well MTPs (HY I – HY VI) for protein expression. The corresponding PUFs were heterologously expressed in DWPs using T7 RNA polymerase expression systems of *E. coli* BL21(DE3) and *E. coli* C43(DE3) induced separately with isopropyl β -D-1-thiogalactopyranoside (IPTG) and lactose (“auto-induction” medium). The expected sizes of protein bands of randomly chosen PUFs detected by Western blot indicate successful protein expression (Fig. 20).

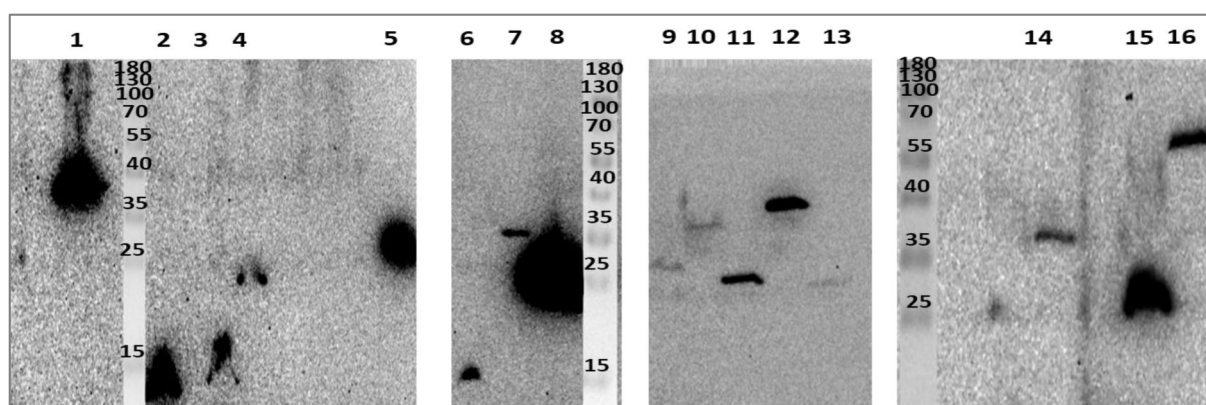


Fig. 20. Western blot analysis of recombinant PUFs expression in *E. coli* BL21(DE3). *E. coli* BL21(DE3) and *E. coli* C43(DE3) strains carrying pGUF-*guf* expression vectors were cultivated in 1 ml of AI medium at 37 °C during 24 h in DWPs. The proteins from 12 μ l of combined cell lysates with OD₅₈₀=40 were separated by SDS-PAGE on 14 % (v/v) gel and detected with 1:5000 anti-C-6xHis HRP conjugate antibody after transfer to PVDF membrane by Western blot. The sample numbers represent: 1 - PA3515 (39.8 kDa), 2 - PA3674 (14.4 kDa), 3 - PA5371 (14.6 kDa), 4 - PA0335 (24.4 kDa), 5 - PA1813 (28.9 kDa), 6 - PA5130 (15.1 kDa), 7 - PA5343 (30.8 kDa), 8 - PA5391 (23.5 kDa), 9 - PA1195 (28.5 kDa), 10 - PA1293 (38.8 kDa), 11 - PA1638 (33 kDa), 12 - PA1730 (52.6 kDa), 13 - PA1784 (26.3 kDa), 14 - PA3070 (36.1 kDa), 15 - PA2764 (24.5 kDa), 16 - PA2448 (62.8 kDa).

Since several hundreds of proteins were expressed, protein dot-blot, as a less time and material-consuming method, was used to test the success of protein expression. Dot-blot signals of produced His-tagged proteins were normalized to the total protein amount, determined by staining a dot-blot membrane with Ponceau S. This step was introduced to estimate the amount of the sample loaded on the membrane. The integration density of each signal in dot-blot and Ponceau S staining was determined using the ImageJ program. Samples with higher signal intensity than empty vector control were considered to contain expressed recombinant proteins.

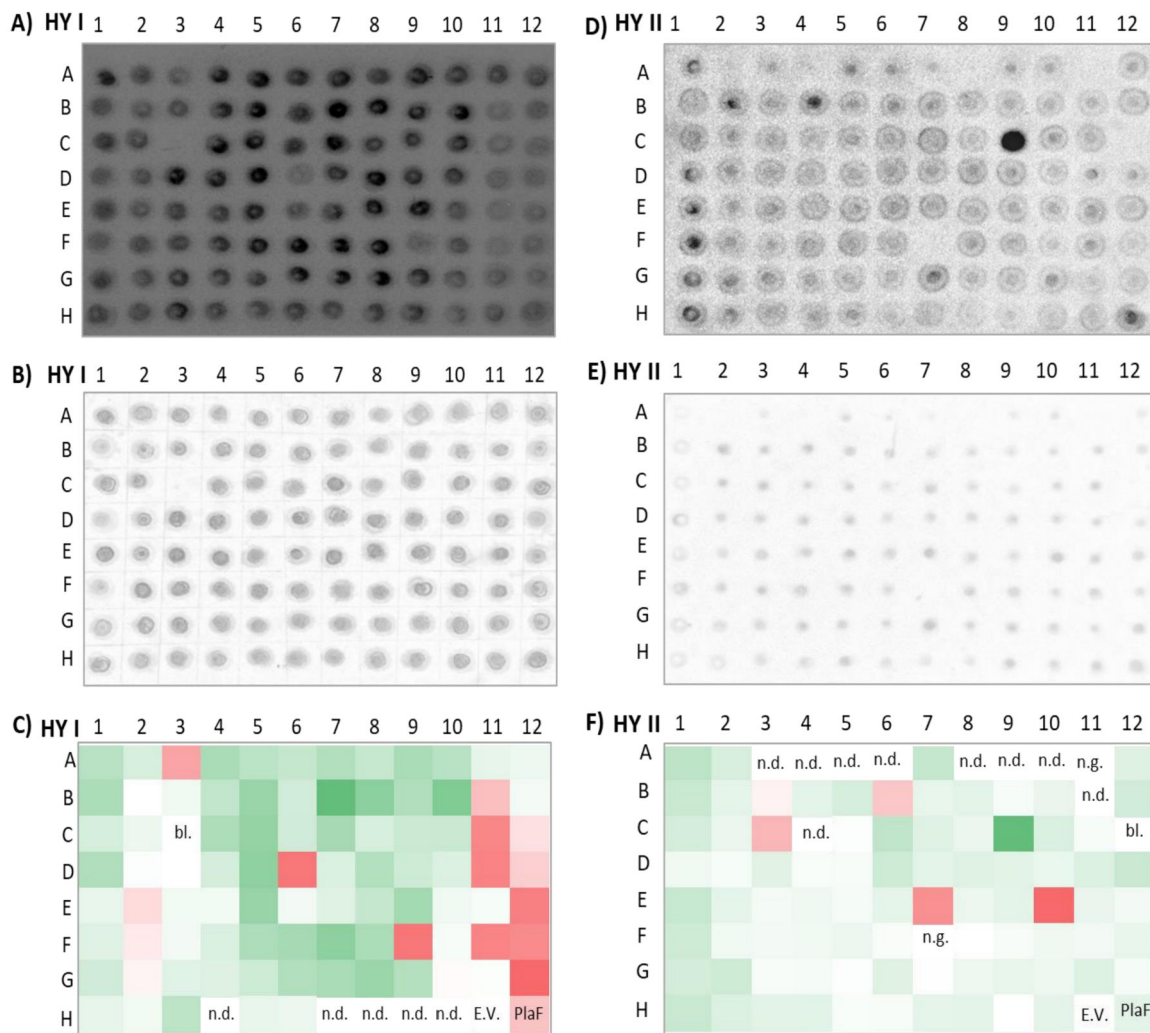


Fig. 21. Dot-blot analysis of expression of PUFs from plates HY I (A-C) and HY II (D-F). Combined *E. coli* BL21(DE3) and *E. coli* C43(DE3) cell lysates (4 μ l) with OD₅₈₀ = 5 were loaded on the nitrocellulose membrane, followed by detection of expressed PUFs using anti-C-6xHis HRP conjugate antibody (**A, D**). Total protein amount was detected after staining with 0.1 % PonceuS dye (**B, E**). Fingerprint showing integration densities of chemiluminescent dot-blot signals normalized to total protein amount. (**C, F**) The green and red colors indicate values higher and lower than the value of the pGUF empty vector (E.V., white-colored), respectively. The intensity of the color is proportional to normalized values. No growth control or blank (bl.) contained only medium; PlaF - phospholipase PlaF expressed from pGUF-*plaF* vector was used as a positive control, n.d. - not determined, n.g. - no growth.

Integration density analysis of normalized chemiluminescent dot-blot signals for PUFs from plate HY I (Fig. 21. A-C) revealed that 74 out of 89 *E. coli* pGUF-*guf* cell lysates have higher signal intensity than cell lysate of empty vector control. These results indicate that 85.4 % of analyzed proteins were expressed. For the plate HY II (Fig. 21. D-F), 78 of 83 *E. coli* pGUF-*guf* cell lysates were positive, indicating 94 % expression rate.

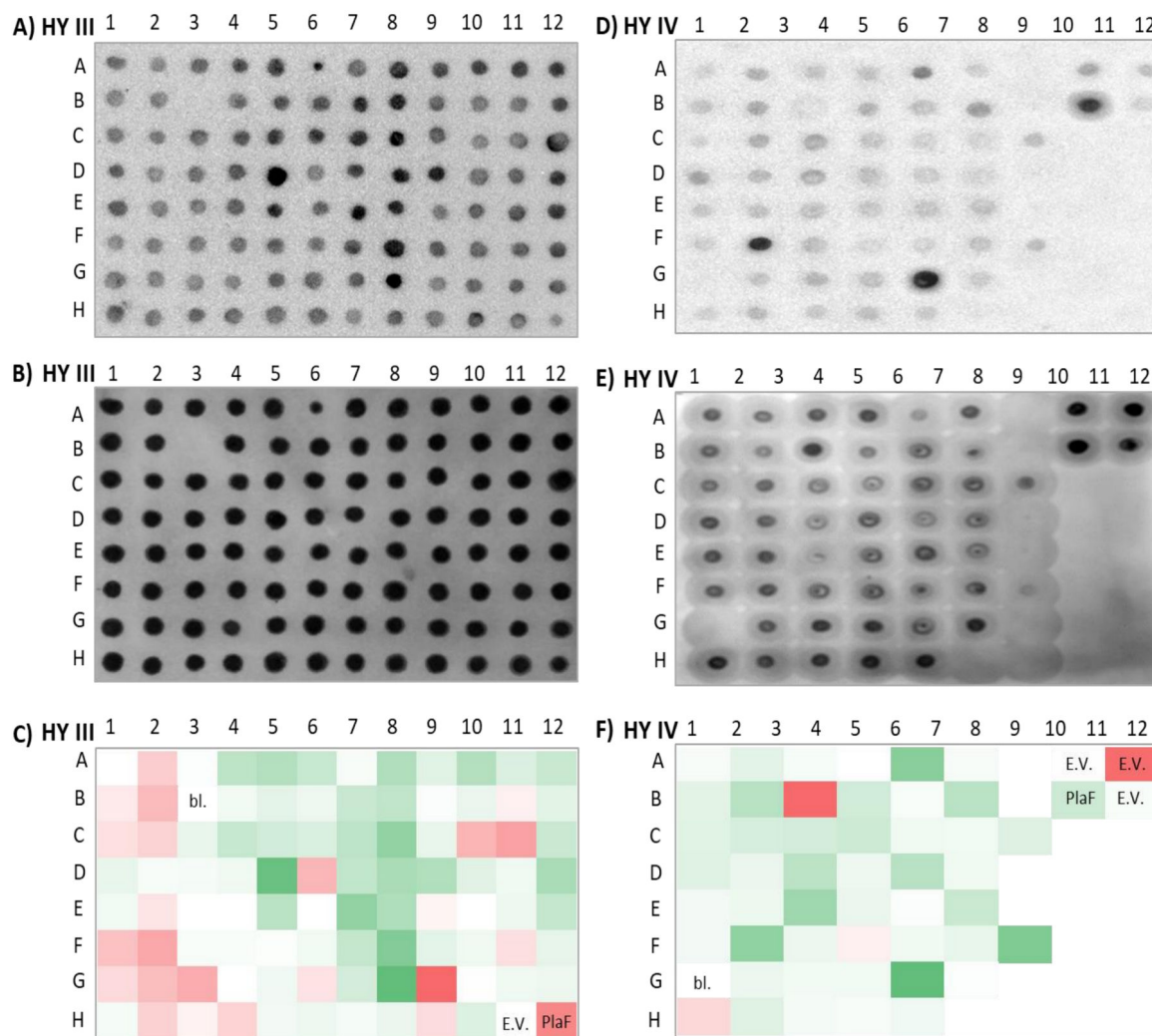


Fig. 22. Dot-blot analysis of PUFs expression in plates HY III (A-C) and HY IV (D-F). Combined *E. coli* BL21(DE3) and *E. coli* C43(DE3) cell lysates (4 μ l) with OD₅₈₀ = 5 were loaded on the nitrocellulose membrane, followed by detection of expressed PUFs using anti-C-6xHis HRP conjugate antibody (**A, D**). Total protein amount was detected after staining with 0.1 % PonceuS dye (**B, E**). Fingerprint showing integration densities of chemiluminescent dot-blot signals normalized to total protein amount. (**C, F**) The green and red colors indicate values higher and lower than the value of the pGUF empty vector (E.V., white-colored), respectively. The intensity of the color is proportional to normalized values. No growth control or blank (bl.) contained only medium; PlaF - phospholipase PlaF expressed from pGUF-*plaF* vector was used as a positive control, n.d. - not determined, n.g. - no growth.

Integration density analysis of chemiluminescent dot-blot signals normalized to total protein amount in plate HY III (Fig. 22. A-C) revealed that 70 out of 94 *E. coli* cell lysates containing pGUF-*guf* constructs have higher signal intensity than cell lysate transformed with pGUF (empty vector), indicating 74.5 % expression success. In the plate HY IV (Fig. 22, D-F), 46 out

of 49 *E. coli* cell lysates containing pGUF-*guf* were positive, indicating 94 % expression success.

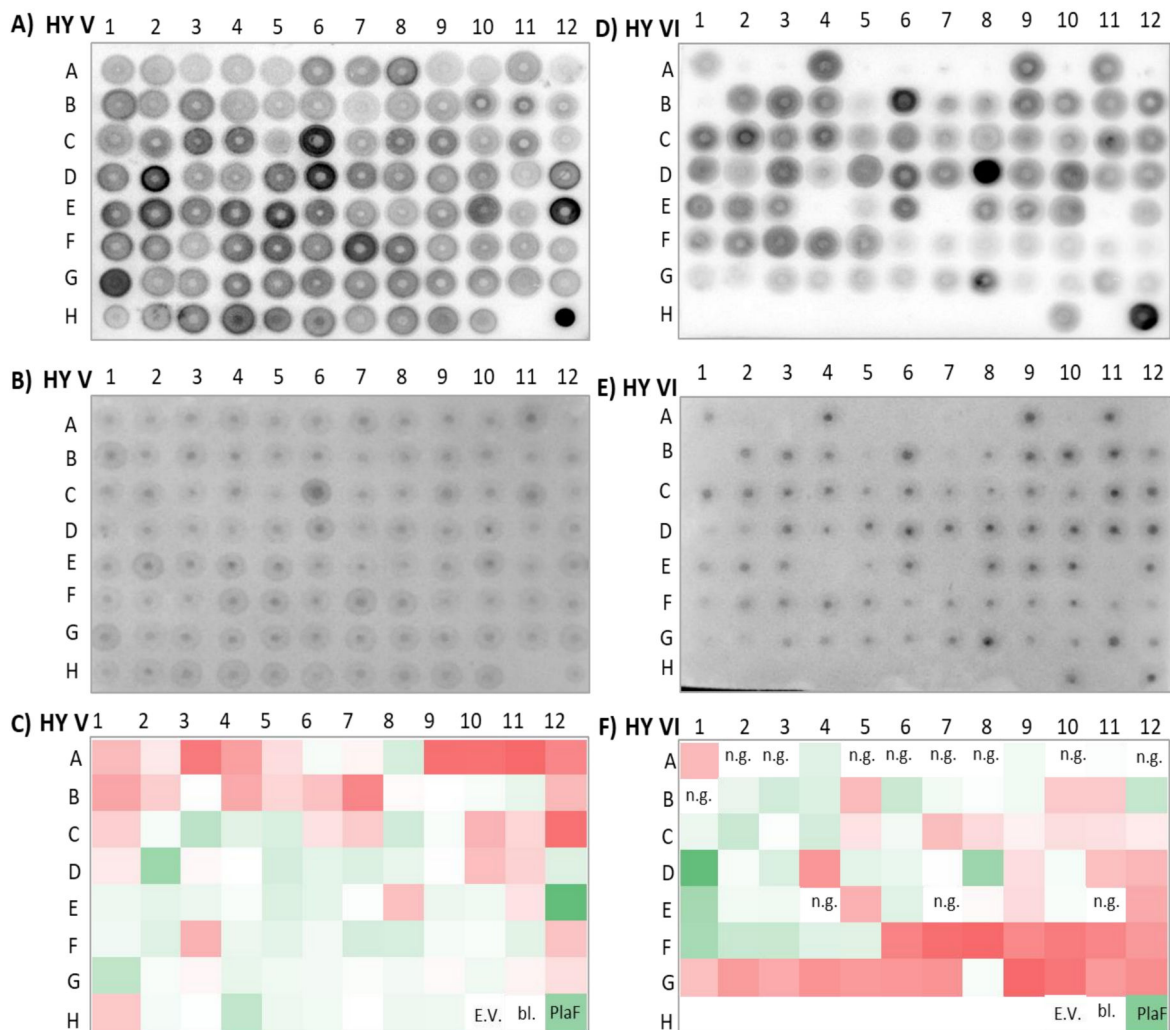


Fig. 23. Dot-blot analysis of PUFs expression in plates HY V (A-C) and HY VI (D-F). Combined *E. coli* BL21(DE3) and *E. coli* C43(DE3) cell lysates (4 μ l) with $OD_{580} = 5$ were loaded on the nitrocellulose membrane, followed by detection of expressed PUFs using anti-C-6xHis HRP conjugate antibody (**A, D**). Total protein amount was detected after staining with 0.1 % PonceuSdye (**B, E**). Fingerprint showing integration densities of chemiluminescent dot-blot signals normalized to total protein amount. (**C, F**) The green and red colors indicate values higher and lower than the value of the pGUF empty vector (E.V., white-colored), respectively. The intensity of the color is proportional to normalized values. No growth control or blank (bl.) contained only medium; PlaF - phospholipase PlaF expressed from pGUF-*plaF* vector was used as a positive control, n.d. - not determined, n.g. - no growth.

Integration density analysis of chemiluminescent dot-blot signals normalized to total protein amount in plate HY V (Fig. 23, A-C) revealed that 59 out of 94 *E. coli* cell lysates containing pGUF-*guf* constructs have higher signal intensity than cell lysate with pGUF (empty vector),

indicating 60 % expression success. In plate HY VI (Fig. 23, D-F), 36 out of 73 *E. coli* cell lysates containing pGUF-*guf* were positive, resulting in a 49.4 % of expression success.

As estimated from the protein dot-blot analysis, the average expression success of six plates containing putative hydrolases was 76.2 %, meaning that 327 putative hydrolases were likely expressed at a level higher than the detection limit of dot-blot.

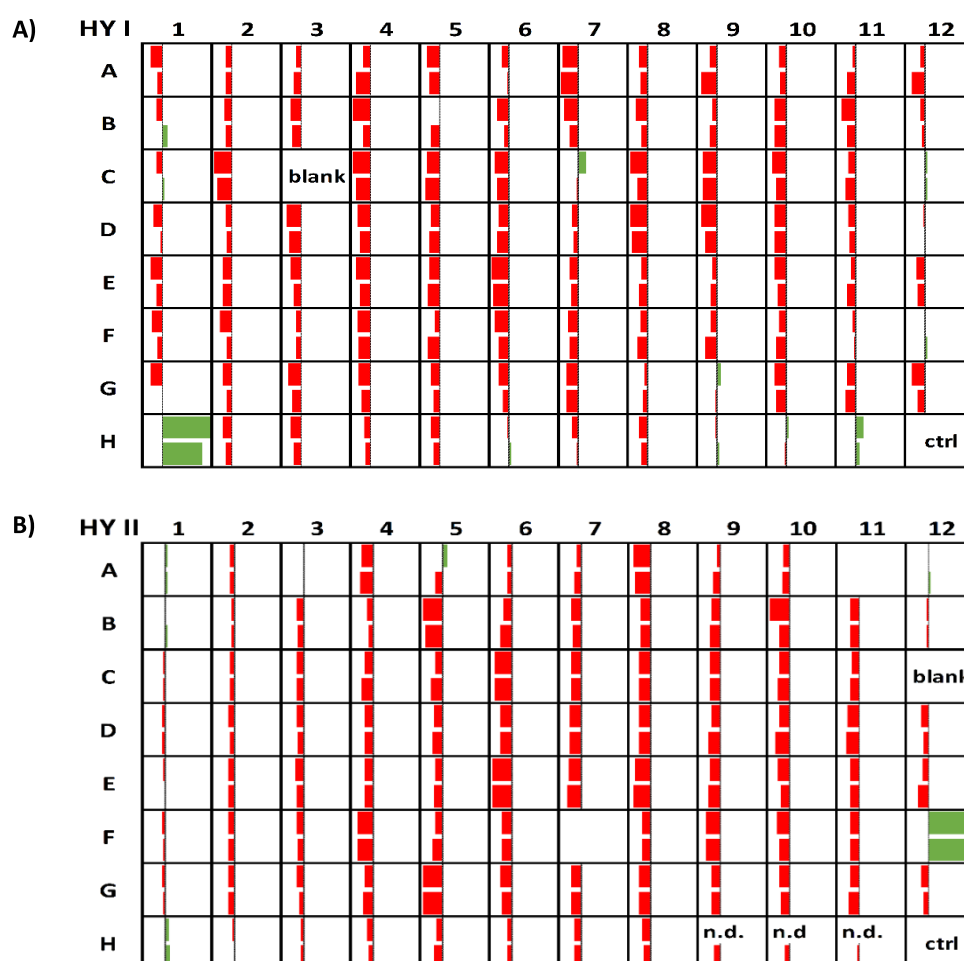
3.4.2. Enzyme activity screening revealed promising novel hydrolases

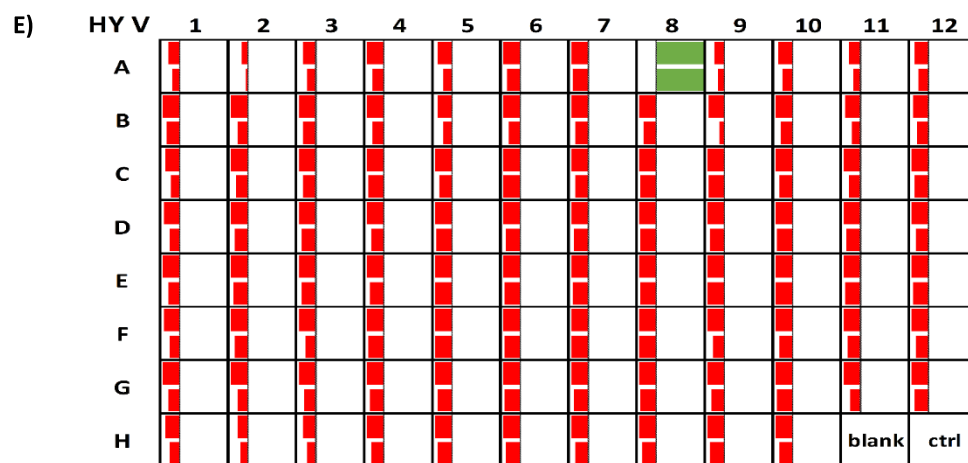
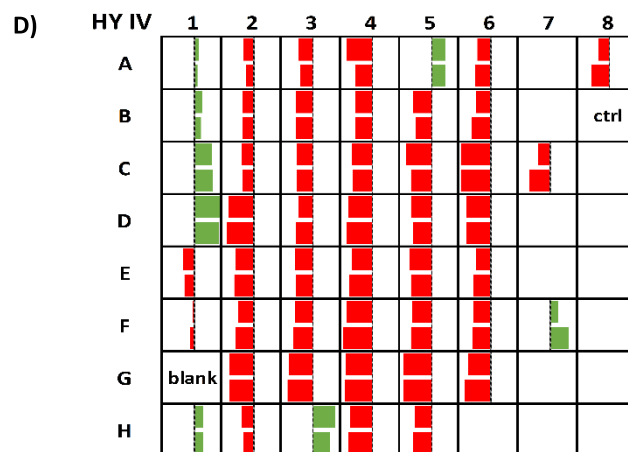
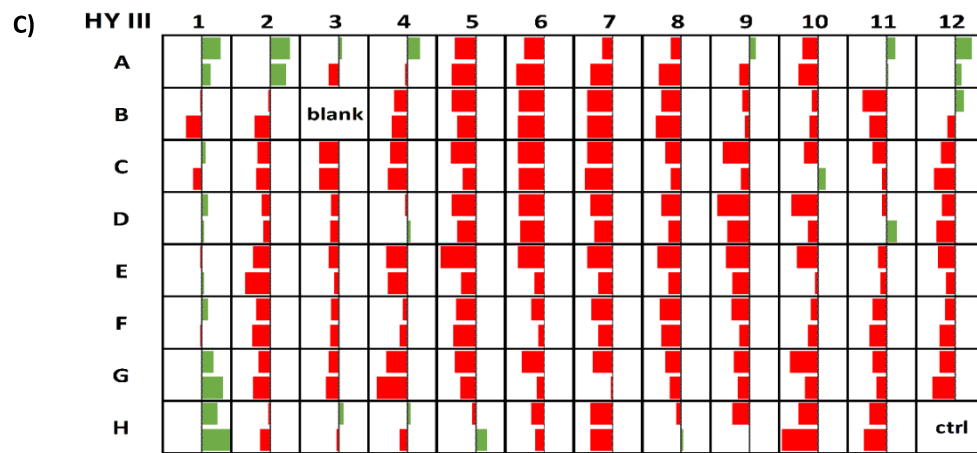
For screening of hydrolytic activities, 460 pGUF-*guf* constructs, including 429 constructs harboring putative hydrolases, were organized in six 96-well plates (Table S4). *E. coli* cells expressing recombinant PUFs were lysed by two freezing/thawing cycles and Triton X-100 (0.2 % v/v), which is mild-detergent useful for solubilization overexpressed membrane proteins [280]. The optical density of cell suspensions was measured and used to prepare cell lysates with the average OD₅₈₀ \approx 2 for activity assays. The activity of each clone was normalized to the number of cells used in the assay by dividing activity with the optical density of each sample. The lysates were tested in 96-well MTP-based activity assays using nine chromogenic and six native substrates for esterase, thioesterase, lipase, phospholipase A, phospholipase C, phosphatase, phosphodiesterase, protease, and α/β -glucosidase enzyme families. In glucosidase, protease, thioesterase, and phospholipase A assays, substrate cocktails consisting of two or three different substrates were used to increase the chance of identification of novel hydrolases and reduce the workload. For example, the substrate cocktail in protease assay included α -benzoyl-L-arginine-*p*-nitroanilide (BA-*p*-NA) substrate, which can be hydrolyzed by serine-, cysteine, and some carboxy- and metallopeptidases and L-leucine-*p*-nitroanilide (Leu-*p*-NA) substrate, which can be hydrolyzed by aminopeptidases and carboxypeptidases. [204] The reaction conditions, including the buffer pH and availability of metal ion cofactors, were adjusted for each assay to match the reaction conditions under which the majority of enzymes from the literature were active. [204] Every enzyme assay in 96-well MTP was performed two times under the same reaction conditions.

The enzyme activity for each sample was calculated by subtracting the sum of average activity and the standard deviation (Ave. + S.D.) calculated for all samples in one 96-well MTP. Hence, positive samples were those whose activity was much higher than that of other samples in the plate. This approach assumes that most GUFs expressed in one MTP do not have tested activity, i.e., they perform as negative controls. The samples that were positive in two

measurements were considered positive in the screening (Tables 9 and S5). They were further categorized regarding the percentage increase relative to the Ave. + S.D. of the corresponding plate. The samples whose activities were <10 %, 10 - 20 %, or >20 % higher than the Ave. + S.D. of the plate in two measurements were considered low, moderate, and high active, respectively. The samples with moderate and high activities identified in activity fingerprints for each tested activity are considered positive hits and will be discussed below.

The screening of the esterase activity measured with the artificial substrate *p*-NPB led to the identification of 23 positive hits (Fig. 24, Tables 9 and S5). The strains carrying pGUF-*pa3518* (plate HY I, position H1), pGUF-*pa0829* (plate HY II, position F12), and pGUF-*pa2315* (plate HY V, position A8) showed very high esterase activities that were \approx 100 %, \approx 200 %, and \approx 300 % higher than Ave. + S.D. in both measurements, respectively. On the other hand, moderate activities were detected in strains carrying pGUF-*pa2074* (HY IV, C1) and pGUF-*pa3074* (HY IV, H3), which showed 17 % and \approx 19 % higher activities than Ave. + S.D. in both measurements, respectively.





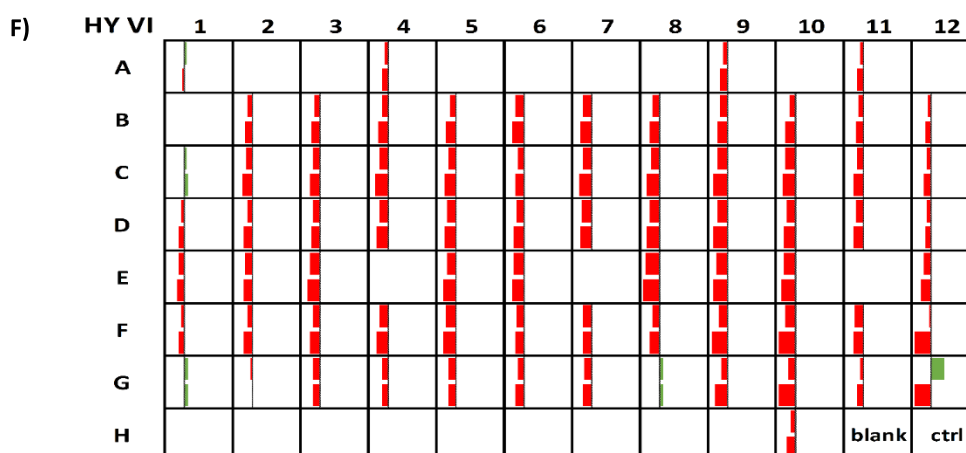
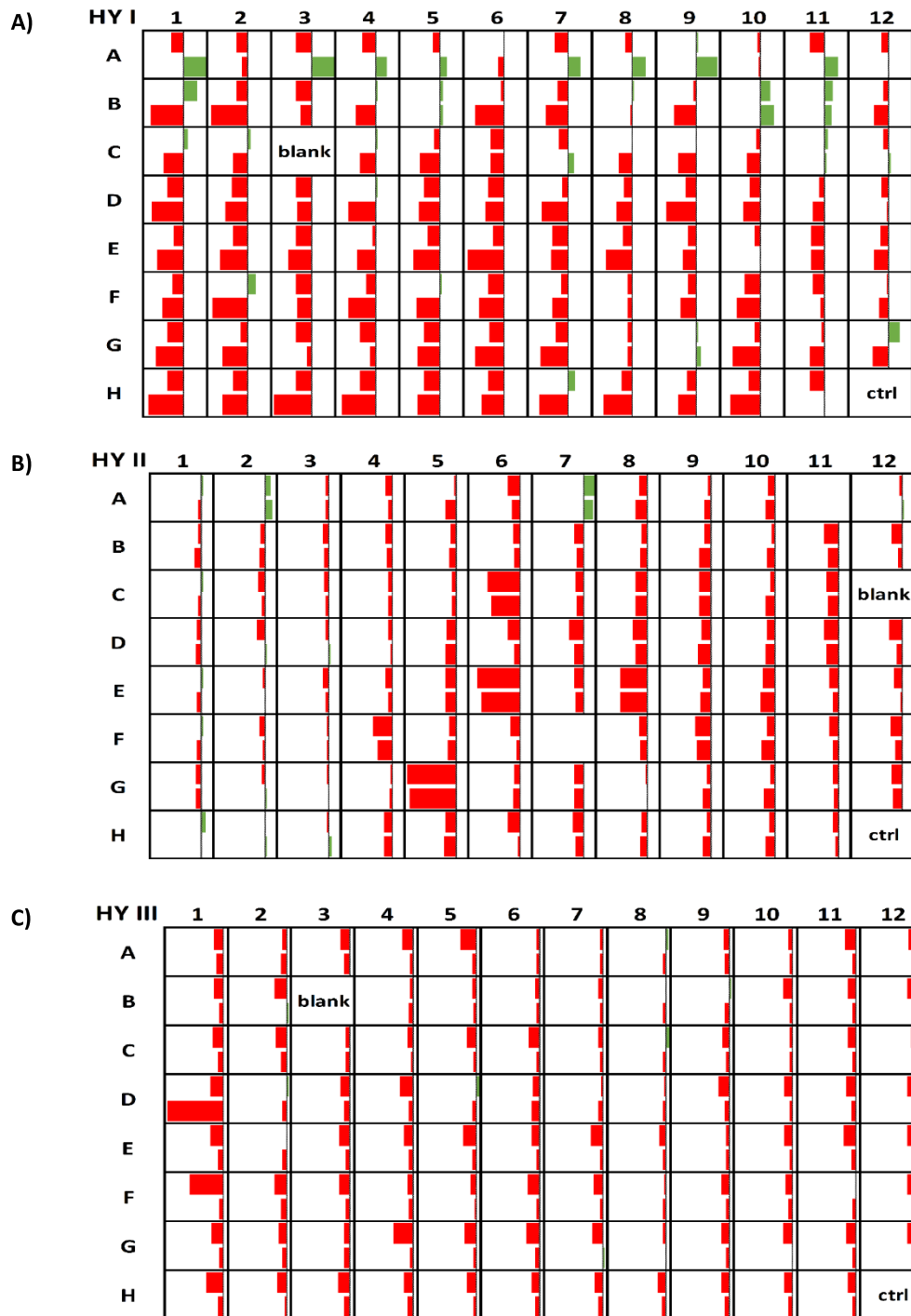


Fig. 24. Fingerprint showing the screening of esterase activity with *p*-nitrophenyl butyrate. The 175 μ l of 1 mM pNPB substrate was added to 25 μ l of *E. coli* BL21(DE3)/*E. coli* C43(DE3) cell lysates expressing GUFs($OD_{580} \approx 2$) and the absorbance of product at 410 nm was measured during 30 min at 37 $^{\circ}$ C. The difference of A_{410nm} with the time normalized to OD_{580nm} . ($\Delta A_{410nm}/OD_{580nm}$) is considered as activity. The bars represent the values of activity of the sample subtracted by Ave. + S.D. for each analyzed plate. The bars are scaled to minimal and maximal values of each plate and colored green or red to indicate positive and negative values, respectively. Two measurements for each sample in 96-well MTP are indicated with two bars per position. **A)** Hydrolase plate I: in H11 is pGUF negative control, **B)** Hydrolase plate II: H11=pGUF, **C)** Hydrolase plate III: H11=pGUF, **D)** Hydrolase plate IV: A8=pGUF, **E)** Hydrolase plate V: H10=pGUF, **F)** Hydrolase plate VI: H10=pGUF. pGUF, empty vector control; blank: buffer negative control containing 25 μ l 100 mM Tris pH 8 0.2 % Triton X-100 and 175 μ l 1 mM substrate, ctrl, positive control containing cell lysate of *E. coli* expressing PlaF from pGUF-*plaf*; n.d. - not determined.

The screening of the thioesterase activity measured with the cocktail composed of natural substrates, acetyl-CoA and palmitoyl-CoA, led to the identification of 24 positive hits (Fig. 25, Tables 9 and S5). The expression strains carrying pGUF-*pa4968* (HY I, B10); pGUF-*pa0057* (HY VI, B4), and pGUF-*pa3087* (HY IV, A5) showed the highest thioesterase activities that were 58 %, 21 % (assay 1, assay 2); 39 %, 28 % and 34 %, 22 % higher than Ave. + S.D. in two measurements, respectively. Conversely, moderate activities were detected in strains carrying pGUF-*pa3226* (HY VI, B10) and pGUF-*pa3785* (HY II, A7), which showed 37 %, 14 % and 22 %, 19 % higher activities than Ave. + S.D. in two measurements, respectively.



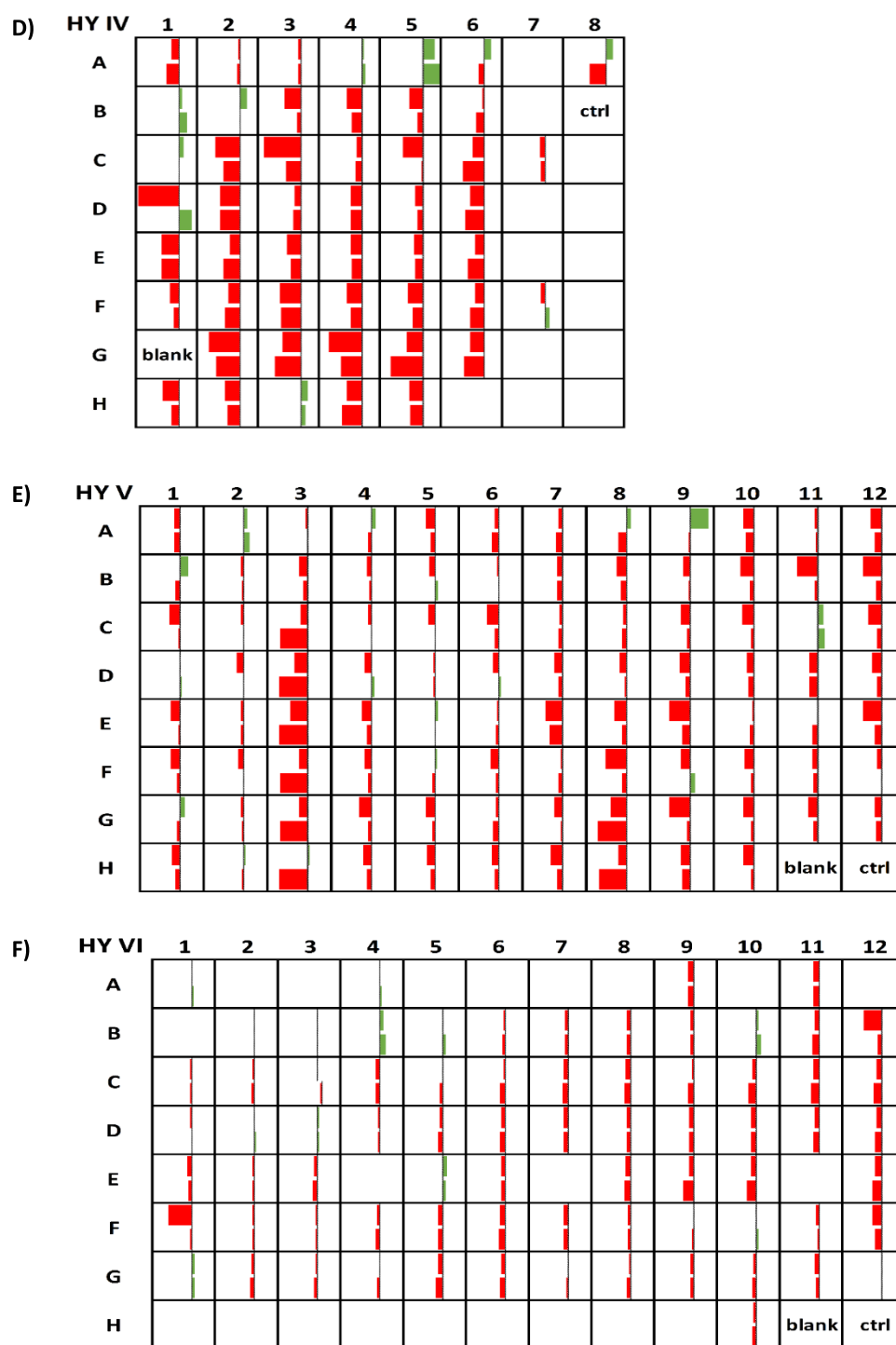
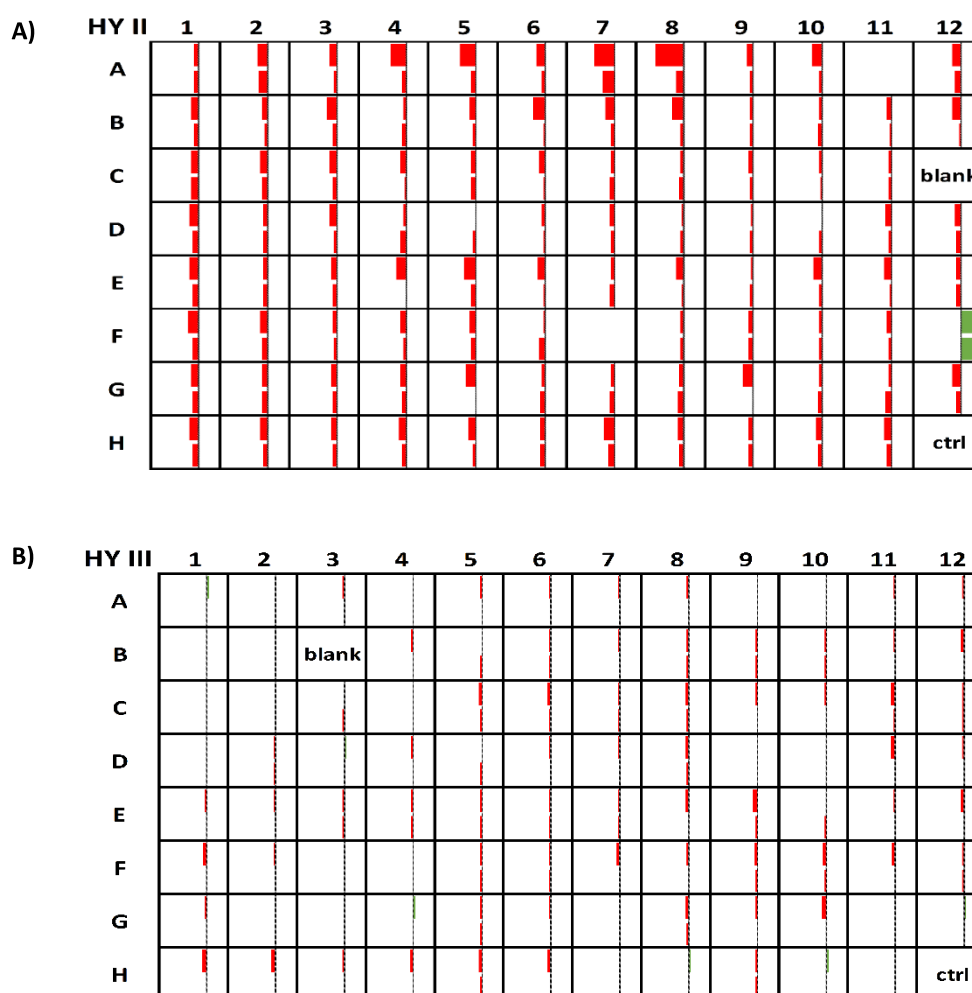


Fig. 25. Fingerprint showing the screening of thioesterase activity measured with acetyl-CoA and palmitoyl-CoA. The 10 μ l of 10 mM DTNB and 150 μ l of substrate cocktail containing 40 μ M acetyl-CoA and 40 μ M palmitoyl-CoA was added to 25 μ l of cell lysates with $OD_{580} \approx 2$ and the absorbance at 412 nm was recorded during 30 min at 37 °C. The difference of A_{410nm} with the time normalized to OD_{580nm} . ($\Delta A_{412nm}/OD_{580nm}$) is considered as an activity. The bars represent the values of activity of the sample subtracted by Ave. + S.D. for each analyzed plate. The bars are scaled to minimal and maximal values of each plate and colored green or red to indicate positive and negative values, respectively. Two measurements for each sample in 96-well MTP are indicated with two bars per position. **A)** Hydrolase plate I: in H11 is pGUF negative controle **B)** Hydrolase plate II: H11=pGUF **C)** Hydrolase plate III: H11=pGUF **D)** Hydrolase plate IV: A8=pGUF **E)** Hydrolase plate V: H10=pGUF **F)**

Hydrolase plate VI: H10=pGUF. Blank - substrate negative control containing 25 μ l 100 mM Tris pH 8 0.2% Triton X-100 and 150 μ l 1 mM substrate.

The screening of lipase activity with the artificial substrate, *p*-NPdec, led to the identification of 19 positive hits (Fig. 26, Table 9 and S5). The expression strains carrying pGUF-*pa0829* (HY II, F12) and pGUF-*pa1062* (HY VI, G12) showed very high activities, which were 5134 %, 341% (assay 1, assay 2), and 109 %, 35 % higher than Ave. + S.D. in two measurements, respectively. On the other hand, the strains carrying pGUF-*pa2625* (HY V, A9) and pGUF-*pa2801* (HY V, F9) were moderately active with 13 %, 17 % and 13 %, 14 % percentage increases relative to Ave. + S.D. in two measurements, respectively.



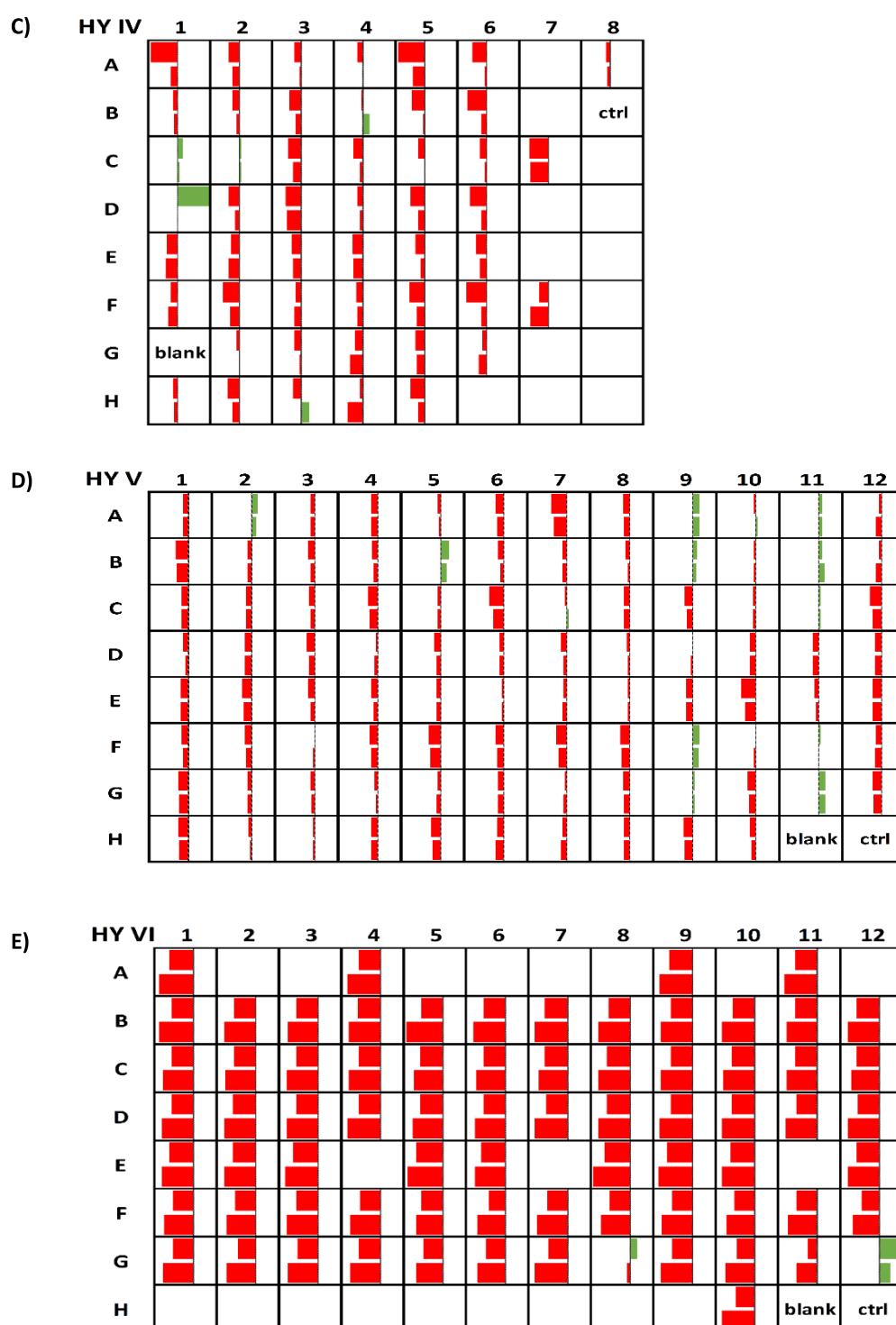
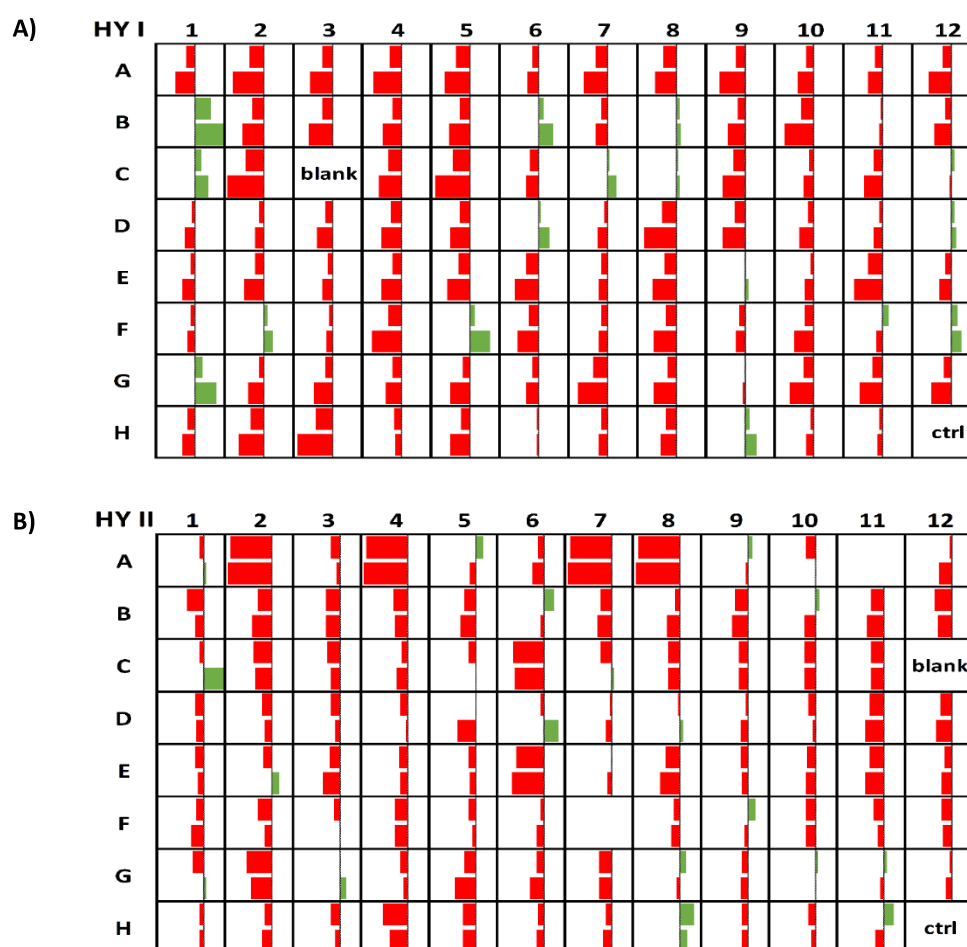
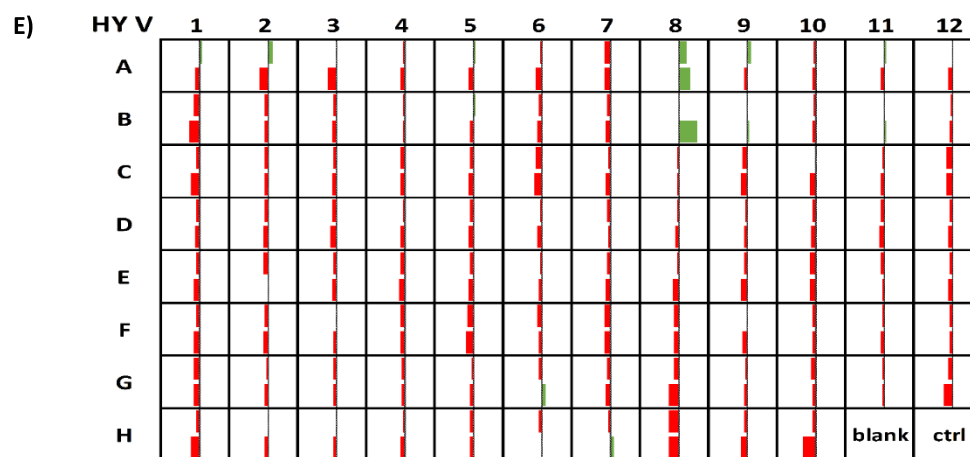
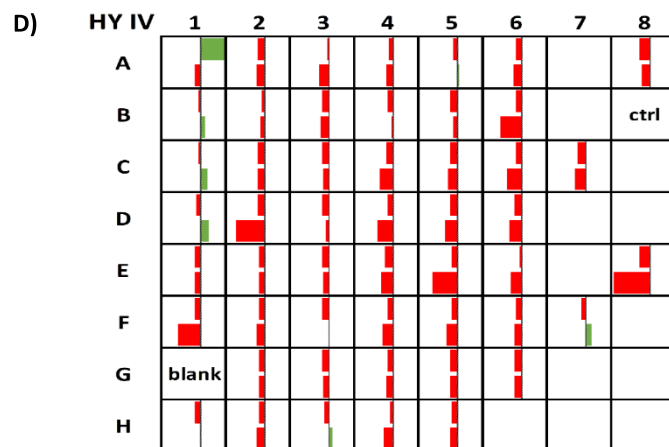
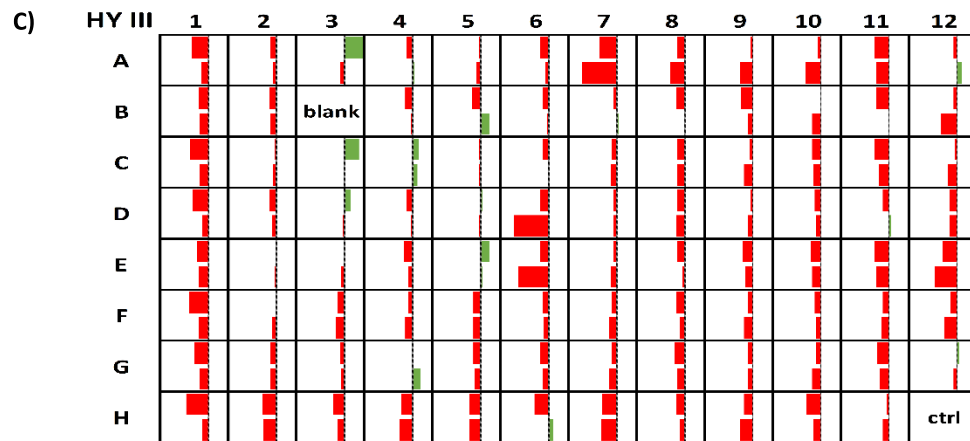


Fig. 26. Fingerprint showing the screening of lipase activity measured with *p*-nitrophenyl decanoate. The 175 μ l of 1mM pNPB substrate was added to 25 μ l of *E. coli* BL21(DE3)/*E. coli* C43(DE3) cell lysates with $OD_{580} \approx 2$ and the absorbances at 410 nm were recorded during 30 min at 37 °C. The difference of A_{410nm} with the time normalized to OD_{580nm} . ($\Delta A_{410nm}/OD_{580nm}$) is considered as an activity. The bars represent the values of activity of the sample subtracted by Ave. + S.D. for each analyzed plate. The bars are scaled to minimal and maximal values of each plate and colored green or red to indicate positive and negative values, respectively. Two measurements for each sample in 96-well MTP are indicated with two bars per position. **A)** Hydrolase plate II: in H11 is pGUF negative controle **B)** Hydrolase plate III: H11=pGUF **C)** Hydrolase plate IV: A8=pGUF **D)** Hydrolase V:

H10=pGUF **E**) Hydrolase plate VI: H10=pGUF. Blank - substrate negative control containing 25 μ l 100 mM Tris pH 8 0.2 % Triton X-100 and 175 μ l 1 mM substrate, ctrl - positive esterase control containing *E. coli* cell lysate with pGUF-*plaf*.

In addition to screening with *p*-NPdec, lipases were screened with the natural substrate, glyceryl tridecanoate (GTD). The released fatty acids were quantified in this assay by a colorimetric NEFA method. This led to the identification of 22 positive hits (Fig. 27, Tables 9 and S5), among which only pGUF-*pa3230* was also positive with *p*-NPdec (Table 9). The expression strains carrying pGUF-*pa2315* (HY V, A8) and pGUF-*pa4968* (HY I, B1) showed high activities, which were 88 %, 43 % (assay 1, assay 2), and 23 %, 28 % higher than Ave. + S.D. in two measurements, respectively. The strains carrying pGUF-*pa0731* (HY VI, F9) and pGUF-*pa3288* (HY II, H8) were moderately active with a 24 %, 13 %, and 34 %, 14 % percentage increase relative to Ave. + S.D. in two measurements, respectively.





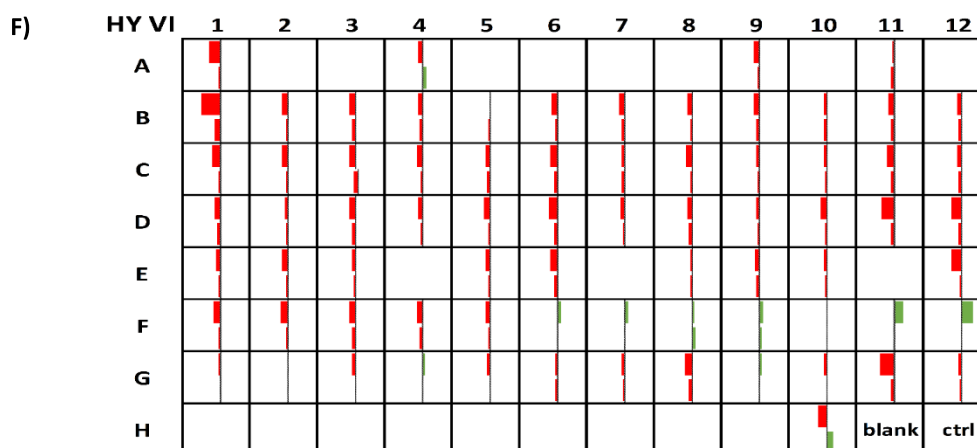
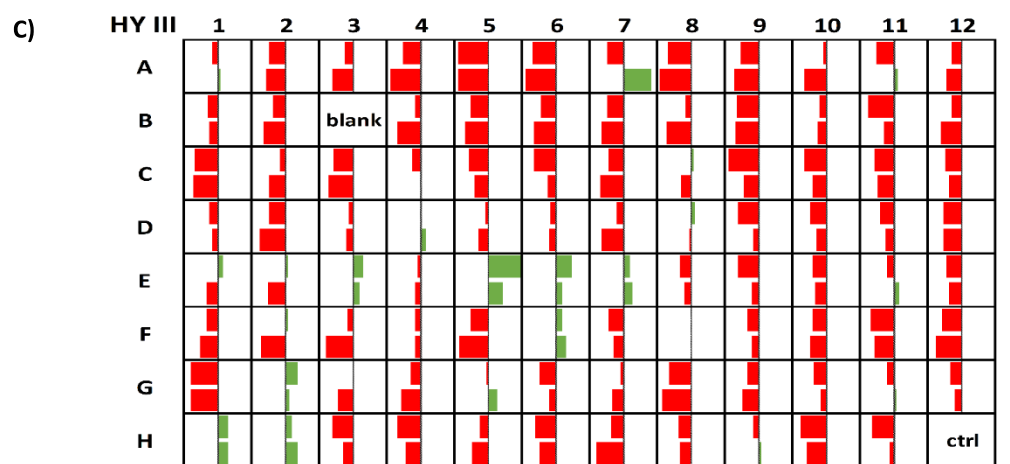
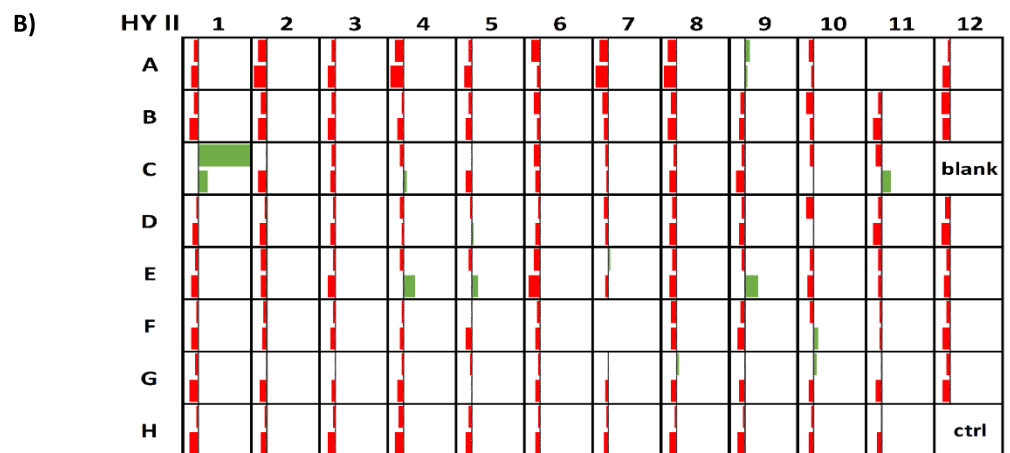
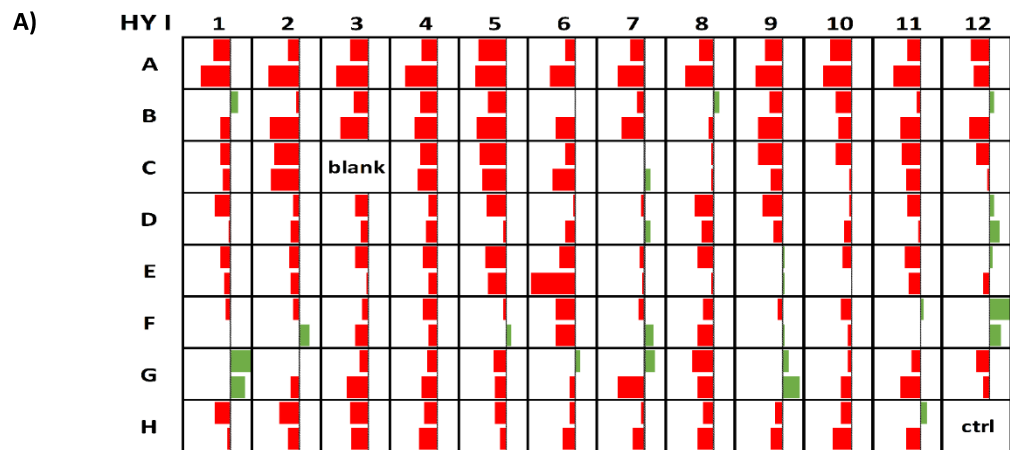


Fig. 27. Fingerprint showing the screening of lipase activity measured with glyceryl tridecanoate. The 10 μ l of 268 mM glyceryl tridecanoate was added to 10 μ l of cell lysates with $OD_{580} \approx 0.4$ and incubated for 24 h at 37 $^{\circ}$ C with shaking at 150 rpm. Fatty acids were quantified with the NEFA assay. The absorbance at 546 nm normalized to OD_{580nm} (A_{546nm}/OD_{580nm}) is considered as activity. The bars represent the values of activity of the sample subtracted by Ave. + S.D. for each analyzed plate. The bars are scaled to minimal and maximal values of each plate and colored green or red to indicate positive and negative values, respectively. Two measurements for each sample in 96-well MTP are indicated with two bars per position. **A)** Hydrolase plate I: in H11 is pGUF negative controle **B)** Hydrolase plate II: H11=pGUF **C)** Hydrolase plate III: H11=pGUF **D)** Hydrolase plate IV: A8=pGUF **E)** Hydrolase plate V: H10=pGUF **F)** Hydrolase plate VI: H10=pGUF. Blank - substrate negative control containing 10 μ l 100 mM Tris pH 8 0.2 % Triton X-100 and 10 μ l substrate, ctrl – *Candida albicans* lipase CalB was used as a positive control.

To identify phospholipases A and B the cocktail containing natural substrates (1,2-dipalmitoyl-sn-glycero-3-phosphocholine (16:0 PC), 1,2-dipalmitoyl-sn-glycero-3-phosphoethanolamine (16:0 PE) and 1,2-dipalmitoyl-sn-glycero-3-phospho-(1'-rac-glycerol) (16:0 PG)) was used and the released fatty acids were quantified by colorimetric NEFA assay. This led to identifying 22 positive hits (Fig. 28, Tables 9 and S5). The expression strains carrying pGUF-*pa3750* (HY II, C1); pGUF-*pa2419* (HY I, G1), and pGUF-*pa2927* (HY V, E7) showed the highest activities, which were 626 %, 56 % (assay 1, assay 2), 34 %, 23 % and 234 %, 226 % higher than Ave. + S.D. in two measurements, respectively. The strains carrying pGUF-*pa1193* (HY I, F12) and pGUF-*pa2729* (HY III, E5) were moderately active with 32 %, 19 %, and 39 %, 16 % increase relative to Ave. + S.D. in two measurements, respectively.



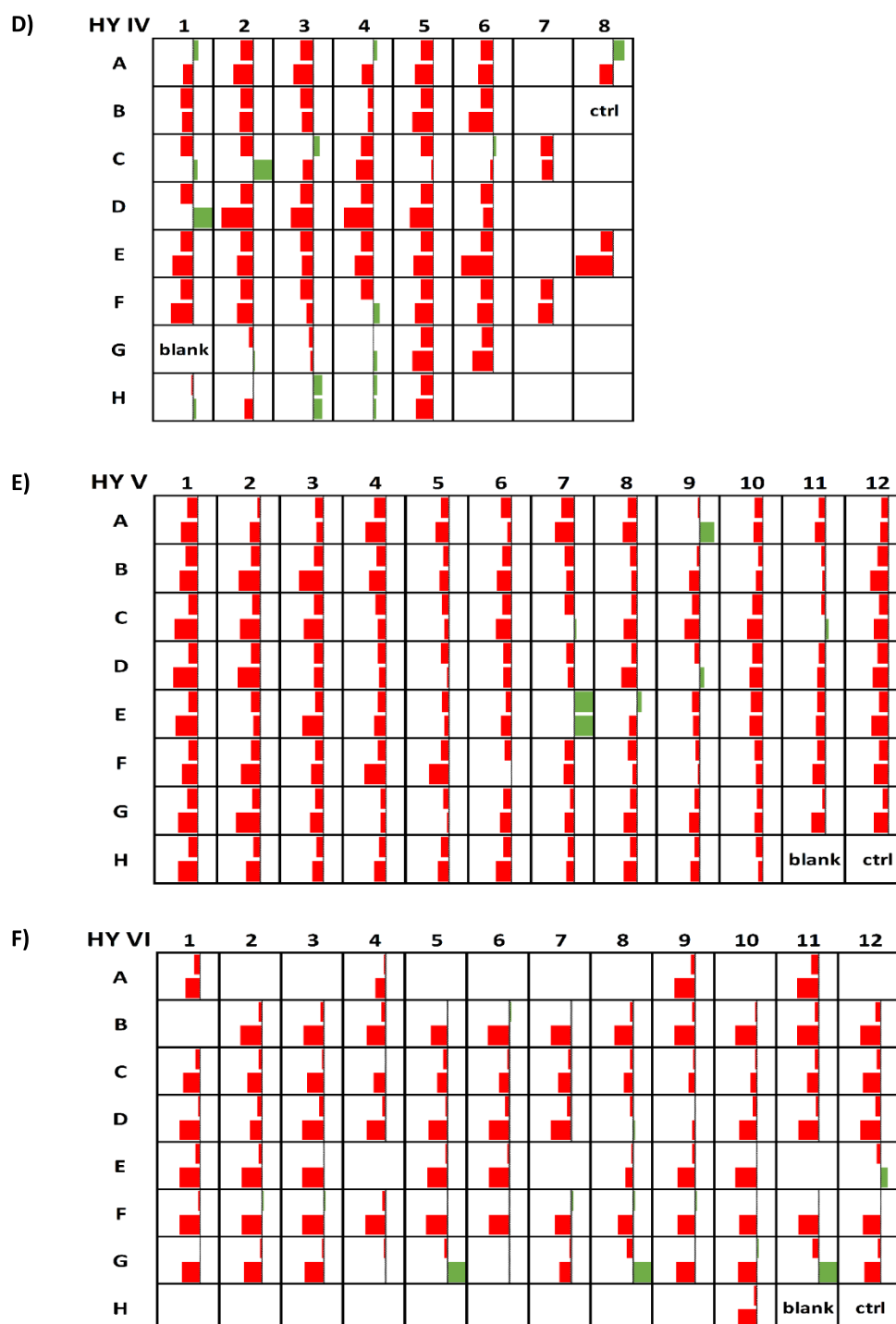
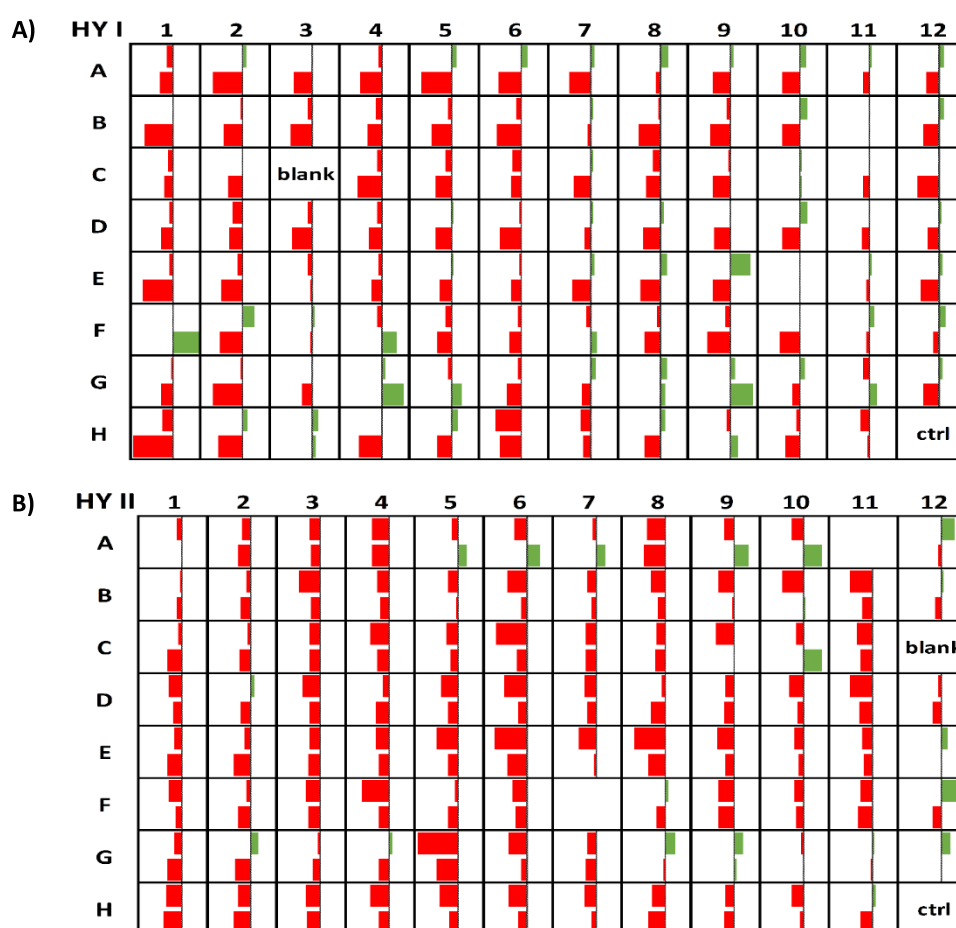
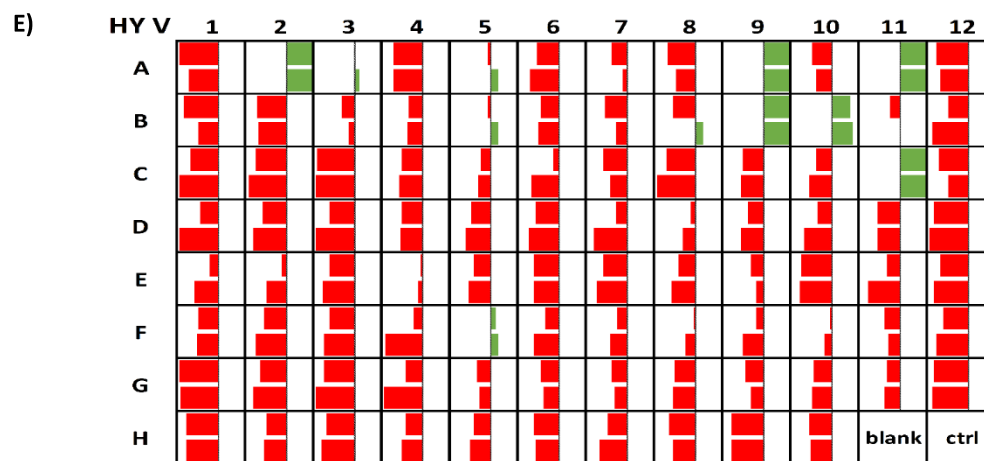
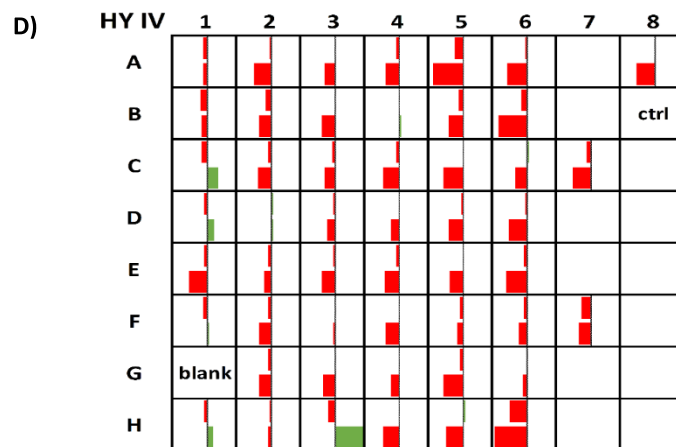
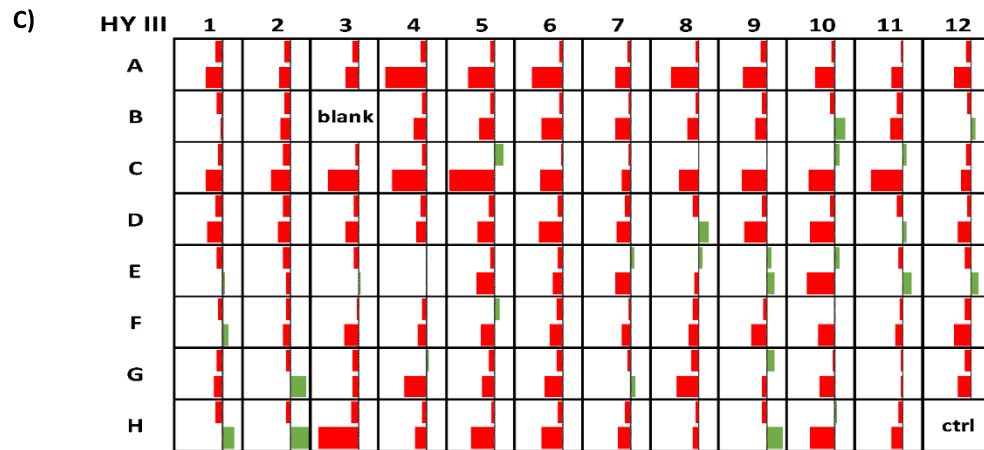


Fig. 28. Fingerprint showing the screening of phospholipase A/B activities measured with 16:0 PC, 16:0 PE, and 16:0 PG cocktail. The 10 μ l of substrate cocktail containing 89.33 mM of each phospholipid was added to 10 μ l of cell lysates with $OD_{580} \approx 0.4$ and incubated for 24 h at 37 $^{\circ}$ C with shaking at 150 rpm. Fatty acids were quantified with the NEFA assay. The absorbance at 546 nm normalized to OD_{580nm} (A_{546nm}/OD_{580nm}) is considered as an activity. The bars represent the values of activity of the sample subtracted by Ave. + S.D. for each analyzed plate. The bars are scaled to minimal and maximal values of each plate and colored green or red to indicate positive and negative values, respectively. Two measurements for each sample in 96-well MTP are indicated with two bars per position. **A)** Hydrolase plate I: in H11 is pGUF negative control **B)** Hydrolase plate II: H11=pGUF **C)** Hydrolase plate III: H11=pGUF **D)** Hydrolase plate IV: A8=pGUF **E)** Hydrolase plate V: H10=pGUF **F)**

Hydrolase plate VI: H10=pGUF. Blank - substrate negative control containing 10 μ l 100 mM Tris pH 8 0.2 % Tween20 and 10 μ l substrate, ctrl - positive lipase control.

The phospholipase C activity screened using an artificial *p*-nitrophenyl phosphorylcholine (*p*-NPPC) substrate resulted in the identification of 23 positive hits (Fig. 29, Tables 9 and S5). The expression strains carrying pGUF-*pa3614* (HY I, G4) and pGUF-*pa1356* (HY I, G9) showed the highest activities, which were 89 %, 43 % (assay 1, assay 2), and 23 %, 28 % higher than Ave. + S.D. in two measurements, respectively. On the other hand, the strains carrying pGUF-*pa1938* (HY I, G8) and pGUF-*pa1918* (HY III, E9) were moderately active with 87 %, 19 % and 64 %, 11 % increase relative to Ave. + S.D. in two measurements, respectively.





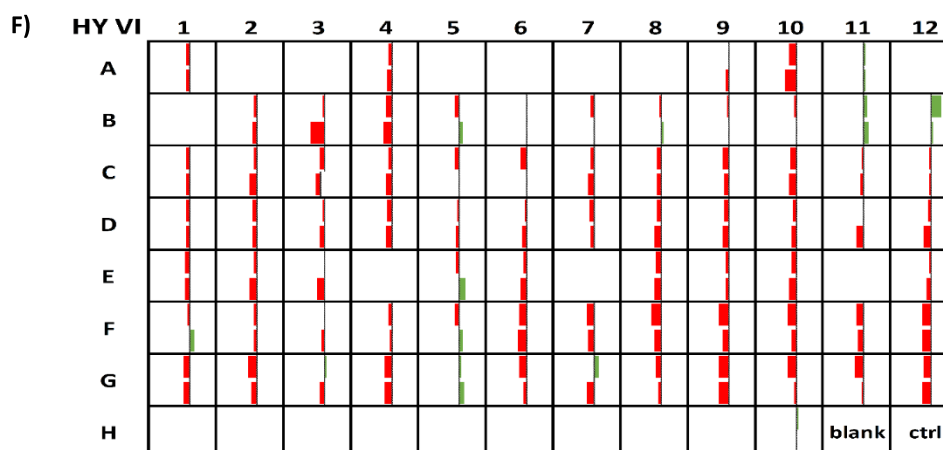
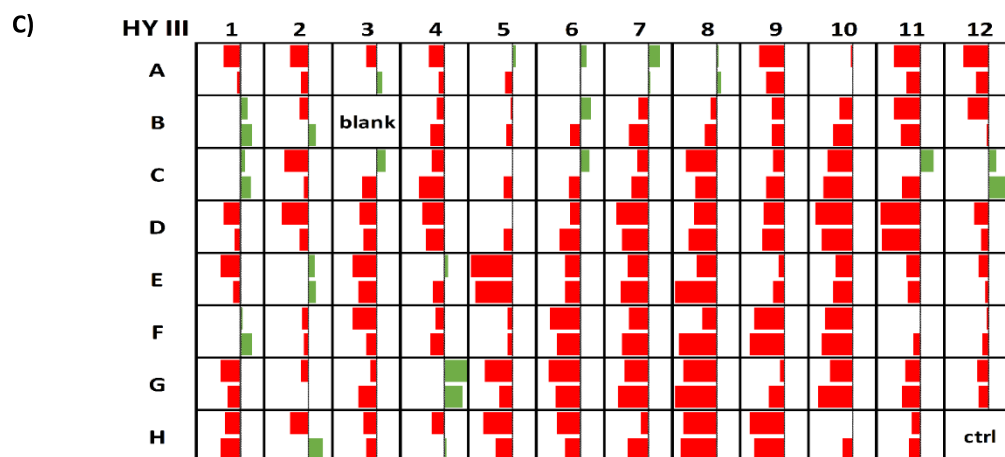
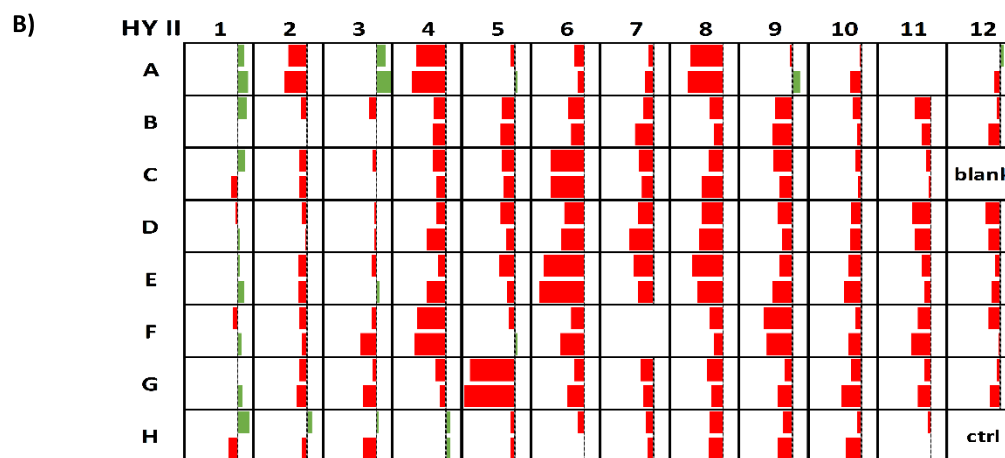
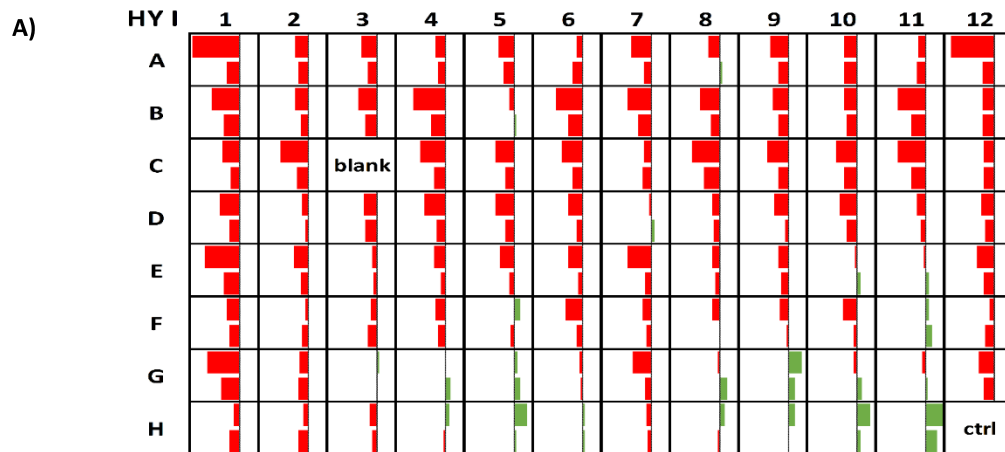


Fig. 29. Fingerprint showing the screening of phospholipase C activity measured with *p*-nitrophenyl phosphorylcholine. The 175 μ l of 1 mM pNPPC was added to 25 μ l of cell lysates with $OD_{580} \approx 2$ and the absorbances at 410 nm were recorded during 30 min at 37 $^{\circ}$ C. The difference of A_{410nm} with the time normalized to OD_{580nm} . ($\Delta A_{410nm}/OD_{580nm}$) is considered as an activity. The bars represent the values of activity of the sample subtracted by Ave. + S.D. for each analyzed plate. The bars are scaled to minimal and maximal values of each plate and colored green or red to indicate positive and negative values, respectively. Two measurements for each sample in 96-well MTP are indicated with two bars per position. **A)** Hydrolase plate I: in H11 is pGUF negative control **B)** Hydrolase plate II: H11=pGUF **C)** Hydrolase plate III: H11=pGUF **D)** Hydrolase plate IV: A8=pGUF **E)** Hydrolase plate V: H10=pGUF **F)** Hydrolase plate VI: H10=pGUF. Blank - substrate negative control containing 10 μ l 100 mM Tris pH 8 0.2 % Tween20 and 10 μ l substrate, ctrl - positive control.

The phosphodiesterase activity screening using an artificial bis-*p*-NPP substrate resulted in identifying 33 positive hits (Fig. 30, Tables 9 and S5). The expression strains carrying pGUF-*pa1906* (HY IV, F7) and pGUF-*pa0543* (HY V, A2) showed the highest activities of 53 %, 46 % (assay 1, assay 2), and 51 %, 30 % higher than Ave. + S.D. in two measurements, respectively. On the other hand, the strains carrying pGUF-*pa3087* (HY VI, E5) and pGUF-*pa5028* (HY V, A11) were moderately active with 36 %, 19 % and 34 %, 12 % percentage increase relative to Ave. + S.D. in two measurements, respectively.



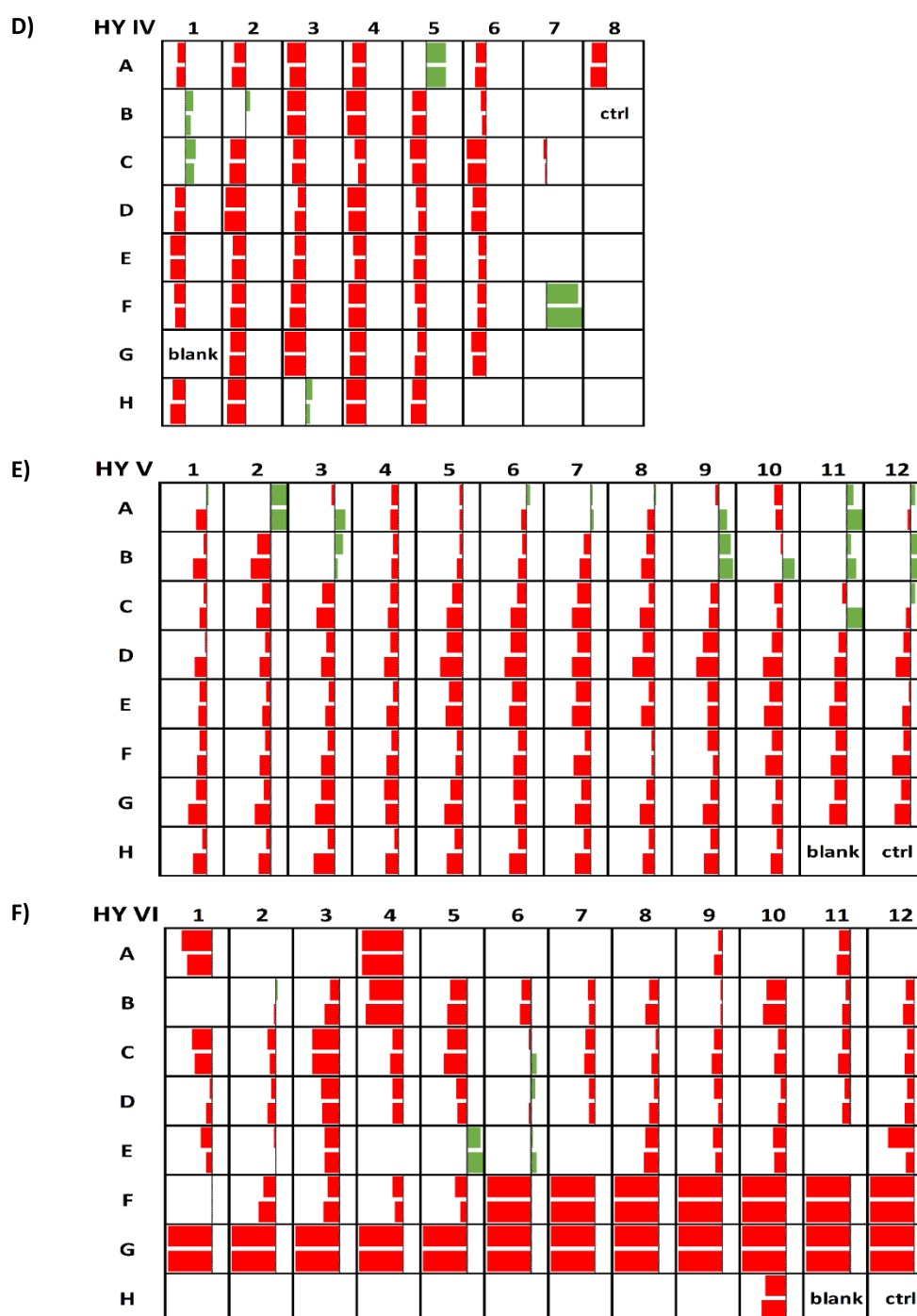
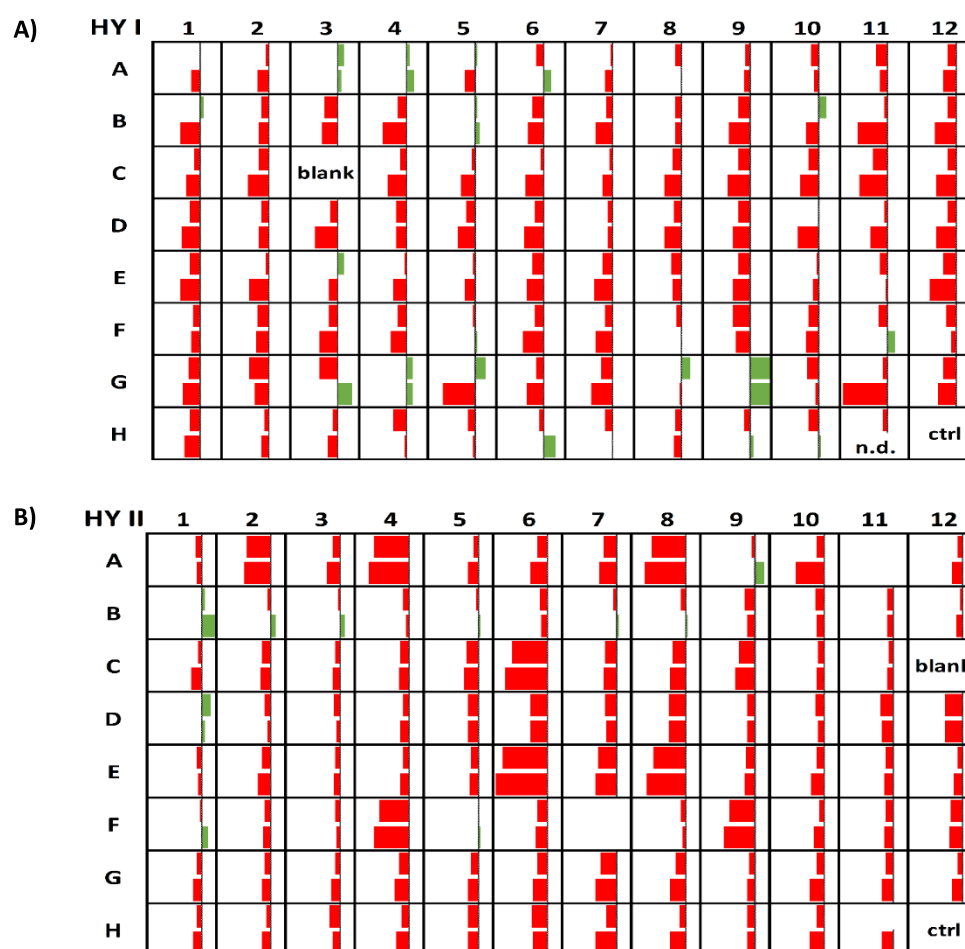
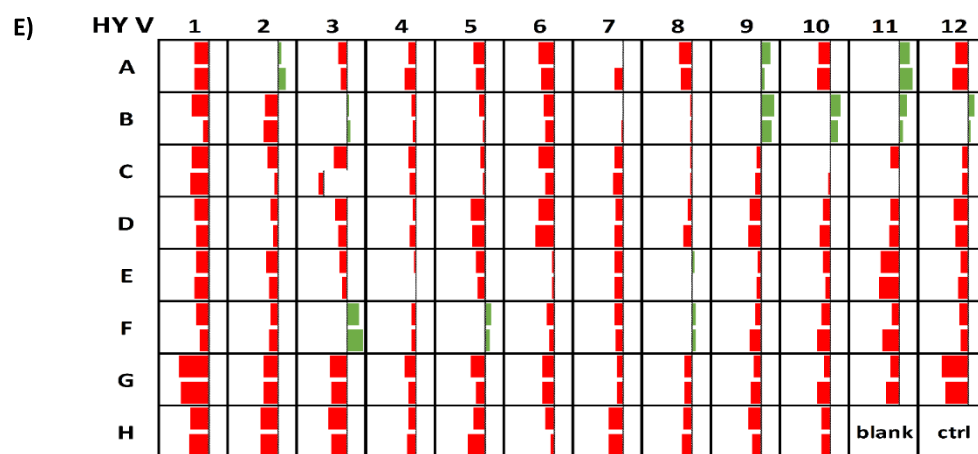
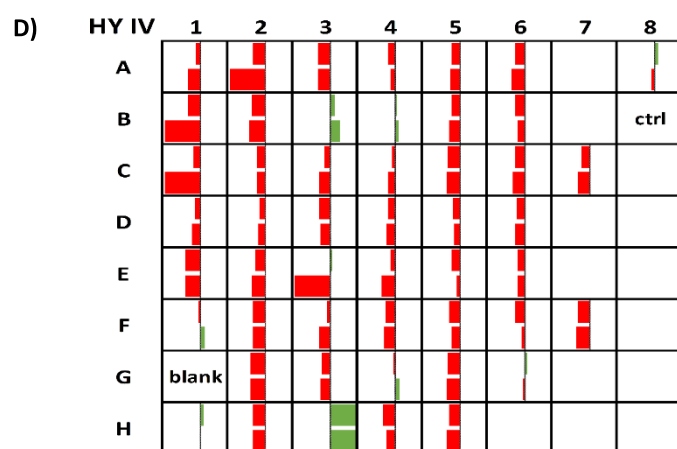
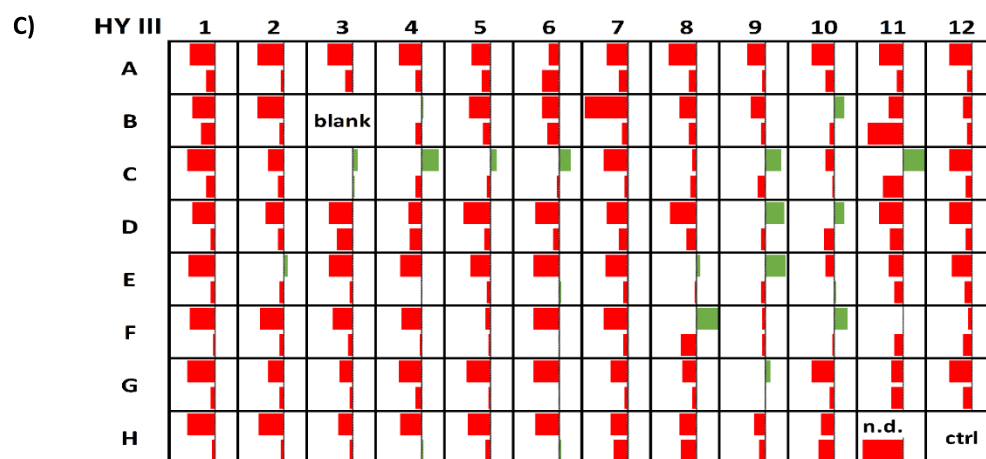


Fig. 30. Fingerprint showing the screening of phosphodiesterase activity measured with bis-*p*-nitrophenyl phosphate. The 175 μ l of 0.83 mM bis-*p*-NPP was added to 25 μ l of cell lysates with $OD_{580} \approx 2$ and the absorbances at 410 nm were recorded during 30 min at 37 °C. The difference of A_{410nm} with the time normalized to OD_{580nm} . ($\Delta A_{410nm}/OD_{580nm}$) is considered as an activity. The bars represent the values of activity of the sample subtracted by Ave. + S.D. for each analyzed plate. The bars are scaled to minimal and maximal values of each plate and colored green or red to indicate positive and negative values, respectively. Two measurements for each sample in 96-well MTP are indicated with two bars per position. **A)** Hydrolase plate I: in H11 is pGUF negative control **B)** Hydrolase plate II: H11=pGUF **C)** Hydrolase plate III: H11=pGUF **D)** Hydrolase plate IV: A8=pGUF **E)** Hydrolase plate V: H10=pGUF **F)** Hydrolase plate VI: H10=pGUF.

The phosphatase activity screening using an artificial *p*-NPP substrate resulted in the identification of 30 positive hits (Fig. 31, Tables 9 and S5). The expression strains carrying pGUF-*pa1356* (HY I, G9); pGUF-*pa3074* (HY IV, H3), and pGUF-*pa3087* (HY VI, E5) showed the highest activities, which were 102 %, 46 % (assay 1, assay 2); 74 %, 68 % and 40 %, 16 % higher than Ave. + S.D. in two measurements, respectively. On the other hand, the strains carrying pGUF-*pa3614* (HY I, G4) and pGUF-*pa5106* (HY V, F3) were moderately active with 30 %, 11 % and 19 %, 14 % increase relative to Ave. + S.D. in two measurements, respectively.





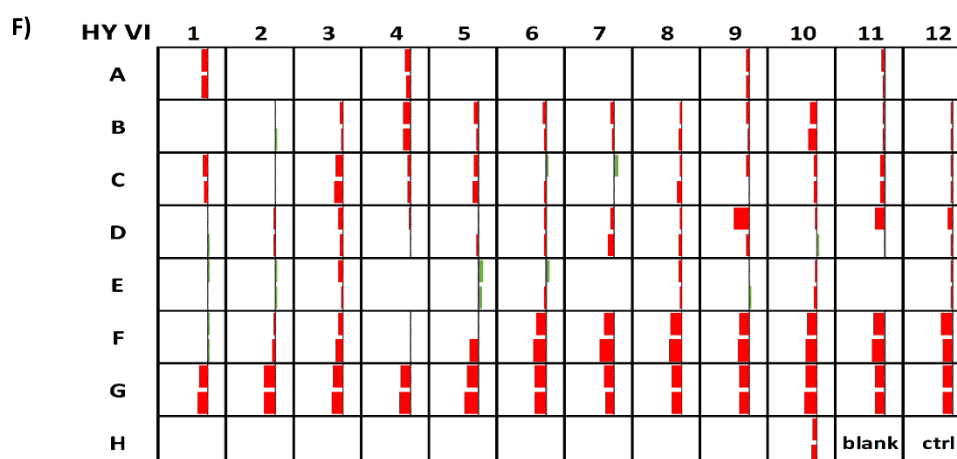
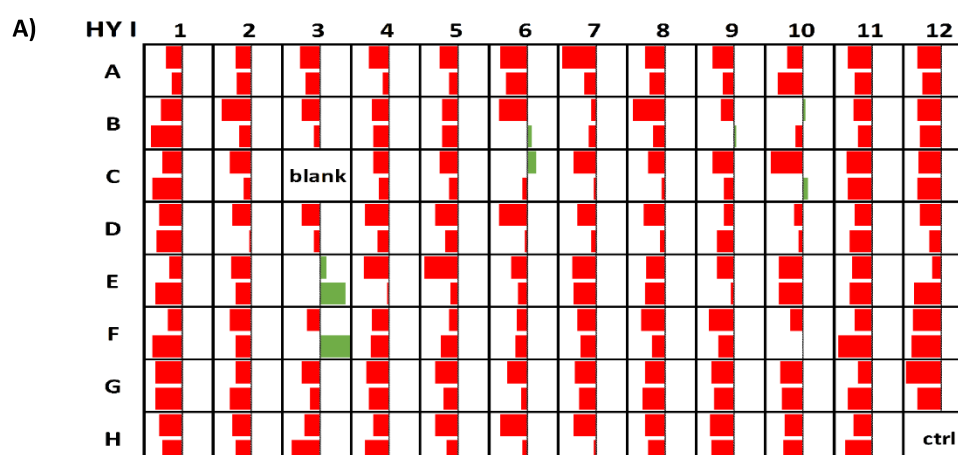
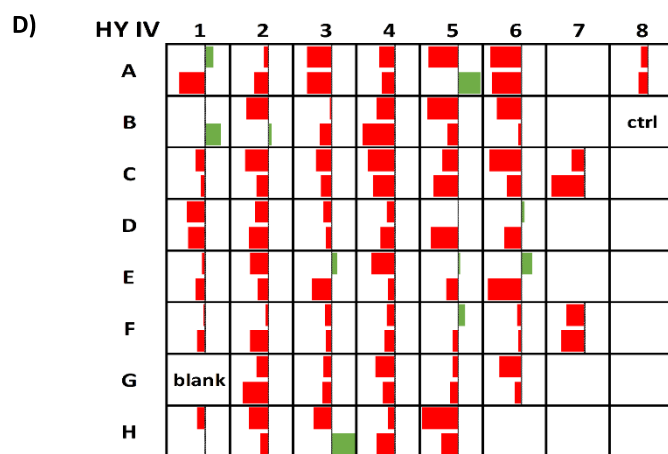
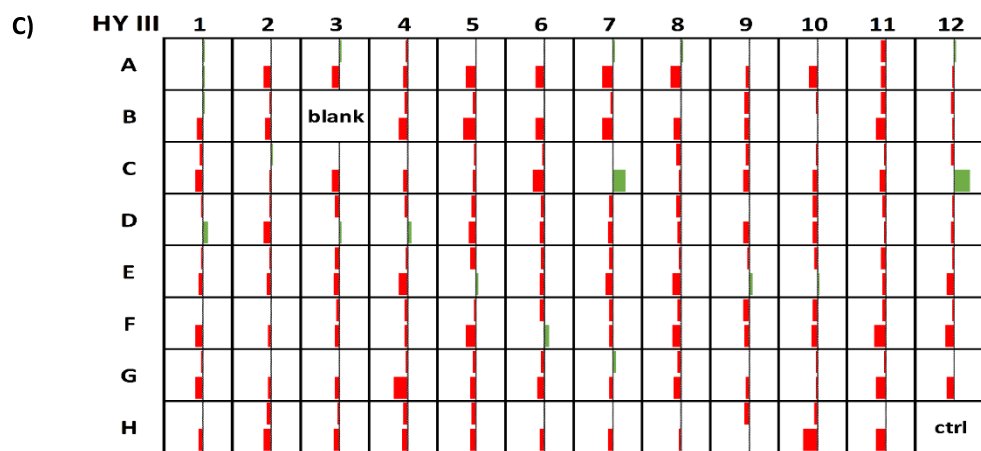
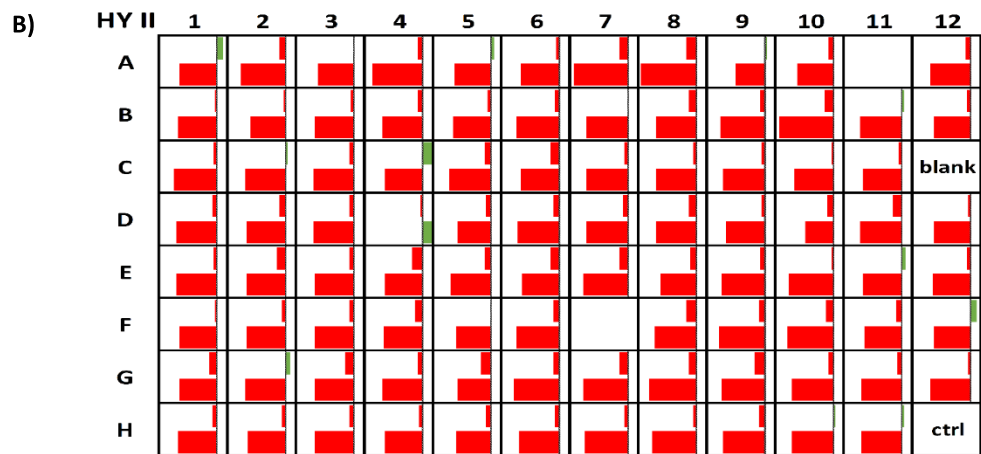


Fig. 31. Fingerprint showing the screening of phosphatase activity with *p*-nitrophenyl phosphate. The 175 μ l of 4 mM pNPP was added to 25 μ l of cell lysates with $OD_{580} \approx 2$ and the absorbances at 410 nm were recorded during 1h at 37 °C. The difference of A_{410nm} with the time normalized to OD_{580nm} . ($\Delta A_{410nm}/OD_{580nm}$) is considered as an activity. The bars represent the values of activity of the sample subtracted by Ave. + S.D. for each analyzed plate. The bars are scaled to minimal and maximal values of each plate and colored green or red to indicate positive and negative values, respectively. Two measurements for each sample in 96-well MTP are indicated with two bars per position. **A)** Hydrolase plate I: in H11 is pGUF negative controle **B)** Hydrolase plate II: H11=pGUF **C)** Hydrolase plate III: H11=pGUF **D)** Hydrolase plate IV: A8=pGUF **E)** Hydrolase plate V: H10=pGUF **F)** Hydrolase plate VI: H10=pGUF. The positive control was alkaline phosphatase.

The protease activity screening using a combination of two artificial substrates, BA-*p*-NA and Leu-*p*-NA, resulted in the identification of three positive hits (Fig. 32, Tables 9 and S5). The expression strains carrying pGUF-*pa5028* (HY V, A11) and pGUF-*pa5396* (HY I, E3) showed high activities, which were 108 %, 237 % (assay 1, assay 2) and 123 %, 41 %, higher than Ave. + S.D. in two measurements, respectively.





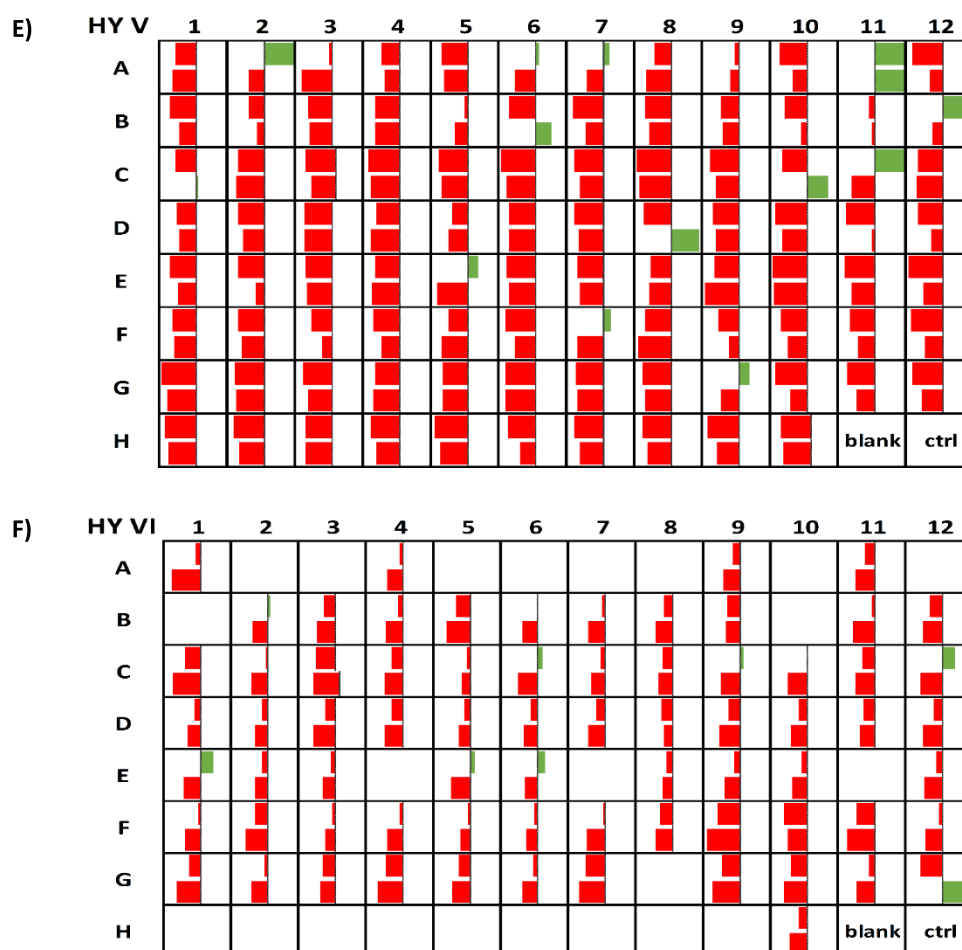
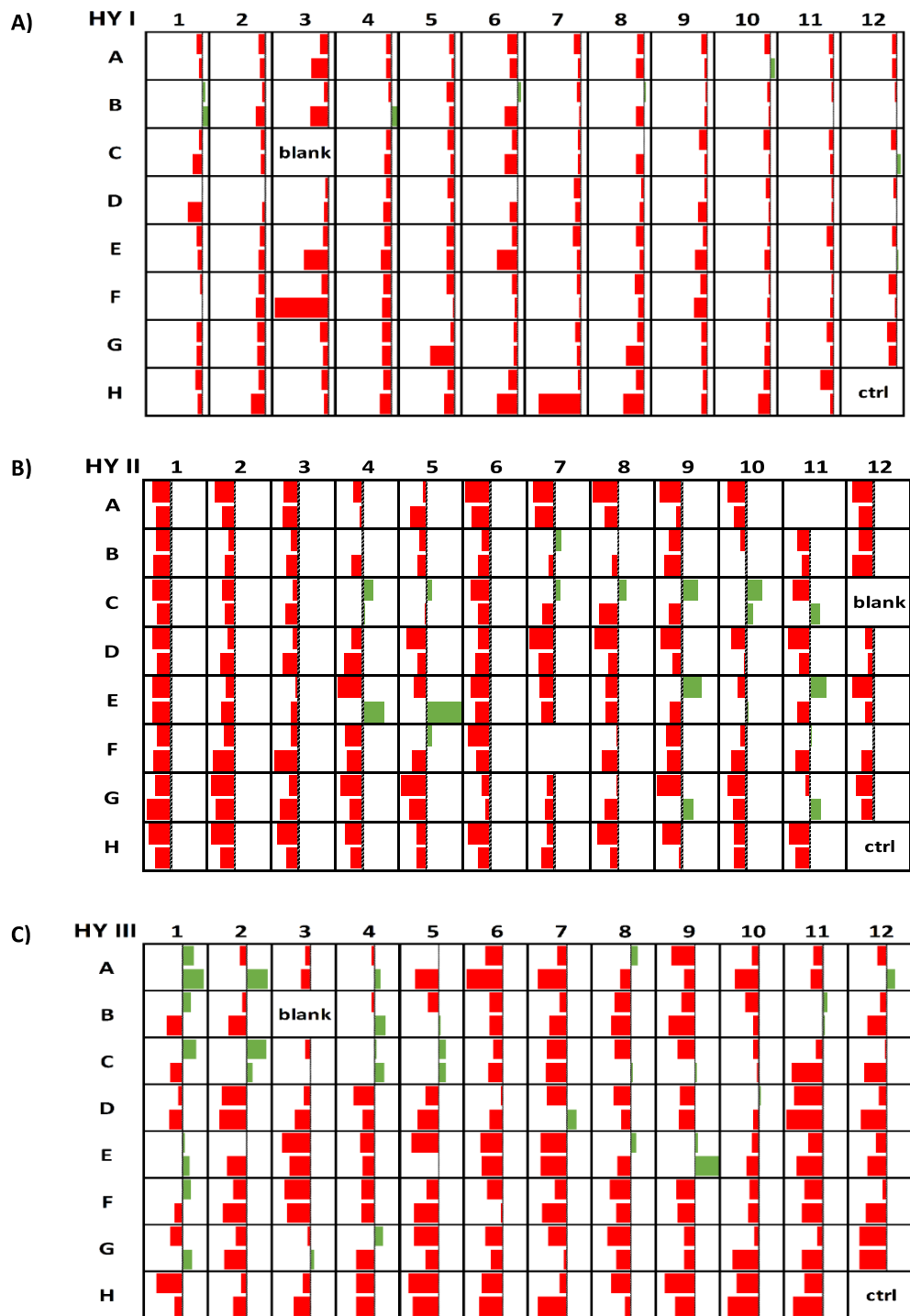


Fig. 32. Fingerprint showing the screening of protease activity measured with α -benzoyl-L-arginine-*p*-nitroanilide and L-leucine-*p*-nitroanilide. The 175 μ l of substrate cocktail containing 1 mM BApNA and 1 mM LeupNA was added to 25 μ l of cell lysates with $OD_{580} \approx 2$ and the absorbances at 412 nm were recorded during 30 min at 37 °C. The difference of A_{410nm} with the time normalized to OD_{580nm} , ($\Delta A_{410nm}/OD_{580nm}$) is considered as an activity. The bars represent the values of activity of the sample subtracted by Ave. + S.D. for each analyzed plate. The bars are scaled to minimal and maximal values of each plate and colored green or red to indicate positive and negative values, respectively. Two measurements for each sample in 96-well MTP are indicated with two bars per position. **A)** Hydrolase plate I: in H11 is pGUF negative controle **B)** Hydrolase plate II: H11=pGUF **C)** Hydrolase plate III: H11=pGUF **D)** Hydrolase plate IV: A8=pGUF **E)** Hydrolase plate V: H10=pGUF **F)** Hydrolase plate VI: H10=pGUF. Positive control was bovine trypsin.

The α/β -glucosidase screening using the mixture of artificial substrates, *p*-nitrophenyl- α -D-glucopyranosid and *p*-nitrophenyl- β -D-glucopyranosid, resulted in the identification of 17 positive hits (Fig. 33, Tables 9 and S5). The expression strain carrying pGUF-*pa1434* (HY II, C10) showed the highest activity, which was 60 % and 38 % (assay 1, assay 2) higher than Ave. + S.D., in two measurements. On the other hand, moderate activity was detected in a strain carrying pGUF-*pa2689* (HY III, A1) which showed a 12 % and 14 % increase relative to Ave. + S.D. in two measurements.



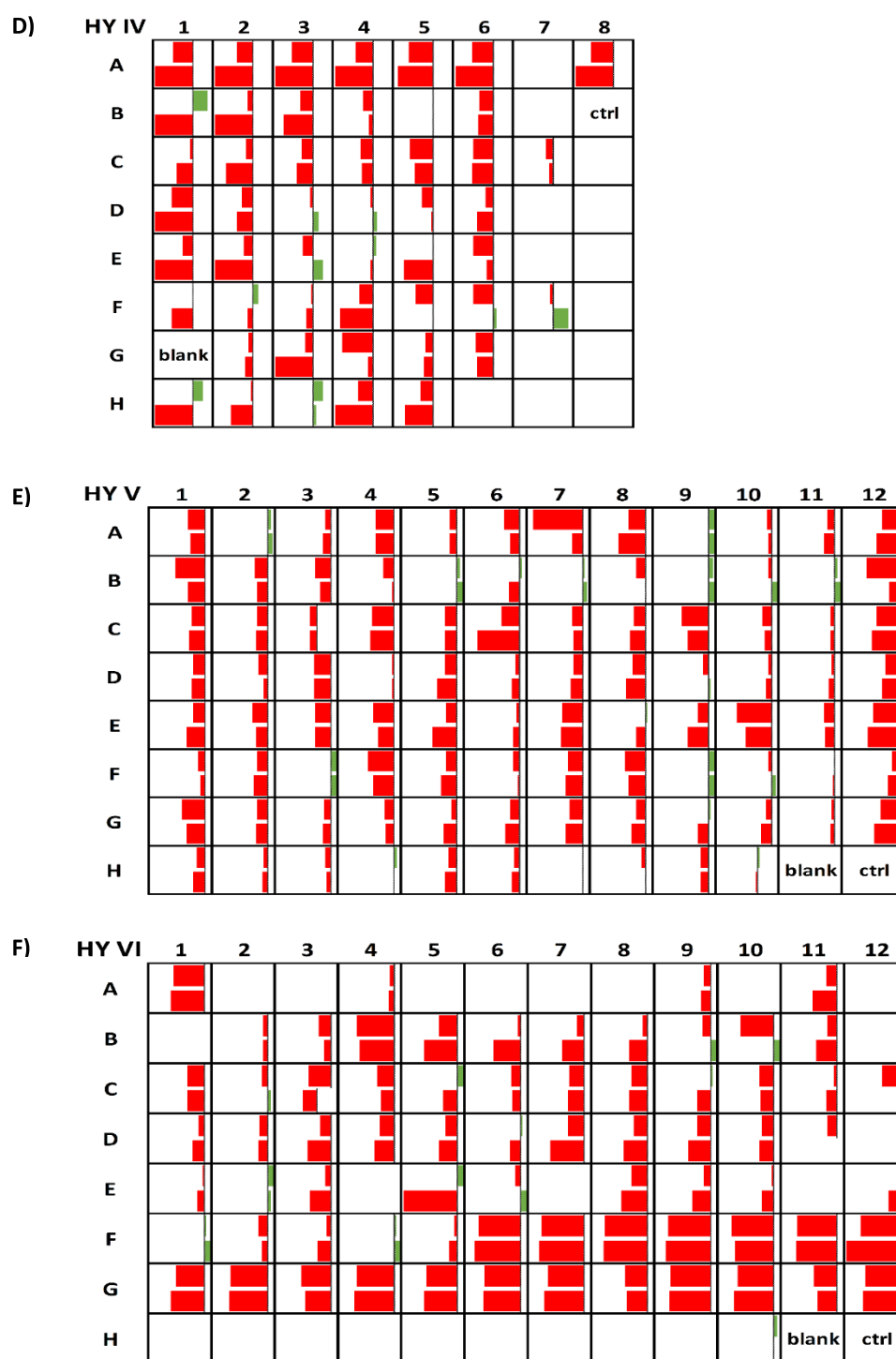


Fig. 33. Fingerprint showing the screening of α/β -glucosidase activity measured with *p*-nitrophenyl- α -D-glucopyranoside and *p*-nitrophenyl- β -D-glucopyranoside. The 175 μ l of substrate cocktail containing 1 mM 4-nitrophenyl- α -D-glucopyranoside, 1 mM 4-nitrophenyl- β -D-glucopyranoside and 0.1 mM glutathione was added to 25 μ l of cell lysates with $OD_{580} \approx 2$ and the absorbances at 410 nm were recorded during 30 min at 37 °C. The difference of A_{410nm} with the time normalized to OD_{580nm} , ($\Delta A_{410nm}/OD_{580nm}$) is considered as activity. The bars represent the values of activity of the sample subtracted by Ave. + S.D. for each analyzed plate. The bars are scaled to minimal and maximal values of each plate and colored green or red to indicate positive and negative values, respectively. Two measurements for each sample in 96-well MTP are indicated with two bars per position. **A)** Hydrolase plate I: in H11 is pGUF negative control **B)** Hydrolase plate II: H11=pGUF **C)** Hydrolase

plate III: H11=pGUF **D)** Hydrolase plate IV: A8=pGUF **E)** Hydrolase plate V: H10=pGUF **F)** Hydrolase plate VI: H10=pGUF.

Table 9. PUFs with high and moderate activities in hydrolase enzyme screenings.

Protein	Well - Plate	Enzyme activity	% difference to plate average + st. dev.*		% difference to pGUF [#]		Dot-blot [§]
			Assay 1	Assay 2	Assay 1	Assay 2	
PA0049	C11 - HY V	phospholipase C	28	28	49	46	-
PA0049	C11 - HY V	thioesterase	27	25	160	43	-
PA0057	B4 - HY VI	thioesterase	28	39	68	100	+
PA0387	C3 - HY III	phosphatase	33	16	-444	45	+
PA0449	B11 - HY I	thioesterase	10	46	11	2709	-
PA0543	A2 - HY V	lipase (<i>p</i> -NPdec)	10	11	23	24	-
PA0543	A2 - HY V	phosphodiesterase	30	51	44	85	-
PA0543	A2 - HY V	phospholipase C	15	26	34	44	-
PA0543	A2 - HY V	thioesterase	14	22	135	39	-
PA0629	D1 - HY IV	esterase	23	26	48	40	+
PA0731	F9 - HY VI	lipase (GTD)	13	24	87	-38	-
PA0788	B5 - HY V	lipase (<i>p</i> -NPdec)	15	15	28	28	-
PA0829	F12 - HY II	esterase	219	206	250	n.d.	+
PA0829	F12 - HY II	lipase (<i>p</i> -NPdec)	5134	341	649	1287	+
PA0978	B10 - HY V	phospholipase C	13	11	31	27	+
PA1062	G12 - HY VI	lipase (<i>p</i> -NPdec)	109	35	3282	-847	-
pa1115	G1 - HY III	esterase	25	16	75	17	-
PA1140	B1 - HY III	phosphodiesterase	19	10	46	24	-
PA1143	G11 - HY V	lipase (<i>p</i> -NPdec)	13	16	25	30	-
PA1193	F12 - HY I	phospholipase A	19	32	53	21	-
PA1198	B9 - HY V	phosphatase	15	12	28	28	+
PA1198	B9 - HY V	phosphodiesterase	23	21	36	49	+
PA1198	B9 - HY V	phospholipase C	19	21	38	38	+
PA1356	G9 - HY I	phosphatase	46	102	-9	153	+
PA1356	G9 - HY I	phospholipase C	95	71	105	226	+
PA1356	G9 - HY I	phosphodiesterase	17	22	-17	17	+
PA1434	C10 - HY II	glucosidase	60	38	822	771	+
PA1495	C12 - HY III	phosphodiesterase	33	11	63	26	+
PA1501	G1 - HY VI	esterase	41	43	321	676	-
PA1501	G1 - HY VI	thioesterase	21	17	59	70	-
PA1597	A9 - HY I	thioesterase	35	11	37	2033	+
PA1878	B12 - HY V	phosphodiesterase	19	17	32	43	-
PA1906	F7 - HY IV	phosphodiesterase	53	46	100	87	+
PA1906	G8 - HY VI	esterase	44	34	332	640	+
PA1918	E9-HY III	phospholipase C	11	64	40	252	-
PA1938	G8 - HY I	phospholipase C	19	87	25	238	+

PA2074	C1 - HY IV	esterase	17	17	41	31	+
PA2074	C1 - HY IV	phosphodiesterase	12	14	47	46	+
PA2074	C1 - HY IV	phospholipase C	14	19	43	45	+
PA2218	A4 - HY I	phosphatase	16	13	-28	41	+
PA2315	A8 - HY V	esterase	321	269	577	473	+
PA2315	A8 - HY V	lipase (GTD)	43	88	65	248	+
PA2419	G1 - HY I	lipase (GTD)	17	12	24	17	+
PA2419	G1 - HY I	phospholipase A	23	34	58	23	+
PA2625	A9 - HY V	lipase (<i>p</i> -NPdec)	13	17	26	31	-
PA2625	A9 - HY V	phospholipase C	19	18	38	35	-
PA2632	A5 - HY IV	esterase	13	13	35	26	+
PA2632	A5 - HY IV	phosphodiesterase	30	29	70	65	+
PA2632	A5 - HY IV	thioesterase	33	20	97	8	+
PA2689	A1 - HY III	esterase	10	26	54	30	+
PA2689	A1 - HY III	glucosidase	12	14	41	43	+
PA2693	A2 - HY II	thioesterase	14	11	22	23	+
PA2693	A2 - HY III	esterase	20	27	67	31	-
PA2729	E5 - HY III	phospholipase A	16	39	21	87	+
PA2801	F9 - HY V	lipase (<i>p</i> -NPdec)	13	14	26	27	+
PA2927	E7 - HY V	phospholipase A	234	226	356	282	+
PA2993	B3 - HY IV	phosphatase	26	10	37	1	-
PA3074	H3 - HY IV	esterase	16	21	40	36	+
PA3074	H3 - HY IV	phosphatase	68	74	83	60	+
PA3074	H3 - HY IV	phospholipase A	21	66	88	-12	+
PA3074	H3 - HY IV	phospholipase C	29	27	63	54	+
PA3087	E5 - HY VI	phosphatase	40	16	103	86	-
PA3087	E5 - HY VI	phosphodiesterase	19	36	76	109	-
PA3087	E5 - HY VI	thioesterase	34	22	76	76	-
PA3226	B10 - HY VI	thioesterase	14	37	50	98	-
PA3230	G4 - HY III	phosphodiesterase	31	34	60	51	+
PA3288	H8 - HY II	lipase (GTD)	14	34	39	8	+
PA3518	H1 - HY I	esterase	100	111	88	81	+
PA3586	B11 - HY VI	phospholipase C	20	25	13	28	-
PA3614	G4 - HY I	phosphatase	11	30	-31	63	+
PA3614	G4 - HY I	phospholipase C	89	43	98	205	+
PA3619	C4 - HY III	lipase (GTD)	14	14	29	19	+
PA3695	E2 - HY VI	phosphatase	17	10	69	77	+
PA3750	C1 - HY II	phospholipase A	56	626	128	670	+
PA3785	A7 - HY II	thioesterase	19	22	27	36	+
PA3886	A3 - HY II	phosphodiesterase	31	17	31	27	+
PA4440	C1 - HY VI	esterase	25	31	275	629	+
PA4792	H1 - HY II	esterase	18	12	29	n.d.	+
PA4968	B1 - HY I	lipase (GTD)	23	28	31	34	-

PA4968	B10 - HY I	thioesterase	21	58	22	2929	+
PA5028	A11 - HY V	phosphatase	13	15	26	31	-
PA5028	A11 - HY V	phosphodiesterase	12	34	24	65	-
PA5028	A11 - HY V	protease	108	237	316	597	-
PA5028	A11 - HY V	phospholipase C	37	18	59	35	-
PA5106	F3 - HY V	phosphatase	14	19	27	35	-
PA5396	E3 - HY I	protease	123	41	914	569	+
PA5481	H1 - HY III	esterase	36	21	90	23	+

*The increase in sample activity relative to plate (% difference to plate) was calculated using formula

$\frac{A_n - (\bar{A} + \sigma_A)}{|\bar{A} + \sigma_A|} \times 100 \%$, A_n - activity (absorbance difference) of a single sample in the plate ($n=1-95$), \bar{A} - average activity of all samples in a plate, σ_A - standard deviation of activities in a plate.

#The increase in activity of the sample relative to pGUF (% difference to pGUF) was calculated using formula

$\frac{A_n - A_{pGUF}}{|A_{pGUF}|} \times 100 \%$, A_n - activity (absorbance difference) of a single sample in the plate, A_{pGUF} - activity

measured in the cell lysate containing empty vector control (pGUF).

[§]PUFs whose expression was confirmed by dot-blot analysis are marked with the plus.

PUFs having a higher than 20 % of activity increase relative to the plate in both assays are underlined green.

n.d. = not determined

The expression and hydrolase screening of 460 PUFs, including 429 homology modeling predicted hydrolases led to an assignment of putative biochemical functions to 126 novel hydrolases of *P. aeruginosa* (Tables 9 and S5). Among them, 57 PUFs (Table 9) showed moderate and high activities, with thirty PUFs showing activities with several tested substrates. As many as 21 PUFs had activities > 40 % higher than the pGUF empty vector negative control. The positive signals in protein dot-blot were detected for 65 % of all PUFs positive in screening and nearly all (96 %) putative hydrolases with the highest activities.

3.5. Validation of hydrolase activities identified in the screening

The medium-throughput screening of enzyme activities using cell lysates might result in false-positive or false-negative results due to the complexity of cellular response to the overproduction of enzymes. Therefore, a new experiment under standard conditions was performed to increase the confidence in hydrolase activities detected in the screening. For this reason, the transformation of *E. coli* with selected pGUF constructs was conducted in Eppendorf tubes. The expression was carried in Erlenmeyer flasks or DWP, where each sample was surrounded by empty wells to eliminate the possibility of cross-contamination. Activ-

ity assays were repeated under identical conditions as in the screening, and the protein expression was analyzed by the Western blot.

The highest esterase activity with the *p*-NPB substrate in the screening was detected for pGUF-*pa2315* (Fig. 24-E, HY V, A8), whose activity was even 20-fold higher than the activity of pGUF (Table 9). In the validation experiment, *in vitro* esterase activity of PA2315 was confirmed as the activity of pGUF-*pa2315* was significantly ($p < 0.0001$) higher than the activity of pGUF control (Fig. 34). Additionally, the signal of recombinant PA2315 at the expected molecular size (42 kDa) was detected in Western blot (Fig. 34).

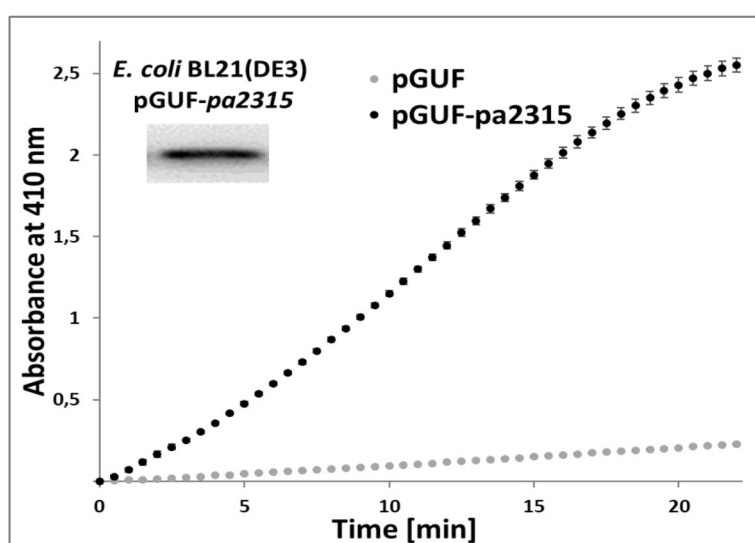


Fig. 34. Esterase activity and Western blot signal of recombinant PA2315 expressed from the pGUF-*pa2315* vector in *E. coli* BL21(DE3). Expression was performed in Erlenmeyer flask, in 5 ml AI medium for 20 h at 37 °C and 150 rpm. The assay was conducted with 25 µl of cell lysates $OD_{580} = 2$ and 175 µl of 1 mM *p*-NPB substrate in three technical replicates, and the increase of A_{410nm} was recorded at 37 °C. Inlet shows the Western blot signal (~42 kDa) from 15 µl cell lysates $OD_{580} = 15$ detected using 1:5000 anti-C-6xHis HRP conjugate antibody.

The moderate esterase activity with the *p*-NPB substrate in the screening was detected for pGUF-*pa2689* (Fig. 24-C, HY III, A12, and Table 9). The esterase activity assigned to PA2689 was reproduced as the activity of pGUF-*pa2689* was significantly higher than the pGUF control ($p < 0.05$), Fig. 35.

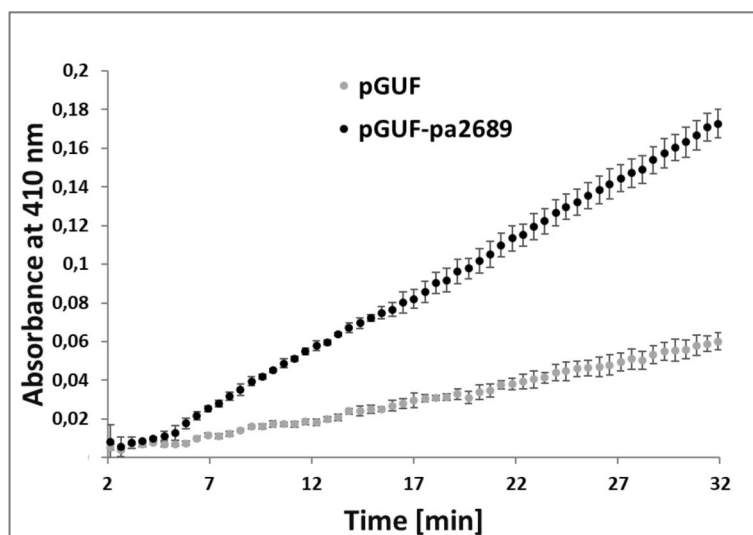


Fig. 35. Esterase activity of recombinant PA2689 expressed from pGUF-*pa2689* vector in *E. coli* BL21(DE3). The bacteria cultivated in 5 ml of TB medium in Erlenmeyer flask were induced for expression with 1 mM IPTG for 4 h at 37 °C and 150 rpm. The assay was performed with 25 μ l of cell lysates $OD_{580} = 2$ and 175 μ l of 1 mM *p*-NPB substrate in duplicates and the increase of A_{410nm} was recorded at 37 °C.

Low esterase activity was identified in the screening in the cell lysates containing pGUF-*pa3615* (Fig. 24-C, HY III, A12), whose activities were 23 % and 6 % higher than Ave. + S.D. of the plate and 2- and 1-fold higher than the pGUF (Table S5). In the separate experiment, *in vitro* esterase activity assigned to PA3615 was reproduced as the activity of pGUF-*pa3615* was significantly ($p < 0.05$) higher than the pGUF control (Fig. 36).

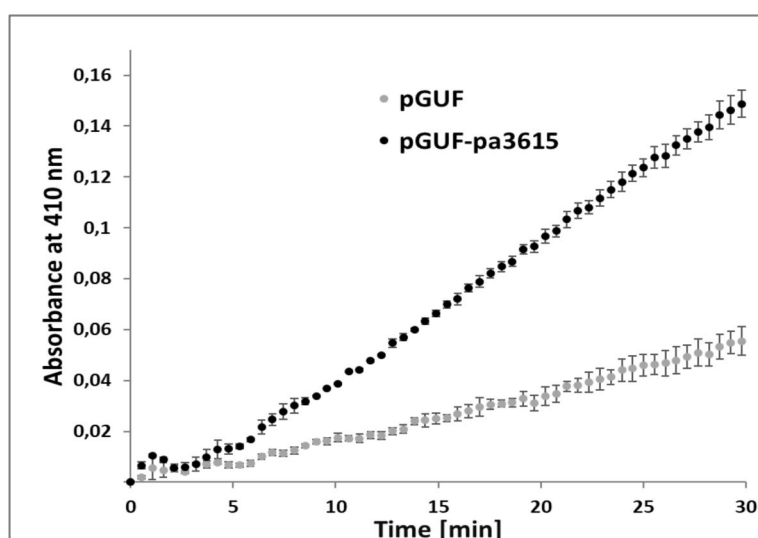


Fig. 36. Esterase activity of recombinant PA3615 expressed from pGUF-*pa3615* vector in *E. coli* BL21(DE3). The bacteria cultivated in 5 ml of TB medium in Erlenmeyer flask were induced for expression with 1 mM IPTG for 4 h at 37 °C and 150 rpm. The assay was performed with 25 μ l of cell lysates $OD_{580} = 2$ and 175 μ l of 1 mM *p*-NPB substrate in duplicates and the increase of A_{410nm} was recorded at 37 °C.

The pGUF-*pa2693* showed moderate esterase activity (Fig. 24-C, HY III, A2, and Table 9) and low thioesterase activity (Fig. 25-B, HY II, A2, and Table S5). In the validation experiments, esterase (Fig. 37-A) and thioesterase (Fig. 37-B) activities of pGUF-*pa2693* were significantly higher than the empty vector with $p < 0.05$ and $p < 0.01$, respectively.

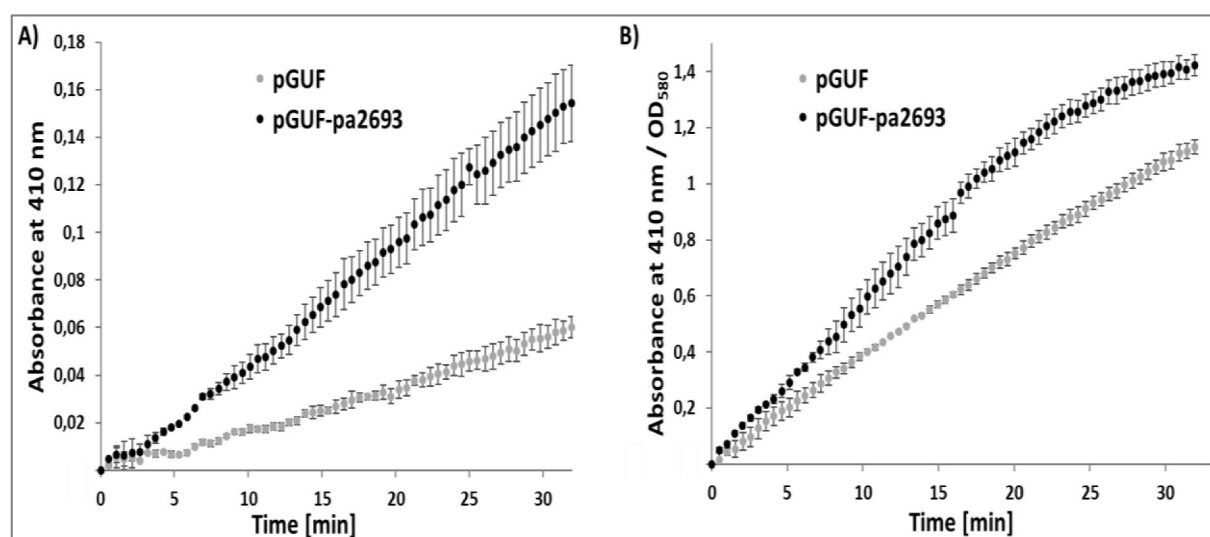


Fig. 37. Esterase (A) and thioesterase (B) activity of recombinant PA2693 expressed from pGUF-*pa2693* vector in *E. coli* BL21(DE3). Expression was conducted in Erlenmeyer flask, in 5 ml of autoinduction medium for 20 h at 37 °C and 150 rpm. **A)** Esterase assay was performed with 25 μ l of cell lysates OD₅₈₀ = 2 and 175 μ l of 1 mM pNPB substrate in triplicates and the increase of A_{410nm} was recorded at 37 °C. **B)** Thioesterase assay was performed with 25 μ l of cell lysates OD₅₈₀ \approx 2, 10 μ l 10 mM DTNB and 175 μ l substrate containing 40 μ M acetyl-CoA and 40 μ M palmitoyl-CoA of the substrate in triplicates and the increase of A_{410nm} was recorded at 37 °C.

The pGUF-*pa3518* at the H1 position in plate HY I showed high esterase activity in the screening (Fig. 24-A and Table 9). This was reproduced in the validation experiment (Fig. 38-A), in which the esterase activity of pGUF-*pa3518* was significantly higher than in the pGUF control ($p < 0.01$). Additional lipase activity with of *p*-nitrophenyl decanoate substrate was detected ($p < 0.0001$) (Fig. 38-B). The presence of the signal at the expected molecular size in the Western blot of cell lysate sample used for enzyme assay additionally supported the finding that recombinant PA3518 is a novel esterase and lipase.

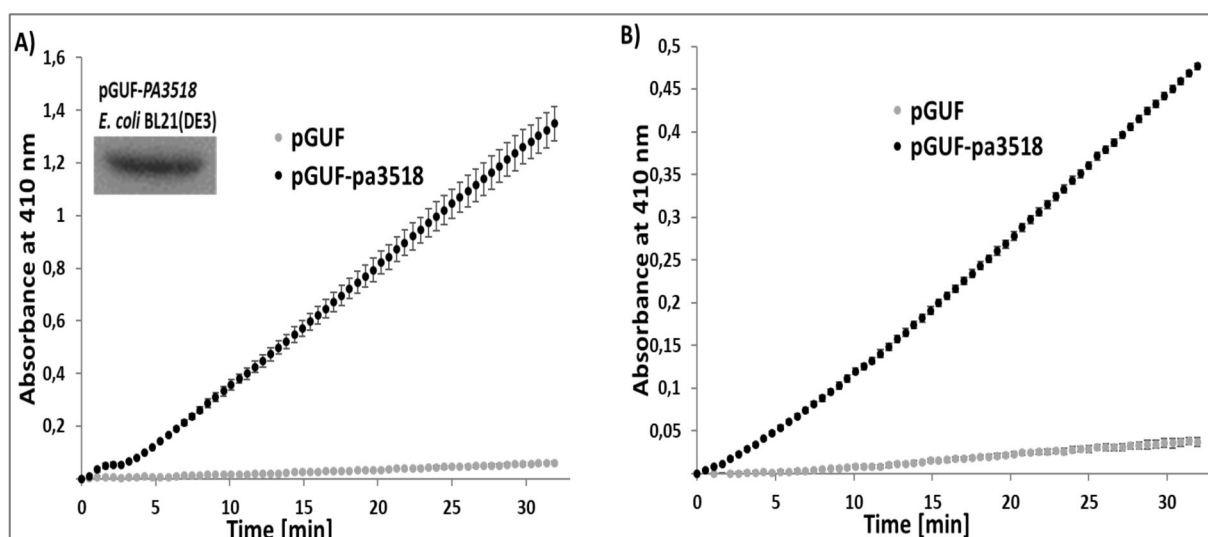


Fig. 38. Esterase (A) and lipase (B) activity of recombinant PA3518 expressed from pGUF-*pa3518* vector in *E. coli* BL21(DE3). The bacteria cultivated in 5 ml of TB medium in Erlenmeyer flask were induced for expression with 1 mM IPTG for 4 h at 37 °C and 150 rpm. **A)** Esterase assay was performed with 25 μ l of cell lysates $OD_{580} = 2$ and 175 μ l of 1 mM pNPB substrate in triplicates and the increase of A_{410nm} was recorded at 37 °C. The Western blot signal (37.5 kDa) from 15 μ l cell lysates $OD_{580} = 15$ was detected using a 1:5000 anti-C-6xHis HRP conjugated antibody. **B)** Lipase assay was performed with 25 μ l of cell lysates $OD_{580} = 2$ and 175 μ l of 1 mM p-nitrophenyl decanoate substrate in triplicates and the increase of A_{410nm} was recorded at 37 °C.

High esterase (Fig. 24-B and Table 9) and lipase activities (Fig. 26-B and Table 9) in cell lysates containing pGUF-*pa0829* at the F12 position in plate HY II detected in the screening were reproduced in the validation experiment, in which measured the esterase (Fig. 39-A) and lipase (Fig. 39-B) activities of pGUF-*pa0829* were significantly higher than empty vector with $p < 0.01$ and $p < 0.0001$, respectively.

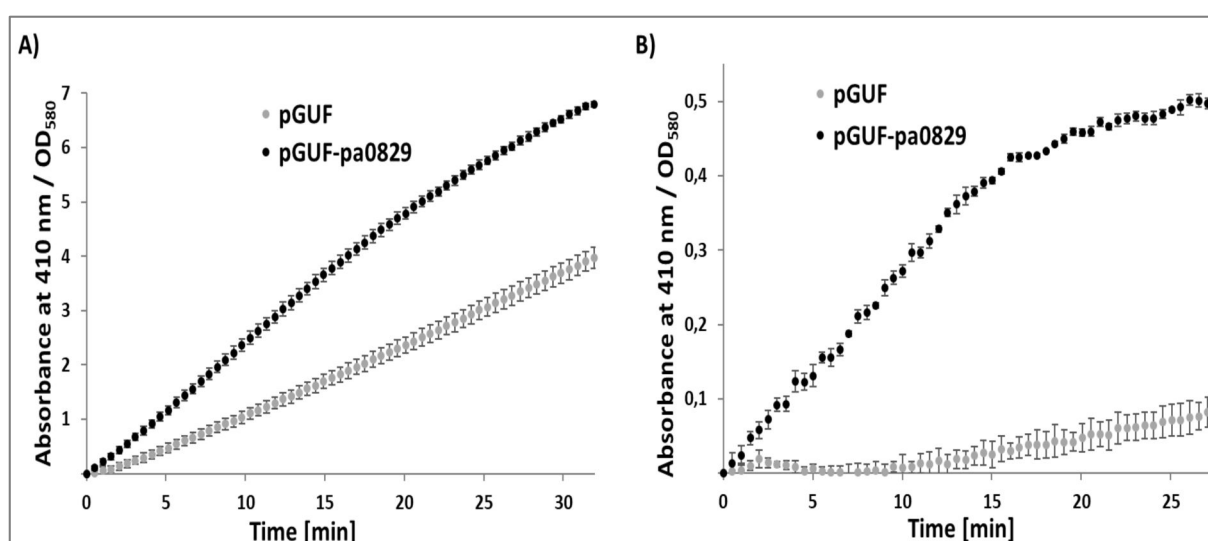


Fig. 39. Esterase (A) and lipase (B) activity of recombinant PA0829 expressed from pGUF-*pa0829* vector in *E. coli* BL21(DE3). Expression was conducted in Erlenmeyer flask, in 5 ml of autoinduction medium for 20 h at 37 °C and 150 rpm. **A)** Esterase assay was performed with 25 µl of cell lysates $OD_{580} \approx 2$ and 175 µl of 1 mM pNPB substrate in triplicates and the increase of A_{410nm} was recorded at 37°C. **B)** Lipase assay was performed with 25 µl of cell lysates $OD_{580} \approx 2$ and 175 µl of 1 mM p-nitrophenyl decanoate substrate in triplicates and the increase of A_{410nm} was recorded at 37 °C.

The highest PLA activity detected in the screening with natural phospholipid substrates was in the cell lysates containing pGUF-*pa3750* (Fig. 28-B, HY II, C1, and Table 9). In a validation experiment, the phospholipase A2 activity of PA3750 was confirmed by measuring the hydrolysis of diheptanoyl thio-PC substrate from the sPLA2 Cayman kit, as the activity of pGUF-*pa3750* was significantly ($p < 0.05$) higher than the activity of the empty vector (Fig. 40). The presence of the band at the expected molecular size in the Western blot of cell lysate sample used for enzyme assay additionally supported the finding that recombinant PA3750 is a novel PLA.

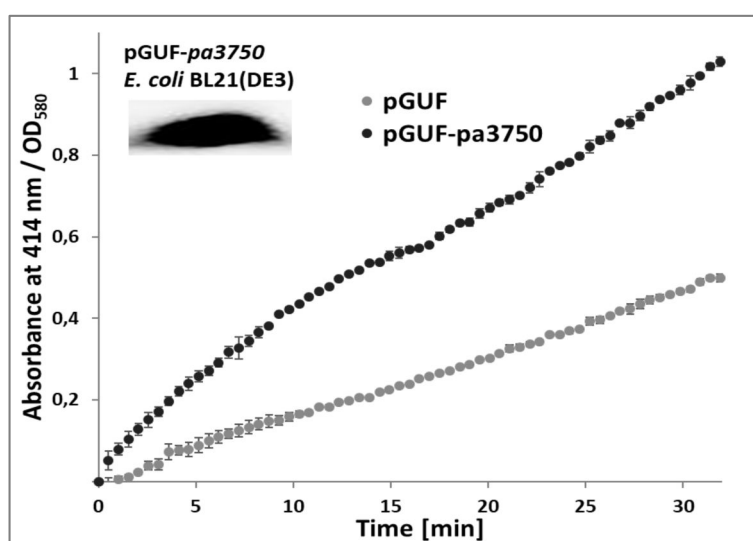


Fig. 40. Phospholipase A2 activity of recombinant PA3750 expressed from pGUF-*pa3750* vector in *E. coli* BL21(DE3). Expression was conducted in 1 ml of autoinduction medium in DWP for 20 h at 37 °C and 1000 rpm. The assay was performed with 20 µl of cell lysates $OD_{580} \approx 2$, 10 µl of 10 mM DTNB and 175 µl of 1.66 mM diheptanoyl thio-PC substrate in triplicates following sPLA₂ Cayman kit instructions. The Western blot signal (26 kDa) from 15 µl cell lysates $OD_{580} = 15$ was detected using a 1:5000 anti-C-6xHis HRP conjugate antibody.

The pGUF-*pa2419* at the G1 position in plate HY I showed strong phospholipase A and moderate lipase activities in the screening (Table 9). The phospholipase A2 activity of pGUF-*pa2419* was significantly higher than the empty vector ($p < 0.05$) as measured using dihep-

tanoyl thio-PC substrate from the sPLA2 Cayman kit (Fig. 41-A) and also in repeated NEFA assay ($p < 0.05$), (Fig. 41-B). The presence of the signal at the expected molecular size in the Western blot of cell lysate sample used for enzyme assay additionally supported the finding that recombinant PA2419 is a novel PLA.

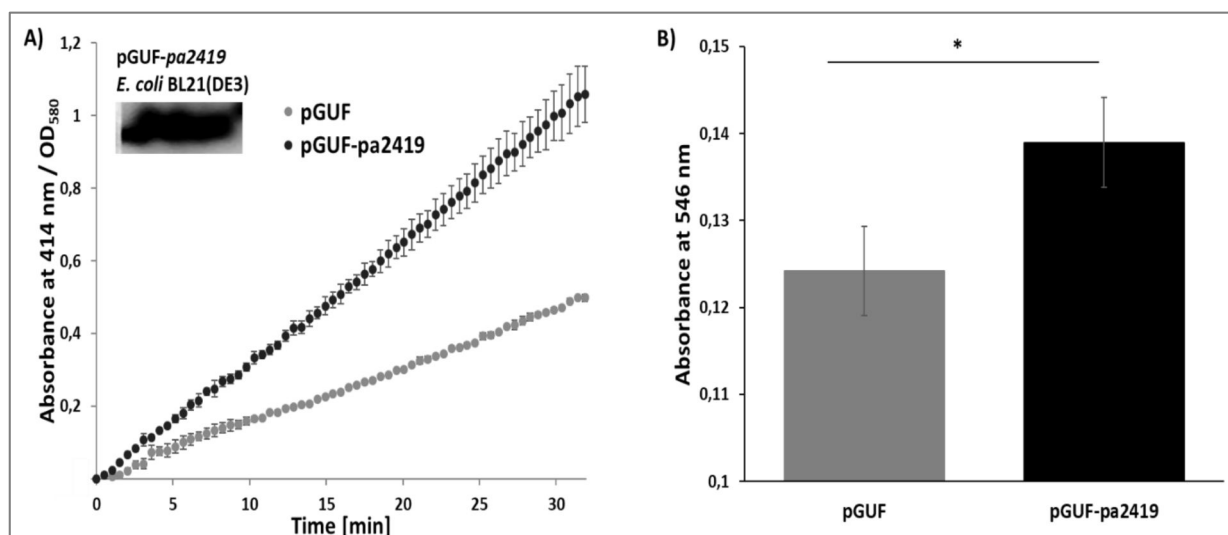


Fig. 41. Phospholipase A2 activity of recombinant PA2419 expressed from pGUF-pa2419 vector in *E. coli* BL21(DE3). Expression was conducted in 1 ml of autoinduction medium in DWP for 20 h at 37 °C and 1000 rpm. **A)** Assay was performed with 20 μ l of cell lysates OD₅₈₀ \approx 2, 10 μ l DTNB and 175 μ l of diheptanoyl thio-PC substrate in triplicates following sPLA₂ Cayman kit instructions. The Western blot signal (24 kDa) from 15 μ l cell lysates OD₅₈₀ = 15 was detected using a 1:5000 anti-C-6xHis HRP conjugate antibody. **B)** Assay was performed in triplicates by incubating 10 μ l of cell lysates with OD₅₈₀ = 0.4 and 10 μ l of 16:0 PC, PE and PG phospholipid emulsion for 24 h at 37 °C and subsequently free fatty acid quantification following NEFA kit instructions.

The pGUF-pa2660 at the G2 position in plate HY III showed low activity in the NEFA phospholipase A assay (Table S5). In the validation experiment using the sPLA2 Cayman kit, the absorbance increase of pGUF-pa2660 was higher than the empty vector but not significant ($p = 0.08$, Fig. 42-A). However, a significant ($p < 0.05$) difference was observed after prolonged incubation of cell lysate with the substrate (Fig. 42-B). This might be due to low expression, as the signal of PA2660 in Western blot could not be detected.

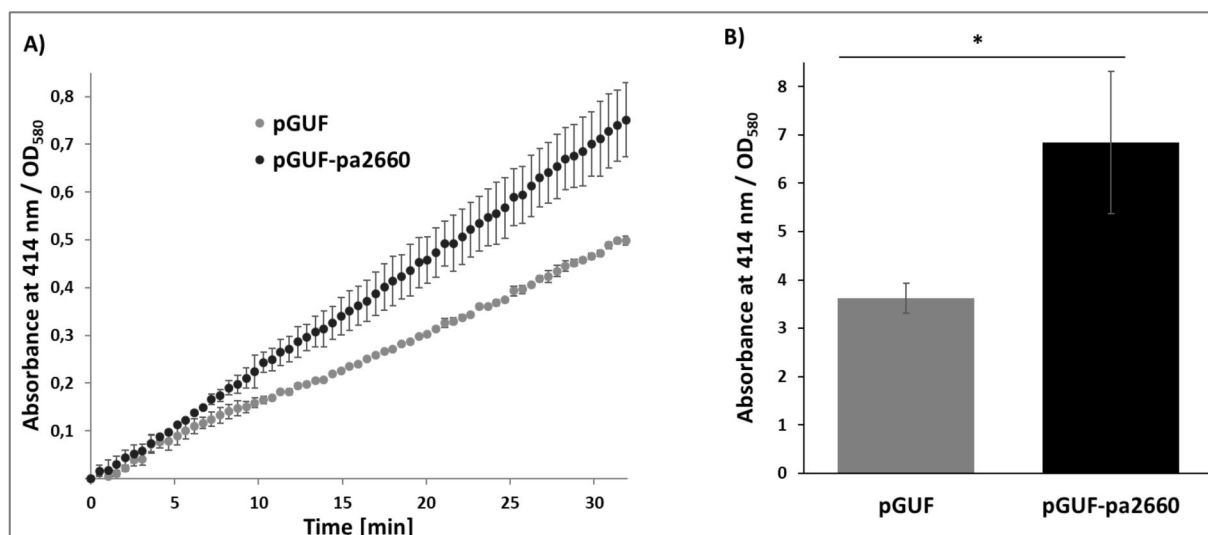


Fig. 42. Phospholipase A2 activity of recombinant PA2660 expressed from pGUF-pa2660 vector in *E. coli* BL21(DE3) in 1 ml of autoinduction medium. Expression was conducted in 1 ml of autoinduction medium in DWP for 20 h at 37 °C and 1000 rpm. The assay was performed with 20 μ l of cell lysates OD₅₈₀ \approx 2, 10 μ l 10 mM DTNB and 175 μ l of 1.66 mM diheptanoyl thio-PC substrate in triplicates following sPLA₂ Cayman kit instructions. **A)** The A_{414nm} was continuously measured for 30 min. **B)** The activity of the same samples was measured after 3 h incubation at r.t.

The pGUF-pa0484 at the E3 position in plate HY III showed low PLA activity in the NEFA phospholipase A assay (Table S5). In the validation experiment using the sPLA₂ Cayman kit, the absorbance increase of pGUF-pa0484 measured during 30 min was higher than in the empty vector but not significantly ($p = 0.13$, Fig. 43-A). However, a significant difference was observed after prolonged incubation (3 h) at r.t. ($p < 0.05$, Fig. 43-B). This might be due to low expression, as the signal in the Western blot could not be detected.

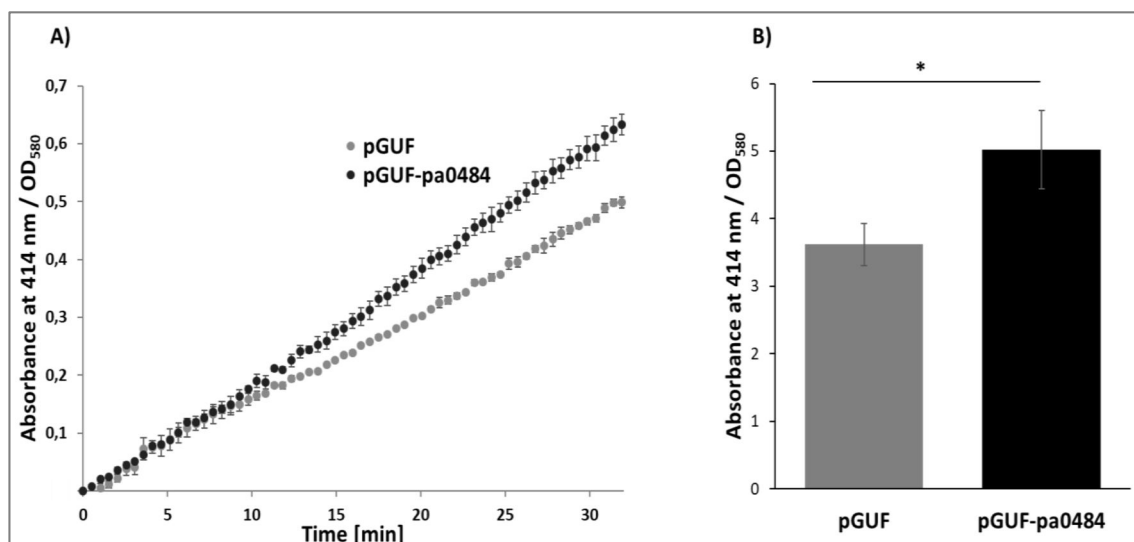


Fig. 43. Phospholipase A2 activity of recombinant PA0484 expressed from pGUF-pa0484 vector in *E. coli* BL21(DE3). Expression was conducted in 1 ml of autoinduction medium in DWP for 20 h at 37 °C and 1000 rpm. The assay was performed with 20 μ l of cell lysates OD₅₈₀ \approx 2, 10 μ l of 10 mM DTNB and 175 μ l of 1.66 mM di-heptanoyl thio-PC substrate in triplicates following sPLA₂ Cayman kit instructions. **A)** The A_{414nm} was continuously measured for 30 min. **B)** The A_{414nm} of the same samples was measured after 3 h at r.t.

The pGUF-pa1193 at the F12 position in plate HY I showed moderate phospholipase A activity and low lipase activity with natural substrates in NEFA assay in screening (Table 9 and Table S5). In the validation experiment, phospholipase A activity was confirmed using natural substrates measured with NEFA assay, as the activity of pGUF-pa1193 was significantly higher than the activity of the empty vector with $p < 0.05$ (Fig. 44). The presence of the signal at the expected molecular size in the Western blot of cell lysate sample used for enzyme assay additionally supported the finding that recombinant PA1193 is a novel PLA.

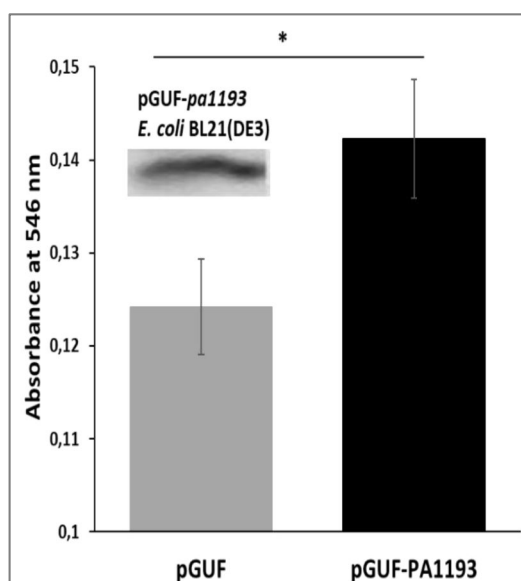


Fig. 44. Phospholipase A activity of recombinant PA1193 expressed from pGUF-pa1193 vector in *E. coli* BL21(DE3) in 5 ml of TB medium with 1 mM IPTG. The assay was performed in triplicates by incubating 10 μ l of cell lysates with OD₅₈₀ = 0.4 and 10 μ l of 16:0 PC, PE and PG phospholipid emulsion for 24 h at 37 °C, and subsequently free fatty acid quantification following NEFA kit instructions. The Western blot signal (25 kDa) from 15 μ l cell lysates OD₅₈₀ = 15 was detected using a 1:5000 anti-C-6xHis HRP conjugate antibody.

The pGUF-pa5535 (HY III, H2) showed low phospholipase A activity in screening (Table S5) with NEFA assay. In a repeated experiment using the NEFA kit (Fig. 45-A), the absorbance increase of pGUF-pa5535 was higher than in the empty vector but not significantly ($p = 0.14$). However, a significant difference ($p < 0.01$) was measured after 3 h of incubation at r.t. with diheptanoyl thio-PC substrate in the Cayman sPLA2 assay kit (Fig. 45-B).

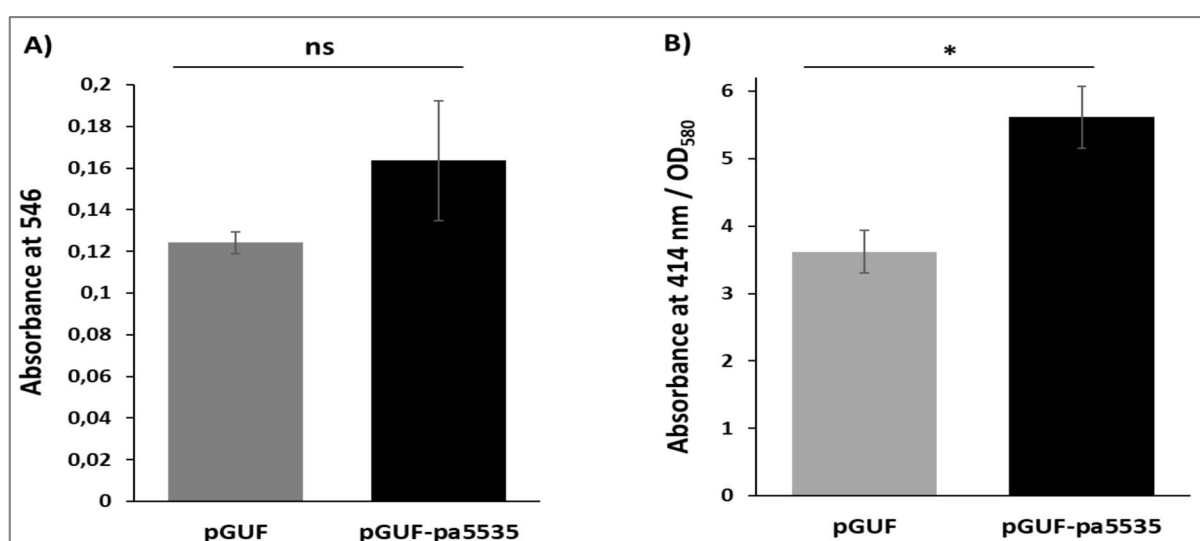


Fig. 45. Phospholipase A activity of recombinant PA5535 expressed from pGUF-pa5535 vector in *E. coli* BL21(DE3) in 1 ml of autoinduction medium in DWP. **A)** The assay was performed in triplicates by incubating

10 μ l of cell lysates with $OD_{580} = 0.4$ and 10 μ l of 16:0 PC, PE, and PG phospholipid emulsion for 24 h at 37 °C, and subsequently free fatty acid quantification following NEFA kit instructions. **B)** PLA2 activity was measured with 20 μ l of cell lysates $OD_{580} \approx 2$, 10 μ l of 10 mM DTNB and 175 μ l of 1.66 mM diheptanoyl thio-PC substrate in triplicates following sPLA₂ Cayman kit instructions.

The pGUF-*pa4961* at the G9 position in plate HY II showed low phospholipase C activity (Table S5). However, high PLC activity was detected in the repeated experiment, showing significantly higher PLC activity of pGUF-*pa4961* in comparison to the empty vector ($p < 0.01$) (Fig. 46), although a Western blot signal was not detected.

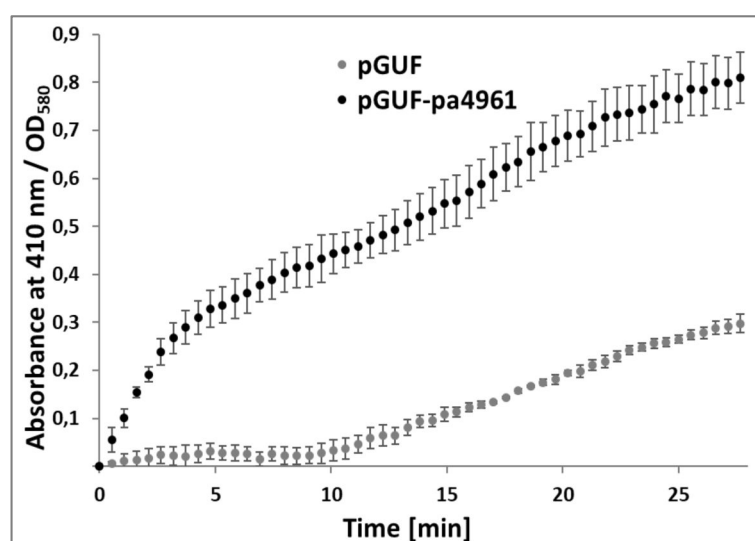


Fig. 46. Phospholipase C activity of recombinant PA4961 expressed from pGUF-*pa4961* vector in *E. coli* BL21(DE3) in 1 ml of autoinduction medium in DWP. The assay was performed with 25 μ l of cell lysates $OD_{580} \approx 2$ and 175 μ l of 2 mM *p*-NPPC substrate in triplicates and the absorbance at 410 nm were recorded during 30 min at 37 °C.

The pGUF-*pa0285* showed high phospholipase C activity in the preliminary screening experiment (data not shown). The PLC activity was confirmed in a repeated experiment, in which significantly higher PLC activity of pGUF-*pa0285* compared to the empty vector with $p < 0.01$ was detected (Fig. 47).

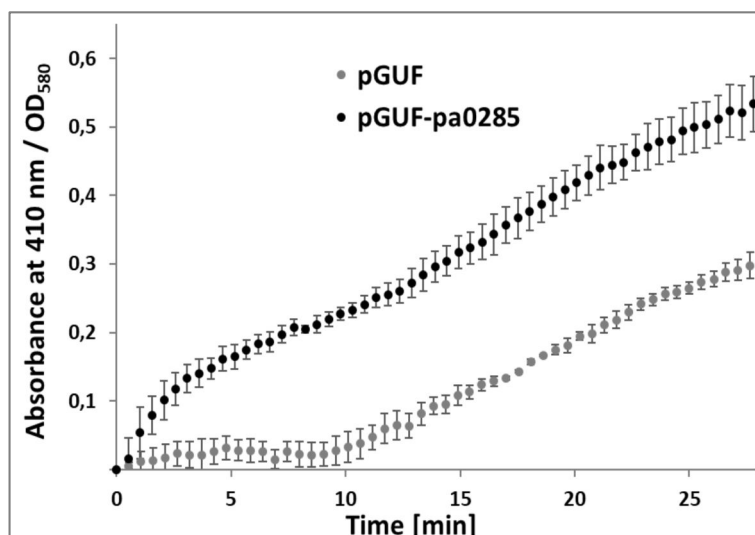


Fig. 47. Phospholipase C activity of recombinant PA0285 expressed from pGUF-*pa0285* vector in *E. coli* BL21(DE3) in 1 ml of autoinduction medium in DWP. The assay was performed with 25 μ l of cell lysates $OD_{580} \approx 2$ and 175 μ l of 2 mM *p*-NPPC substrate in triplicates and the absorbances at 410 nm were recorded during 30 min at 37 °C.

The pGUF-*pa5028* at the A11 position in plate HY V showed high protease and moderate phosphodiesterase, phosphatase, and PLC activities in the screening experiment (Table S5). However, only phosphodiesterase activity could be confirmed in the validation experiment, as the activity of pGUF-*pa5028* was significantly higher than in the empty vector with $p < 0.01$ (Fig. 48). The presence of the band at the expected molecular size in the Western blot of cell lysate sample used for enzyme assay additionally supported the finding that recombinant PA5028 is a novel hydrolase.

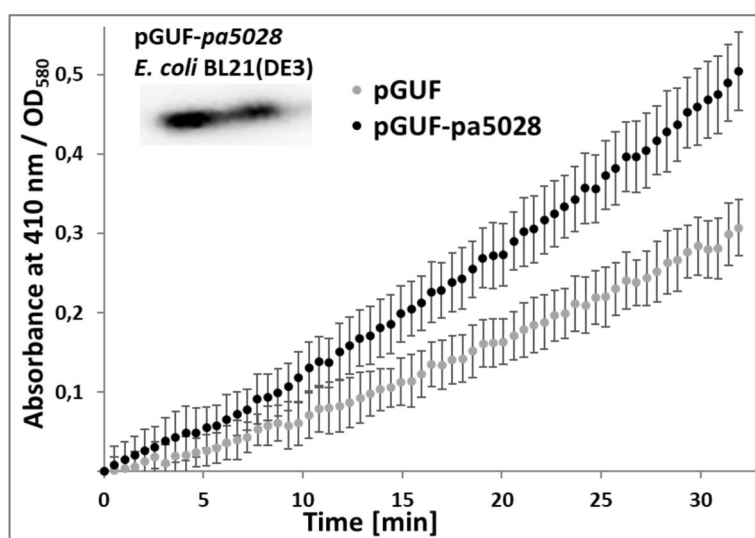


Fig. 48. Phosphodiesterase activity of recombinant PA5028 expressed from pGUF-*pa5028* vector in *E. coli* BL21(DE3) in 1 ml of autoinduction medium in DWP. The assay was performed with 25 μ l of cell lysates $OD_{580} \approx 2$ and 175 μ l of 2 mM bis-*p*-NPP substrate in triplicates and the absorbance at 410 nm were recorded for 30 min at 37 °C. The Western blot signal (28.6 kDa) from 15 μ l cell lysates $OD_{580} = 15$ was detected using a 1:5000 anti-C-6xHis HRP conjugate antibody.

The pGUF-*pa0543* at the A2 position in plate HY V was positive for several activities in the screening, showing high phosphodiesterase, moderate PLC and thioesterase (Table 9), and low phosphatase activities (Table S5). In the validation experiments, the phosphodiesterase activity was confirmed as the absorbance increase of pGUF-*pa0543* was significantly higher than the empty vector with $p < 0.05$ (Fig. 49-A). Furthermore, phosphatase activity was also validated (Fig. 49-B). Other activities were not tested, and the Western blot signal could not be detected.

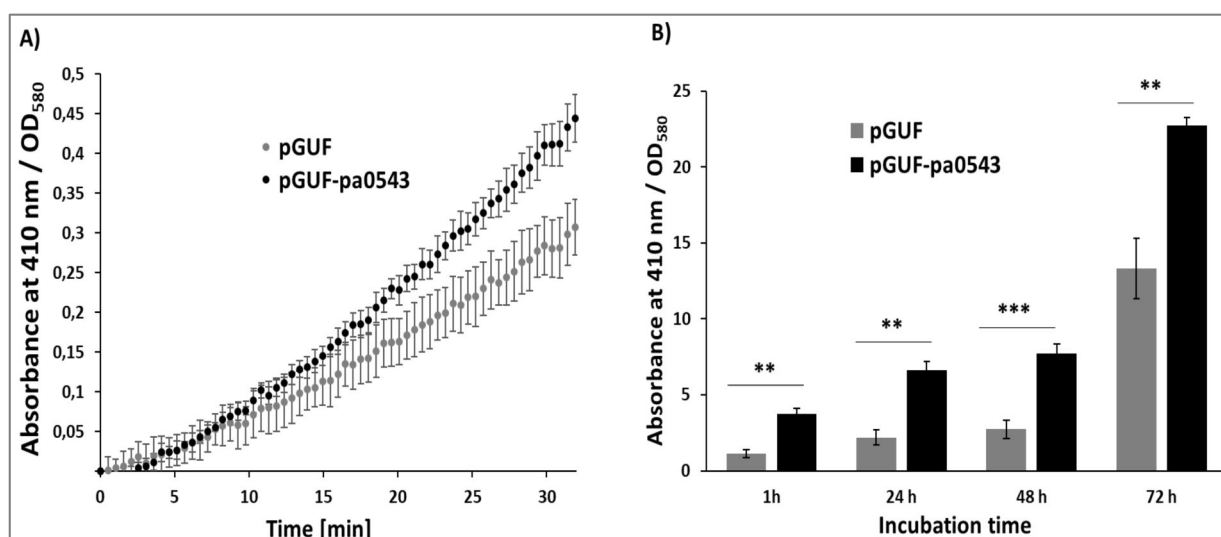


Fig. 49. Phosphodiesterase (A) and phosphatase (B) activity of recombinant PA0543 expressed from pGUF-*pa0543* vector in *E. coli* BL21(DE3) in 1 ml of autoinduction medium in DWP. A) Phosphodiesterase assay was performed with 25 μ l of cell lysates $OD_{580} \approx 2$ and 175 μ l of 2 mM bis-*p*-NPP substrate in triplicates and the absorbances at 410 nm were recorded during 30 min at 37 °C. B) Phosphatase assay was performed in triplicates by incubating 25 μ l of cell lysates $OD_{580} \approx 2$ with 175 μ l of 10 mM *p*-NPP substrate at room temperature and recording A_{410nm} after 1, 24, 48, and 72 h.

The pGUF-*pa3074* at the H3 position in the plate HY IV was identified as positive in the screening in several assays, showing high phosphatase, phospholipases C and A activities (Table 9), low esterase, phosphodiesterase, and glucosidase activities (Table S5). The phos-

phodiesterase ($p < 0.01$, Fig. 50-A) and phosphatase (Fig. 50-B) activities of pGUF-*pa3074* were significantly higher than the empty vector in the validation experiments.

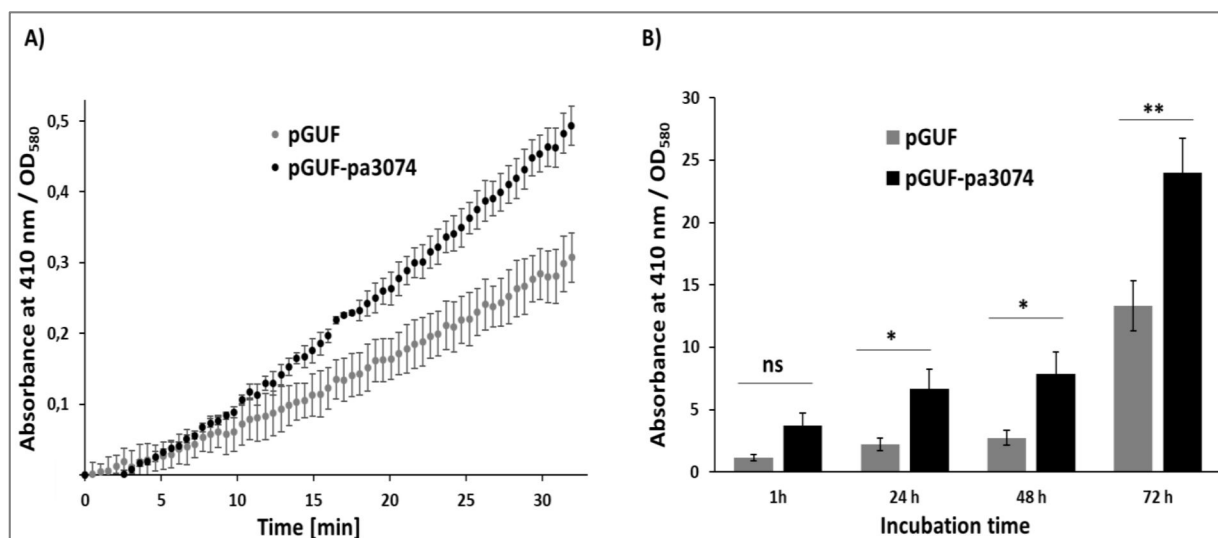


Fig. 50. Phosphodiesterase (A) and phosphatase (B) activity of recombinant PA3074 expressed from pGUF-*pa3074* vector in *E. coli* BL21(DE3) in 1 ml AI medium in DWP. A) Phosphodiesterase assay was performed with 25 μ l of cell lysates OD₅₈₀ \approx 2 and 175 μ l of 2 mM bis-pNPP substrate in triplicates and the increase of A_{410nm} was recorded at 37 °C. **B)** Phosphatase assay was performed in triplicates by incubating 25 μ l of cell lysates OD₅₈₀ \approx 2 and 175 μ l of 10 mM *p*-NPP substrate at room temperature and recording A_{410nm} after 1, 24, 48, and 72 h.

The PA1089 is an example of a protein whose phosphatase activity was bioinformatically predicted but was not detected in the screening. However, in the repeated experiment, pGUF-*pa1089* showed significantly higher phosphatase activity than the empty vector strain (Fig. 51). This can be due to an improved expression rate in the repeated experiment, as the expected molecular size bend was detected (Fig. 51).

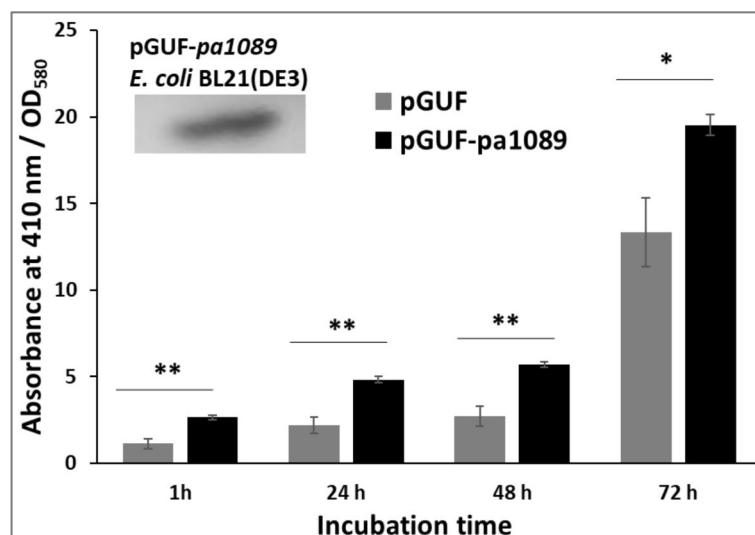


Fig. 51. Phosphatase activity of recombinant PA1089 expressed from pGUF-*pa1089* vector in *E. coli* BL21(DE3) in 1 ml AI medium. Phosphatase assay was performed in triplicates by incubating 25 μ l of cell lysates OD₅₈₀ \approx 2 and 175 μ l of 10 mM *p*-NPP substrate at room temperature and recording A_{410nm} after 1, 24, 48, and 72 h. The Western blot signal (22.5 kDa) from 15 μ l cell lysates OD₅₈₀ = 15 was detected using a 1:5000 anti-C-6xHis HRP conjugate antibody. ** indicates $p < 0.01$.

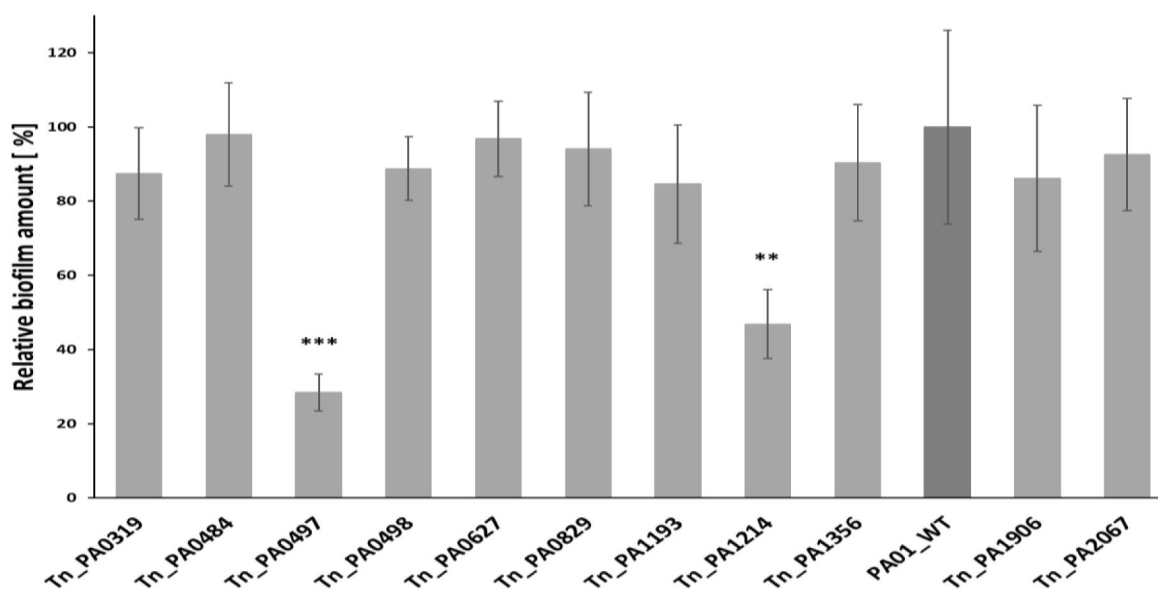
Conclusively, five esterase (PA2315, PA3615, PA2693, PA3518, PA0829), one thioesterase (PA2693), two lipase (PA0829, PA3518), six phospholipases A (PA3750, PA2419, PA2660, PA0484, PA1193 and PA5535), two phospholipase C (PA4961, PA0285), three phosphodiesterase (PA5028, PA0543, PA3074, PA1214) and three phosphatase (PA0543, PA3074, PA1089) activities of *P. aeruginosa* PUFs were validated which strongly suggest that these proteins are novel hydrolases.

3.6. Biological roles of characterized *P. aeruginosa* GUFs

After identifying novel *in vitro* hydrolase activities of *P. aeruginosa* genes, the further step was to examine the biological context and significance of their biochemical functions for *P. aeruginosa* physiology. Since many *P. aeruginosa* hydrolases are involved in virulence, toxicity, and biofilm formation (Chapter 1.5.), these traits were measured in *P. aeruginosa* PA01 transposon mutant strains of the investigated genes and compared to the respective wild-type strain. To ensure comparability, the original *P. aeruginosa* PA01 wild-type strain (Washington wild-type), used to generate the transposon-mutant library, was included in these assays.

3.6.1. Novel *P. aeruginosa* biofilm effectors

The biofilm formation assay under static conditions was performed in 96-well MTPs containing 7-8 biological replicates of transposon mutants, the wild-type strain, and several medium controls to test the influence of validated hydrolases on biofilm. In addition to the genes with validated hydrolase activities, the genes with bioinformatically predicted biofilm-relevant functions, including putative adhesins *pa0498* and *pa0497*, putative lectins *pa5033*, *pa0627*, and *pa5178*, and putative pili biogenesis factor *pa5441*, were also analyzed.



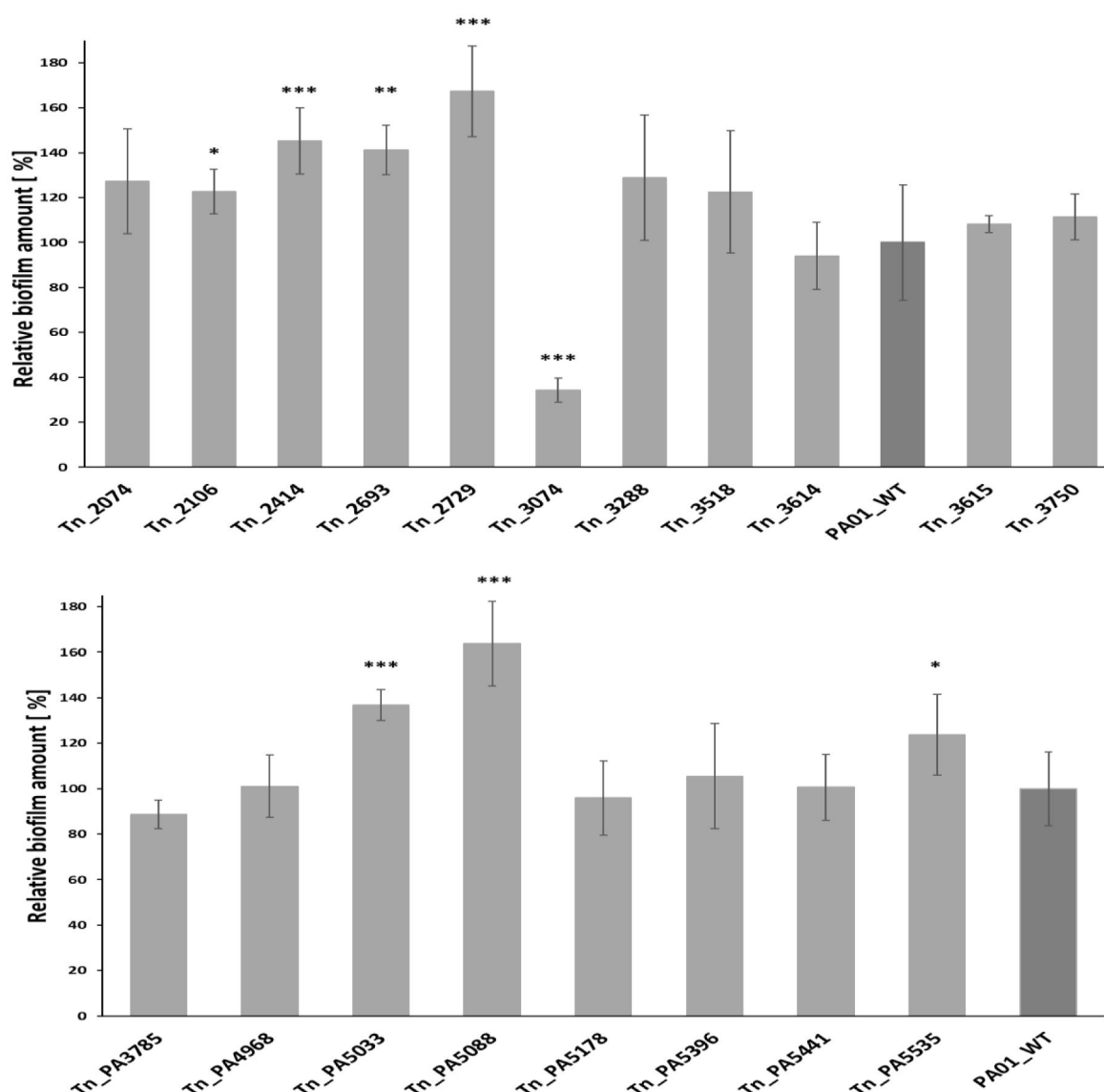


Fig. 52. Biofilm formation assay with *P. aeruginosa* transposon mutants (Tn). For each strain, 7-8 clones from LB agar plate were inoculated in 100 μ l LB medium in 96-well MTP and the cultivation preceded for 16 h at 37 $^{\circ}$ C without shaking. Upon the end of the cultivation, OD₅₈₀ was measured and the biofilm was stained with 0.1 % (w/v) crystal-violet and quantified at A_{550nm}. Biofilm amount normalized to OD₅₈₀ is shown as a percentage of the biofilm produced by the wild-type (WT), which is set to 100 %. ** indicate $p \leq 0.01$ and *** $p \leq 0.001$ for *** in a two-sample unequal variance t-test.

In the crystal-violet biofilm assay (Fig. 52), three transposon mutant strains produced significantly less biofilm than the wild-type under tested conditions. Transposon mutant of *pa0497* gene (Tn_PA0497) produced 72 % less biofilm, *pa1214* gene (Tn_PA1214) produced 53 % less biofilm and *pa3074* (Tn_PA3074) produced 66 % less biofilm than the wild-type. In addition to negative effectors of biofilm, seven mutant strains (Tn_PA2106, Tn_PA2419, Tn_PA2693, Tn_PA2729, Tn_PA5033, Tn_PA5088, Tn_PA5535) produced significantly (p

<0.05) more (23 – 67 %) biofilm (Fig. 52). Among identified biofilm effectors, the proteins with verified *in vitro* hydrolase activity are phosphatase/phosphodiesterase PA3074, phospholipases A PA2419 and PA5535, and thioesterase PA2693.

3.6.2. Novel *P. aeruginosa* virulence factors in the *Galleria mellonella* model

The corresponding transposon mutants were tested in *G. mellonella* caterpillar larvae virulence assay to examine the virulence role of selected *P. aeruginosa* genes. This assay is shown to be a suitable and not-demanding infection model for *P. aeruginosa*, allowing the assessment of temperature-dependent virulence factors due to its growth at 37 °C. [281]

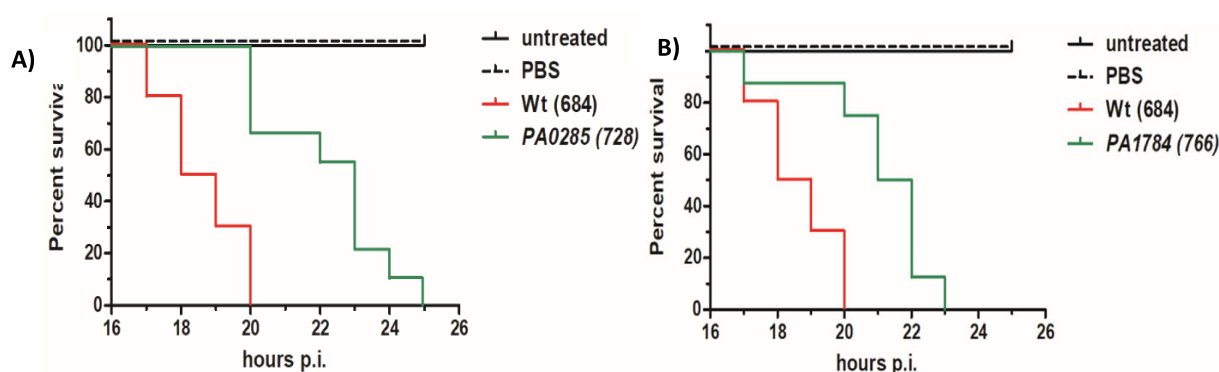


Fig. 53. Kaplan-Meier plots of *P. aeruginosa* transposon mutant strains of PA0285 (A) and PA1784 (B) in *G. mellonella* virulence assay. The representative plots show larvae survival 24 h after injection of 500 bacterial cells. Two independent experiments with ten larvae per test group were conducted. The percentage of survival was determined relative to the untreated (not infected) group, while PBS-treated larvae served as negative controls. Wt - wild type, PBS - phosphate saline buffer, p.i. – post-infection. WT plots in panels A and B are identical. The experiment was performed by Dr. S. Felgner at the Institute for Molecular Bacteriology in Braunschweig.

In Fig. 53-A, a significant difference in survival rates between *P. aeruginosa* Tn_PA0285 transposon mutant and Wt strain is observed, as *P. aeruginosa* WT killed 50 % of larvae, while all larvae injected with Tn_PA0285 strain remained alive 18 h after injection. Two hours later, all the larvae infected with *P. aeruginosa* WT strain were dead, while the survival rate of larvae infected with Tn_PA0285 strain was 70 %. The inactivation of the PA0285 gene prolonged the larvae's life for five hours.

Similarly, 18 h after the infection with *P. aeruginosa* WT strain, 50 % of larvae died, opposite to only 10 % of larvae infected with Tn_PA1784 strain. Two hours later, all the larvae infected with *P. aeruginosa* WT strain were dead, while the survival rate of larvae infected with

Tn_PA1784 strain was 75 %. Conclusively, *pa0285* and *pa1784* genes were identified as novel putative virulence factors in the *G. mellonella* infection model.

3.7. Inhibition of virulence factor LecB sugar-binding activity by glycoamidoamines

The potential of synthetic glycoamidoamines as anti-virulence drugs was examined by testing their competitive inhibitory effect on virulent factor lectin LecB fucose binding and *P. aeruginosa* PA01 biofilm formation. The tested compounds consisted of an amidoamine oligomer backbone functionalized with 1, 2, 3, 4 and 6 fucose units (K. Bücher, Ph.D. thesis, HHU Düsseldorf, 2019). The glycooligomers containing three fucose units were synthesized by variation of spacing between the fucose, giving three different compounds. The method used to test their inhibitory potency was modified enzyme-linked lectin assay (mELLA), in which binding of LecB to the fucosylated surface of 96-well MTP was quantified by measuring the luminescence signal originating from LecB-specific antibody. In addition, the decrease in luminescence signal upon the addition of glycoamidoamines (2×10^{-7} - 9 mM concentration range) was measured to identify the most potent inhibitor (the one with the lowest IC₅₀ value).

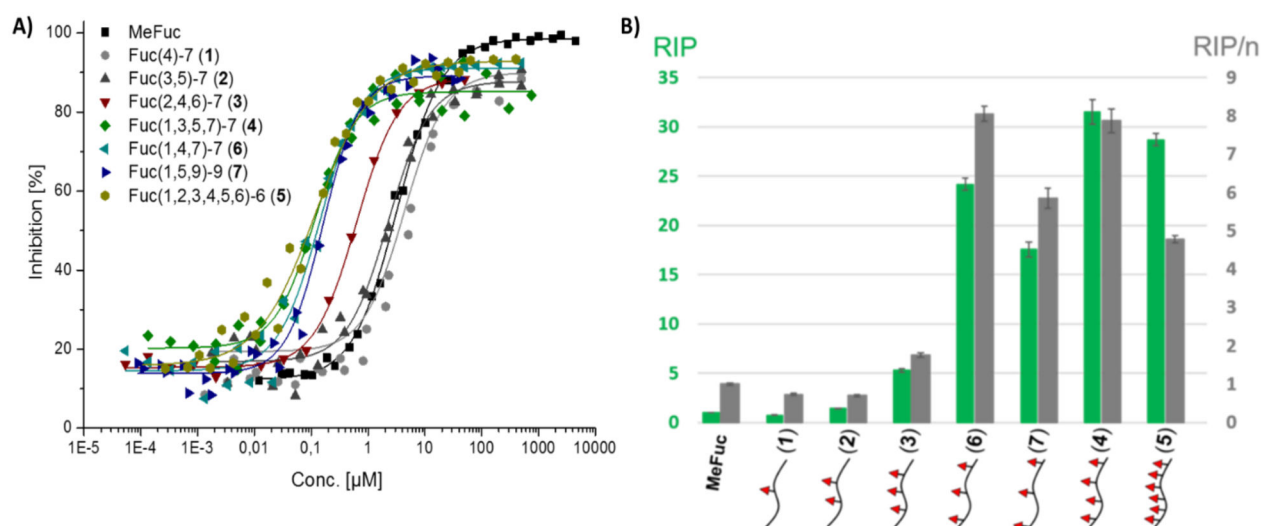


Fig. 54. Inhibition of LecB binding to α -L-fucose-PAA-biotin by glycoamidoamines [267] **A)** Inhibition curves of fucosylated glycooligomers and α -L-methylfucose obtained after testing their effect on LecB binding to α -L-fucose-PAA-biotin in mELLA assay. Sigmoidal inhibition curves represent averaged three independent experiments performed in triplicates. The percentage of inhibition was calculated according to the equation $(A_{\text{without inhibitor}} - A_{\text{inhibitor}}) / A_{\text{without inhibitor}} \times 100 \%$ and IC₅₀ values were obtained from inhibition curves using sigmoidal logistic fit in OriginPro. **B)** Relative inhibitory potencies (RIP) and inhibitory potencies per fucose unit (RIP/n) of seven glycooligomers, whose schematic structures are depicted underneath the diagram. The inhibitors 3, 6

and 7 have 3 fucose units with different spacing between them. $RIP = IC_{50} (MeFuc)/IC_{50} (glycooligomer)$. Errors are standard errors of the mean (SEM) of nine independent measurements. The purified LecB was provided by T. Schwabroch (HHU Düsseldorf).

The inhibition curves (Fig. 54-A) showed that glycooligomers with 1 and 2 fucose units have similar IC_{50} values as the methyl-fucose, glycooligomer with 3 fucose units and the lowest spacing is in the middle, while two oligomers with 3 fucose units, but the larger spacing between them, and oligomers with 4 and 6 fucose units behave relative similar and have the lowest IC_{50} values. For better comparison of inhibitors, their IC_{50} values were normalized to IC_{50} of methyl fucose standard (labeled as RIP, relative inhibitory potencies) and the number of fucose units (RIP/n). The RIP values presented in Fig. 54-B showed that the most potent oligomers contained four and six fucose units, demonstrating 31 and 29-fold better binding to LecB than the modified natural ligand, α -L-methyl-fucose, respectively. Although the general tendency of increase in RIP with the increase in the number of fucose moieties is observable, it is not linear, as the highest RIP per fucose unit is obtained for glycooligomers with 4 and 3 fucose molecules

In the biofilm formation assay performed in the presence of 2 mM fucosylated glycooligomers, the reduction of *P. aeruginosa* PA01 biofilm amount up to 20 % was observed (Fig. 55).

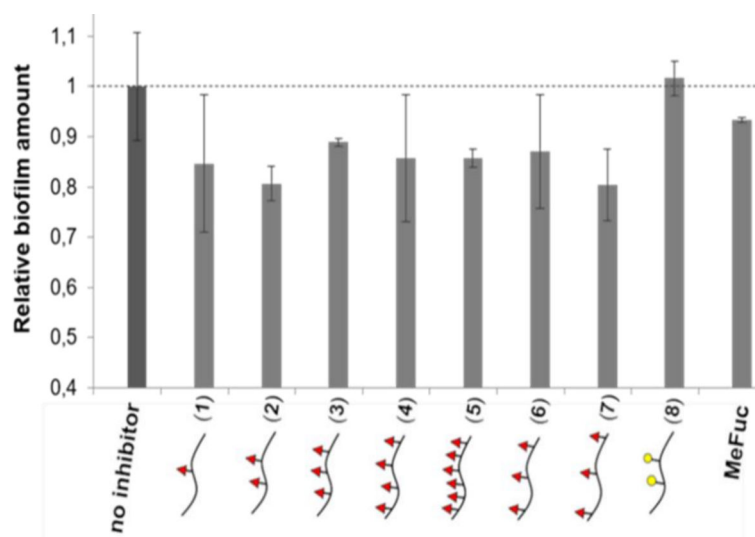


Figure 55. Biofilm formation assay with *P. aeruginosa* incubated with glycoamidoamine inhibitors. [267]

Inhibitory effect of glycooligomers 1 – 7 (2 mM) on the formation of *P. aeruginosa* PA01 biofilm in a microtiter plate after 21 h incubation. The attached biofilm was quantified with crystal violet. The mean \pm standard errors of three independent experiments are normalized to cultures grown without an inhibitor.

4. Discussion

Given that a) functional annotations for even more than 50 % of genes are unknown, uncertain, or incorrect [282], and b) the number of new sequences deposited in databases is exponentially growing, a reliable, functional characterization of these genes is an important striving in contemporary biology. However, the pace of experimental functional characterization significantly lags behind the sequencing projects, as less than 1 % of protein sequences in the Uniprot database had an experimentally confirmed function by April 2019. [283] This also negatively reflects the investigation of virulence factors and drug targets of pathogenic bacteria, including *P. aeruginosa*, which has nearly 40 % of GUFs (Fig. 3). [284] Considering the large number of GUFs in prokaryotic genomes, a bioinformatically guided high-throughput experimental approach is recommended by the Enzyme Function Initiative, a consortium assembled to promote a multidisciplinary approach to identifying novel enzymes in bacteria. [285]

In this project, the medium-throughput cloning and expression pipeline (Fig. 15) for screening several hundreds of *P. aeruginosa* proteins of unknown function, whose hydrolytic activities were predicted by a structure homology modeling-based approach (Fig. 6), was established. The screening resulted in the assignment of *in vitro* hydrolase functions to 18 PUFs (Table 10). Further analysis of these genes led to identifying two putative virulence factors (*pa0285*, *pa1784*) and three biofilm effectors (*pa3074*, *pa1214*, *pa0497*). These five proteins are novel candidates for anti-virulence drug targets. Moreover, Phyre2 homology modeling resulted in confident hints for further investigation of biochemical or biological functions for the additional 1249 GUFs. [286]

4.1. Structure homology modeling guided deciphering the functions of *P. aeruginosa* GUFs

Bioinformatics methods are valuable tools to guide and complement experimental work in the genomic era. The methods used to assign putative biochemical functions to proteins mostly rely on protein sequence or structure similarities or integrate both. Comparative genomics uses information about genes of similar sequences to predict their biological functions. [287] Besides the standard sequence similarity analysis by the BLAST algorithm, more sophisticated methods for functional annotations of genes have emerged, including phylo-

genetic relationships, functional domain recognition, and identification of gene operon/metabolic genomic context. [283, 285, 288] Comparative genomics was previously used to identify the genes which might be promising drug targets.

One approach encompassed the comparison of the genomes of 100 *P. aeruginosa* clinical isolates containing highly-virulent strains with the genomes of less virulent strains to identify the virulence-relevant genes. [289] Similarly, differential genome analysis of *H. pylori* with its closest relatives, *H. influenzae* and *E. coli* allowed the identification of species-specific genes, thereby narrowing down the search for genes involved in interactions with the host. [290] Besides assisting in identifying anti-virulence drug targets, comparative genomics is useful for identifying promising antibiotic targets. A good antibiotic should target essential bacterial gene, preferably conserved within several pathogen strains (broad-range). Furthermore, it should exert no or minimum toxic effect on a host. In the work of Sakharkar *et al.* (2004), [291] 306 *P. aeruginosa* genes were identified as promising antibiotic drug targets by BLASTP analysis, which revealed that these genes share homology to essential genes of other bacteria deposited in DEG (Database of Essential Genes) and do not have homologs within the human genome. [291] These criteria indicate that drugs targeting these genes might be effective antibiotics exerting weak or no toxic effects on humans.

To find the promising drug targets among *P. aeruginosa* GUFs, they were scrutinized according to the comparative genomic PGD annotations to identify proteins with sequence homologs among human proteins, other pathogenic bacteria, and well-known virulence factors (Fig. 3). Compared to similar work [291], the essentiality was not ascribed based on sequence similarity with the essential genes in other bacteria but exclusively based on the experimental data obtained by generating transposon mutant libraries. [292] The analysis revealed that most *P. aeruginosa* GUFs (96 %) do not have human homologs and are therefore expected to be safe targets (Fig. 4). Among them, highly prioritized targets for novel antibiotic and antivirulence drugs include 106 GUFs with essential, pathology-related, or virulence functions (Fig. 4). Conclusively, the genomics mining of 2137 *P. aeruginosa* GUFs narrowed the search for novel drug targets by more than 20-fold.

Furthermore, the prioritization of GUFs aimed to identify the genes with putative hydrolase functions for experimental characterization because many pathology and virulence relevant proteins belong to this enzyme family. [293] Functional prediction based on comparing sequences appears to be reliable only when sequence similarity is very high. [294] One of the

reasons this approach should be taken with caution is that duplicates of genes can divergently evolve into proteins with different functions [295]. Furthermore, proteins can be homologous although they do not share significant sequence similarity; their homology relies on significant structural similarity or high sequence similarity to an intermediate sequence. In these cases, 3D structural information can significantly contribute to protein annotation since, in evolution, protein folds are often kept conserved long after sequences are strongly changed. [296] Moreover, certain structural features can be correlated with specific biochemical function, e.g. the identification of an active site groove or ligand-binding sites, such as helix-turn-helix secondary structures, which are often found in DNA binding proteins. [295] Therefore, one of the approaches to annotate functions of hypothetical proteins is computational structural genomics, in which experimental determination of protein structures is followed by bioinformatics analysis of obtained structure. [297, 298] Since the structures of most proteins with unknown functions are still unknown (94 % of *P. aeruginosa* PUFs have unknown structures), *in silico* methods for the prediction of model structures are used. One of the most often used internet servers for protein structure prediction is Phyre2, which relies on template-based modeling, in which protein structure is built according to the homologous template(s) with known structure. [274] The advantage of this method is that it can detect remote homologs and accurately model protein structures even if sequence identity to a known protein structure is less than 20 % [275]. This was observed for the homology modeling of 2137 *P. aeruginosa* PUFs, as the majority of the proteins were confidently modeled, despite low sequence identities (Fig. 5-A). Besides here presented genome-wide functional annotations of *P. aeruginosa* PUFs [299], Phyre2 server was used for genome-wide analysis of *M. tuberculosis* [300], *M. mycoides* [301] and *T. pallidum* [302]. In all studies, the functions of modeled proteins were predicted from the functions of corresponding reliable templates. To define a reliable template, the main criterium in modeling 4160 *M. tuberculosis* proteins and 2137 *P. aeruginosa* PUFs was the confidence of modeling, which was set to be greater than 75 %. For modeling 149 *M. mycoides* PUFs [301] and 978 *T. pallidum* proteins [302], confidence greater than 90 % was used. It is thought that higher modeling confidence results in a more reliable structural model; however, a confidence cut-off for functional annotation *via* homology modeling is not clearly defined. [275] A total of 1589 (74 %) of modeled *P. aeruginosa* PUFs satisfied confidence criteria (Fig. 5-B), similar to those reported for *M. tuberculosis* (80 % reliably modeled proteins) [300]. The remaining 548 *P. ae-*

aeruginosa PUFs might have very distant homologs, or the structures of their homologs were not yet solved [302], or they have developed unique folds that cannot be matched with any fold in the library. A second criterium, related to the size of protein aligned to the template, was applied to assign the biochemical functions (enzyme, transport, ligand-binding) among *P. aeruginosa* PUFs modeled with high confidence. As modeled PUFs have different sizes, we did not consider the alignment coverage parameter as in the above-mentioned studies [300], but set the criterium that the range of protein aligned to the template should be at least the average domain size, which is 50 amino acids for ligand-binding domains and 100 amino acids for enzymes and transporters [299]. This resulted in the assignment of putative biochemical functions to 1267 PUFs, including 1020 putative enzymes, 486 ligand-binding proteins, and 155 transport proteins (Fig. 7-A). Notably, some proteins have two or three assigned functions, which is reasonable in multi-template homology modeling, as many enzymes and transporters bind cofactors and large proteins usually have more domains, exerting different functions. [299] The enzyme function is assigned to the largest number of *P. aeruginosa* PUFs and enzymes are also the most abundant among essential and virulence-related PUFs (Fig. 7-C). This is understandable, taken that enzymes have great importance for various processes in a cell. Putative hydrolases and transferases were the most abundant functions in *P. aeruginosa* PUF (Fig. 8-A) and interestingly, the same observation emerged after homology modeling of *T. pallidum* PUFs [302]. As concluded in the previous studies [300, 302], Phyre2 is a useful complementary tool in the functional annotation of genes to other bioinformatics methods and databases, and this was also observed for *P. aeruginosa* PUFs (Table 10). Eight of 18 proteins with experimentally validated hydrolase activities (Table 10) had enzyme subclass correctly predicted by Phyre2. In the case of PA2315, PA0829, PA2660, PA0285 and PA5028, Phyre2 prediction was more accurate or precise in comparison to sequence-based Uniprot functional annotations obtained by InterPro domain prediction or Gene Ontology phylogenetic or sequence computational analysis (Table 10).

Table 10. Phyre2 models and Uniprot annotations of proteins with validated *in vitro* hydrolase activities.

Gene	Validated activity	Uniprot annotation	Phyre2 hydrolase template(s)
PA2315	esterase	β -lactamase domain (InterPro)	esterase ^{T1-T6,T9} , β -lactamase ^{T7,T8} , amidase ^{T10}
PA3615	esterase	AMP nucleosidase (GO)	phosphoribohydrolase ^{T1-T3,T8-9}
PA2693	esterase, thioesterase	Acyl-CoA hydrolase (GO)	thioesterase ^{T1-T10}
PA3518	esterase, lipase	glycosylase (GO)	thiaminase ^{T8,T9}
PA0829	esterase, lipase	hydrolase (GO)	epoxide-hydrolase ^{T1,T2} , PLA ^{T3} , carboxylesterase ^{T7} , lipase ^{T8}
PA3750	PLA	lysophospholipase (GO)	lypolytic enzyme ^{T1,T10} , esterase ^{T2,T4,T5,T7-9} , lipase ^{T6}
PA2419	PLA	hydrolase (GO)	ribonuclease ^{T2} , isochorismatase ^{T5,T7,T8}
PA2660	PLA	uncharacterized	PLD ^{T2} , PLA ^{T3,T4,T6,T7}
PA0484	PLA	Gly cleavage system/transcription	phosphatase ^{T3} , deformylase ^{T5-T9}
PA1193	PLA	glycosylase (GO)	glycosylase ^{T1-T7} , nuclease ^{T8,T10}
PA5535	PLA	CobW C-terminal domain (InterPro)	urease ^{T6,T8,T9}
PA4961	PLC	uncharacterized	/
PA0285	PLC	transcription regulator (GO)	phosphodiesterase ^{T1-T5}
PA5028	phosphodiesterase	AAA_31 domain (InterPro)	ATPase ^{T3}
PA1214	phosphodiesterase	asparagine synthase/glutaminase (GO)	/
PA0543	phosphodiesterase, phosphatase	hydrolase (GO)	peptidase ^{T1,T2,T4-T6}
PA3074	phosphodiesterase, phosphatase	TPR_REGION domain (InterPro)	proteasom ^{T11}
PA1089	phosphatase	phosphatase (GO)	phosphatase ^{T1-T5}

The proteins whose experimentally determined hydrolase function matched with Phyre2 prediction are labeled green. For each PUF, up to 10 templates (T1-T10) were analyzed and those having hydrolase functions with confidence $\geq 75\%$ and size of aligned query ≥ 100 residues are indicated in superscripts. The ordinal numbers of templates with corresponding biochemical functions are noted in superscripts. GO, gene ontology annotation.

Besides biochemical functions, many templates in Phyre2 homology modeling of PUFs have described biological functions. Text mining of specific virulence or antibiotic resistance-related biological functions can assist in the identification of priority groups for experimental studies (Fig. 8). A successful example is hypothetical protein PA0497, which was selected to be tested in biofilm formation assay due to multiple confident templates having a role in the cell adhesion. The corresponding *P. aeruginosa* transposon mutant strain Tn_PA0497 was significantly impaired in biofilm formation compared to the wild-type strain (Fig. 52). It is the experimental indication that PA0497 might be an adhesin.

Although the structure is 3 to 10 times more conserved than the sequence [303], the functional inference based on homology modeling is not always reliable, as similar folds might diverge to have distinct functions. [304] Another possible reason for homology modeling false-positive functional assignments is that the template's active and binding sites might not be aligned in the query protein. This can be examined in more detail by Phyre2 single protein analysis and ideally experimentally verified.

4.2. The pGUF is a novel cloning and expression vector

To generate the *P. aeruginosa* GUFs expression plasmid library and subsequently produce protein in *E. coli* and *P. aeruginosa*, a novel pGUF vector was constructed as a derivative of pBBR1mcs3. The generated vector unified β -galactosidase α -peptide selection marker and broad-host-range feature of pBBR1mcs3 cloning vector with the T7-system expression elements for inducible protein production from pET22b expression vector.

The complete nucleotide sequence of the new vector was verified by walking primer Sanger sequencing with $\geq 99.8\%$ of sequence identity (Table 5). Only a few mutations found in the 6358 bp long sequence were identified in nonfunctional regions, except for CG⁵⁹⁵⁵ deletion in the T7-terminator sequence. However, this mutation likely does not affect the functionality of the T7-terminator since the RNA-hairpin secondary structure, which terminates transcription, still should be formed (Fig. 56). The minimum free energy change of secondary structure formation of the T7-terminator with GC deletion (-12.40 kcal/mol) was similar to the intact terminator (-11.30 kcal/mol), as predicted by the online RNA fold server (Fig. 56). [305]

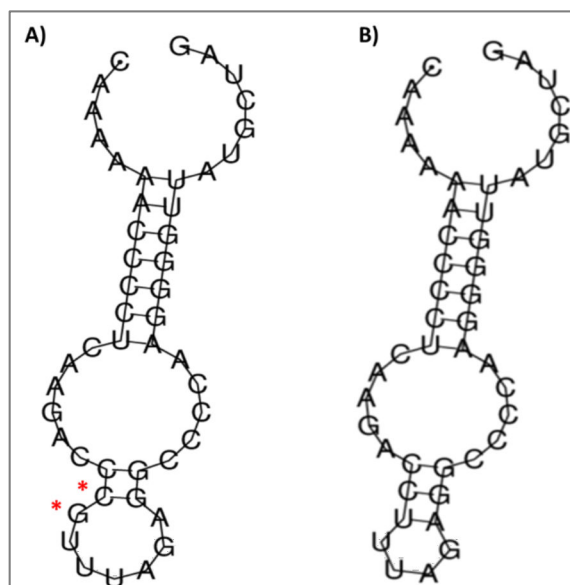


Fig. 56. Secondary structures of T-7 terminator RNA sequences. A) Native T7-terminator sequence from pET22b vector B) T7-terminator sequence from pGUF vector in which CG (indicated by red asterisks) were missing. The figures were obtained by the RNA fold server. [305]

A desirable trait of cloning vectors, especially those used for high-throughput cloning, is the presence of a selection marker for recombinant clones, such as the gene for β -galactosidase α -peptide (*lacZ α*) in pBBR1mcs3, commonly used in white-blue clone selection [277]. Besides

deleting unwanted sequences from multiple cloning site (MCS), the original *lacZα* was shortened in the pGUF vector to decrease the plasmid size since plasmid size negatively correlates with transformation efficiency. [306] Despite these changes, the functional amino acids of original *LacZα* were successfully preserved in mutated *LacZα** of pGUF, which was confirmed by the blue color of *E. coli* colonies carrying pGUF (Fig. 13-A). Although beneficial for recombinant clone identification, the insertion of the genes encoding enzymes into MCS of *lacZα* was correlated with the impairment of enzyme activity upon fusion of the short fragment of *lacZα*. [277]. Since this project aimed to identify novel enzymes expressed using pGUF constructs, the *Afl* II and *Sma* I cloning restriction sites were positioned outside of the *lacZ** gene, similar to what was previously done for several pBBR1MCS vectors. [277] Therefore, complete excision instead of disruption of *lacZ** selectable marker was responsible for the absence of β-galactosidase activity, as demonstrated for pGUF-*plaf* construct (Fig. 13-A). Although *E. coli* is the most common microorganism for heterologous recombinant protein expression [307], *Pseudomonas putida* has recently been found to be a good alternative host due to its high growth rate, metabolic versatility, and tolerance toward chemical and proteinaceous toxins. [308] Considering the expression of *P. aeruginosa* GUFs, the homologous expression might have advantages over the heterologous expression in *E. coli* due to the presence of systems for proper post-translational modifications [309], which might be absent in *E. coli*. Additionally, *Pseudomonas* may be suitable for efficiently translating high G+C content *Pseudomonas* genes to avoid codon bias and consequent mutation or truncation of the target gene. [307, 310] Concomitantly, testing different bacterial hosts may result in a higher probability of recombinant protein production. [311] For that purpose, *E. coli* - *Pseudomonas* expression vectors were constructed, including broad-host-range vectors, which harbor its *ori* region with *rep* gene enabling host-independent replication and shuttle vectors, which contain different *ori* regions, each functioning in one strain with the corresponding Rep protein, which can be provided by the host. [312] The pGUF was designed to propagate in both strains (*E. coli* and *P. aeruginosa*) based on pMB1 *ori* and *rep* gene from pBBR1msc3 vector and to allow homologous gene expression in *P. aeruginosa* PA01 under the control of *lac* promoter and heterologous gene expression in *E. coli* under the control of *lac* and T-7 promoters. The functionality of pGUF expression elements in both strains was confirmed by Western blot detection of recombinant phospholipase PlaF of *P. aeruginosa* [313, 314] expressed using the pGUF-*plaf*

construct (Fig. 13-B). A similar example of a broad host range dual-expression vector is the pEPB41 vector, which harbors pBBR1mcs replicon and T7-promoter used for the expression of *B. subtilis* lipase A and *F. solani pisi* cutinase in *E. coli* BL21 (DE3) and *Pseudomonas putida* KT2440-T7. [311] *E. coli* - *Pseudomonas* expression vectors such as pBSP II KS/pBSP II KS and pCon2(3) in addition to T-7 promoter, also contain lac promoter, which eliminated the need for T7 RNA polymerase-engineered *Pseudomonas* strains. [315, 316] However, since all mentioned vectors did not contain *lacI* repressor gene, *lacI* has to be provided from an additional plasmid or expressed from the chromosome of modified strains, such as *E. coli* BL21 (DE3) and *P. aeruginosa* LAC, to achieve inducible gene expression. [315, 316] Furthermore, in the absence of LacI, basal overexpression of the target gene may take place, thus decreasing cell viability and inducing loss of plasmid, especially in the case of toxic proteins [317]. Since the leaky basal expression is related to insufficient chromosomal repressor production [311], pGUF incorporates *lacI* gene and LacI binding sites (lac operator) upstream of T-7 and lac promoters, enabling lactose-induced gene expression in *E. coli* and *P. aeruginosa* PA01. However, the absence of leaky basal expression in pGUF was not experimentally evidenced. Like pGUF, broad host range expression vector pMEKm12 (9.9 kbp), which harbors tac promoter, *lacI* repressor and *lacZα* selection marker was used for IPTG-induced expression of the gene encoding syringomycin synthetase in *P. syringae* and *E. coli* DH10B. [318] A similar strategy was used in *E. coli* - *P. aeruginosa* arabinose-inducible expression shuttle vector pHERD20T (5 kbp), which harbors *lacZα* selection marker, P_{BAD} promoter, and the *araC* regulator. [319]

As pGUF was constructed to screen *P. aeruginosa* putative hydrolases in highly sensitive colorimetric enzyme assays using *E. coli* cell lysates expressing respective GUFs, the functionality and solubility of produced proteins were more important than the quantity of produced proteins. One of the factors affecting all these parameters is a plasmid copy number. The higher the plasmid stability and less possibility for inclusion bodies formation [320], the higher possibility for the expression of toxic proteins in *E. coli* [321], but also the lower protein yields were correlated with the low plasmid copy number. pGUF also belongs to low copy number plasmids as it harbors pMB1 ori. [322] The potential of pGUF to be used for the expression and identification of enzymes and virulence factors was confirmed by high esterase activity detected in *E. coli* BL21(DE3) and *P. aeruginosa* PA01 strains carrying pGUF-*plaf*, clearly indicating the presence of correctly folded and active potentially toxic mem-

brane phospholipase, PlaF (Fig. 13-C, D). [323] However, native Ni²⁺-affinity chromatographic purification of recombinant proteins produced using the pGUF construct requires more optimization (data not shown), which can be correlated with a lower quantity of produced recombinant and consequent higher extent of non-specific protein binding.

4.3. Medium-throughput cloning of *P. aeruginosa* GUFs

The expression plasmid library consisting of 606 pGUF-*guf* constructs carrying *P. aeruginosa* GUFs was generated following the cloning pipeline in 96-well plates and automatic identification of positive Sanger sequencing results after BLASTN sequence alignment. The genome-wide plasmid libraries, often comprised of thousands of ORFs (open reading frames), were previously constructed for pathogenic bacteria, including *P. aeruginosa* [324], *S. aureus* [325], *B. melitensis* [326], *C. pneumoniae* [327], *F. Tularensis* [328], and *V. Cholerae* [329]. These libraries were used in high-throughput and global (“omics”) studies to elucidate bacterial virulence and pathogenesis. To identify positive constructs in these projects, recombination-based cloning strategies, highly automated cloning pipelines, i.e. robotic liquid handling stations and specialized software were utilized. A rare example of employing a classical restriction/ligation cloning strategy for library construction is the generation of constructs for nearly 2000 human ORFs using a commercial Flexy cloning system (Promega). [330] This system overcomes the main concern of the classical cloning approach - the occurrence of recognition restriction sites among such a large number of genes and the tedious procedure including restriction and ligation steps, which often require DNA purification in between. In the Flexy system gene of interest and vector are hydrolyzed with Sgf I and Pme I DNA endonucleases, whose 8 bp-long recognition restriction sites occur very rarely among many genomes. [331] However, even 107 or 5 % of all *P. aeruginosa* GUFs contain Sgf I restriction site and no one contains Pme I recognition site. However, placing Pme I restriction site on the 3'- end of the gene, followed by the C-terminal protein tag, requires subsequent inactivation of the stop codon in the recognition sequence of this enzyme. [331] In the Flexy system, this is achieved in an additional sub-cloning step in which the Sgf I/Pme I hydrolyzed gene of interest is transferred from the entry vector into the Sgf I/EcoICRI hydrolyzed expression vector. [331] In the generation of the pGUF-*guf* plasmid library, the genes were hydrolyzed only with Afl II restriction enzyme at 5' terminus. This restriction site occurs only in 8 (0.36 %) *P. aeruginosa* GUFs, which were excluded from cloning. The genes with 5' Afl II

sticky-overhang were ligated directly into the linearized pGUF expression vector, which had 5' Afl II sticky overhang and 3' blunt-end generated by SmaI enzyme. The absence of 3' restriction site in amplified genes eliminated the need to exclude from cloning GUFs, which could harbor the second restriction site. Additionally, the length of oligonucleotides, the most costly reagent in the library generation, was minimized as only forward oligonucleotides included six bp for Afl II restriction site. Although this approach results in the loss of Sma I restriction site in the construct, thereby disabling its use for eventual sub-cloning of a gene into another expression vector, it also results in nearly seamless cloning as only GGG (coding for the small glycine) remains between C-terminal 6xHis tag and the recombinant protein. This is not the case in the Flexi cloning, in which three amino acids are inserted upstream of the N- or C-terminus protein tag or in recombinase-based cloning, in which even 9 to 12 amino acids are incorporated. These exogenous residues might affect protein expression and activity. [331]

The recombinase-based strategy employed in the generation of ORF libraries of pathogenic bacteria [324] - [329] relies on the Gateway cloning system (Life Technologies), in which the recombination reaction catalyzed by Clonase enzyme mixture occurs between attB sites flanking the gene of interest and attP sites on entry vector. [331] The gene is transferred from the entry vector into the expression vector in the second recombination reaction. [331] Contrary to restriction/ligation cloning, this cloning method has the advantage that it is amenable for any insert sequence, as att recombination sites long at least 25 bp do not occur within many gene sequences. [331] However, att sites increase the average size of primers used to amplify genes for Gateway cloning to 45-55 nucleotides, which is two times higher than the average size of primers used to amplify GUFs (23 bp). The long primers increase not just the costs but also the mutation rates in final constructs, including frame-shift mutations at both gene termini since the synthesis of large oligonucleotides is more prone to mistakes. [331] To avoid these negative effects, two sets of shorter primers in two rounds of PCRs, in which PCR product from the first reaction served as a template in the second reaction, were used to amplify ORFs. Two sets of primers were used either in two consecutive PCR reactions for the generation of *P. aeruginosa* [324] and *F. tularensis* [328] libraries or in one nested PCR reaction for the generation of *S. aureus* [325] and *C. pneumoniae* [327] libraries. Although performed in two steps, the success of PCR gene amplification in these projects was high: 99 % in *P. aeruginosa* [324], 100 % in *F. Tularensis* [328], 97 % in *B. melitensis* [326]

and > 99 % in *V. cholerae* [329] and *C. pneumoniae* [327] libraries, as inspected by agarose gel electrophoresis of at least several hundred amplified genes. The success of touch-down PCR amplification of *P. aeruginosa* GUFs was comparably high (93 %) as judged by the agarose gel electrophoresis of 42 randomly selected genes (Fig. 17). This is similar to PCR success during the generation of the complete *P. aeruginosa* genome library [324], although primer design strategy, PCR conditions, and criteria used to arrange primers in one 96-well plate differed. In the complete *P. aeruginosa* genome library project [324], PCR primer pairs were designed by specifying T_m of all primers at 65 °C, while primer pairs in pGUF-*guf* library presented here were designed by setting the primer length at 20 nucleotides to reduce costs. The T_m values for pGUF-*guf* primers were then calculated, and the primer pairs with T_m difference higher than 10 °C were adjusted manually. The primers for amplification of *P. aeruginosa* GUFs in one 96-well plate were organized according to similar T_m values in a way that the range of annealing temperatures for all primer pairs in the same plate was covered in the first 10-15 cycles of the touch-down PCR program. Since in both cases the genes were amplified using G+C rich (66 % GC content) [332] *P. aeruginosa* PA01 genomic DNA as a template, GC rich buffers (*P. aeruginosa* complete ORF library) or betaine and BSA in case of pGUF-*guf* library were used to decrease the secondary structure formation and high T_m , thereby increasing the specificity and yield. [333, 334] Notably, all tested GUFs larger than 1500 bp were amplified, which were reported to be overrepresented among a small fraction of failed PCRs in other projects. [326]

The number and complexity of steps in the cloning pipeline used to generate the pGUF-*guf* library are similar to the Flexi restriction/ligation procedure used for the human library project [331]. The difference is that the last step of cultivation of clones and plasmid isolation was part of the cloning pipeline in the human ORFeom project [330]. In contrast, in the GUF project, the company performed plasmid isolation and sequencing, saving time and costs (Fig. 57). Although the preparation of linearized pGUF in the GUF project is more demanding, the cloning pipeline of *P. aeruginosa* recombinase-based ORFeom project has additional steps, including two rounds of PCR for ORFs amplification and sub-cloning of the insert from entry to an expression vector, which requires two transformation steps and plasmid isolation in between them (Fig. 57). The reported time efficiency for cloning of complete *P. aeruginosa* ORFeom [324] of 337 ORFs per week and person is similar to time efficiency of 190 GUFs per week and person reported here. The higher time efficacy in the complete genome *P.*

aeruginosa ORFeom project [324] can be attributed to shorter enzyme incubation times and the application of an almost completely automated procedure by robotic pipetting and clone selecting systems instead of only a partially automated approach using a 96-well plate master pipettor for the construction of the pGUF-*guf* library.

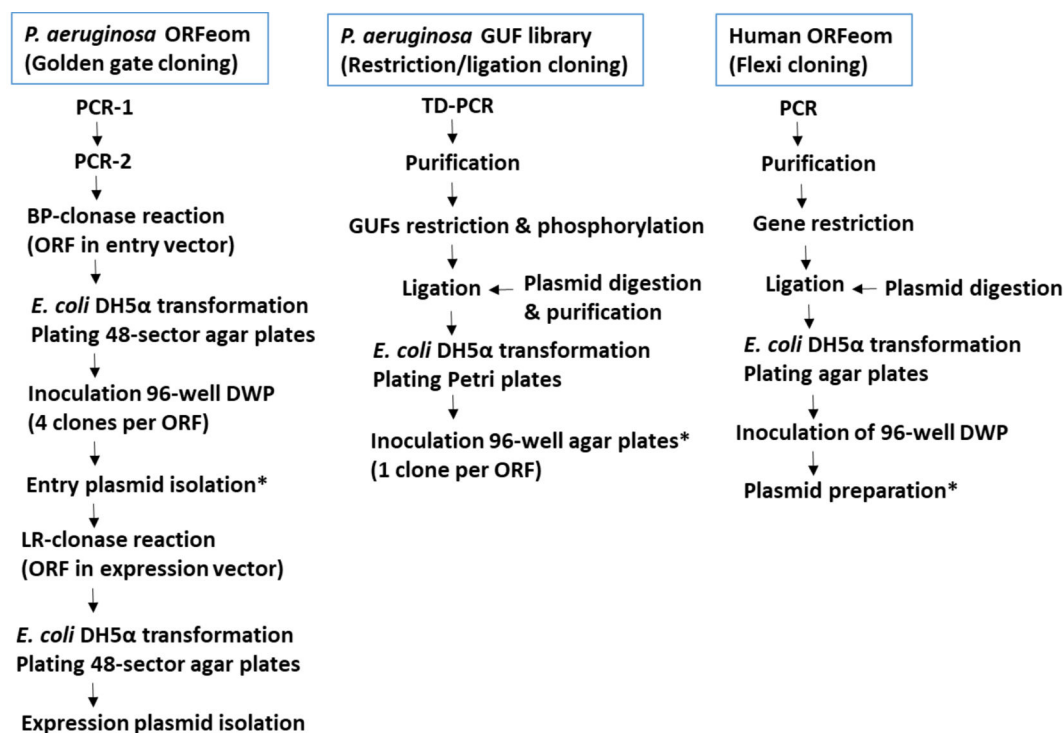


Fig. 57. Comparison of the cloning pipelines used in high/medium-throughput projects: complete *P. aeruginosa* ORFeom project [324], human ORFeom project [330], and here presented *P. aeruginosa* GUF project. Asterisks are assigned to the step at which the samples are submitted to sequencing.

The sequencing results in ORFeom projects [324] - [329] were analyzed at the nucleotide and protein levels mostly using specialized in-house developed software. In these projects, the results with any deletions, insertions, nonsense, and frameshift mutations were excluded, while silent and usually up to 2 missense mutations were tolerated. [324, 328] Since the DNA sequencing method is error-prone, especially in the first and last 100 nucleotides, the quality of sequences was validated by Phred software [328] and two to seven reads per single clone were performed to achieve good sequence quality. [328, 329] Considering that the pGUF-*guf* library was constructed to allow the identification of novel enzymes and only one read per submitted clone was performed due to the cost limitations, the sequencing results were analyzed only at the nucleotide level, and less stringent rules were applied to define a positive result for subsequent experimental characterization.

Since the rejection criteria, the number of sequenced clones per gene, and even the number of sequencing reactions per clone were different between the pGUF-*guf* library and libraries from the literature, the cloning success cannot be directly compared. The number of perfectly aligned sequencing results to reference genes, calculated as a ratio of the total number of accepted sequences, was comparable in GUF, *V. cholerae* [329], and *F. tularensis* libraries [328]. However, we need to consider that the rejection criteria for accepted results in the pGUF-*guf* library were less stringent (Table 11).

Table 11. Comparison of plasmid libraries validation results from *F. tularensis* ORFeom [328], *V. cholerae* ORFeom [329], and here presented *P. aeruginosa* GUF project.

	<i>P. aeruginosa</i> GUFs	<i>V. cholerae</i> ORFs	<i>F. tularensis</i> ORFs
Average gene length	993	922	1025
Clone per gene	1,7	1,5	1,8
Read per clone	1	3,2 ± 2,7	2,8 ± 2,7
Perfect match	70%	93%	84%

Overall, the developed cloning pipeline was successfully used to generate expression constructs for hundreds of *P. aeruginosa* GUFs. With the increase in DNA sequencing efforts, the procedure should be amenable for high-throughput projects focused on generating thousands of constructs.

4.4. Medium-throughput *P. aeruginosa* PUFs production and enzyme activity screening

The success of a recombinant gene expression and the functionality of a produced protein cannot be efficiently predicted. [335] This complex process depends on the features of the expression plasmid such as replicon and promoter type, a host organism, cultivation temperature, and medium composition, and the gene intrinsic properties, including codon usage and toxicity. [307] Two *E. coli* strains cultivated in two different media were used to increase the expression rate of hundreds of studied hydrolases. However, the cells obtained from all four conditions were pooled together for subsequent analysis. We selected *E. coli* BL21(DE3), which is the most widely used host for gene expression under the T-7 promoter [307], and its derivative - *E. coli* C43(DE3), which showed higher tolerance to the production of recombinant membrane and toxic proteins, that is at least partially due to the mutations in *lacI* gene and lacUV5 promoter, resulting in the lower level of protein production. [336]

Each strain was cultivated in an auto-induction medium, which is a preferable medium in high-throughput projects as tight protein regulation is achieved without monitoring cell density [309], and TB medium with the use of non-metabolizable IPTG as an expression inducer, which is shown to be more efficient for production of some proteins. [337] Our preliminary analysis of the expression of several *P. aeruginosa* GUFs confirmed that all conditions were useful for protein production, although, as expected, with different yields. Besides increasing the chances of protein production, this strategy leads to possible dilution of protein concentration in case the protein is produced under only several of four expression conditions. However, the enzyme activity should still be detected using sensitive hydrolase assays, as was the case in the esterase activity of pGUF-*plaf*, which was active although it was below the detection limit of dot-blot analysis in some experiments (Fig. 19-C). Among 429 expressed pGUF-*guf* constructs, we estimated that 76 % of proteins were produced according to protein dot-blot. This result is similar to other high-throughput projects, in which proteins were produced using *E. coli* and expression plasmids harboring elements of the inducible T-7 expression system. For example, 77 % of ≈ 380 tested constructs from *V. cholerae* library showed the expected size of GST-fused recombinant proteins in Western blot [329]; 85 % of 20 arbitrary chosen constructs from *S. aureus* library produced 6xHis-tagged recombinant proteins according to Western blot [325]; 90 % of 71 constructs from *P. aeruginosa* library showed expected N-terminal 6xHis-tagged recombinant proteins in SDS-PAGE [324]; the genes from 72 % of 1961 constructs from *F. tularensis* library were expressed and purified based on N-terminal 6xHis-tag, analyzed by Labchip90 automated electrophoresis [328]. Although the information about the molecular size of produced protein is missing in dot-blot, this method is shown to be suitable for fast immunodetection of proteins in 96-well plate format, as it was used in the screening of 6xHis-tag labeled proteins in high-throughput structural genomics projects. [338, 339]

In the library of *P. aeruginosa*, putative hydrolases expressed in DWP, 81 and 399 proteins were predicted by the SOSUI database as membrane-bound and soluble, respectively. The dot-blot results revealed that a similar percentage of predicted membrane proteins (70 %) and predicted soluble proteins (86 %) were produced. In the *P. aeruginosa* ORFeom project [324], the success of non-membrane protein expression (91 %) was nearly two times the success of membrane-associated protein expression (59 %). These results indicate that the expression conditions (low copy number pGUF vector, *E. coli* C43(DE3) and BL21(DE3)) used

in our project are better for membrane proteins compared to the conditions used in the *P. aeruginosa* ORFeom project (high-copy number vector (pDEST17) and *E. coli* BL21(DE3)) [324]. These expression results obtained with pGUF are in agreement with previously observed good performance of low copy vector pBBR1mcs-3 for expression of membrane phospholipases PlaF [340] and PlaB [341]. Here used expression conditions leading to a better expression of membrane proteins might be advantageous in drug target-focused research, as around 50 % of all drug targets are membrane proteins [280].

The produced proteins from expression plasmid libraries were used in downstream screenings for various purposes: identification of the most optimal high-throughput expression conditions yielding soluble proteins [338]; determination of the protein structures [342]; identification of novel antigens in immune response assay as potential vaccine candidates [324]; identification of novel promising biocatalysts and enantioselective enzymes [343] and novel enzymes from metagenomes [344]. The high-throughput screening of enzyme activities might be performed in agar plate-based assays [345, 346], but using more sensitive chromogenic and fluorogenic substrates is more common [347]. These substrates were previously used in MTP or microarray fluorimetric or colorimetric assays with crude cell lysates or, in most cases, purified proteins. [265, 348] However, the success of high-throughput purification of proteins with 6xHis-tag under non-denaturing conditions was only 30 % in the *P. aeruginosa* ORFeom project [324], while the addition of protein denaturation agents increased the success to 100 %. [324] As the general success rate of purification of procaryotic His-tagged proteins is ≈ 50 % [349], the hydrolase screening of expressed GUFs was performed using cell lysates to avoid: a) the possible loss of protein, b) additional renaturation step, which often leads to poor recovery of functional protein [350], c) interference of imidazole from elution buffer in hydrolase assays [265], and d) difficulty of defining reliable negative control in enzyme assays in case of partially purified (enriched) protein samples. The co-elution of *E. coli* endogenous proteins together with low-expressed recombinant protein was the primary source of false-positive activities measured with purified proteins. [265] However, a high probability of false positive and false negative results emerges also in screenings using cell lysates. The false-positive results may be due to the biological complexity of the cell lysate sample, e.g., the measured activity might originate from a genome-derived enzyme, which is positively regulated by the overexpressed recombinant protein. False-negative results can emerge if a protein is completely expressed

in an insoluble fraction of inclusion bodies and therefore inactive (although detected in dot-blot) or the generated product of tested enzyme activity or the recombinant protein itself is degraded by endogenous enzymes [351]. Therefore, the stringent criteria were set to identify the positive enzyme activities in screening of *P. aeruginosa* PUFs library: the measured activity in positive sample has to be a) higher than the empty vector control representing „background“ cell activity and the eventual influence of the vector, b) higher than the average activity and standard deviation of all samples from the 96-well plate and c) criteria mentioned under a) and b) should be fulfilled in two independent measurements.

The assays in hydrolase screening were performed using well-established and simple substrates with broad specificity under similar reaction conditions suitable for most enzymes belonging to a specific enzyme subclass. [265] Except for PLAs and lipases, for which natural substrates were used, the chromogenic artificial substrates were used to screen proteases, esterases, thioesterases, phosphatases, glucosidases, PLCs, and phosphodiesterases. These substrates are the most common hydrolase substrates, in which the natural substrate moiety is bound to *p*-nitrophenol or *p*-nitroanilide at the hydrolase cleavage site. In these assays, chromophore released upon hydrolysis is the measure of enzyme activity. [352] A total of 141 positive samples in the screening of 429 PUFs, including 27 PUFs which showed more than 20 % increase in activity relative to the average activity plus standard deviation of all samples in a plate, in two experiments were identified. Among 71 PUFs that were screened as positive, the hydrolase activities were reproduced for 18 PUFs (27 %) in an experiment performed in an Erlenmeyer flask. This accounts for 4 % of all tested PUFs, which is comparable to 6 % of identified enzymes in the project in which similar enzyme assays were used to test purified proteins [265]. As shown in Table 10, some *P. aeruginosa* PUFs were positive in screening with more than one substrate. This was observed for PA3614, which showed PLC and phosphatase activities, and PA1501, which showed esterase and thioesterase activities. This can be due to the use of artificial substrates which are rather general than specific, e.g., bis-*p*-nitrophenyl phosphate acts as a substrate of PLC and phosphodiesterase. [265] Furthermore, substrate promiscuity of enzymes might be responsible for these results, e.g., some lipases have thioesterase, esterase, or phospholipase activity. [180, 353] The activities of recently published phospholipase A PA2927 [354] and esterase PA2789 [355], both being hypothetical proteins at the beginning of this project, were also identified in the screening (PA2927, E7-HY V, Fig. 23.-E and PA2789, A1-HY III, Fig.

22-C), what represents the valuable proofs of the principle of here applied cloning, expression and enzyme screening pipeline.

4.5. Novel *P. aeruginosa* hydrolases and their biological significance

This chapter will discuss the proteins that showed the highest hydrolase activity or effect in the biological assays in the light of their newly identified *in vitro* biochemical function and bioinformatics data.

In the screening and validation experiments, the highest carboxylesterase activity with *p*-nitrophenyl butyrate substrate was detected for **PA2315** (Figs. 24-E and 34). The PA2315 is annotated in the PGD and Uniprot databases as a 42.4 kDa hypothetical protein with predicted cytoplasmic membrane subcellular localization and β -lactamase-like domain. [271, 356] Phyre2 homology modeling of PA2315 revealed highly confident esterase, β -lactamase, and carboxypeptidase structural homologs. [299] The best structural model of PA2315 was built using the structure of esterase EstB [357] from *Burkholderia gladioli* (100 % confidence, 96 % query coverage, 56 % seq. identity). According to this model, PA2315 has a β -lactamase/transpeptidase fold comprised of antiparallel β -sheets flanked with α -helices and putative Ser-Lys-Tyr catalytic triad. [240] Despite the β -lactamase fold, EstB does not have β -lactamase activity since steric hindrance in the tunnel of the active site prevents β -lactam entry. [357] In the preliminary experiment using cell lysates of *E. coli* pGUF-*pa2315* and CEN-TA chromogenic cephalosporine substrate, the β -lactamase activity could not be detected. The analysis of the primary structure of PA2315 revealed the Ser-x-x-Lys motif, typical for class C β -lactamases, in the N-terminal part and conservation of Ser-Lys-Tyr catalytic residues (Fig. 54). This implies that PA2315 is a new member of class VIII esterases. [358] The transposon mutant of *pa2315* was not generated in the *P. aeruginosa* PA01 strain [254] but is available for *P. aeruginosa* PA14. [359] The precise biological role of *B. gladioli* EstB is unknown, although it is likely involved in antibiotic resistance as it has high deacetylation effect on cephalosporins. [360]

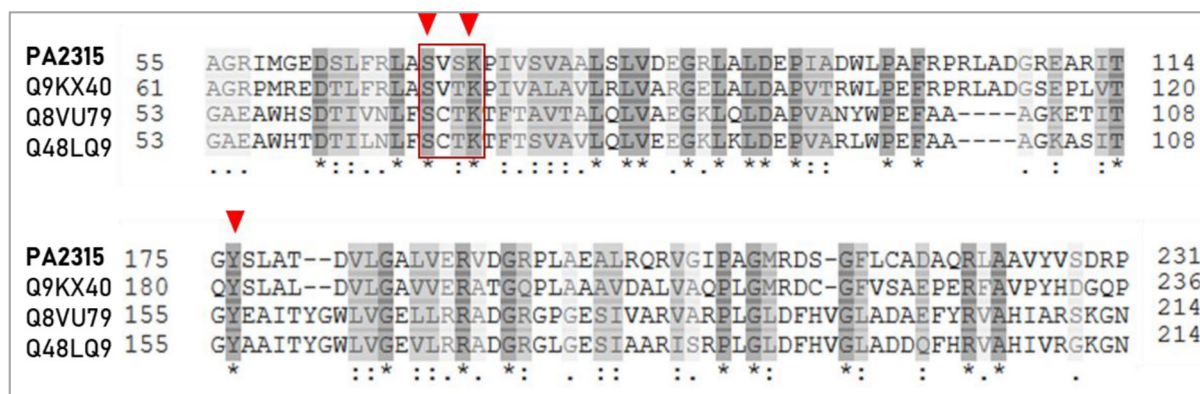


Fig. 58. Multiple protein sequence alignment between PA2315 and three esterases from lipolytic enzyme family VIII [358]: esterase EstB from *Burkholderia gladioli* (Q9KX40) [357], *Pseudomonas fluorescens* putative carboxylesterase (Q8VU79), *Pseudomonas syringae* esterase EstC (Q48LQ9). The catalytic residues are labeled with red triangles, Ser-x-x-Lys motif with a red square, the identical residues with the star, and similar with the colon. The numbers next to the sequences indicate the range of aligned regions in the corresponding protein. The alignment was performed using the Uniprot database.

High phospholipase C activity was identified for **PA4961**, 56.7 kDa hypothetical protein whose outer membrane vesicle localization in *P. aeruginosa* was previously experimentally confirmed. [361] Only the C-terminal half of the protein could be modeled with Phyre2, revealing homologs with transferase and lyase activities and no homolog with hydrolase activity. Although PA4961 was not listed in the PGD list of (putative) virulence factors, based on Conserved Domain Database (CDD) analysis and Pfam domain annotation in PGD, it revealed similarity with the protein family Smp members, which includes membrane proteins with a role in hemolysis. [362] Interestingly, the sequence alignment between PA4961 and Smp family member, *Pasteurella multocida* AhpA, revealed high similarity in the N-terminal region of the protein (Fig. 59). Since the aligned region also contains transmembrane peptides, one might reasonably assume that the structural similarity between two proteins in this region is also high, but Phyre2 could not detect it, as the structure of AhpA has not been solved. More intriguingly, although the *P. aeruginosa* PA01 transposon mutant library contains *pa4961*, this gene is identified as a condition-specific essential gene required for *P. aeruginosa* growth on agar medium with cystic fibrosis patients' sputum. [363] Given that *P. aeruginosa* hemolytic phospholipase C PlcH has a role in providing the nutrients through hydrolysis of lung surfactants, including phosphatidylcholine [364], a similar biological role might be hypothesized for PA4961 to explain its role in the survival of bacteria on sputum

agar. These assumptions based on bioinformatics mining and the newly identified PLC activity of PA4961 remain to be experimentally confirmed.

PA4961	1	MTRPTSVKPDNEFLLFRALRQRRVPIALRIASHSLILVALALL-----IYAWVMGMQF	54
Q9L8J3	1	---MHLTKKEF-----IKLSMIS-SIIILCIAIVSVILFGVQQFKIGSQL	41
		:. :.*	
PA4961	55	RQAMQQQADALGQSLITQTAASATELLVSNL-ILSLNVLLNNLVKNPLVAHAATYSVDQR	113
Q9L8J3	42	AS--VNOVSNLSHLLIRCOANLLSMLLVNNASTEQLTESLDAFAKEEFVLDASIYSNRGE	99
		. :.*. :.* :.* :.* :.* :.* :.* :.* :.* :.* :.* :.* :.* :.*	
PA4961	114	ILAEAGSRPKQSL-LGA-----TEGLYSTPITFQEVLAGHLRISLDMQFQCP--M	161
Q9L8J3	100	LLAHTSHFQNLRLTLGLNSPTQPDEENTQQIVEPTISLNGIEGFLRVTFDSKYGRKTTQSK	159
		:*.*. :.* :.* :.* :.* :.* :.* :.* :.* :.* :.* :.* :.* :.*	
PA4961	162	M--ISLQSMGLISLILL-----ILALYESLRLLGRQISTPLLQLRVWLRDPDPNPAP-GAE	212
Q9L8J3	160	IDHLFHQLYGEIILIFLAGVLLASSIHVELSHYRRT-----YRKVTENKAVKVLK	209
		: :.* :.* :.* :.* :.* :.* :.* :.* :.* :.* :.* :.* :.*	
PA4961	213	LQNEIGDLADLEERLVPEKPPAPEPEEAPLPQNFDDILLEDDEADLRSRKVEASAFEED	272
Q9L8J3	210	TKQNVGNYHR-----	220
		:*.*. :.*	
PA4961	273	DIPLGDALLDETKPVEFTSIDEDPLDQDAFDENGAEAGEQPAAPAAAREPQHSAVLAIQL	332
Q9L8J3	221	-----	220
PA4961	333	GAQEQLRRLPRSRRLVDLLQRYRDCLEQAARQYKGSLSLHTSDGGSLLLFHSRDNRADYLTN	392
Q9L8J3	221	-----RRRLNK---	226
		.* :	
PA4961	393	ALCCGELMRALGHALQIEVADSGITLQLQLGLSLGEDLSEQTQADLLLNETVQNALALNQ	452
Q9L8J3	227	-----	226
PA4961	453	HSRNLLLVERSIADDAVVRERARIRAIASPEGACCVERLLEPYPSMLERQLARMHDRAP	512
Q9L8J3	227	-----	226

Fig. 59. Protein sequence alignment between PA4961 and *Pasteurella multocida* AhpA (Q9L8J3). [365] Identical residues are labeled with the star and similar with the colon. The numbers next to the sequences indicate the range of aligned regions in the corresponding protein. The alignment was performed using the Uniprot database.

In vitro lipase activity of PA0829 was validated with *p*-NPdec and *E. coli* pGUF-pa0829 cell lysate (Fig. 39-B). Probable hydrolase **PA0829**, 35.1 kDa was reliably modeled with several structural templates with an α/β hydrolase fold. The majority had epoxide hydrolase or dehalogenase biochemical functions, which are all distinctive features of family V lipolytic enzymes. [358] Therefore, the protein sequence of PA0829 was analyzed by alignment with the family V lipases [173] together with two putative lipase/carboxylases that were structural templates. The sequence alignment revealed that PA0829 has a 35-39 % sequence similarity to family V members, which is within the literature range for this family. [358] Moreover, the presence of lipase pentapeptide G-X-S-X-G forming Ser-nucleophilic elbow between β 5-sheet and adjacent α -helix [366] and the conservation of catalytic triad residues Asp-His-Ser (Fig. 60) shows that PA0829 indeed belongs to family V lipolytic enzymes. Interestingly, the

highly confident structural homolog of PA0829 was PA2949, phospholipase PlaF (100 % confidence, 97 % query coverage, and 22 % seq. identity), which also exerts activity toward *p*-nitrophenyl decanoate. [314]

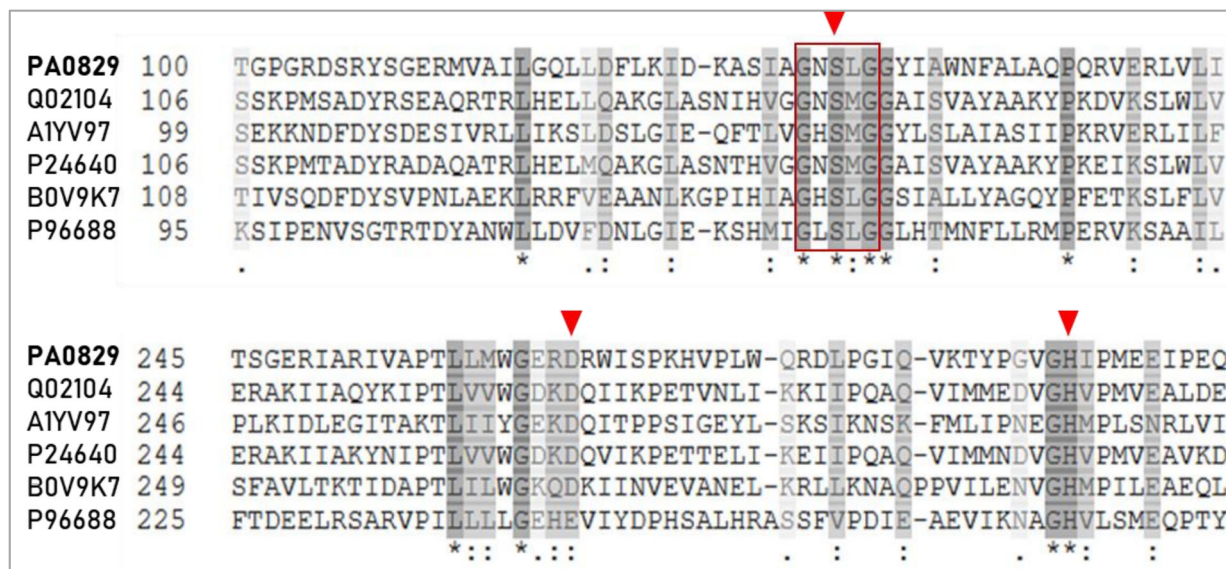


Fig. 60. Multiple protein sequence alignment between PA0829, lipolytic enzymes from family V [358] (Q02104, A1YV97, P24640) and Phyre2 structural templates (B0V9K7 and P96688). Q02104 - *Psychrobacter immobilis* lipase Lip1, A1YV97 - *Fervidobacterium changbaicum* lipase, P24640 - *Moraxella* sp. lipase Lip3, B0V9K7 - putative *A. baumani* lipase, P96688 - putative *B. subtilis* carboxylesterase. The residues from the catalytic triad are labeled with red triangles and lipase pentapeptide G-X-S-X-G with the red square. The numbers next to the sequences indicate the range of aligned regions in the corresponding protein. The alignment was performed using the Uniprot database.

Another validated lipase activity with *p*-nitrophenyl decanoate belongs to hypothetical protein **PA3518**, 37.5 kDa with predicted cytoplasmic/periplasmic localization (Fig. 38-B). The protein structure of PA3518 is determined, and surprisingly, instead of the typical hydrolase α/β fold, it consists exclusively of α -helices. [356] The gene ontology suggested glycosylase activity for this protein [356] and Phyre2 homology modeling transferase, oxidoreductase, and thiaminase (glycosylase) activities. [299] The glycosidase activity was not detected in our screening, but the homology to acyltransferases and human glycosylases is characteristic of lipolytic enzymes from family XIV. [173] Although there is a 22 % sequence similarity and conservation of Asp and His catalytic residues between PA3518 and class XIV member, *Thermoanaerobacter tengcongensis* esterase EstA3, Phe instead of Ser nucleophile is present

in PA3518, and characteristic CHSMG pentapeptide [367] is absent, making its classification still elusive.

The highest phospholipase A activity detected in the screening with a natural phospholipid substrate cocktail (Fig. 23-B) was in *E. coli* cell lysates overexpressing hypothetical protein **PA3750** (26.3 kDa) with predicted cytoplasmic membrane localization. The PLA2 activity was confirmed in the validation experiment with the artificial diheptanoyl thio-PC substrate (Fig. 340). The best structural model of PA3750 had an $\alpha/\beta/\alpha$ fold and was assembled based on homology to *Bacteroides thetaiotaomicron* lipolytic enzyme BT4096 (100 % confidence, 82 % query coverage, 16 % seq. identity). The present GDSL motif in the BT4096 template and $\alpha/\beta/\alpha$ fold are determinants of family II of lipolytic enzymes. [173] The protein sequence alignment between PA3750 and family II members revealed conservation of catalytic Asp and His in the D-X-X-H motif (Fig. 61). However, the GDSL motif encompassing catalytic Ser was not conserved in PA3750, but interestingly, the GEST region in PA3750, instead of the GDSL motif, could contain a putative nucleophilic Ser (Fig. 61).

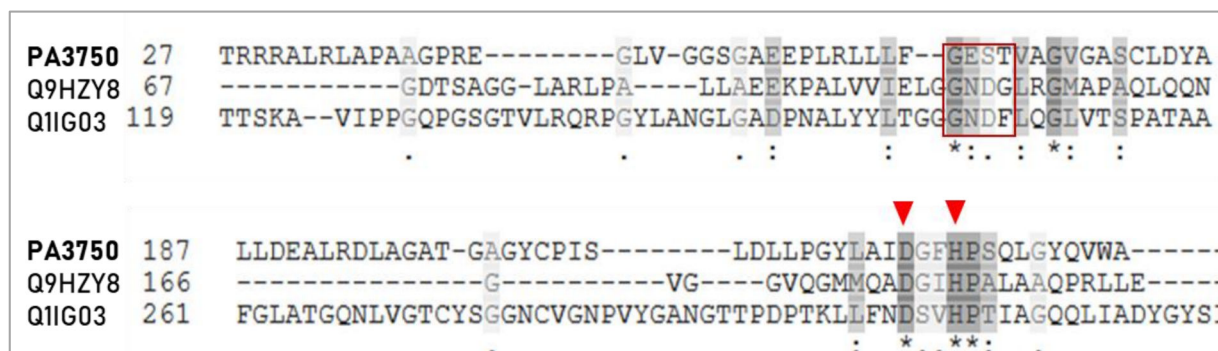


Fig. 61. Multiple protein sequence alignment between PA3750 and lipolytic enzymes from family II. [358] Q9HZY8 - *Pseudomonas aeruginosa* esterase TesA [368], Q1IG03 - *Pseudomonas entomophila* putative esterase EstA. The residues from the catalytic triad are labeled with red triangles and GEST region with the red square. The numbers next to the sequences indicate the range of aligned regions in the corresponding protein. The alignment was performed using the Uniprot database.

In the *G. mellonella* virulence assay, novel phospholipase C **PA0285** (Fig. 47) was identified as a promising novel virulence factor (Fig. 53-A). The structural model of this 86.4 kDa large protein with predicted cytoplasmic membrane localization contains three distinct domains, indicating its complexity: N-terminal PAS domain comprised of five antiparallel β -sheets and few α -helices [369], GGDEF domain comprised of five β -sheets surrounded by α -helices [370]

and EAL domain with $\alpha\beta(\beta\alpha)_7$ -barrel fold [371]. The PAS domain is often found in signaling proteins, in which it allosterically propagates the signal to the adjacent domain upon ligand binding. [372] The GGDEF domain, named after the conserved sequence motif, usually functions as diguanylate cyclase synthesizing an important bacterial second messenger, cyclic di-GMP [373]. The EAL domain is also named after its conserved residues and predominantly exerts phosphodiesterase activity responsible for di-GMP hydrolysis. [374] PA0285 has structural homology with *P. aeruginosa* diguanylate cyclase/phosphodiesterase RbdA (100 % confidence, 71 % query coverage, 30 % seq. identity), which promotes biofilm dispersal *via* c-di-GMP hydrolysis. [375] Based on phospholipase C (phosphoric-diester hydrolase) activity of PA0285 and functions of its structural templates, the putative virulence role of PA0285 might be mediated through hydrolysis of the c-di-GMP, a second messenger which regulates many virulence factors [376]. The protein sequence alignment between PA0285 and diguanylate cyclase/phosphodiesterase homolog templates from Phyre2 revealed the conservation of catalytic motifs (Fig. 62).

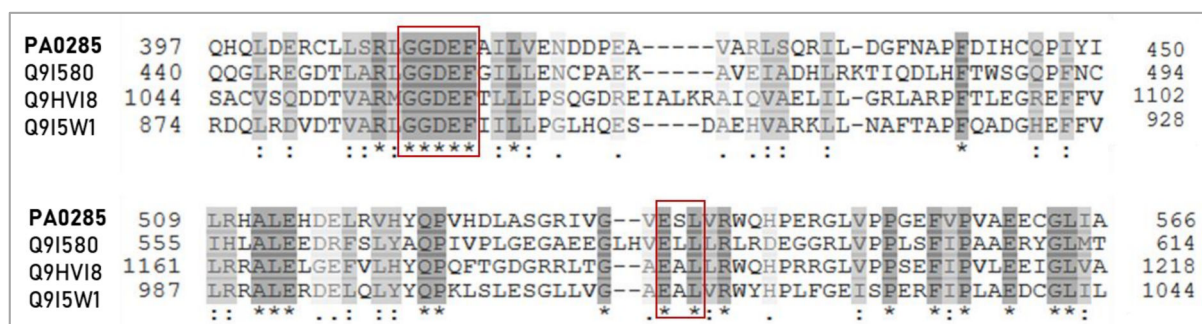


Fig. 62. Multiple protein alignment between PA0285 and Phyre2 templates. Q9I580 - *Pseudomonas aeruginosa* putative transcription regulator (Uniprot annotation), RbdA GGDEF protein [377] (PDB annotation); Q9HVI8 - *Pseudomonas aeruginosa* MorA motility regulator (Uniprot annotation), diguanylate cyclase - phosphodiesterase c-di-GMP regulator [378] (PDB annotation); Q9I5W1 - *P. aeruginosa* uncharacterized protein (Uniprot annotation), diguanylate cyclase [379] (PDB annotation). The conserved motifs are labeled with red squares. The numbers next to the sequences indicate the range of aligned regions in the corresponding protein. The alignment was performed using the Uniprot database.

The hypothetical protein **PA1784**, also a promising virulence factor according to the *G. mellonella* virulence assay (Fig. 53-B), was positive in the screening for esterase activity. However, this activity was not reproduced in the validation experiment, probably due to the unsuccessful expression as concluded by missing the Western blot signal. In Phyre2 homology modeling, many highly confident templates of PA1784 with alginate lyase function were

detected, which might be correlated with reported catalytic promiscuity between esterases and lyases. [380]

PA3074, annotated as 65.6 kDa hypothetical protein with predicted cytoplasmic membrane localization, showed *in vitro* phosphatase and phosphodiesterase activities (Fig. 50-A and B) and an essential role in biofilm formation (Fig. 47-B). Phyre2 could reliably model only one-third of PA3074 protein. The structural templates of PA3074 include human transcriptional and DNA repair factors, which exert their functions by dephosphorylation of proteins [381] or ATP hydrolysis [382]. Furthermore, PA3074 harbors tetratricopeptide (TPR) repeat consisting of 34 degenerate amino acids folded into a pair of antiparallel α -helices, which has a role in protein-protein interactions. [383] Strikingly, TPR repeat is necessary for functions of many bacterial virulence factors, including *P. aeruginosa* FimV regulator of twitching motility and TIIS and PilF pili biogenesis factor. [384] *S. mutants* Vick is an example of phosphatase, which is a positive biofilm effector. It belongs to the two-component regulator system responsible for extracellular polysaccharide (EPS) synthesis and cell division. [385]

Another protein essential for biofilm formation was **PA1214**, annotated as 59.3 kDa hypothetical protein with a predicted cytoplasmic localization. Homology modeling revealed many templates with asparagine synthase (glutamine-hydrolyzing) activity, indicating that this protein might be involved in bacterial metabolism.

A significantly higher biofilm amount was produced in **PA2693** *P. aeruginosa* PA01 transposon mutant compared to the wild-type strain, indicating that this protein might be a negative biofilm effector/regulator (Fig. 52-B). The PA2693 is annotated as 18.9 kDa conserved hypothetical protein with predicted cytoplasmic localization and putative thioesterase function. [271] The thioesterase activity detected in the screening with *E. coli* pGUF-*pa2693* cell lysate using a substrate cocktail containing acetyl-CoA and palmitoyl-CoA was validated in a separate experiment (Fig. 37-B). Recombinant PA2693, similarly to *E. coli* TAP and *P. aeruginosa* TesA thioesterases [175], also shows esterase activity (Fig. 32-A). Accordingly, many highly confident thioesterase structural homologs of PA2693 were identified by homology modeling. [299] The structural model of PA2693 assembled based on the homology with *Bacillus cereus* BcACT1 acyl-CoA thioesterase [386] (100 % confidence, 95 % query coverage, and 34

% seq. identity) reveals hotdog fold, commonly found in enzymes of thioesterase II family (Chapter 1.5). The influence of PA2963 on the biofilm can be correlated with frequently found thioesterase roles in signal transduction and gene transcription, e.g., *P. aeruginosa* thioesterase PqsE indirectly induces biofilm formation (Chapter 1.5).

Performing enzyme assays using cell lysates is suitable for the initial detection of enzyme activity [387], as the protein is in the isotonic cell-like surrounding with the majority of cofactors available. However, due to the complexity of the cell lysate samples containing overexpressed protein, the next step would be confirming detected activities with purified proteins and the natural substrates. Three genes (*pa3074*, *pa0497*, and *pa1214*), whose transposon mutant strains were significantly impaired in biofilm formation compared to the wild-type, are promising targets for anti-biofilm (anti-virulence) drugs. Identifying these targets is crucial since as much as 65 % of all microbial and 80 % of chronic infections are biofilm-related [388]. Additional two promising anti-virulence drug targets are PA0285 and PA1784, whose transposon mutants have a positive effect on the killing rate of *G. mellonella*. The observed effects may reflect the involvement of the genes in host-pathogen interactions in the case of *G. mellonella* assay or the importance of genes in the biofilm formation or regulation. However, it is possible that the inactivation of these genes negatively influences bacterial growth leading to less biofilm amount or higher larvae survival rates. In this case, these genes are probably important factors in bacterial metabolism, growth, or reproduction and, therefore, the valuable targets of bacteriostatic antibiotics. Although the biofilm amount was normalized to cell density, an additional comparison of growth curves of transposon mutants and wild-type strains would help to distinguish between these causalities.

4.6. Glycoamidoamines as *P. aeruginosa* lectin LecB inhibitors

The equally important tasks in developing anti-virulence therapy are the exploration and identification of diverse virulence factors (targets) and design, testing, and structural optimization of their inhibitors (drugs). Therefore, besides identifying novel hydrolase virulence factors, α -l-fucosylated glycooligomers [267] were tested as inhibitors of already established adhesion and biofilm-related *P. aeruginosa* virulence factor, lectin LecB (Chapter 1.2). Since lectins perform their function by binding to mono or polysaccharides, the design of high-affinity ligands (glycomimetics), which would interfere with natural ligand binding, is one of the strategies for developing anti-adhesion therapy.

The mELLA binding experiment showed that the relative LecB inhibition potencies of α -l-fucosylated glycooligomers generally increased with the number of fucose units bound to the glycoamidoamine backbone (Fig. 54-B). Better binding of glycooligomers to the higher number of fucose units can be explained by the tetrameric LecB quaternary structure and the multivalence effect. The affinity of binding of joined molecules to a protein is higher than the sum of affinities of individual ligand molecules. [389] Additionally, the proximity of fucose units on multivalent oligomers increases the probability of rebinding after protein-ligand dissociation. [390] However, the increase in binding with the number of fucose units is not linear since inhibitor 5 (6 fucose units) has slightly lower relative potency than inhibitor 4 (4 fucose units) (Fig. 54-B). This effect can be correlated with the absence of higher LecB oligomers than tetrameric LecB. Besides the number of fucose units, the size of spacing blocks between them showed a strong influence on the inhibition potencies. This is demonstrated by the finding that the 3-valent inhibitor 6 with a larger spacer had almost the same inhibitory potency per fucose unit as 4-valent inhibitor 4 (Fig. 54-B). Previously designed LecB inhibitors include synthetic oligomers based on pentaerythrityl phosphodiester [391], dendrimers based on lysins and cyclopeptides [392], and glycoclusters based on trithiocyanuric acid [393]. Considering the inhibition potencies of synthesized compounds, it seems that creating tightly binding multivalent inhibitors is mostly an empirical endeavor [394]. Significant improvements in affinity compared to the L-fucose standard were observed in the case of octavalent cationic dendrimer that showed a 440-fold enhancement in potency over fucose [395]. As the binding of α -L-methyl-fucose to LecB is 7-fold higher than the L-fucose binding to LecB [396], it can be inferred that this dendrimer is a better inhibitor than the most po-

tent α -L-fucosylated glycooligomer (inhibitor 4), which achieved 31-fold better binding to LecB than α -L-methyl-fucose (Fig. 54-B).

In the biofilm formation assay, 15 – 20 % reduction in biofilm amount was achieved with 2 mM glycooligomers, and no correlation with the number or spacing of fucose ligands was observed (Fig. 55). The glycopeptide dendrimers outperformed the glycooligomer also in *in vivo* studies, as the reduction in biofilm formation for 40 – 55 % in the micromolar range of dendrimers was reported. [397] Conclusively, the first generation of α -L-fucosylated glycooligomers has the potential to be used in anti-adhesion therapy but needs further structural optimization.

5. Supplementary data

Table S1. List of oligonucleotides

Plate position*	Gene	Gene length [bp]	Forward primer sequence (5'→3')	Rewerse primer sequence (5'→3')
-	lacZα	-	CGTATAACGTTACTGGTTTCACATTC	GCTCACTCATTAGGCACCCCTAATAC
-	linpBBR1 mcs3	-	GGGGTGCCTAATGAGTGAGCTAAC	TGTTAAAATTCGCGTTAAATTTTG
-	lacI	-	GAGTCAATTCAGGGTGGTGAATGTGAAACCAG-TAACGTTATAC	CAAAAATTTAAC-GCGAATTTTAACATCAC-TGCCCGCTTCCAGTCG
-	pGUF-GUF	-		TAAGAGACACCGGCATACTCTG
-	pGUF-GUF, P1_pGUF	-	AACGCAATTAATGTGAGTTAGC	-
-	P5_pGUF	-	TAAGAGACACCGGCATACTCTG	-
-	P6_pGUF	-	AACGCAATTAATGTGAGTTAGC	-
-	P7_pGUF	-	GGCCATCGTCCACATATCC	-
-	P8_pGUF	-	GGATATGCAGGCCAAGGCCG	-
-	P9_pGUF	-	CGGCGGTGCTCAACGGCCTCAAC	-
-	P10_pGU F	-	ACGCGTTGCGCGAGAAGATTG	-
-	P13_pGU F	-	ACCTGCCAGCCTTGACCGAAAC	-
A1_P1	PA0498	1008	CTTAAGATGAATGCAATTAC	CTTGTAAATAGACCTCTATCG
B1_P1	PA0716	1326	CTTAAGATGAATTTTCAGATAG	ACTAAGGAAGTCACTAAGGG
C1_P1	PA4692	1014	CTTAAGATGCTGATCAAGAT	GTAGTACTTCTCAGATCCA
D1_P1	PA3755	555	CTTAAGATGAAATTCTGCAG	GTCTTTCTTATAGGAAGCCA
E1_P1	PA1888	1410	CTTAAGATGAAAATACTCGC	GAGAGGGTTTTCATAGAGGA
F1_P1	PA0565	339	CTTAAGATGCTGAACAACCTG	CTTTTTGAACTGGTCGTAGG
G1_P1	PA3367	339	CTTAAGATGAAATTCGGACT	CTTTCTCCGATAGCTTTTCT
H1_P1	PA2839	771	CTTAAGATGCTACCGACTCT	ATCGAAGCGATAGATATCCA
A2_P1	PA0625	2238	CTTAAGATGAGTAAAGACATGG	AACCATCGCCGGGTGCG
B2_P1	PA0981	624	CTTAAGATGAAAAAATCACTTG	GTTTAAAACCACTTTATTATTC
C2_P1	PA4872	864	CTTAAGATGCATAGAGCCTC	CTCTTTGACTTCCATGTAGT
D2_P1	PA0642	789	CTTAAGGTGGCCATCACTAT	AGCCTTTATTATCGGAATTG
E2_P1	PA4584	813	CTTAAGATGAACAGGGAAGA	TGAGGTTTCCCTGTGTATT
F2_P1	PA2036	522	CTTAAGATGTGGTTTCTTGG	GAAAACCAACCCGAAAATAAT
G2_P1	PA3497	1221	CTTAAGATGATGAAAACCCA	GAAGTAGTAGCCGATGTTCA
H2_P1	PA3093	1119	CTTAAGATGCGTAAGCTGAT	TAGCCAGAGATTGACCAGTT
A3_P1	PA1090	663	CTTAAGGTGTCGCCTATTGA	ATCATTGAGTTCCAGTTAT
B3_P1	PA5201	2340	CTTAAGATGGACAGCATCAA	CTTCTTCTTCAGTTGCTTGG
C3_P1	PA2459	606	CTTAAGATGACTCAGTGGCA	TGCCAATTGCAAAAATCTAT
D3_P1	PA0442	117	CTTAAGATGGTGAGAACCTT	GATGCTGATCATCGATTGAG
E3_P1	PA4377	243	CTTAAGATGAAATTAGAAATCACTC	GCGCGACAGGCTGGC
F3_P1	PA5138	753	CTTAAGATGCAAGAAGCCT	GAGATAGCTGTTGAGGATGT
G3_P1	PA4940	186	CTTAAGATGTGGCAGGAATT	GTGAATCCAGTAAAGAAGCA
H3_P1	PA2501	168	CTTAAGATGGATTCTACGG	GTAATGGGTGGCGATATAGA

A4_P1	PA2461	480	CTTAAGATGATAACTATTTTTTTTG	GCCTTTAATCGACCAAAA
B4_P1	PA4592	1482	CTTAAGATGAATAGGTGGGG	GTGGTCATTGAGCGAAATCT
C4_P1	PA2455	528	CTTAAGATGACCGAAGAACG	TAGATTGAACACCAGATGAA
D4_P1	PA0255	687	CTTAAGATGGTGGGTAGCAG	ACGCACCATATAGTCCATCT
E4_P1	PA0060	234	CTTAAGATGAAAACCATCGG	GTCGTCGTTCTTCTGGTAGA
F4_P1	PA2538	453	CTTAAGATGCCTGAGCAAAC	GGTTTGAGCGTTGAATAGAG
G4_P1	PA0939	327	CTTAAGATGGACAGCTACCG	GTTTCCAAGGTGTGAAGATG
H4_P1	PA1132	690	CTTAAGGTGTCGTCCTGGTT	GCGAAATACCGAATGGATGA
A5_P1	PA4441	447	CTTAAGGTGGAACAGTCGCT	GTACTTGCCTTTCAGGCCGT
B5_P1	PA5509	669	CTTAAGGTGGTCTCTGGTCTG	GAGCCAGGGATACAGACGCT
C5_P1	PA1197	771	CTTAAGATGGACAGCCACAG	TCGATAAATGTGACTTACCA
D5_P1	PA3754	612	CTTAAGATGAACTGCACGCT	ACTCAGTTTGATGAACGAAG
E5_P1	PA0715	957	CTTAAGATGAAGAAGAGACCTTTAG	GAGCTTCGGTGATTTATGAA
F5_P1	PA3826	498	CTTAAGATGCCGAAACACAT	CTTCTTGAGTGTTCTTCG
G5_P1	PA0722	252	CTTAAGATGTCAGGCGTTGT	CTTGGCTTTACGAAGAAGTG
H5_P1	PA2037	1461	GAGCTCATGAAGAAGTCTATGATTC	CTTCAAACCATATCCAAGCT
A6_P1	PA1369	753	CTTAAGATGAACCAGGAGCA	TTTAGTCTCTTCAGTGCCCA
B6_P1	PA1372	2136	CTTAAGATGTCAATAGATATTCTGGT	TTTATCTTTCTCTCCAGAG
C6_P1	PA2902	849	CTTAAGATGTCCTTTCGCTG	CAAGTCACTTTCCTGCGTAG
D6_P1	PA4746	459	CTTAAGGTGTCGAGCAAGCT	ATCAAAACGGGGAATGATGT
E6_P1	PA1370	1866	CTTAAGGTGTCGAGCAAGGA	GCTCGCATTTTCTTGAATCG
F6_P1	PA1231	909	CTTAAGATGTCCATCGTTCG	AAGGTACTCTGCAACCAGC
G6_P1	PA1764	1599	CTTAAGATGAAGATGCGCAT	GAAGGTCGTACGGTAGGTC
H6_P1	PA2228	1212	CTTAAGATGATAAATAAGAGAAATGC	CCTCACCCCTACTGTTCTTG
A7_P1	PA3518	987	CTTAAGATGAATACCCGCAA	CTTGACGCTCTGCATCTCTT
B7_P1	PA0539	831	CTTAAGATGCTAGCCACCAG	GAGCTTCATCAGCAGCATTC
C7_P1	PA1305	474	CTTAAGATGAATGAACAAGACTATCT	CAGGCGCGGCTCGATG
D7_P1	PA2218	1104	CTTAAGATGGAAACCAAGCA	CAGATGCTCGTGAAGAATC
E7_P1	PA4294	507	CTTAAGATGACGACTAGTATTAAGGA	CAGCAACAGGTTGGCAC
F7_P1	PA3353	792	CTTAAGGTGCTATCATTGAGGC	GAACAGTTCGTCTTCTCG
G7_P1	PA2730	954	CTTAAGGTGGCGCTGAATC	CTGGATTGAGTATTCCTCAG
H7_P1	PA0982	549	GAGCTCATGTCTATCGTACCGG	GAGATCCTTGGCTAGCCAG
A8_P1	PA0497	1002	CTTAAGATGAATGCCTTCATCC	CTTGTAGTAGACCTCTATCG
B8_P1	PA0007	1707	CTTAAGGTGAAACGCTGAA	CAGGACCTTCAGATACTCC
C8_P1	PA1917	348	CTTAAGATGAACCTTCGCT	GTCGAAGATCAGGTAGGTCT
D8_P1	PA4471	396	CTTAAGATGTCCTTCGAGGC	GTCATCTTGGTTTCCTTGTT
E8_P1	PA1371	702	CTTAAGATGAATAGAACAGACGTAAC	CGCGAAATAGAATGATCT
F8_P1	PA2458	1122	CTTAAGGTGCAGGACGTCAC	GAGTAGGGAAAATAAATCTGTC
G8_P1	PA0560	489	CTTAAGATGATCCCCCTCAA	GAGACTCTTCAGGTCAGGT
H8_P1	PA1831	711	CTTAAGGTGGGAGCATCTA	TCGATAGGTGATGAGTCCG
A9_P1	PA2189	555	CTTAAGATGTCCAAGCAGCA	AGAATGGATACTCCACTGGC
B9_P1	PA3054	1905	CTTAAGGTGTTCCCTTGCCCT	GAACACCACTCCTACCGGAT
C9_P1	PA0754	984	CTTAAGATGATGATGAAACTGTCTT	CTGGATCAGGCCGAAGTCC
D9_P1	PA0805	228	CTTAAGATGTCTATTCAACATCGTAC	GGCAGCCAGTGTTTTCTTGC
E9_P1	PA1688	870	CTTAAGATGCTGACCAAACG	CAATTCGCTCTTCTGTCGTT
F9_P1	PA2990	723	CTTAAGGTGACTCTCATCTATGGAC	GCGATCCCCGAGGGTGGC
G9_P1	PA3305	1995	CTTAAGGTGCCATTCACTG	TGCAGACTCATGGCTTCC

H9_P1	PA4562	1539	CTTAAGATGAATCTTCTCAAATCAT	CAGCACCGCCCGGC
A10_P1	PA0340	804	CTTAAGATGGAGTTTCTCTATAT	CGACAGAAAAGCGAGATCGG
B10_P1	PA1936	201	CTTAAGGTGATGTTGAGCG	AGAGAGCCTGTTGATGGCC
C10_P1	PA2734	1296	CTTAAGGTGCTGCGTAATGG	GTCTTCAGCATCGGCTTCC
D10_P1	PA3390	303	CTTAAGGTGTAATGATCTTTATCA	GCGCAGCGGATTGAGCG
E10_P1	PA4735	3267	CTTAAGATGCCCAAAGGACT	CTCGCTATCCAGGTGCAGTT
F10_P1	PA2372	573	CTTAAGATGAACTATTTATTCGTGC	AGGTACTCTGTCTTGCTT
G10_P1	PA4379	684	CTTAAGATGAACAATCCGCC	TTCTTTTCGCAAGATATAG
H10_P1	PA1387	1557	CTTAAGGTGCCAAGCGATG	CAAGACGTAGTGGAATCGC
A11_P1	PA4958	1464	CTTAAGGTGGTCCAGGAAGC	CAGAGACTTCAGAGCGAG
B11_P1	PA5182	414	CTTAAGGTGTTGGTTGCGT	GTCGTCGTAGTAGCGACGAT
C11_P1	PA1536	540	CTTAAGATGAACCTCCCCCT	GGTGAAGTCCAGGTGCTAAT
D11_P1	PA2737	258	CTTAAGGTGCTGCGCTACTG	CTTCTTCAGGACCAGCAGGA
E11_P1	PA2820	774	CTTAAGGTGTCGCCACTCCT	GTCGTAGACGTTCTTCTTCTCC
F11_P1	PA4838	1155	CTTAAGATGCCCAACTCCAT	GAAGTATTCAACCAGGCG
G11_P1	PA2038	315	CTTAAGATGGTCTGGGCAGT	AATCAGCCACCACTTGAAC
H11_P1	PA2606	360	CTTAAGATGAGCCAGTCGCT	GAGGGTAATCACCTGGTCG
A12_P1	PA2759	315	CTTAAGATGAAGATTCTTATTGCTG	GGAACAGGTCTGGCC
B12_P1	PA5494	291	CTTAAGATGCGTACGCTGAA	CCAGCTGAAGATCTCCATT
C12_P1	PA1040	498	CTTAAGATGAGCGAACCGAT	CCACCAGTACTTGCCGAAG
D12_P1	PA1298	276	CTTAAGGTGGCCCATACCAT	CTTCAGGTAGGAACGCAGCG
E12_P1	PA2529	1434	CTTAAGATGATCGACCCGTT	GGTATCTCCCCGAATACG
F12_P1	PA4583	1215	CTTAAGATGAAAGACATGAATATCCT	TCCTTTCACGCACACCACC
G12_P1	PA4699	780	CTTAAGGTGAAGAAGATTTCTGATT	GGAGCTGACCTTGGCCTTC
H12_P1	PA1874	7407	CTTAAGATGTGATCCAGGC	GACCACGACCTGTACCGTG
A1_P2	PA2074	813	CTTAAGATGGCCAAGGTTACCGTCGC	ATACAGCTCGGGTCGCCGGT
B1_P2	PA2090	1080	CTTAAGATGAGCATCGAACTGCGCG	TGCGACGCGCCTCAGG
C1_P2	PA2336	1341	CTTAAGATGCCAGATTCCCGATGCT	ACGCCGCGCCGTGAC
D1_P2	PA2352	1128	CTTAAGATGCGGCAAAGATTCTGGCA	GTAGCCGTGCCGGCGC
E1_P2	PA2415	426	CTTAAGATGGCCACCGCACTACGCT	GCCATGCGCCACCTCCTC
F1_P2	PA2440	963	CTTAAGATGCGAAGCCTGATCGGGAT	TGGGCGGGCTCCACGATA
G1_P2	PA2594	960	CTTAAGATGTCTCGTCCGTTCTGCG	GTGCCGCGGCTGCCATAC
H1_P2	PA2989	765	CTTAAGATGGGTGCGACGTTTGCC	GGTCGAAGAAGGTTGGCCCG
A2_P2	PA3022	807	CTTAAGATGTTCCGTCTCTCCGCGCT	GTCGAGGATTTCCACCGGCA
B2_P2	PA3783	630	CTTAAGATGTCCGCACGTCAACCCA	GCGGTTGGCCAGGGCTC
C2_P2	PA3785	477	CTTAAGATGCGCACATCCTTCTCGC	GTGGCCGTGCTGCTCGTG
D2_P2	PA3908	720	CTTAAGATGACGGACGCCAAGGCTTT	GCCGCGCAGCGGC
E2_P2	PA3928	171	CTTAAGATGGTCCGTACGCCGAGTCA	GTGCGGGACGCCAGC
F2_P2	PA4200	867	CTTAAGATGCGAACCCTCACCACCT	GGCCTCGAGGTTCTCGACCC
G2_P2	PA4347	1155	CTTAAGATGTAGGGTTGCCCTCGA	TGGCCGCGCTCCC
H2_P2	PA4348	786	CTTAAGATGCGACGCGAACCATC	GCCTGGCATGCGGTAGTCGT
A3_P2	PA4420	942	CTTAAGATGAATGCCACCTACGCCA	TCTCAGCTTCTCCGCCACGC
B3_P2	PA4639	588	CTTAAGATGCTGCATCGCTGTTGCT	TTGCTGGCCGAGGGTCTGAG
C3_P2	PA4773	483	CTTAAGATGGCAATTCAACCGTTGCG	GGCCACCCCGTGCC
D3_P2	PA4879	2070	CTTAAGATGACGCGCGGCCG	GCGCTTGCCGGCCG
E3_P2	PA4928	2244	CTTAAGATGCAAGCCGCCAAGCC	GCGCGGGATGTTGCGCT
F3_P2	PA5108	258	CTTAAGATGGCGTGTTCGTACCT	CTTGAGCCCCTGGCCGG

G3_P2	PA5212	330	CTTAAGATGCGTTCCGTCAAACCTCGC	CTGCTGGACGGCGGACTG
H3_P2	PA5357	537	CTTAAGATGCCCAGCAATGCGCTCT	TACGTCGGCGATTCCCGC
A4_P2	PA5442	2856	CTTAAGATGACCGTCCATGTCGAGCC	ACGAGCCTGGCGCAAACCTT
B4_P2	PA5507	654	CTTAAGATGTTGAGCCTGCCCCACC	CAGGTTGTCCGGCCGAG
C4_P2	PA0855	1020	CTTAAGATGAACGGAACCGCCGC	CCAGCGCGCGCGG
D4_P2	PA1966	372	CTTAAGATGCCGCATCTCGTCATCG	GCGCTGCCGGGCGA
E4_P2	PA2868	360	CTTAAGATGGGCAAACGTCATCCCAA	CTTATGCCGTTTCGCGCCAAG
F4_P2	PA3939	921	CTTAAGATGAGCGAAGCCCGGCTC	CAGGGCCGCGCCCA
G4_P2	PA3978	549	CTTAAGATGTTCCGTACCGGCCGC	GGGCAGCGCGCGCA
H4_P2	PA0814	435	CTTAAGATGCAGACATCCCCGCTC	TGGCCGACCGCCG
A5_P2	PA0851	963	CTTAAGATGCCTTTTTCTCTCGCCGC	GTCGCCGGCGGCCA
B5_P2	PA3904	396	CTTAAGATGAGCGGCAAACCCGCT	CGGTGCGCCGCCGA
C5_P2	PA0239	879	CTTAAGATGAACGCATCCACCTCCCC	GCGGCCACGGCGCC
D5_P2	PA2498	633	CTTAAGATGCTGGTCTGCGCAGCATT	TTGGGCGCCGGCGG
E5_P2	PA4623	390	CTTAAGATGAAACGCCCGCTGATCCT	GGCGGGGCGCCGC
F5_P2	PA0446	1224	CTTAAGATGCCCGGCGCCCT	GATCACCTTGCCGTCGCGCA
G5_P2	PA3911	516	CTTAAGATGCTGAACCGCCAACGC	GCCGCCCGCGCG
H5_P2	PA0063	1128	CTTAAGGTGCTGGTAGGGCGGCG	GGGCGCTGCGGCGG
A6_P2	PA2186	171	CTTAAGATGACCGCCAAGCGC	GGCGGGACGACGGGC
B6_P2	PA2331	561	CTTAAGATGTCACGCGTTCCCG	GGCCTGCGGGTTGGTCC
C6_P2	PA5303	354	CTTAAGATGCCCATCCAGCGC	GGGCAGCGAGCGACC
D6_P2	PA0543	969	CTTAAGATGCGTACGCTGATCCGCC	GCGCGGCAACTGGCTG
E6_P2	PA2464	525	CTTAAGATGAACGCAAGGATCGCCG	CTTACCAGGAGGTCCTTGC
F6_P2	PA0168	591	CTTAAGATGCCGAGCACCTGCAAG	GGCGTCCAGCCGCTGC
G6_P2	PA0209	882	CTTAAGATGAACGCCATCGCGAACC	GAGACTCCCAGCCCACCCAC
H6_P2	PA0309	753	CTTAAGATGCGCGCTTTGCTCGC	GGGGGCGACCGCCTG
A7_P2	PA0660	969	CTTAAGATGTCTTGCCCGCCCTG	GCGCGGCCAGCGGT
B7_P2	PA0731	738	CTTAAGATGCCAACCTTCTCCGTGC	TTTGAGCAGGCTGGCGATGA
C7_P2	PA1398	342	CTTAAGATGCGTAGCCCGCTTGCC	GGGCTTCGCCGCTTG
D7_P2	PA1468	417	CTTAAGATGCCTGCAATACCCCTGCG	GGCGATGCCGCGCAG
E7_P2	PA1550	540	CTTAAGATGCAGTCCGAGACCCACCC	TGGGCGCTTCGCTTCTGC
F7_P2	PA1817	390	CTTAAGATGCGCAGCGCTTATCGGA	GCGTGTGCCCCGTCC
G7_P2	PA1906	537	CTTAAGATGCATATCCCGCCGAGC	TGCGTCTGCGCGGACT
H7_P2	PA2423	795	CTTAAGATGCTCAGGGAACGGGTTTCG	GAGCGGCCGCAACTTGC
A8_P2	PA2559	543	CTTAAGATGAGAAGCAAGGCGTCCGG	GCGCAGGACCAGGCTGG
B8_P2	PA2569	342	CTTAAGATGCCCTGCCGACTTTCCC	GCGCGGGCAGGAAACCT
C8_P2	PA3021	387	CTTAAGATGAACAAGCCCTCGCCAC	GAGCTTGCGTCGACGCA
D8_P2	PA3040	330	CTTAAGATGCCCGCAAGACCACTG	GCGCCGGCTGACCAACA
E8_P2	PA3323	876	CTTAAGATGTCCAAGGCGCCTGG	TGCGGCTCCCGTCT
F8_P2	PA3359	1011	CTTAAGATGTCCGCAACGACCTGC	GTGGCTGTAGTGCCGGGTGG
G8_P2	PA3772	897	CTTAAGATGACCCACCGCACCGC	GAACACATGGACCAGGCGCA
H8_P2	PA3786	390	CTTAAGATGCCCTGTACAGGCG	GGCGACAGGAGAAGCGCG
A9_P2	PA3886	900	CTTAAGATGAGCGATGCCCGACCT	GACCAGCCCTGGCGCG
B9_P2	PA4657	984	CTTAAGATGAGCGTCCCCATCGCC	GAGATGTTCCAGCAGGCGCC
C9_P2	PA4766	306	CTTAAGATGGCTGAGATCGCCGTCG	ACCGCCTTCGCGTTCGC
D9_P2	PA4849	867	CTTAAGATGGAACGCATCCGCCG	GCCGGCGCTGCCACTC
E9_P2	PA5123	573	CTTAAGATGATCCGCGCATTCTCG	GCGCTCGTTGGCTCTATCG

5. Supplementary data

F9_P2	PA5444	429	CTTAAGATGCTGGCATCCTGGGCCT	TGGGCGGATTGCCAGGAC
G9_P2	PA5534	642	CTTAAGATGAGCGCACTGCCGCAG	GGCAAGCCAGTCCAGGGTCA
H9_P2	PA0751	1038	CTTAAGATGCCTGAGCGCGTCACCT	GCCGGCGCGCTTCCT
A10_P2	PA1352	1212	CTTAAGATGCCATCCTCGCCATCCTC	GGCGCCGTTGGCGC
B10_P2	PA2441	876	CTTAAGATGAGCATGGCTTCCAGCCC	CGGGTGTTTCGGCCGCT
C10_P2	PA2600	1068	CTTAAGATGATCACCGCCACACCGAG	ACCGCGGTGCCCAAC
D10_P2	PA2768	483	CTTAAGATGACTGCCTCCCCTTCCCC	CTTCCGCTCGACGGCGAG
E10_P2	PA2799	300	CTTAAGATGCAGCCATCGAGCACA	GTGGATCGCGACGATGCTCA
F10_P2	PA3003	630	CTTAAGATGCGCTTGTTCGGTTGCC	TTGCGCAGGAGGTGCGG
G10_P2	PA3465	1716	CTTAAGATGTCCAGTCCGTTTCGCC	GCTCCCCGCCGTCGC
H10_P2	PA3753	525	CTTAAGATGAAATACCGCCTGGGCGA	CGCCGGGTCTCGACG
A11_P2	PA4325	423	CTTAAGATGCGTGCCCTGTGGTTCTG	GCGGCAGCGTTCGGACTC
B11_P2	PA4686	2847	CTTAAGATGAGCCAGACCCGCTACGG	CGCCGGTTCGCCGG
C11_P2	PA4993	921	CTTAAGATGCCCCGTATGCTCGCC	GGCGCTGGCGCGGT
D11_P2	PA5469	765	CTTAAGATGGAATGGCTGACCAGCCC	GTCGCCGAGCACTTCCTTGC
E11_P2	PA0244	855	CTTAAGATGAGCGCGCCGCG	GTCGCCCAGGCTGGCGAAGT
F11_P2	PA1872	792	CTTAAGATGAGCCTTTCCCCCGCC	GCCGCGCCGGGGC
G11_P2	PA2650	810	CTTAAGATGCCACCTTCCACGAAATC	ACCGGCGGCGGACCT
H11_P2	PA0859	603	CTTAAGATGTGCTCCTGGTGCTGG	CTCATGCCGGCCCCGTT
A12_P2	PA2806	831	CTTAAGATGCAGCATCCCGCCGA	CTGGCGCACCAGGCGTC
B12_P2	PA3293	816	CTTAAGATGACGCCGAACCCCCG	TGCGCGACTCGTTCCTCG
C12_P2	PA3680	786	CTTAAGATGACCGATTCCGCCGCTC	GCCCTTGCCAGGGCCT
D12_P2	PA3907	786	CTTAAGATGAGCGGCATAGGCGCG	TGCGCAATACCCCGGGTCT
E12_P2	PA4010	720	CTTAAGATGTCCCGCGATCCCATCC	TTGAGGTGCGGGTCTGAT
F12_P2	PA4364	402	CTTAAGATGGCTGGCGAAACCTCGC	GTGTGCCTCCGCCGCC
G12_P2	PA4667	1773	CTTAAGATGATGGCGCCACCCTCG	AGGAGTCTCGGCGCCGGT
H12_P2	PA4734	882	CTTAAGATGGAAGCGTCCGTCGCC	GTGGCTCACCGGCGGC
A1_P3	PA2731	465	GATCTTAAGATGGGCGATAGTCTG	CCGGTGAAGATTACATTGAC
A2_P3	PA3429	897	GATCTTAAGATGACCGCGGCGCTGCC	GTGCAAAAGCGCCTCTGG
A3_P3	PA0065	666	GATCTTAAGATGCGTGACGCCGCGCTG	TAGTCGCTCGATTCTTCCG
A4_P3	PA5047	1440	GATCTTAAGATGAAGACCGCCTG	GGGGCGGATCTCGATCAG
A5_P3	PA1211	636	GATCTTAAGATGAGCGGCGCGTCTG	ACCTGCCCCAAGATGTCTT
A6_P3	PA2993	1029	GATCTTAAGATGGCTGAGCGTTT	TTCCCCCTCCCGGCATTC
A7_P3	PA3804	1044	GATCTTAAGATGATGAAAGCGCC	GGACCTGTGCTGGCGG
A8_P3	PA3869	384	GATCTTAAGATGGCCATCGAGAA	CAGATAGGCGCTCTGGGC
A9_P3	PA0990	639	GATCTTAAGATGCCATCGGTCAG	CTGCGCTGGGCCTGTT
A10_P3	PA2223	1020	GATCTTAAGATGAATAGAGAATTGGATCA	GTCTTCGCGAGGCTTCTTCG
A11_P3	PA2871	798	GATCTTAAGATGAATTTTCCGAATTG	GGCGAAGCGCACGCAGTA
A12_P3	PA4011	1314	GATCTTAAGATGAGTCTCGACAGGATCTTC	CTGTTGCTGCACCTGCAGCA
B1_P3	PA5310	1590	GATCTTAAGATGAGCCGGTCTGTT	AGAAAAGTCTGAATCATCCAGTCG
B2_P3	PA0318	666	GATCTTAAGATGAGTTACCAGCATCAATA	GAGTCCAGGGATCGTTGGA
B3_P3	PA0431	555	GATCTTAAGATGAGCGCTCCAC	CTGCGACTTGCGAACCCG
B4_P3	PA2286	1545	GATCTTAAGATGAAGGGCACGGT	CCGGCTTTCCCGTGG
B5_P3	PA1935	705	GATCTTAAGATGATGGCGCAGCTGCG	GGCGTTCTCCGATGCC
B6_P3	PA0588	1923	GATCTTAAGATGAGCATTTTCAGTCAGATCTT	GGCGCGCTGCGAGC
B7_P3	PA1753	498	GATCTTAAGATGATTCTGTTCTCTCTA	TTTCATCAGCGCTTCCAGG
B8_P3	PA4924	696	GATCTTAAGATGTTGATCTTCAGATTGCTGATCTT	TGGGGCGAGCAGCTCC

B9_P3	PA2814	672	GATCTTAAGATGCAGTCTACCTACAATC	GAGCAGGCGTCGGCCG
B10_P3	PA4968	621	GATCTTAAGATGACCGGACCCAG	CTTCTTCGTGCCGAAGCTCT
B11_P3	PA4948	468	GATCTTAAGATGTCTGAAGTGATCCTGTC	GCGACGTGGCAAATATTGCA
B12_P3	PA1046	2274	GATCTTAAGATGGAGTTAAGGAAAACAGG	TCGGAGCGCCTCCCG
C1_P3	PA3756	501	GATCTTAAGATGCGCTGGTTGCT	GTGGGATTCCAATACCTGC
C2_P3	PA2283	1458	GATCTTAAGATGAGCCACGATACGC	GCCGAACACCGTGACCATCT
C3_P3	PA1193	672	GATCTTAAGATGCGCGACTACGC	CAGGTCGCGACTACGGTGCT
C4_P3	PA2209	1098	GATCTTAAGATGCGATCTTATTTTGAGTGGAC	ATGATTGACCGTATGTGCCA
C5_P3	PA2699	1839	GATCTTAAGATGACCGCCGACCT	GTCCCCCGGAAGGAAAGG
C6_P3	PA2698	681	GATCTTAAGATGAGCCACTATCTCGAAGT	GGGACGCTTGTCAGCTTGA
C7_P3	PA4404	924	GATCTTAAGATGCACATCATTTTCTGAG	CTCGCCCCAGACGTCGC
C8_P3	PA4539	1092	GATCTTAAGATGTGATCTTTCGGTTGATCTTTTC	CGGAGAAGTGTTTTGGCGCA
C9_P3	PA1166	789	GATCTTAAGATGCGCCTGCTCTG	CGCTCTTCCCCGCCATTG
C10_P3	PA1239	885	GATCTTAAGATGAGATCTTCGTTGACTCAACA	GAGGCCGAGTCTTCGCT
C11_P3	PA1506	330	GATCTTAAGATGCACCGGTCTCT	CCGCAACTGCTGCTCCC
C12_P3	PA3017	438	GATCTTAAGATGCCCTATCAACACATTCT	GGCCGAGTCGCGGACC
D1_P3	PA4717	894	GATCTTAAGATGCTCTGGCGCAA	GCGTACGACTTTAAGCCAAT
D2_P3	PA5281	699	GATCTTAAGATGAGCAGCCTGCG	CAGCGGCCGGTAGCGC
D3_P3	PA4048	645	GATCTTAAGATGCTGCGGCTGTG	GGACGGCGGCAGCAGG
D4_P3	PA1307	774	GATCTTAAGATGTGTGAACATTGGGCAT	CTGGCGAAGCCAGCCG
D5_P3	PA1280	585	GATCTTAAGATGAGCCTGCGCCT	GGCTTTCTTCAGGTGCACCG
D6_P3	PA0391	1968	GATCTTAAGATGAGCATGGAAAGACTCAG	GGTGCCTGCGACCTGGC
D7_P3	PA2044	1875	GATCTTAAGATGCCCCGTCATCC	GTCCCAGCCGAACAGCTC
D8_P3	PA2958	1134	GATCTTAAGATGAATTGTTACCAGGACGA	CTTGCCGATGCAGAAACTCG
D9_P3	PA4792	936	GATCTTAAGATGAATCGAAGTATTGCGAT	GCGGAGTTCGTCAACCAGCA
D10_P3	PA5081	477	GATCTTAAGATGGCCGAGGCGATCTT	GATCTCGATGCGTTCGCC
D11_P3	PA5551	510	GATCTTAAGATGCCGAAGCCTGC	GGCTGCGCCGAGAAAGCT
D12_P3	PA0496	978	GATCTTAAGATGTGCGATTAAGGTGCTCAA	GGGCCACTGCATCTCGCC
E1_P3	PA3170	1335	GATCTTAAGATGCCAACGTCCG	ATTATTAGATTGATAAGGGCACG
E2_P3	PA5209	1365	GATCTTAAGATGCAGAAAGAAACCGAAAT	GAGCATCTTTTCCAGTCCGA
E3_P3	PA5396	978	GATCTTAAGATGAGCCCAGCCGA	TCGACGCCCTTCATCTTGTC
E4_P3	PA3564	678	GATCTTAAGATGGTGCTCGGCGT	GAAAGCGAAGCAGGAACAGC
E5_P3	PA3301	951	GATCTTAAGATGCCCGCGCTGCCA	GAGCGTCTGGGCTTGAAGG
E6_P3	PA3941	597	GATCTTAAGATGAGGCTGCGCGA	CCCGCCGGGCTGATC
E7_P3	PA5513	879	GATCTTAAGATGTGCTATCCCCCTG	TGTTCTCTCTTTGTGCAATGATC
E8_P3	PA3681	696	GATCTTAAGATGCGCCGCTGGTT	CCCCGCGATCCGACC
E9_P3	PA4458	540	GATCTTAAGATGAGCGATACCCATTCTG	GCGAATGAAGTTGCGGCTGA
E10_P3	PA3251	810	GATCTTAAGATGCGCCACGACGT	CATGAAGGTGCCATCGAGT
E11_P3	PA4965	525	GATCTTAAGATGACGCAACGGGC	TAAAGGAAGGGCGTAGGTACCGGT
E12_P3	PA5567	1368	GATCTTAAGATGCAAGCCGCCAC	TCCACCTCTTCATCGGCCA
F1_P3	PA0469	858	GATCTTAAGATGGCCACAGTGGAATACT	TGGACGTTCTCCTTGTTGC
F2_P3	PA3971	432	GATCTTAAGATGCAGGCGCATCC	GAGCACGCGGGTCTCGAAAC
F3_P3	PA4952	1020	GATCTTAAGATGGCCAAACGCCA	GTCAAAAGTCGAAAAGTCGG
F4_P3	PA0277	759	GATCTTAAGATGAAGATCCGTGATCTTCCCT	CTTGCCGGATTGCGGGC
F5_P3	PA0542	420	GATCTTAAGATGTCCATTGTCGATCTTCACT	TTGCAGGCGGGCGAG
F6_P3	PA2635	2019	GATCTTAAGATGAGCCTGGAGAAAAAGA	GCGCTGCAGGCCAAGGT
F7_P3	PA3320	456	GATCTTAAGATGCCCAATTATCTGATGGT	CGGCGTTTGCAGTTGCTC

F8_P3	PA2831	1128	GATCTTAAGATGCAGATCCGCGC	TTCGGCCAGCGCCAC
F9_P3	PA3846	543	GATCTTAAGATGCTGATCCGCGC	TAGGCGGATCGACAGGCCAT
F10_P3	PA4065	1266	GATCTTAAGATGTATCTGATCTCCGACTGGC	CGGCAGTCCTTCGAGCAG
F11_P3	PA5079	438	GATCTTAAGATGAAGGCATTGCTGCA	TGGCGGACTCCCGGC
F12_P3	PA2915	867	GATCTTAAGATGTTGAAACCCGACATCAC	GATGTTGTACGCCGAGGGCG
G1_P3	PA3767	549	GATCTTAAGATGCGGGTGACTAAGCTG	TTGTCTACCTTCAGACGGG
G2_P3	PA1202	618	GATCTTAAGATGTCGATCTTACCTACAAGCG	GTAGTACTGGCGGTAGTGCT
G3_P3	PA2682	1242	GATCTTAAGATGGGACAGTACGTCAGCAT	TGCTCCCATGGTCAGGGT
G4_P3	PA3614	1404	GATCTTAAGATGGCATCACTGACGTTTCT	CTCGGAAACAGACGCGCG
G5_P3	PA4382	795	GATCTTAAGATGACCCAGGCCGC	ATGCTTGGCCTCGATAAGCA
G6_P3	PA5177	666	GATCTTAAGATGCCACCTGCC	TCGGCTCGGCAGTACCGTAT
G7_P3	PA0968	447	GATCTTAAGATGCGCGCGCAACACG	TGGATTGGGCGAGGAGAAAGT
G8_P3	PA0978	828	GATCTTAAGATGGAAGTGGTCTGTTACGC	GTAGTCCGTTTCCGGCATGC
G9_P3	PA1356	1107	GATCTTAAGATGAGCGAGCGACTCTATGT	ACTCTCCAGCAGGAAGGTCA
G10_P3	PA3623	894	GATCTTAAGATGGATAAGGGGAAGGATT	ATCTCTGTGAAAAAGAATCCGG
G11_P3	PA3969	1086	GATCTTAAGATGCCCTCCCTGCG	TCCACGGGCCTCCCTGG
G12_P3	PA0480	798	GATCTTAAGATGGGCAACCTGTGATCTTTCT	GAGCGGAAGGGGCGCT
H1_P3	PA0957	408	GATCTTAAGATGAACGCGGCGCAGG	TACCGGTAATCCGGCACTTT
H2_P3	PA5488	879	GATCTTAAGATGTTGCGCCGCTG	GTTTCTTGCATGGGGATTCT
H3_P3	PA0333	1272	GATCTTAAGATGCGTATTCTGCTGGTAGG	TGAACCGGCTGAATCCTCGC
H4_P3	PA0370	597	GATCTTAAGATGAGCAAACCTACTGCGAA	ACAGCGAAGCTGGCGCA
H5_P3	PA1732	801	GATCTTAAGATGAGACTCTCGATACCCA	GACCCGCCCTTGCC
H6_P3	PA2086	903	GATCTTAAGATGAATACCGATCCGTTGC	GCGCAGGAAGAAGTGCTGGA
H7_P3	PA5194	804	GATCTTAAGATGGATAATGCCTCTCCGTT	CCGGCAGACCTTCATAGGC
H8_P3	PA0057	888	GATCTTAAGATGTCGCGCCATGG	CTTGCGATCCGCAGCGAT
H9_P3	PA0451	1332	GATCTTAAGATGCGGATGCCGTG	GAACAGATCCAGCGGGATCT
H10_P3	PA1733	732	GATCTTAAGATGACCTACTGTGTCGCGAT	ACCCATCCCGACAGTGGGT
H11_P3	PA1792	723	GATCTTAAGATGAGCGTCTGTTTCATCTC	GGCTCCCGCTGCCAG
H12_P3	PA1050	1113	GATCTTAAGATGTTCGAACTGGATTCGAC	CCCGCGGCGCGGAA
A1_P4	PA0495	879	GATCTTAAGATGCACGCCAACAT	ATCGACATGCAGTACCTC
A2_P4	PA3172	681	GATCTTAAGATGAAGCGCATGCG	GCAGTCGCAGAGCGCG
A3_P4	PA0545	1305	GATCTTAAGATGAACTGTTATGGGGAG	GCGCATGCGGAAGGCTTC
A4_P4	PA0976	675	GATCTTAAGATGAACCAGAAGAAAGCG	GAAATATGGCGTCGGGTCGG
A5_P4	PA1089	603	GATCTTAAGATGCGCACTGCCTA	CAGCATGTTCAATAGCGGAC
A6_P4	PA2301	543	GATCTTAAGATGGTTCTGCGCGA	ACCGGCTTCGCTGAGTTC
A7_P4	PA3515	1074	GATCTTAAGATGACAAAGGCTAACGAG	GGGTCGCAGTTCGAACAGCG
A8_P4	PA2222	648	GATCTTAAGATGGCCGAGATCAATATCTA	GATCGCTGCAAAATAGGCCA
A9_P4	PA3332	426	GATCTTAAGATGAATGCCAAGGAAATTCT	GGCTCCCTGGACGATCTTGG
A10_P4	PA3674	399	GATCTTAAGATGAAAAAAGTCCATTGC	GCGCGCCGATTCGACCT
A11_P4	PA4372	1065	GATCTTAAGATGTTCCGCCACG	GTCGCCATCGTTGGCGTT
A12_P4	PA5135	774	GATCTTAAGATGTCGGCGTTCCG	GTGCGGCGCTGGC
B1_P4	PA5371	405	GATCTTAAGATGATCGAGCTTGAACAAG	GCCCCGGCGTGGCG
B2_P4	PA0335	654	GATCTTAAGATGCGTCTGCCCT	ACGCAGGGAATGATCGGCC
B3_P4	PA0562	675	GATCTTAAGATGCCCCACCCAT	GACTGTCCGGCGCAAGC
B4_P4	PA0573	336	GATCTTAAGATGGATTACAGCCCGATAG	TGCCAAAGCCTGTGACCTGC
B5_P4	PA0820	813	GATCTTAAGATGCCCGCGTTATCGCTG	AACGACTACATCAGCCTC
B6_P4	PA1568	354	GATCTTAAGATGCATATCGAACGTTTCG	CTGCGGGCGGGCGGCGAC

B7_P4	PA1813	777	GATCTTAAGATGATACAGATCGACGCC	GAAGTGGTCTTCCAGGCC
B8_P4	PA2732	3441	GATCTTAAGATGAAACCCACCGATACC	TCGCCATGCGCAATCCT
B9_P4	PA3046	345	GATCTTAAGATGGCTACTAATCGTTCCC	GAGCTTCGGCAGGACAGGCT
B10_P4	PA4445	759	GATCTTAAGATGGCTATCGCCTGAGC	GGCAGGATTAGGACAGTC
B11_P4	PA4535	630	GATCTTAAGATGAACGAAGCGGATTATCT	CAGGCCTACCCCGGCGTC
B12_P4	PA0049	1662	GATCTTAAGATGCGCTACGCCCC	GTCCGCTTGCGCC
C1_P4	PA0351	474	GATCTTAAGATGCCCCAGTCCC	GAGGGTGATCAGCTCCGCT
C2_P4	PA0462	705	GATCTTAAGATGTTGAGAAGCAGCAGAAG	CTTGCAAGTGGGCTTGTCCG
C3_P4	PA0630	363	GATCTTAAGATGAGCCGGCTCGC	TAGTCCAGCTCCCGTCTGA
C4_P4	PA0868	414	GATCTTAAGATGCTGATCATCTCCAATGC	GAAATCCACCTTGCCGCG
C5_P4	PA1035	495	GATCTTAAGATGAATTACCAGGCGCAAAT	TTCTGGGATGAAATCGCCGG
C6_P4	PA1558	633	GATCTTAAGATGTCGCTGAAATGGAACC	ATGGCCCTGGAGCCCC
C7_P4	PA1621	813	GATCTTAAGATGTCGAATCGGTTTTCTT	TGCCGAACGCTCCTCGGT
C8_P4	PA1762	762	GATCTTAAGATGTTGAGATTTTGCTGGG	CTTGGTGCGCAGGTGTATGA
C9_P4	PA1768	540	GATCTTAAGATGAAACTCAAGCCCTAGC	CTCAGCAGTTTTGTCATCAG
C10_P4	PA1842	363	GATCTTAAGATGAAATTCCTCACTCCC	CTCGAAGAAGTTGTGCCAGC
C11_P4	PA1938	822	GATCTTAAGATGGTCTGTTCAGCTTTCG	ACCCATCCCGGACAGTGGGT
C12_P4	PA2164	1752	GATCTTAAGATGGCGATCCGGCG	CTCATGGCGGGCTCCAG
D1_P4	PA2325	1236	GATCTTAAGATGAGCGCACTGGAAG	GAGCCAGGCGTGCCGCG
D2_P4	PA2695	1104	GATCTTAAGATGAAAGCAGTACGCCAG	GCGTTTCCGCACGCG
D3_P4	PA2823	891	GATCTTAAGATGGATTCCCGATTGAGC	TGCCTGGCGCTCCAGC
D4_P4	PA3066	573	GATCTTAAGATGAACACAGCACTGATCG	GAGCGCTGCCAACTGGTC
D5_P4	PA3762	318	GATCTTAAGGCATGTACAAGCTGTGTTTC	GAAGACCATGTCGGTCAGGC
D6_P4	PA4122	780	GATCTTAAGATGAAACACGCACGCATC	TTCTGCGTGCTCCTGTGC
D7_P4	PA5130	420	GATCTTAAGATGCAATTCGTTTCCCGTC	CTTACCAGCGGCAGGTGT
D8_P4	PA5196	435	GATCTTAAGATGGTCGGGCTGCG	AACCGGGCTCCGTCGAG
D9_P4	PA5343	852	GATCTTAAGATGTCGCAACAGTGATGAT	GGCGTCCCCGAGCACC
D10_P4	PA5391	675	GATCTTAAGATGACCTTTCCATCGTCG	CTCGTCGCCGGGCAC
D11_P4	PA0127	501	GATCTTAAGATGCGCCTGCCTGC	GAGCCCTTGGTCTTCGG
D12_P4	PA0544	744	GATCTTAAGATGAAGATCCGCTGCTG	GACCTCGAAGACGAATCCG
E1_P4	PA1111	624	GATCTTAAGATGCAGTCACGCTGATC	AAGCAAGGCGACCATTTCTT
E2_P4	PA1195	765	GATCTTAAGATGTTCAAGCACATCATCGC	GAAGCGCAGCGACATGCAAC
E3_P4	PA1293	1062	GATCTTAAGATGAAGAAGCTCAGCGGAAT	GGGAATCGCCAGACGGCC
E4_P4	PA1638	909	GATCTTAAGATGCAGCAACTGTTGAACG	GAAGATCGACAGCCGATCC
E5_P4	PA1730	1413	GATCTTAAGATGGCACGCATGTTTTACG	TTCTCCACCACCCAGGTGT
E6_P4	PA1740	999	GATCTTAAGATGATGAGACGACAGGCTTC	ACGGCCCCGGCCG
E7_P4	PA1784	696	GATCTTAAGATGATCGATCTCAGCACCTG	GCGATGGGCGGTGTTTACG
E8_P4	PA2091	1284	GATCTTAAGATGAGCGGCGTTCGC	GTCTCGCCATGGCTGC
E9_P4	PA2745	864	GATCTTAAGATGAGTGGCGAACTCGC	GGACGTTTCCACGTCCGG
E10_P4	PA2756	435	GATCTTAAGATGCGGCATTTCTGATGAAC	GCCCGGCACAGGCC
E11_P4	PA2833	447	GATCTTAAGATGTTCCATACGCTCCTGG	ACTCCCTGCGCATCTCCCT
E12_P4	PA2927	1332	GATCTTAAGATGCCCCGTTGATCGTC	GGGGTTCCTGAAGACGAATA
F1_P4	PA3226	828	GATCTTAAGATGCCTGACTTCCAGCAC	GGAGACGTTTGAGCATGGTT
F2_P4	PA3472	597	GATCTTAAGATGCGTTTACCTTTTTGAC	GCGCTTGGGGTGCTTTC
F3_P4	PA3499	435	GATCTTAAGATGACCGGGTGCG	GGCTTCGTGCGAGTTCGCCA
F4_P4	PA4012	594	GATCTTAAGATGAAGTTGCCGTTGTTTCC	GTCGATACCAACTCGCCCT
F5_P4	PA4030	831	GATCTTAAGATGTGGTCGTTCCGCG	GCCGTTAGTCGTGTCGCC

5. Supplementary data

F6_P4	PA4060	279	GATCTTAAGATGGAGCTGAGCTATTCGG	GGCTTGCCCGGTTTCG
F7_P4	PA4093	417	GATCTTAAGATGACCGACAAGAAAGAGCA	GCGGCGGTGCGCC
F8_P4	PA4510	678	GATCTTAAGATGATCCGCATCGAACCC	TTCGCGCCCGCCCA
F9_P4	PA4604	1005	GATCTTAAGATGTCCGAAGTAGCCAACG	GCGGCCCTTCGACGATGC
F10_P4	PA4789	306	GATCTTAAGATGGACCTGCACGAACTC	TGGCAGGAAGCGCCGTTTC
F11_P4	PA5106	1362	GATCTTAAGATGTCCGAATTTTCGCTG	GTCGAGCAGTTCCCCAGCA
F12_P4	PA5295	1677	GATCTTAAGATGTCAGCGCCCGC	ATTGCCGAGCGGCTGGC
G1_P4	PA0457	525	GATCTTAAGATGAAGCCTGTGCAATCCC	CTGAGCGGCGAGCGC
G2_P4	PA0667	1344	GATCTTAAGATGTTCCCTCGAGCGA	GCGCTGCTTGTTACGGGC
G3_P4	PA0824	519	GATCTTAAGATGAGTGGAACCCGCC	TGCGTCGCACCTCTGCAC
G4_P4	PA0988	405	GATCTTAAGATGCCGACCCCGTT	TGCGAGGAGCGCGC
G5_P4	PA1005	1434	GATCTTAAGATGAATGTACTGCGCCCTG	GCGGAACATTTCTTGACCA
G6_P4	PA1616	465	GATCTTAAGATGAAGCTCTGGCTGTTGC	GCCGTGCCGCGGGT
G7_P4	PA1640	1038	GATCTTAAGATGAGCAAACAGGTGCGC	GGCGTTGTCTTCTCGTAGC
G8_P4	PA1865	1680	GATCTTAAGATGCATGAACAGTACCAGGC	GTCATCGACATGCCAGCG
G9_P4	PA1893	2430	GATCTTAAGATGTCGAAGAACGCACGTT	TGGTCGTGGCTCGCCG
G10_P4	PA2151	1995	GATCTTAAGATGAGTTCGATTGTCCGCAA	TGCGTCGACGCGCC
G11_P4	PA2172	1077	GATCTTAAGATGCGCGAAGAAGACCG	GGCTTCGTCTGCCGCG
G12_P4	PA2448	1743	GATCTTAAGATGAAGCAACGGATTCCAC	GCCCTCGTGGAATACACCG
H1_P4	PA2596	987	GATCTTAAGATGAAACGACCCCTGTGTG	ACGCTGGCCGACGCG
H2_P4	PA2764	696	GATCTTAAGATGAGCAACCTGCCTGC	GTGGGCGGTGGCCAC
H3_P4	PA2801	405	GATCTTAAGATGGCTGACAGACAATTGCT	GGCGATCGCGGCGC
H4_P4	PA2875	918	GATCTTAAGATGCTGAACACCTGGAAG	GAGCGCCGGGACTTCGC
H5_P4	PA3070	981	GATCTTAAGATGAGCAACGAGCCAGAAAG	GGCCACGGCGACCAC
H6_P4	PA3130	438	GATCTTAAGATGAATTGGGACTACGCCG	GGCCCCGGCGAGCAG
H7_P4	PA3576	423	GATCTTAAGATGTTCTCCATTCTCGCCC	GTACCCATCCGCCACCGG
H8_P4	PA3586	987	GATCTTAAGATGCGTGCTTTCATCTTCT	GAGCTGGACGACGCTGGC
H9_P4	PA3726	540	GATCTTAAGATGGCCCTGCAATCCAC	ACGCTCGCCCTGCAGC
H10_P4	PA3787	849	GATCTTAAGATGCCCCGACCCCT	GGGCTGGAAGGCACCGAT
A1_P5	PA0006	537	GATCTTAAGATGTCCCGTCCCTGCTG	CTGAAGTAATGCGCTGCGCA
A2_P5	PA0013	654	GATCTTAAGATGTGAGCCTCTTCTCGGC	AGCGTTGCTCTGCGGCC
A3_P5	PA0404	435	GATCTTAAGATGGCCAGCGACAAGCC	ATCCGGGTGTTGCGCCAG
A4_P5	PA1135	876	GATCTTAAGATGAGCAACGAGCGGATAC	GCGGGCGAAGCGTTTCG
A5_P5	PA1213	960	GATCTTAAGATGACAACCATCCATCGTCG	CGGGCGGGGCTCCTG
A6_P5	PA1415	729	GATCTTAAGATGAGAATCGTCAGCCGC	TCGATCGTGGTTCCTGAACC
A7_P5	PA1508	261	GATCTTAAGATGGACATCATTCGCCTTGG	GTTTTGCGCAGCGCCCAA
A8_P5	PA1593	474	GATCTTAAGATGTCGGAATCCTCTCC	TGCCGCACCTCCCTGC
A9_P5	PA1618	438	GATCTTAAGATGAGCCTCTGGCGACAAAC	GCCCGCCTGCCCG
A10_P5	PA1645	408	GATCTTAAGATGCGTCCCGTATTGCCG	GTCCGCGCGCCGCA
A11_P5	PA2156	738	GATCTTAAGATGATCTGCCGCGCCT	TGGTCCACCTCCACCGC
A12_P5	PA2178	609	GATCTTAAGATGACCCGCGAAATGGCTC	GCGCAGGTAATCGCCGCT
B1_P5	PA2211	960	GATCTTAAGATGGCTGAGCTGTACGACG	TGGGGAAGTCTCGGGTC
B2_P5	PA2315	1176	GATCTTAAGATGTCCAGTTTCGAACGAG	GCGCACCTCCGCGGA
B3_P5	PA2353	1155	GATCTTAAGATGCCCCGATACCTCTCCG	GCCGCGCTGTGCT
B4_P5	PA2496	516	GATCTTAAGATGTCCGACCCACCT	TTCCCGCGCTCCG
B5_P5	PA2625	471	GATCTTAAGATGAGCTGGCATCCCCATG	GGCCTGGGGTAGGGAGGG
B6_P5	PA3982	483	GATCTTAAGATGCCGCTTGAGCT	TTTTCTTGCTCGGTGGCT

5. Supplementary data

B7_P5	PA4642	291	GATCTTAAGATGCGCAAAGACAAGAAAC	GGCGCCCTTGGCCG
B8_P5	PA4679	702	GATCTTAAGATGCCTGTGCGTGCGC	TTGAATCTCGCTCGACCAGC
B9_P5	PA5028	768	GATCTTAAGATGCGGCGCGTGGT	GCTTTCGAGCAGCCCGTG
B10_P5	PA3953	582	GATCTTAAGATGAATGACGATGCCCAGC	GGCCGGAAGCGCTG
B11_P5	PA4152	1113	GATCTTAAGATGAGCCGATCCATACACT	ATGCTGGCGGAGGAAGTCGA
B12_P5	PA4308	1491	GATCTTAAGATGTCGAAGCGAATGAGTT	GCGCCGCTTCTCCCG
C1_P5	PA4673	1101	GATCTTAAGATGGGATTCAACTGCGGC	CACGTTGAAGCGGAAATGCA
C2_P5	PA5113	1395	GATCTTAAGATGACGCGCTCCTTTTCG	TGGCTTGTTGCGCGAGGAAC
C3_P5	PA5176	567	GATCTTAAGATGCGTCAGAAACCCACC	TGCCTGGTACTGCGCCG
C4_P5	PA5547	624	GATCTTAAGATGAACGAGACCGTATCCCT	GCGGAACGTTTCCAGAAGC
C5_P5	PA0285	2283	GATCTTAAGATGAGCCCCGCCTG	GTCTTCCGCGCAGCGCCAC
C6_P5	PA0788	3126	GATCTTAAGATGAATTGCGCAGCTACAGG	CAGGCGGCCGATCTGTTG
C7_P5	PA0829	942	GATCTTAAGATGTCCGCGACACCTATC	GGCCATCAGGAAGCGCAGTG
C8_P5	PA0832	642	GATCTTAAGATGTCGACATCCCCCGC	GCCCCTGACGAAGGGGTTCT
C9_P5	PA0935	831	GATCTTAAGATGTACCGACTCGACGACC	ACAGCCGGGCGCGCT
C10_P5	PA0955	957	GATCTTAAGATGCCACCGGAAGACC	GGGCGTCTCGCCAGGGT
C11_P5	PA1167	672	GATCTTAAGATGCCTGACCTGAGTACCTG	TTGATGGCTAACGCGCAGCT
C12_P5	PA1198	618	GATCTTAAGATGCCATGCTTAAACGCTT	GCGCTTGCTCGTCAGGGC
D1_P5	PA1517	927	GATCTTAAGATGAGCGCTGACTACCCAC	TGCTCGGTCTCCTGGAAAG
D2_P5	PA1622	861	GATCTTAAGATGAGCCTGCAGGTCGAG	GCGCGGAAGAAGGCC
D3_P5	PA1878	579	GATCTTAAGATGTCCCTCGAACTGCTGAG	GGCGTCGCGCCGAAC
D4_P5	PA2817	411	GATCTTAAGATGGCCAACTCTACCTCG	GTGCCGCGGCTGTCC
D5_P5	PA2872	771	GATCTTAAGATGACGGGGTTCATCGATGA	GTGCCCCGCAAGCGC
D6_P5	PA3037	867	GATCTTAAGATGCCTTCTGTATCGCCT	TTCCAGCCAGTGCGGGAAGT
D7_P5	PA3076	1080	GATCTTAAGATGCGCTTCCGTACCCT	CTTGAGCACCTTGATCGGCT
D8_P5	PA3132	858	GATCTTAAGATGAGCAGCCTGACCTGG	GGAAGCGCTCGCCGTCTTTT
D9_P5	PA3180	438	GATCTTAAGATGCACGATGTCCCTCCC	TTCGCCGATGCGCCGG
D10_P5	PA3200	888	GATCTTAAGATGCGTGTGATCTGCATTG	TTCGGCCCCCTTGCTTC
D11_P5	PA3241	1170	GATCTTAAGATGTCCGATCCCTTGCC	CCGCTCGATCCGACAGGAA
D12_P5	PA3247	1290	GATCTTAAGATGCGCGCAGAACTCAAC	GGGCAGCTCGCTGCTGG
E1_P5	PA3258	1806	GATCTTAAGATGAAATACGGGGCCGGT	GGCGGCCTCGATCAGGTG
E2_P5	PA3501	219	GATCTTAAGATGCAAGACCGTTACCTCGA	CGCGCCAGGCGGG
E3_P5	PA3727	693	GATCTTAAGATGGACTTCGACGGATTGGA	GCGCGGGGCGTAGC
E4_P5	PA3734	1206	GATCTTAAGATGCCGCGCAAATAGC	AAGGGCAGCGCGAGTTTGT
E5_P5	PA4344	1221	GATCTTAAGATGGCTCGACATCGACACAT	GGCCGCGCGTTATTGG
E6_P5	PA4632	822	GATCTTAAGATGGCTCATCCCTCCGATT	CTTGCCGCGCTGGC
E7_P5	PA5392	423	GATCTTAAGATGCCTACCCATACCCGC	TTGCTGCCAGTCGTGGG
E8_P5	PA5539	897	GATCTTAAGATGAATGCCTTGACGCTTCC	TGCTGCACCTCGCTGCC
E9_P5	PA0142	1350	GATCTTAAGATGTCCGACCTGGATTTC	ACCGGCGATCAGGGCACT
E10_P5	PA0371	1488	GATCTTAAGATGAGTGAGCGCACAGGG	ATGCTCCGGAACGCCGC
E11_P5	PA0485	897	GATCTTAAGATGGCGACCGCCAACC	GCCCGTTGCGGCAG
E12_P5	PA0581	570	GATCTTAAGATGGTCTGGCTACTGGCGA	GAAATGCCGTTGCGGGC
F1_P5	PA0589	333	GATCTTAAGATGAGCGACACCTCCAGC	CTCCGCTTCCGCGCTG
F2_P5	PA0629	630	GATCTTAAGATGAACTGACCGAGCAGCA	TGACAGCACCGCCTGG
F3_P5	PA1143	654	GATCTTAAGATGCCACTTGCCCTCTTCG	GCGCCATTCCAGCACTGG
F4_P5	PA1289	480	GATCTTAAGATGGGTATTTCCGCCAACGA	GGCGACCTGGCTGAGGCT
F5_P5	PA1575	552	GATCTTAAGATGCCTCACTGGTGGAATC	ATGCTCCACCGCAATACCA

F6_P5	PA1680	984	GATCTTAAGATGAAGACCTCCATGCCGC	GCGGCCTTTTTCCGCTC
F7_P5	PA1767	1527	GATCTTAAGATGCGCTCTCTCAACCTGC	GTCTTGAGCAGGGCCTTGA
F8_P5	PA2072	2595	GATCTTAAGATGCTTGCTTCAGCGATTGC	AGGCCGGCGCGCAG
F9_P5	PA2110	942	GATCTTAAGATGAACGACTCCATCCACGG	TGCGTCCCAGGCCGC
F10_P5	PA2160	2151	GATCTTAAGATGAGCAGAAAGCGTAGCCC	TCCTTCCGCTCCGGCG
F11_P5	PA2375	396	GATCTTAAGATGGGCTGCCCGCAGGTC	GGGAATCAGCATCTGCACCT
F12_P5	PA2451	600	GATCTTAAGATGCTGTTCGACGAGGACC	ATGCGCCGGCAACAAGG
G1_P5	PA2452	927	GATCTTAAGATGTCTGCCGTTTCCACCTC	GTGGCGCTGGTTGGCCA
G2_P5	PA2959	777	GATCTTAAGATGCTGGTCGATTCCTACTG	GCGGGCCAACGGAAACAG
G3_P5	PA3087	981	GATCTTAAGATGCAACTCGACCCCGG	CTCGTCAGCCTCCGGCC
G4_P5	PA3288	504	GATCTTAAGATGCCTGGCCTGTTCTTCC	ATCCGCCAGCACCTCGG
G5_P5	PA3289	414	GATCTTAAGATGCGCCCGATGTACGC	TTCGGCGCGGATGTCTG
G6_P5	PA3374	1164	GATCTTAAGATGTCGTCTGAACGCGTTCT	GAACACTCTCTGCCCGCC
G7_P5	PA3470	459	GATCTTAAGATGACCGACAACCTGCTGAG	GCGCACATGATCGGGGC
G8_P5	PA3509	870	GATCTTAAGATGAACATGGCGCAGACCC	TCCATTGGCGGTTCTCTCAA
G9_P5	PA3829	924	GATCTTAAGATGCAACGACTGAACGTGGA	TTCGACGACTGTCTGCTGGCT
G10_P5	PA3856	483	GATCTTAAGATGGCCACCCCAACG	GCCGGCCCGCGGAT
G11_P5	PA3919	1392	GATCTTAAGATGGATGACCACGGACGTTT	CATGTGCGCTCGGCGTA
G12_P5	PA4322	1008	GATCTTAAGATGAGCGAACAGACGCC	TACGCGGGGGGCCG
H1_P5	PA4440	630	GATCTTAAGTTGTCTACCCGCGAAATCCC	GTCTGCAGGCGTGGCAG
H2_P5	PA4767	435	GATCTTAAGATGAGCACCCATATCCAGCG	GCCATAGAGTTGCTTGGCGC
H3_P5	PA4830	540	GATCTTAAGATGGAACAGCCCGGCC	TCCGGCCATGTGCAGGAC
H4_P5	PA4972	747	GATCTTAAGATGCGCCTTCTGAAATTCGC	GCCGCGCGCGGGAAC
H5_P5	PA5246	474	GATCTTAAGATGAGCGAAACGCCCTCC	GCCGCACAGATAGGTACCGG
H6_P5	PA5290	1494	GATCTTAAGATGTCCCTGGCGATTGTCC	CGTGAGAGTCAATGCCCGAT
H7_P5	PA0201	582	GATCTTAAGATGCACAGCGAACCGGTC	GGCGCGCGCAGGGG
H8_P5	PA0599	1062	GATCTTAAGATGCCGGCCTTCTCTACT	CTCCGCAGGTTTCTGCGCAT
H9_P5	PA0891	1113	GATCTTAAGATGGAGCGTATCGACCACCT	GTCGCTGAGCAAGCGTCCCT
H10_P5	PA0954	276	GATCTTAAGATGGCGAGGATCTGCTTGC	GCGACGGACGACGAAGCC
A1_P6	PA2228	1212	GATCTTAAGATGATAAATAAGAGAAATG	CCTCACCCCTACTGTTCTTG
A2_P6	PA2871	798	GATCTTAAGATGAATTTTTCCGAATTG	GCCGAACACCGTGACCATCT
A3_P6	PA5519	567	GATCTTAAGATGACGATTGAAAATTTG	TCCGTCTTCGGAATCGC
A4_P6	PA2218	1104	GATCTTAAGATGGAAACCAAGCA	CAGATGCTCGTCAAGAATC
A5_P6	PA4635	705	GATCTTAAGATGGATTGAAAGTATTTT	GTGCGCCGCCAGTTCGAA
A6_P6	PA4833	618	GATCTTAAGATGTATCACGGTGAAAG	GAGTACGTAGCGCCAGATCG
A7_P6	PA4792	936	GATCTTAAGATGAATCGAAGTATTGCG	CCCGCCGGGCTGATC
A8_P6	PA1383	1806	GATCTTAAGATGCTCAAAAGAACTACT	GTTGCGGTTGTACCAGCCT
A9_P6	PA5202	390	GATCTTAAGATGAGCGAGATGCC	CAACTGGGCGAAGGTACCTT
A10_P6	PA0826	639	GATCTTAAGATGAAAAAGGAACCGAAAG	TAGTGGCGTGTTTCGAACT
A11_P6	PA3400	1134	GATCTTAAGATGAAGAACTACCTGCAG	CCAACCTTGACGTTGTCCC
A12_P6	PA1835	438	GATCTTAAGATGAGTCAGATGATGCAG	GGCCTGGCTGACGTACATGG
B1_P6	PA1887	669	GATCTTAAGATGAAAACCTCTCTAGC	TTGGCGGATGAGCCGCT
B2_P6	PA3797	795	GATCTTAAGATGCGCGATCTGAC	AGGATGGATTTCTGAAGCGAT
B3_P6	PA1888	1410	GATCTTAAGATGAAAATACTCGCCCTTC	GAGAGGGTTTTATAGAGGA
B4_P6	PA4824	777	GATCTTAAGATGACCCTGCACGA	GAAACGCAAGGTCGCTCC
B5_P6	PA0947	705	GATCTTAAGATGAAACCTATTCAGCTTCC	CCAGCCGAGGGTTTCTTGA
B6_P6	PA1597	726	GATCTTAAGATGAGTGAGATTCGTGTAGA	GGCGAAGACTTCCGCCAG

5. Supplementary data

B7_P6	PA1089	603	GATCTTAAGATGCGCACTGCCTA	CAGCATGTTCAATAGGCGAC
B8_P6	PA2927	1332	GATCTTAAGATGCCCCGTTCGAT	GGGGTTCCTGAAGACGAATA
B9_P6	PA3233	1800	GATCTTAAGATGCCTGACAGTTTCAAC	TCGGGTCTCCAGGTGGAATT
B10_P6	PA1763	1026	GATCTTAAGATGAGAATCAGGGGGTAC	CTGGGCCCTTCAGCCCTTT
B11_P6	PA3224	318	GATCTTAAGATGAAAAGGCTTTGCTGTTT	TTTCGCGATCTTGACAGGTCA
B12_P6	PA1594	447	GATCTTAAGATGAGCCCCGACCAG	CGGCTCGTCCACCTTGAAAT
C1_P6	PA4968	621	GATCTTAAGATGACCGCGACCAG	GTCAAAAGTCGAAAAGTCGG
C2_P6	PA0481	444	GATCTTAAGATGAACGAGCCGGG	TTTCTTCGGGTAGCCATGCA
C3_P6	PA5414	642	GATCTTAAGATGAAACGCCCGCT	GGGTAGCTTGTCAGCTTCA
C4_P6	PA0474	405	GATCTTAAGATGATGAACGTCCCCG	GGGCAGATGAAACACGCC
C5_P6	PA1593	474	GATCTTAAGATGTCGAAAAATCCTCTCC	TGCCGCACCTCCCTGC
C6_P6	PA1797	1833	GATCTTAAGATGTTTCGTGCAATGCATC	TGGGGACTCCTTCCTTGCA
C7_P6	PA1166	789	GATCTTAAGATGCGCCTGCTCTG	ACCTGCCCCAAGATGTCCT
C8_P6	PA4387	468	GATCTTAAGATGCGCGCTTTCCT	GTTGCGCAATCGTCGC
C9_P6	PA0469	858	GATCTTAAGATGGCCACAGTGGAATAC	CCCCGCGATCCGACC
C10_P6	PA2117	981	GATCTTAAGATGGCGTTCAAACGGATAG	CGACCTTAAGTGAGAGGCGT
C11_P6	PA2822	483	GATCTTAAGATGATCGATCTGCAGCAATC	GCAGTCCGTCAGGCGCAG
C12_P6	PA4093	417	GATCTTAAGATGACCGACAAGAAAGAGC	GCGGCGGTGCGCC
D1_P6	PA4929	2043	GATCTTAAGATGAGCAATTCCGACGTTTT	GGAGATACGCTCCGGTGCCA
D2_P6	PA1478	177	GATCTTAAGATGAGCTTGAATCGTTCTG	CTGCTGGGCCTCCCGG
D3_P6	PA0065	666	GATCTTAAGATGCGTGACGCCGCGC	GTGGGATTCCAATACCTGC
D4_P6	PA1506	330	GATCTTAAGATGCACCGGTCTCT	GTCCCGCCGAAGGAAAGG
D5_P6	PA5329	465	GATCTTAAGATGAGCAGCGCAGC	CTCGGCGTGAGTCCCTGATT
D6_P6	PA0449	540	GATCTTAAGATGGCGCAGGCAG	GGGCAGGACTTCGTCTTCCT
D7_P6	PA2358	390	GATCTTAAGATGCTTCGTCCGCG	GTTCAGCTTGTAGGCCTGGA
D8_P6	PA2803	744	GATCTTAAGATGCCAGCTCCGA	TGGTTTTTCTCCTTCAGGC
D9_P6	PA5396	978	GATCTTAAGATGAGCCCAGCCGA	CTCGCCCCAGACGTGCG
D10_P6	PA3941	597	GATCTTAAGATGAGGCTGGCCGA	CGGCGTTTGAGTTGCTC
D11_P6	PA3971	432	GATCTTAAGATGCAGGCGCATCC	TTCGGCCAGCGCCAC
D12_P6	PA1095	381	GATCTTAAGATGTACGCGATGAAAGCG	GTGCGAAATACCGTCCCAAC
E1_P6	PA2801	405	GATCTTAAGATGGCTGACAGACAATTGC	GGCGATCGCGGCGC
E2_P6	PA1433	1953	GATCTTAAGATGTCACTGCTCAAGCAATTG	GGCATCCCCGGACCAGG
E3_P6	PA2581	1041	GATCTTAAGATGAAAACATCGCTCGG	TCTTGCCTTGCGTTTCAAGG
E4_P6	PA4317	738	GATCTTAAGATGAACGACACCAGCAATC	GTTGCCAGCGGGCG
E5_P6	PA1675	558	GATCTTAAGATGCAAGACGACGACTTTTC	CTCGTCGCGGCCCTTCGAG
E6_P6	PA0959	630	GATCTTAAGATGTTTCGGCGTCGC	GGCCTCCCCGGCAAAAC
E7_P6	PA0492	759	GATCTTAAGATGACTGAAGTCGACCTCAA	ACGCGGCGCCTTGATG
E8_P6	PA1450	1260	GATCTTAAGATGGATCGAACCTTGCTCTGA	CCAACTGTCCGAGGCACC
E9_P6	PA3372	771	GATCTTAAGATGCGCCTGACCTT	CAGCGGCAGGCACATCC
E10_P6	PA1291	840	GATCTTAAGATGAGTACCGCAGTGGAG	CGCCGCGTCGGGCA
E11_P6	PA3301	951	GATCTTAAGATGCCCCGCCGCT	TGTTCTCTCTTTGTCGAATGATC
E12_P6	PA3564	678	GATCTTAAGATGGTGCTCGGCGT	GTCCCAGCCGAACAGCTC
F1_P6	PA0308	1020	GATCTTAAGATGTGTTTCGCGCGC	GGCCCCAGCGCGTC
F2_P6	PA0480	798	GATCTTAAGATGGGCAACCTGTCTTTCT	GGCTGCGCCGAGAAAGCT
F3_P6	PA0957	408	GATCTTAAGATGAACGCGGCGC	TAAAGGAAGGGCGTAGGTACCGGT
F4_P6	PA1792	723	GATCTTAAGATGAGCGTCTGTTCATCTC	GAGCGGGAAGGGCGCCT
F5_P6	PA3464	1326	GATCTTAAGATGAAGTTGCTGTTGCGTTG	CTCCTTCGCCCCACCCTC

5. Supplementary data

F6_P6	PA2750	519	GATCTTAAGATGATCTTCCGCACCCTC	AGTTCGCGGAGATCCATCTC
F7_P6	PA0174	603	GATCTTAAGATGAATCTCCAGGCCCG	GAACAGGTCGATGGGGCC
F8_P6	PA3981	1023	GATCTTAAGTTGAACGCCCCCA	AGCGGCATCGTGACCGC
F9_P6	PA1451	1344	GATCTTAAGATGTCTGCAATCACGCGTTA	CCAACTACCGGAGGCGCC
F10_P6	PA0351	474	GATCTTAAGATGCCCCAGTCCCG	GAGGGTGATCAGCTCCGCT
F11_P6	PA0368	999	GATCTTAAGATGACCGCGTCCCC	GTGCTGCCGAGGCG
F12_P6	PA0107	555	GATCTTAAGATGAGCGATGCCAAGGTC	TCGTCCCGCAACCGGTAC
G1_P6	PA1870	426	GATCTTAAGATGGCTACACGACGGAAAAC	GCGTTCCTCGTCGGAGGAAC
G2_P6	PA3955	657	GATCTTAAGATGAATCCTCTGCTGCCG	CATCCCGTTGCGTGCG
G3_P6	PA3130	438	GATCTTAAGATGAATTGGGACTACGCCG	GGCCCCGGCGAGCAG
G4_P6	PA3727	693	GATCTTAAGATGGACTTCGACGGATTGG	GCGCGGGCGTAGC
G5_P6	PA1012	759	GATCTTAAGATGCGGTTCCGCGT	GGCGATCTCGCGCCAATC
G6_P6	PA3219	813	GATCTTAAGATGAGCACC CGCA	TGCCCGCGGCTCGAC
G7_P6	PA2728	2661	GATCTTAAGTTGCGCGAGGAGCA	TTGGGAGGCCTCCGCTG
G8_P6	PA1181	3363	GATCTTAAGATGTTCAGTGGCAAAACCGA	GCCCAACTCCTGGCGACG
G9_P6	PA5177	666	GATCTTAAGATGCCACCCTGCC	CGGCAGTCCTTCGAGCAG
G10_P6	PA2764	696	GATCTTAAGATGAGCAACCTGCCTGC	GTGGGCGGTGGCCAC
G11_P6	PA2146	168	GATCTTAAGATGGCACAGCATCAAGGTG	GTTCCCGCGTGGCTG
G12_P6	PA3726	540	GATCTTAAGATGGCCCTGCAATCCAC	ACGCTCGCCTGCAGC
H1_P6	PA4789	306	GATCTTAAGATGGACCTGCACGAACTCA	TGGCAGGAAGCGCCGTTT
H2_P6	PA3829	924	GATCTTAAGATGCAACGACTGAACGTGG	TTCGACGACTGTGCTGGCT
H3_P6	PA1518	381	GATCTTAAGATGTCCGCCAGCGG	GCTGCCGCGATAGGTGCAAT
H4_P6	PA2419	681	GATCTTAAGATGAGCGCTCCCGC	CTTGCGCTGCGAATCCAGTT
H5_P6	PA2411	765	GATCTTAAGATGGGCGGTACGCC	GCAGATCGCCGCCGACTC
H6_P6	PA4926	936	GATCTTAAGATGTCCGCACCCGC	GCCGGCTGTTCTCTGTAGCG
H7_P6	PA5052	696	GATCTTAAGATGGCAAAGAAGAAACCCGC	GCGGGCCTTGCGTTGCT
H8_P6	PA0968	447	GATCTTAAGATGCGCGCGCAACAC	ATCTCTGTGAAAAAGAATCCGG
H9_P6	PA1047	1179	GATCTTAAGATGCCCCGACCACTTTCC	CAGACACTCCCCGCGAC
H10_P6	PA0285	2283	GATCTTAAGATGAGCCCCCGCT	GTCTTCCGGCAGCGCCAC
A1_P7	PA3502	318	GACTTAAGATGAGCGACACCTTGTTG	TTGGCCTCCAGTGCGGAC
A2_P7	PA5295	1677	GACTTAAGTTGTGAGCGCCCGC	ATTGCCGAGCGGCTGGC
A3_P7	PA2769	411	GACTTAAGATGCCGGCACCGC	GCGCTTCGGGTGCAAGG
A4_P7	PA3912	891	GACTTAAGATGAACTGAGCCTGGGAC	GCATAGCCCTGCCTCTCTG
A5_P7	PA3461	1197	GACTTAAGATGACCCTCTGCCACAAC	GCCCTTGTCGCTGTTGTTGC
A6_P7	PA1939	1998	GACTTAAGATGCTGGCGCTGCG	CCGCCCTCATCTCCGG
A7_P7	PA4782	246	GACTTAAGATGCTGCGGCGCAG	GGGCGTCAGGCGGAAC
A8_P7	PA2860	441	GACTTAAGATGCGCCGATTTAAACAGC	GCGCAGGATACGGCGGG
A9_P7	PA0589	333	GACTTAAGATGAGCGACACCTTCCAGC	CTCCGCTTCGCCGCTG
A10_P7	PA1154	534	GACTTAAGATGCCAAGCTACCGACGAAC	AACCCGCTCGGCCGC
A11_P7	PA2451	600	GACTTAAGATGCTGTTGACGAGGACC	ATGCGCCGGCAACAAGG
A12_P7	PA2452	927	GACTTAAGATGTCTGCCGTTTCCACCTC	GTGGCGCTGGTTGGCCA
B1_P7	PA2539	1314	GACTTAAGATGCTCTGGCTGCTGTTCC	GGCATGGCGCACCTCG
B2_P7	PA3741	426	GACTTAAGATGACCCCCAGAGAGCAAG	AGCCGCTGGCTGGC
B3_P7	PA4015	456	GACTTAAGATGCCATTGTAACCGTAGC	GACGAAGCAGAGGCTGAGGG
B4_P7	PA0536	1026	GACTTAAGATGCGCCGGCTGCT	CCAGCGTCCGGAGGCG
B5_P7	PA3310	1656	GACTTAAGATGGGTGGGGGTATCAAG	CTGGGCTGCCCTGGGC
B6_P7	PA4701	1563	GACTTAAGATGAGCCAGACCCTGATCG	GAGACCGGGCAGGCGCT

B7_P7	PA4278	705	GACTTAAGATGCGCTGGTCTTCTCTGTT	GGGGGATGCAACACCTTTGC
B8_P7	PA3728	5241	GACTTAAGATGTCGGACACTCAAGCCG	GGGTTGATCGTTCTCCAGCG
B9_P7	PA3069	618	GACTTAAGATGCGCGCCGGCGAATTC	CTGCACCGGCAGGAAATGC
B10_P7	PA0989	561	GACTTAAGATGGGCAAACCATTCCTTC	CTCGTTGCCGAGCATCGC
B11_P7	PA1639	606	GACTTAAGATGTCCCGTCCGATCCC	GCGGCTGAACTCGAGGAC
B12_P7	PA0466	303	GACTTAAGATGCGCTGTTCTTCGAGT	TTTCCAGCACACCAGGCG
C1_P7	PA1030	756	GACTTAAGATGAGCGAGATCTGGCGA	CGCCGGATGCGGCAA
C2_P7	PA1618	438	GACTTAAGATGAGCCTCTGGCGACAAAC	GCCCGCCTGCCCCG
C3_P7	PA2898	369	GACTTAAGATGATCCGCCAGCCCC	GAAACGCAACGCGTCCGC
C4_P7	PA4677	1239	GACTTAAGATGTGCGACACCCTGATC	CAGCGCGGCGTGGCTAC
C5_P7	PA4830	540	GACTTAAGATGGAACAGCCCGGCC	TCCGGCCATGTGCAGGAC
C6_P7	PA5026	453	GACTTAAGATGCCACTGCCACCG	GGGTGCGCGTGGCT
C7_P7	PA0575	3738	GACTTAAGATGCAGCGTCTGCAGGC	TACCGGCGCTTCTCGGG
C8_P7	PA4391	1002	GACTTAAGATGTCGCTCAGAGCCCTC	CCAGCCGACGCCGACC
C9_P7	PA0822	447	GACTTAAGATGACCAAGAACCACCG	ATAGCGGGAATCATCG
C10_P7	PA1118	684	GACTTAAGATGCTGCGCAAGAAACCG	GACCATCCGCCGGAACCTG
C11_P7	PA2485	279	GACTTAAGATGGTAACACCGGCGAAC	TTTCTTCTCGTGGTCGGCG
C12_P7	PA0097	1200	GACTTAAGATGGCGCTATCTTCCAG	TGCCTCGTCTCTCGGC
D1_P7	PA0758	837	GACTTAAGATGAGCAAGCTTGCCGAC	TTGCAGCATGCTGGTGGC
D2_P7	PA0858	939	GACTTAAGATGACATCCATCGTCGTGG	GTTCTCCAGCGTGGACTGGC
D3_P7	PA1680	984	GACTTAAGATGAAGACCTCCATGCCGC	GCGGCCTTTTCCGCCTC
D4_P7	PA2072	2595	GACTTAAGATGCTTGCTTCAGCGATTG	AGGCCGGCGCGCAG
D5_P7	PA2661	894	GACTTAAGATGAACTGGCCGTAGCG	ACAAAGCTCAGCAAGCGGCC
D6_P7	PA3241	1170	GACTTAAGATGTCCGATCCCCTTGCC	CCGCTCGATCCGAGGAA
D7_P7	PA3258	1806	GACTTAAGATGAAATACGGGGCCGGTT	GGCGGCCCTCGATCAGGTG
D8_P7	PA3379	630	GACTTAAGATGACCAGCGCTTCGCTTC	GGCCACCTCCTCGACGG
D9_P7	PA3509	870	GACTTAAGATGAACATGGCGCAGACC	TCCATTGGCGGTTCTCTCAA
D10_P7	PA4312	762	GACTTAAGATGGCTGAACGCAGCCTG	TGCCGCGTGGTCCAGG
D11_P7	PA5185	444	GACTTAAGATGGCGACCCGCCCC	CTGGGCCCTTAAGTGAAGCG
D12_P7	PA5246	474	GACTTAAGATGAGCGAAACGCCCTC	GCCGCACAGATAGGTACC
E1_P7	PA3994	891	GACTTAAGATGAGCCGCTATGCCTTC	GTCATCCGCGCAGAACCG
E2_P7	PA5363	900	GACTTAAGATGCTAGGGCGCCTTCTC	AGGCTCGCGGACGATGG
E3_P7	PA3695	906	GACTTAAGATGAAGCGCTGCTGATC	TGGATTGCCTTCGGGTTTCG
E4_P7	PA3043	1332	GACTTAAGATGGACTGCGAGACCCTG	GGAGGGGCTCGAGCGTCC
E5_P7	PA1209	936	GACTTAAGATGCGTGAACCTGCAACCC	GGCGTTCCGCACGACCT
E6_P7	PA3110	660	GACTTAAGATGGCCTTGCTGGAAAGAG	ACCGCGTTCCGGCTGG
E7_P7	PA1189	498	GACTTAAGATGCCCCGAACCTCAAC	CTCGCGGAGCACTTCGCC
E8_P7	PA2549	1044	GACTTAAGATGGCAGCTCTGCATGCAT	GCGTGGGTGTCCAGACGTTT
E9_P7	PA0061	438	GACTTAAGATGCGTCCACTCACCCGTC	GTACGGCGGGCAGCGG
E10_P7	PA0201	582	GACTTAAGATGCACAGCGAACGCGTC	GGCGCGCGCAGGGG
E11_P7	PA1907	1641	GACTTAAGATGACCGCTGTCGACCTGC	GGGAAGATCCAGCCCGGTCT
E12_P7	PA2004	1392	GACTTAAGATGAGCGTGATCATCGCCC	GACCAGGCCGGTGGCGTA
F1_P7	PA2049	1434	GACTTAAGATGCTGGTGCCATCCATG	GCGACCCGGCGCGA
F2_P7	PA2063	1224	GACTTAAGATGGACGATCTCTCCCC	GCGGTAGCCGTCAAGCAACG
F3_P7	PA2156	738	GACTTAAGATGATCCTGCCGCGCCT	TGGCTCACCTCCACCGC
F4_P7	PA2636	555	GACTTAAGATGGAATGCAGGCTCCCC	CCTGGGGGCTGCGGTAGC
F5_P7	PA2793	1035	GACTTAAGATGAGACTGCCCCGCC	TTTCAATGACAGCGGCACGC

5. Supplementary data

F6_P7	PA3087	981	GACTTAAGATGCAACTCGACCCCGGA	CTCGTCAGCCTCCGGCC
F7_P7	PA3401	1173	GACTTAAGATGGCGTGGGCCGC	TATCGGGCTCAGGTCCAGGC
F8_P7	PA4643	486	GACTTAAGATGTTCCGCCGTAGCCTG	ACGCGCGCGTACCGCGCCGGTGTG
F9_P7	PA5222	483	GACTTAAGATGCCGGTCTGGTCGAGG	GGCCGCGTTCCGCAG
F10_P7	PA3750	750	GACTTAAGATGCGCCGGCTGGCAAC	GGCTACCGCGACGCCGCC
F11_P7	PA2471	699	GACTTAAGATGAACCATCTCTCGCGC	GACCACGCGGACGCTGAG
F12_P7	PA1469	723	GACTTAAGATGACCGTCCAGGCCGAC	CGGCTTGC GCGCAT
G1_P7	PA2168	777	GACTTAAGATGACGGCGAACAGCGAAC	GAAAGCCGGATGGATGGTGG
G2_P7	PA4509	930	GACTTAAGATGAATGGTTTGCGGGTCG	GCCGCGAAAAGAAGCGGTAGA
G3_P7	PA2922	1170	GACTTAAGATGACCGAGCCTGCCGTC	GGCCAGGAAGCGCTCGG
G4_P7	PA5133	1287	GACTTAAGATGCTCCGCCTCTTCCTC	TCCCTGTGCGCGGCAC
G5_P7	PA2567	1764	GACTTAAGATGGCAACCCACCTATC	ACGCCGCGAGCCAGTCTC
G6_P7	PA1969	393	GACTTAAGATGCCACTGTAAGGTG	GCCGCGAGCAGGCCGC
G7_P7	PA0099	1161	GACTTAAGATGGCCAACGAGGTGTAC	GCGGACTCGACTCCTCGTGG
G8_P7	PA2503	1254	GACTTAAGATGGAACCTCCCCGCC	GCCTGGCAGCTCGGCG
G9_P7	PA0454	2202	GACTTAAGATGCCGCCCTCTTCGTTG	GGGCTGGCCTGGCAGC
G10_P7	PA0800	534	GACTTAAGATGGCGCGGCGGAC	TGGACGCGCTCCGTAGTCGA
G11_P7	PA0064	984	GACTTAAGATGACCGACAACCCCTTC	GGCGGCGAGCTGGTCG
G12_P7	PA1622	861	GACTTAAGATGAGCCTGCAGGTCGAGG	GCGCGCGAAGAAGGCC
H1_P7	PA3414	585	GACTTAAGATGCCGCGACAACCTGCC	GCGGCGTCGCGAGCT
H2_P7	PA3908	720	GACTTAAGATGACGGACGCCAAGGC	GCCGCGCAGCGGC
H3_P7	PA3958	1140	GACTTAAGATGCGCGGCGGCAAGCTC	ATGGGGCAGCAGGAAGCG
H4_P7	PA5442	2856	GACTTAAGATGACCGTCCATGTCGAGC	ACGAGCCTGGCGCAAACC
H5_P7	PA1677	597	GACTTAAGATGCCTCATCCGCTCACCC	GAGCAGTTCCCGGGCCTG
H6_P7	PA1434	714	GACTTAAGATGTCCCAACCCCGG	ATCTCCTTGGGTGCGTCGA
H7_P7	PA4543	729	GACTTAAGATGAACGCCTGGCTGACC	GTCCTGGAGCCAGACCAGGC
H8_P7	PA5180	840	GACTTAAGATGCCTTGCCAGCCTGCAT	CTCGGTTGCGGCCGG
H9_P7	PA2984	2226	GACTTAAGATGCGCCTGGGATTGCC	TTTTTCCCGCCAGAAGTGCG
H10_P7	PA0543	969	GACTTAAGATGCGTACGCTGATCCGC	GCGCGGCAACTGGCTG
A1_P8	PA0238	816	GATCTTAAG ATGGAATCTAGGATTCTTTC	CAGGCGGGCGAGCAGCGCCC
A2_P8	PA2599	945	GATCTTAAG ATGAACTCAAGCAATACCT	GTGGAAGGCTTCGTTGAAGG
A3_P8	PA3259	480	GATCTTAAG ATGAACTCTGAATGGATCTG	GAGACCGAGCGCGGACGCCC
A4_P8	PA3519	1038	GATCTTAAG ATGACTTCAAATCCGTTACA	GGCCATGGCCAGGGAATTCTG
A5_P8	PA0732	1044	GATCTTAAG ATGAAAAGATCCCTTGCCGT	CTTTTTAAGCGATTTCTGTCG
A6_P8	PA1746	507	GATCTTAAG ATGATTCTGGAAGTTGAAGG	GGCCAGCTTTCTCGGCCG
A7_P8	PA1788	468	GATCTTAAG ATGTCTCGCAAAGAATCAA	TCTGTGATCGCCTGCAGGA
A8_P8	PA5088	882	GATCTTAAG ATGATGCGTCCATTATGTTT	CTGCCCCGTTTCCAGTCGG
A9_P8	PA0565	339	GATCTTAAG ATGCTGAACAACTGGACCGA	CTTTTTGAAGTGGTCGTAGG
A10_P8	PA2102	459	GATCTTAAG ATGAATACGAACGTGTTGAC	CTCGTCTGGCTCGATGGCC
A11_P8	PA0100	921	GATCTTAAG ATGTTGAAGAACTCTCGCC	ATCTATGCGCGTCCATTGCT
A12_P8	PA1069	2295	GATCTTAAG ATGGATATCTGGAAGTGGGT	CAGGCCGTAGCGCTCGATAG
B1_P8	PA1140	837	GATCTTAAG ATGTCCAAGTCCAGCTACTA	ATGCGGCGCATTGAGAGTCA
B2_P8	PA1791	1332	GATCTTAAG GTGATCATCTCGAAGGGAAA	GTCCTTGACCTTGAGGTCTGA
B3_P8	PA2075	1662	GATCTTAAG ATGCTTCTTCAACCATCAG	TTCCAGTTCGGCTGCGCTCT
B4_P8	PA2293	966	GATCTTAAG ATGACCTGTAAAAACGCCAC	TGCCGGCATCCGAGTTGCG
B5_P8	PA2418	861	GATCTTAAG GTGAAAAAGGTCTGGGAAT	GTGGGCGCGGATGAAGCGCC
B6_P8	PA2941	645	GATCTTAAG ATGGGTGCGGATGCCAGGAG	GACTTCGTTCAATTCGCTGA

B7_P8	PA3513	1008	GATCTTAAG ATGTCCAAGTCATTGCTCAA	TGGGCGGGCTCCGTGCTGCG
B8_P8	PA3664	348	GATCTTAAG ATGACCTACGTTCTCTACGG	GGCCAGGGCGGCGGCGTAGG
B9_P8	PA4069	885	GATCTTAAG ATGCGAATGCGCCTGATGCT	AACATGCCTGTAGTACCTGT
B10_P8	PA4390	1008	GATCTTAAG GTGCTCATGTTGTCGAGAAT	CCAGCCGACCCGAGGCCGA
B11_P8	PA4474	1443	GATCTTAAG ATGAGCGAGTTGTTGTCATC	GGCGCCGGTGCCGCCGACGG
B12_P8	PA4685	696	GATCTTAAG ATGCATCTTGATCTCTCCGA	TGCGTCAGCCTCCTGTTGCG
C1_P8	PA5330	618	GATCTTAAG ATGGTCGGACAGGATGTAAT	GGGACTCACGCCGAGTAGCT
C2_P8	PA0360	987	GATCTTAAG ATGTTCAAGTCAGTGGGTGTT	CTGGCTCGCCGCTTCAACCG
C3_P8	PA0387	594	GATCTTAAG ATGATCAAGCTCGAACAGCT	GAGACCCAGGCGCTGCTTGA
C4_P8	PA0726	1275	GATCTTAAG GTGTCGATCAAGATCCACCA	TTTCTGCCTCCAGGGCCGCG
C5_P8	PA1488	1239	GATCTTAAG ATGAGCATCACTGAACAGGT	GTGGCCGGAGGTGAGGAAAG
C6_P8	PA2610	975	GATCTTAAG ATGGGACAGTTGATCGATGG	GCCTTCTCCCCAGATGCCCT
C7_P8	PA3598	816	GATCTTAAG ATGAAAGTCGAACCTCGTCCA	GGGAATCAGCAGCTCGCGCA
C8_P8	PA3923	1926	GATCTTAAG ATGACAACCCGTAATCCGTT	GAAGTTCATGCCGAAGCTGA
C9_P8	PA4631	1026	GATCTTAAG GTGGACGAACAGCCACTCTC	GGCATTGAAATAGCCGTTGT
C10_P8	PA5532	759	GATCTTAAG ATGCTTCGAGAGATACCCAC	GCCAGGCGTCCACTGCGGCC
C11_P8	PA0055	507	GATCTTAAG ATGTCCCTGTCGATCTACC	GGCGCCGCCGAGGAAGTCCA
C12_P8	PA0257	792	GATCTTAAG ATGAGCCGACAGGCTTACTA	AAACGCCCGATGCACCGCAT
D1_P8	PA0741	642	GATCTTAAG ATGAAAATCGCCCTGATCGG	GTAGGCCACGTTGAAGCGCT
D2_P8	PA1188	1182	GATCTTAAG ATGAAAGGCCCGTTGTCATC	GGCGATGGCCCCGGCCGCT
D3_P8	PA1205	948	GATCTTAAG ATGAGCAATACCGAAGAGCG	CTCGGCGTCGATCTTCCAGG
D4_P8	PA1206	474	GATCTTAAG ATGCAATTGCAACACCTGGT	ACTCCGCTGGCGGCGCTGG
D5_P8	PA1841	498	GATCTTAAG ATGAGTGCGAAAATGGACGA	CGCCCGGATCAGGCGCGGTT
D6_P8	PA2017	930	GATCTTAAG ATGAGTCGGCTGATGACCTA	GTCGGCCGCTGGCAGCGCTC
D7_P8	PA2530	1326	GATCTTAAG ATGCACCAGAGACAGCATTT	GAGCGTGAGGGTGAAGCGCC
D8_P8	PA2705	1182	GATCTTAAG ATGCTGCTCAACCTGTTCAA	ACCGCGCGAGAGGAAGCGCA
D9_P8	PA2974	693	GATCTTAAG ATGACTGACTACGCGTTGCT	GACATGCTCAACCACTCTG
D10_P8	PA3716	1707	GATCTTAAG ATGCAAAGACTGTCGCGTAT	GCTCTCGCTGGTTTCCTCGC
D11_P8	PA4336	585	GATCTTAAG GTGATGGCTGCGAAGAAGAT	GTGGCTGATGCGGGTGCCGA
D12_P8	PA5086	642	GATCTTAAG ATGCACAACCTGGCGAATCT	CCGCTCCGGCTTCCAGTCTG
E1_P8	PA5087	870	GATCTTAAG ATGGCTATTGGACTTTGGGC	CTGACCCGGCTTCCAGTCGG
E2_P8	PA0310	699	GATCTTAAG ATGGGGCGCTATTGTCGACA	GGAGAGTTGCAGGAGGGATT
E3_P8	PA0484	516	GATCTTAAG ATGGATCACCTGGTCCTGAC	GGACGCGTCCAGCACCAACT
E4_P8	PA0587	1272	GATCTTAAG ATGAGCTACGTCATCGACCG	TGCGACGAGCCTCCTCTGGA
E5_P8	PA0862	783	GATCTTAAG GTGAGCGAGTTCTTTGACCG	CTCCGCGCCGACCGCGAGCT
E6_P8	PA1210	699	GATCTTAAG ATGATCGAACGTCGTCCCTT	GGCCACTTCCACCAGCAGCA
E7_P8	PA1567	1398	GATCTTAAG ATGACCTTCCGACCCCTTCTG	ACCTTGTGCGCCTTGCCCG
E8_P8	PA1573	597	GATCTTAAG ATGGACAAGGACGTATCCGG	GCCCTGCGGGAAGCGGTAGT
E9_P8	PA1918	1401	GATCTTAAG ATGAAACTCACGCTCACCCC	GGATTTGTCTTCAAGGCCGG
E10_P8	PA2141	549	GATCTTAAG ATGCCCCGACCTGCAACTCGC	TGGTGGTTTCTCTCTGTGCG
E11_P8	PA3283	855	GATCTTAAG ATGCAACGGGAATTCGTCAG	TGTGCCGTACCCAGGCTGC
E12_P8	PA3731	696	GATCTTAAG ATGACGGTATGGAGCAAGCT	GGCCTTGCCCTTTTCCTTCA
F1_P8	PA4115	1386	GATCTTAAG ATGTCTCATCGCCCTGTGAT	GGCCGCTCGGTCTGCACCA
F2_P8	PA4321	1272	GATCTTAAG ATGATGAGCCGGCGCGCGCG	TAGGGCATTCTGAGGCTTT
F3_P8	PA4579	1857	GATCTTAAG ATGCCGAAACGCTGTTGCC	GTAGTAGTACCAGCGCAGCT
F4_P8	PA5245	669	GATCTTAAG ATGCACAAGAAAGTTGCCGT	GGCCTTGTCTGCTGTCACCA
F5_P8	PA0144	627	GATCTTAAG ATGAGCCGATCCAACGGTTC	GCCGTGGCGCCGGCTGGCGA

F6_P8	PA0878	828	GATCTTAAG ATGAGTGAGTCCGCTTTCGC	GTCGAATTCACGTCGCCGC
F7_P8	PA0882	1203	GATCTTAAG ATGACACAATCCACCGACC	TACCGTTCCGGTCGCGCGCA
F8_P8	PA0987	843	GATCTTAAG ATGCAGGCGCGAACCGGCAT	GTTAGTAGGCCCTGGGGTTG
F9_P8	PA1214	1599	GATCTTAAG ATGTGCGGCATCCTCGGTTA	TAGCGAGGCTCCGTATTCTT
F10_P8	PA1274	657	GATCTTAAG ATGTCCGATTCTTCCACGC	TGCTCGCTCGCCCCAACGGT
F11_P8	PA1689	2103	GATCTTAAG ATGGACCAAACGGAAGTCCG	GTCCTTGTCGGGATCCCGT
F12_P8	PA1885	534	GATCTTAAG ATGACCGAACCGACGATTCTG	GCCGGCAGCAGCCAGGCGCT
G1_P8	PA2540	1761	GATCTTAAG ATGCGCGACGTACAGGAATT	GCGGGCGACCTTCTGCGCCA
G2_P8	PA2660	1083	GATCTTAAG ATGCCAGCCATCCAGATCAA	GTCCAGCGCTTGCAGGCGTT
G3_P8	PA2707	846	GATCTTAAG ATGAAGTTCGAAGGCACCCA	GCGGCTGGCGGGCGGCTCA
G4_P8	PA3075	1632	GATCTTAAG ATGATCCGCCTGTTCTGCAG	GCGCGGATAGACGGTGGCA
G5_P8	PA3481	1095	GATCTTAAG ATGTCCGCTATCACTCGCCA	GTCGTGCTGATGCTGATGT
G6_P8	PA3618	507	GATCTTAAG ATGACCTGATGGAGTCCGA	GCCCGGTTCTCGCCGTTGC
G7_P8	PA4106	831	GATCTTAAG ATGACCTGATCGACAACGC	TCCATGACGGCGTCCCTCGT
G8_P8	PA4106	831	GATCTTAAG ATGACCTGATCGACAACGC	TCCATGACGGCGTCCCTCGT
G9_P8	PA4465	861	GATCTTAAG ATGCGCCTGATCATCGTCAG	GCTGCTGAGATCGCGGTGGC
G10_P8	PA4612	552	GATCTTAAG ATGACGACGATGCGAGGTTG	CCTCGCCGCCGAGTGCCGT
G11_P8	PA4923	588	GATCTTAAG ATGACCTTGCCTCCGCTCTG	CTGCGGGGTGCGGTGACCC
G12_P8	PA4927	2493	GATCTTAAG ATGCCCGAGCTGCTTGCCCA	GGTGGATACCGTTCTCTGGC
H1_P8	PA5481	468	GATCTTAAG ATGCGACTCATGCGTAACCT	GTACCAGTTCGGATCGGCCT
H2_P8	PA5535	1203	GATCTTAAG GTGAACCAACGCCTACCTGT	TGCGGCGTGCCCCAGTCTT
H3_P8	PA0344	1380	GATCTTAAG ATGACTGAGCCGCTGATCCT	TTCCCCGCGCCGCTCTCCA
H4_P8	PA0735	816	GATCTTAAG ATGAATCGAACCGTCGCAA	GCGGCGAACGGCGTTGGTGA
H5_P8	PA1219	615	GATCTTAAG ATGCTGATCCTGCTGCCTGA	TTGGACGGACTCCTTGCTGA
H6_P8	PA1357	477	GATCTTAAG ATGAGCCTCGAATCCGTCCG	GGCTTCTGGAGGACTTCTT
H7_P8	PA1559	732	GATCTTAAG ATGAACATGCATGCCGACGG	CGTCGATCTGCTGCTCCAGG
H8_P8	PA2106	735	GATCTTAAG ATGACGCAGACCGCTCCCT	ACCCAGTACCAGTACCACCC
H9_P8	PA2230	672	GATCTTAAG ATGCATGGAGTGCCGAAAG	CCAGAACCAGCCGCCGCGCG
H10_P8	PA2309	1023	GATCTTAAG ATGAACCGCATCCCCGTTT	ACTCCCCTGCAACGGCGCGC
A1_P9	PA2689	915	GATCTTAAG ATGAGAACCTCCCTGCTCGT	GCGCTGGCGTTCCACCGCCG
A2_P9	PA3073	1023	GATCTTAAG ATGTTTGAGTTCGCTGGCC	TGGTTGCTCCCGGAACGGC
A3_P9	PA3074	1761	GATCTTAAG ATGAACCTGTTGCTGGACGC	TGGCGTGGCTTCTGGCGTT
A4_P9	PA3240	858	GATCTTAAG ATGACCCGCTACCGTGATGT	GACGGCCAGGACACCGTCGC
A5_P9	PA3615	1071	GATCTTAAG ATGCCCTACGAAGCCGATGA	GTCCAGTTTTCCGGCAGGT
A6_P9	PA3619	1008	GATCTTAAG ATGAACATCGCGCCACTCAA	GCGTGCCGCGGTATAGCTGG
A7_P9	PA4008	1224	GATCTTAAG ATGCGCTACCGTACCGACTA	GGCGACCTCCGCTCGCTCCC
A8_P9	PA4163	1710	GATCTTAAG ATGATCGAGGTACCGAGGT	CTTGCTTGCCAGCGGTGGAG
A9_P9	PA4437	963	GATCTTAAG ATGCGCCTTTATCTGCTCGC	GCGCTGCGCGGTGTTCTGCT
A10_P9	PA4532	690	GATCTTAAG GTGATCGCTGCCGAATTGCT	GGGCTTGCGCTCTTCGCTCT
A11_P9	PA4802	723	GATCTTAAG ATGACGCTGATCGCCGCCGC	AGCGTCTATCTCGGTCCGTT
A12_P9	PA5136	1482	GATCTTAAG ATGGCCCGCCCTCCCCCTCC	GTTCAAGTCGTAGGCCTGGA
B1_P9	PA0145	519	GATCTTAAG ATGACCGCATCTACCTGGC	GGCGTTCCCGCCGAGTCTCT
B2_P9	PA0586	1554	GATCTTAAG ATGAGCAAGCGCCAGCCCAT	AATGGGCGGGATGATCAGGT
B3_P9	PA1495	627	GATCTTAAG ATGGGAAGTCTTGACCGGCA	GGCCGCTGTTCCAGGCGCT
B4_P9	PA2067	669	GATCTTAAG ATGGACGGCGTCTGATCAG	TGGGACGCCAACGCTCTCT
B5_P9	PA2182	270	GATCTTAAG ATGACTACGCCCGCATGAT	GGAACAGGCGCGCCCGATCC
B6_P9	PA2474	912	GATCTTAAG ATGACCACCGCATCCGGGC	GAAGACCTGCGAGTAGCGCA

B7_P9	PA2595	957	GATCTTAAG ATGCGTCAGACCCTGAGCCT	CCGGATATCCGCATCCGACG
B8_P9	PA2613	1326	GATCTTAAG GTGGATCTGTTCCGAGCGA	GGATTTTCTGCGTTGGCGGG
B9_P9	PA2693	501	GATCTTAAG ATGGAACCTGGCAGCTACCA	GGCCGGCATCGCGTGATCCA
B10_P9	PA2729	1350	GATCTTAAG ATGAGCGGACCGAAAGTCGT	CAACCCCTCTGCCGCGCCA
B11_P9	PA2972	579	GATCTTAAG ATGCCCCACCTGATCCTCGC	GGGGATTTCGACGCCTTCCT
B12_P9	PA3080	1098	GATCTTAAG ATGCGTGAGCCCATGACGTG	TTGTTGTTGTTGAGCGCGG
C1_P9	PA3238	1362	GATCTTAAG ATGCCCCACTTCTCCGTTT	GTTTCTGCCTGCTGGGTGA
C2_P9	PA3682	825	GATCTTAAG ATGACCAGCCAACGCCAACG	GCGGAACAGGTCGTTGATGC
C3_P9	PA3868	1011	GATCTTAAG ATGCTGTTGAGCGTGGTGGA	GTCCGTAGCCAGGGTCTCGC
C4_P9	PA4620	540	GATCTTAAG ATGGCTAACCGCAAGCTCCA	AGCCTCCTTGACCAGGCCGA
C5_P9	PA4908	933	GATCTTAAG ATGCACAGCCTGCGCTTTTT	GGCGGCGTTATCCACAACCC
C6_P9	PA0146	1098	GATCTTAAG ATGAAACACCGTCGCACGCA	CTTCGGCAGGTCGGCCTTGA
C7_P9	PA1045	2145	GATCTTAAG ATGCTCAGCGCCGAACCTCAA	GGCGATTTCGCGGCGGAACG
C8_P9	PA1112	1149	GATCTTAAG ATGCCGGGCTGTCTTTGAA	GCGCGCCAACCCAGGCGCA
C9_P9	PA1115	2325	GATCTTAAG GTGCGTCCACTCAGCCGTTG	GTGCGAAAGGATCAGGGCCT
C10_P9	PA2162	2781	GATCTTAAG ATGATTGAGCCCCGCGCTAC	TGGGGTGTCTCTGCGCGA
C11_P9	PA2296	1407	GATCTTAAG ATGCGACTGCGTGCAATCCT	GCGGAGCGCCAGCGCCTGCT
C12_P9	PA2719	687	GATCTTAAG ATGACCAAGCGCATCTGCA	GCCGAGCAGGGCGGCCACCT
D1_P9	PA3230	1125	GATCTTAAG ATGCCGATCCAGACGCTTGC	GGCCTGGCGGTAGGGCAACA
D2_P9	PA3424	1407	GATCTTAAG ATGTCGGCCTGGCGCCACCT	GCGCATCAGGCTTTCATGC
D3_P9	PA4017	642	GATCTTAAG ATGCACTCGACGCCAAGCG	TTTCCCCAGCTTGCGCAGTT
D4_P9	PA4040	1008	GATCTTAAG ATGCGCCTGCGTAACGTAGC	GCACTTGGGCGACGAGGGCT
D5_P9	PA4121	660	GATCTTAAG ATGAGCCGCGCACTGAATGA	TTCGCGCAGATGCTGTTGG
D6_P9	PA4360	474	GATCTTAAG GTGCGCCTGCAGGTCAAGCA	GCGGGTATTGAGCTGCTGCT
D7_P9	PA4478	606	GATCTTAAG ATGCCGTGCTGTATCTCGC	CGGCGGGTTGCCACCCACGG
D8_P9	PA4517	1803	GATCTTAAG GTGTCCCCACTCCACCAAG	GCCTTCGTTGCGCTGGCGGG
D9_P9	PA0319	990	GATCTTAAG ATGCCCTTTCATGGCGACGC	ATCGGCGTCGCTGGTGGCCA
D10_P9	PA1018	867	GATCTTAAG ATGGCGCTCGATCTGAGGT	GTCCGGCCGCTCTGGCGGCG
D11_P9	PA2134	573	GATCTTAAG GTGCCGAAGTCCCGGCATT	CTTGATGGGTGCGCCTTGG
D12_P9	PA2221	1206	GATCTTAAG ATGACTGCGGCAACTTGC	TCCAGGGCAGCGCGATATC
E1_P9	PA2632	621	GATCTTAAG ATGAGCGACACCCCGAGAC	CAGGAGGAAGTCCGCGAGGT
E2_P9	PA2963	1050	GATCTTAAG ATGCGCAAACCTGCTGGTGCT	TTGTGGCGCGGGGTGATGG
E3_P9	PA3449	1002	GATCTTAAG ATGATCGCCGCTCTCCGTCG	GGGCTCCGTGCGCGCCAACG
E4_P9	PA3580	471	GATCTTAAG ATGACCCCTGCCATCGACCT	TTCACGGCCGATGGCGGCGA
E5_P9	PA3693	522	GATCTTAAG ATGACCGAGGTCCGCGTCTG	GCGGGCCACAGGCCGCTCGC
E6_P9	PA3951	504	GATCTTAAG TTGAGTCGTCCCGAGTCGCC	GCCCTTGAGCAGCAGTCCGC
E7_P9	PA0468	951	GATCTTAAG ATGCGTCACCTGCCCTACCC	GTCGCGGACGACGCGCAGAC
E8_P9	PA0639	771	GATCTTAAG ATGGAACCTGAGCCGAGCCT	CTGCGGCATCCGCGTGTGCC
E9_P9	PA0924	1929	GATCTTAAG ATGTTGCCCCACCCAGCAC	TGGCGTCAACGAAGTCGCGA
E10_P9	PA1009	558	GATCTTAAG ATGTCCACCAGCCAACCCG	GGGGTGTGGGGGCGCCAGG
E11_P9	PA2328	1200	GATCTTAAG ATGTGCTGGACGACCCGAC	CGGGCTGATCTCTCGCTGC
E12_P9	PA3419	813	GATCTTAAG ATGGACCCGCGTCAAGCCTG	GTGACGGGCGCGCTGGTGC
F1_P9	PA3445	972	GATCTTAAG ATGCGCACCATCGCTTTGCG	GGGTGCGCTGGCGACCTTGC
F2_P9	PA4045	798	GATCTTAAG ATGCGCTCGTTCTGGTGCT	GCGCGCCCCGCGAGCGAGC
F3_P9	PA4118	570	GATCTTAAG ATGCCCCGCTCCGCTCCG	GTTACCGCGTACTGCGCCA
F4_P9	PA4788	858	GATCTTAAG ATGCCACCGCTGGCTCGA	GCCCTGTAGCCGGCTCCAAT
F5_P9	PA5520	744	GATCTTAAG ATGCCTGCCGCATACGCAT	GTCGTCCCTGGCTGACTGG

F6_P9	PA1894	693	GATCTTAAG ATGCCGCCAACCAGCCCCAC	ATAGACCCGCCGGTCCGGT
F7_P9	PA1915	1548	GATCTTAAG ATGCCGCAGAGCATCCGCCA	GTCCATGTCGCCGCCATGGT
F8_P9	PA2111	714	GATCTTAAG ATGAGCCAACCGCAACCGCG	TGCCTGGACCTCCAGGGGCG
F9_P9	PA2163	2055	GATCTTAAG ATGAGTGACGCACGCCTGGC	ATCATGGGCGGGCTCCTCGG
F10_P9	PA2421	921	GATCTTAAG ATGCGTGACGCCCTGCTACC	GAACGCCAGCAGGTAGCGCA
F11_P9	PA3255	579	GATCTTAAG ATGGCGAGTCTCGGCTGGGT	GCGCCAGGCGTTGACCGGCC
F12_P9	PA3733	1230	GATCTTAAG ATGCGCACACTGCAGCCTGA	GATGGCGCCTCCCGGCGCA
G1_P9	PA4516	816	GATCTTAAG ATGCGCCACCTGCTGCTTCG	GACGGGCAGTTGCGCGTGCC
G2_P9	PA4966	1014	GATCTTAAG ATGCGCCGCTGCTGGCCAT	CTTGTCGCCCAACCAGCCGC
G3_P9	PA0356	825	GATCTTAAG GTGCCGCCGCAACCCAGAT	GTAGCTGCCCTGGCCGACGC
G4_P9	PA0671	552	GATCTTAAG GTGCCGGCCGGCGCTTCCCT	TTGCCAGGCGCTGGCTGGCA
G5_P9	PA0787	1164	GATCTTAAG ATGCTGACCACCTGGCGGT	GCGCACCGGCCAGTACCAGG
G6_P9	PA0813	1248	GATCTTAAG ATGAGCGCGCTCTTCCCGC	ACTGGCGGCGCGCTGTCGCA
G7_P9	PA1605	1035	GATCTTAAG ATGGTGCGCCCCGTACGCG	TTCGCTCGCGGATCGGCGG
G8_P9	PA1866	2277	GATCTTAAG ATGACTGAGCAGGGCGGCGA	ACGCAGTTGCCACCAGCCCG
G9_P9	PA1972	1704	GATCTTAAG ATGTCGAAAGCCCGCGCCGT	GGAAGCCGGCGGCTCCTGGC
G10_P9	PA2858	2493	GATCTTAAG GTGCCCCCTCCCGCCTGCT	GCCCTCGCGCAGGACCCGCA
G11_P9	PA3071	939	GATCTTAAG ATGCTGAGCGCCGCCCGGG	TGCGCGATACCCCGGCTGGT
G12_P9	PA3091	1440	GATCTTAAG ATGCGGGCCGCTCGCCAGG	GCTCACGGTGCAGGCGGCC
H1_P9	PA3492	1035	GATCTTAAG ATGGCCCTGCCCCGCCAC	GTCGCTGCCTGAAGCCGC
H2_P9	PA4016	1740	GATCTTAAG ATGCTTCGCCCCGCCAGGTC	TTTGCCCGCCGCGCCCTCGC
H3_P9	PA4323	1332	GATCTTAAG ATGAAGCCATCGCGCGCCCT	AAGCACGCCGGCGCGCTTCC
H4_P9	PA4841	537	GATCTTAAG ATGGCCGCGCCGATCAGCGC	GGCGTCCAGGTACAGGCGCA
H5_P9	PA4955	1512	GATCTTAAG ATGACAGACCGCTCGCCGC	TTCCGTGCGGCGCTGGCGGC
H6_P9	PA4961	1539	GATCTTAAG GTGACCCGGCCACGTCCGT	CGGGCGGGCGCGGTCTGTGCA
H7_P9	PA5022	3357	GATCTTAAG ATGCCTGCCCTTCGCTCCCT	GCGGGTTCGGTTCGGCGGGAC
H8_P9	PA5299	1860	GATCTTAAG ATGGGCTGCCCTCGGGCT	GCCCCGCTCTCTCGGCTGG
H9_P9	PA5390	1155	GATCTTAAG ATGCCCGGCAGCCGCGACAT	AGGCTCCCGCAGCCACGCCG
H10_P9	PA5395	471	GATCTTAAG ATGAGCGACGTCCGTCCCC	GAGGCCGAGTTCGCCGAGCG

*In the plate position column letter before underline represents position of the primer (gene) in 96-well plate and symbol after underline the ordinal number of the plate. The primers were synthesized by Eurofins Genomics (Louisville, KY, USA).

Table S2. Sequencing results of pGUF-*guf* expression plasmids obtained using forward primer.

Gene name	Gene length [bp]	Alignment coverage [%]*	Mismatches	Gaps	Δ coordinate [#]
PA2146	168	100	0	0	0
PA2501	168	99	0	0	1
PA1478	177	100	0	0	0
PA4940	186	100	0	0	0
PA3501	219	100	2	0	0
PA4782	246	100	0	0	0
PA0722	252	100	0	0	0
PA2737	258	100	0	0	0
PA1508	261	100	0	0	0
PA2182	270	100	0	0	0
PA0954	276	100	0	0	0
PA2485	279	100	0	0	0

5. Supplementary data

PA4060	279	100	0	0	-1
PA0466	303	100	0	0	0
PA3390	303	100	0	0	0
PA4789	306	100	0	0	0
PA2038	315	100	0	0	0
PA2759	315	100	0	0	0
PA3224	318	100	0	0	0
PA3502	318	100	0	0	0
PA3762	318	100	0	0	0
PA0939	327	100	1	0	0
PA1506	330	100	0	0	0
PA0589	333	100	0	0	0
PA0573	336	100	0	0	1
PA0565	339	100	0	0	0
PA3046	345	100	0	0	0
PA1917	348	100	0	0	0
PA3664	348	100	0	0	0
PA1568	354	100	0	0	0
PA5303	354	99	0	0	-4
PA0630	363	100	0	0	0
PA1842	363	100	0	0	0
PA2898	369	100	0	0	0
PA1966	372	99	0	0	0
PA1095	381	100	0	0	0
PA1518	381	100	0	0	-1
PA5339	381	99	0	0	0
PA3869	384	100	0	0	0
PA2358	390	100	0	0	0
PA3786	390	100	1	1	0
PA5202	390	100	0	0	0
PA1969	393	100	0	0	0
PA5347	393	99	0	0	0
PA2375	396	100	0	0	0
PA4471	396	100	0	0	0
PA3674	399	100	1	0	0
PA5144	399	99	1	0	0
PA0474	405	100	0	0	-1
PA0988	405	100	0	0	0
PA2801	405	100	0	0	0
PA5371	405	100	0	0	0
PA0925	408	99	0	0	0
PA0957	408	100	1	0	0
PA2769	411	100	0	0	0
PA0868	414	100	0	0	0
PA3289	414	100	0	0	0
PA4093	417	100	0	0	1
PA5130	420	100	0	0	0
PA4325	423	99	0	0	0
PA5392	423	100	0	0	0

5. Supplementary data

PA1870	426	100	0	0	0
PA3332	426	100	0	0	0
PA3741	426	100	0	0	0
PA2120	429	99	0	0	0
PA1428	432	99	0	0	0
PA0404	435	100	0	0	0
PA2756	435	100	0	0	1
PA3499	435	100	0	0	1
PA4767	435	100	0	0	0
PA5196	435	100	0	0	0
PA0061	438	100	0	0	0
PA0315	438	99	0	0	0
PA1835	438	100	0	0	0
PA3017	438	100	0	0	0
PA3130	438	100	0	0	0
PA3180	438	100	0	0	-1
PA5079	438	100	0	0	0
PA2860	441	100	0	0	1
PA0481	444	101	1	0	3
PA0822	447	100	0	0	0
PA0968	447	100	0	0	0
PA1594	447	100	0	0	0
PA2833	447	100	0	0	0
PA2538	453	100	0	0	0
PA5026	453	100	0	0	0
PA3320	456	100	0	0	0
PA4015	456	100	0	0	0
PA2102	459	100	0	0	0
PA3470	459	100	1	0	0
PA4746	459	100	0	0	-2
PA1616	465	100	0	0	-1
PA5329	465	100	0	0	0
PA1788	468	100	0	0	0
PA4387	468	100	0	0	0
PA4948	468	100	0	0	1
PA5481	468	100	0	0	0
PA2625	471	100	0	0	0
PA5395	471	100	0	0	0
PA0351	474	100	0	0	0
PA1206	474	100	0	0	0
PA1593	474	100	0	0	0
PA4360	474	100	0	0	0
PA5246	474	100	0	0	0
PA1357	477	100	0	0	0
PA3785	477	99	0	0	0
PA1289	480	100	0	0	0
PA3259	480	100	0	0	0
PA2768	483	100	0	0	0
PA2822	483	100	0	0	0

5. Supplementary data

pa3856	483	100	0	0	0
PA3982	483	100	1	1	0
PA5222	483	100	0	0	0
PA4643	486	100	0	0	0
PA0560	489	100	0	0	0
PA1035	495	100	0	0	0
PA1040	498	100	0	0	0
PA1189	498	100	0	0	0
PA1753	498	100	0	0	0
PA1841	498	100	0	0	0
PA0127	501	100	0	0	0
PA2693	501	100	0	0	0
PA3756	501	100	0	0	0
PA3288	504	99	0	0	0
PA3951	504	100	0	0	0
PA0055	507	100	0	0	0
PA1746	507	100	0	0	0
PA3618	507	100	0	0	0
PA5551	510	100	0	0	-1
PA0484	516	100	0	0	0
pa3911	516	100	0	0	0
PA0145	519	100	0	0	0
PA0824	519	100	0	0	0
PA2750	519	100	0	0	0
PA1062	522	99	0	0	0
PA3693	522	100	0	0	0
PA0457	525	100	0	0	0
PA2464	525	100	2	0	0
PA4965	525	100	0	1	1
PA0800	534	100	0	0	0
PA1154	534	100	0	0	0
PA1885	534	100	0	0	0
PA0006	537	100	0	0	0
PA1906	537	99	0	0	0
PA4841	537	100	0	0	0
PA0449	540	100	0	0	-1
PA1536	540	100	0	0	0
PA1550	540	100	1	1	-7
PA1768	540	100	0	0	0
PA3726	540	100	0	0	0
PA4458	540	100	0	0	0
PA4620	540	100	1	0	0
PA4830	540	100	0	0	0
PA2301	543	100	0	0	0
PA3846	543	100	0	1	0
PA2141	549	100	0	1	0
PA3978	549	99	0	0	0
PA0671	552	100	0	0	0
PA1575	552	100	0	0	0

5. Supplementary data

PA4612	552	100	0	0	0
PA0107	555	100	0	0	0
PA0431	555	100	0	0	0
PA2189	555	99	0	0	0
PA2636	555	100	0	0	-1
PA1009	558	100	0	0	0
PA1675	558	100	0	0	0
PA0989	561	100	0	0	0
PA2331	561	100	0	1	0
PA5176	567	100	0	0	0
PA5519	567	100	0	0	0
PA0581	570	100	0	0	0
PA4118	570	100	0	0	0
PA2134	573	100	0	0	0
PA2372	573	100	2	2	0
PA3066	573	100	0	0	0
PA5123	573	100	0	0	1
PA1878	579	100	0	0	0
PA2972	579	100	0	0	0
PA3255	579	100	0	0	0
PA0201	582	100	0	0	0
PA3953	582	100	1	0	0
PA1280	585	100	0	0	0
PA3414	585	100	0	0	0
PA4336	585	100	0	0	0
PA4639	588	99	0	0	0
PA4923	588	100	0	0	0
PA0168	591	100	0	0	0
PA0387	594	100	0	0	0
PA4012	594	100	0	0	0
PA0370	597	100	0	0	0
PA1573	597	100	0	0	0
PA1677	597	100	0	0	0
PA3472	597	100	0	0	0
PA3941	597	100	0	0	1
PA2451	600	100	0	0	1
PA0174	603	100	0	0	0
PA1089	603	100	0	0	-1
PA1639	606	100	0	0	0
PA2459	606	100	0	0	0
PA4478	606	100	0	0	0
PA1219	615	100	0	0	0
PA1198	618	100	0	0	-1
PA1202	618	99	0	0	-5
PA3069	618	100	1	0	0
PA4833	618	100	0	0	0
PA5330	618	100	0	0	0
PA2632	621	100	0	0	0
PA4968	621	100	0	0	0

5. Supplementary data

PA0981	624	100	0	0	0
PA1111	624	100	0	0	0
PA5547	624	100	1	0	0
PA0144	627	100	0	0	0
PA1495	627	100	0	0	0
PA0629	630	100	0	0	0
PA0959	630	100	0	0	0
PA3379	630	100	0	0	0
PA4440	630	100	0	0	0
PA4535	630	100	0	0	0
PA1558	633	100	0	0	-1
PA2498	633	100	1	0	0
PA1211	636	100	0	0	0
PA0826	639	100	0	0	0
PA0990	639	100	0	0	0
PA0741	642	100	0	0	0
PA0832	642	100	0	0	0
PA4017	642	100	1	0	0
PA5086	642	100	0	0	0
PA5414	642	100	0	0	0
PA5534	642	100	0	0	0
PA2941	645	100	0	0	0
PA4048	645	100	0	0	0
PA2222	648	100	0	0	0
PA0013	654	100	0	0	0
PA0335	654	100	0	0	1
PA1143	654	100	0	0	0
PA1274	657	100	0	0	0
PA3955	657	100	1	0	0
PA3110	660	100	0	0	0
PA4121	660	100	0	0	0
PA1090	663	100	0	0	0
PA0065	666	100	0	1	0
PA0318	666	100	0	0	0
PA5177	666	100	0	0	0
PA2067	669	100	0	0	0
PA5245	669	100	0	0	0
PA1167	672	100	0	0	0
PA1193	672	100	0	0	0
PA2230	672	100	0	0	0
PA2814	672	100	1	1	0
PA0562	675	100	0	0	0
PA0976	675	100	0	0	0
PA5391	675	100	0	0	0
PA3564	678	100	0	0	-1
PA4510	678	100	0	0	1
PA2419	681	100	0	0	0
PA2698	681	100	0	0	0
PA3172	681	100	0	0	-1

5. Supplementary data

PA1118	684	100	0	0	0
PA4379	684	100	0	0	0
PA4532	690	100	0	0	0
PA1894	693	100	0	0	0
PA2974	693	100	0	0	0
PA3727	693	100	0	0	0
PA1784	696	100	0	0	0
PA2764	696	100	0	0	0
PA3681	696	100	0	0	1
PA3731	696	100	0	0	0
PA5052	696	100	0	0	0
PA0310	699	100	0	0	0
PA1210	699	100	0	0	0
PA2471	699	100	0	0	0
PA5281	699	100	0	0	0
PA1371	702	85	0	0	-3
PA4679	702	100	0	0	1
PA0462	705	100	0	0	-1
PA0947	705	100	0	0	0
PA1935	705	100	0	0	1
PA4278	705	100	0	0	0
PA4635	705	100	0	0	0
PA1831	711	100	0	0	0
PA1434	714	100	0	0	0
PA2111	714	93	0	0	0
PA4010	720	100	0	0	0
PA1792	723	100	0	0	0
PA4802	723	100	0	0	0
PA1597	726	100	0	0	0
PA4543	729	100	0	1	0
PA1559	732	100	0	0	0
PA1733	732	100	0	0	0
PA2106	735	100	0	0	0
PA0731	738	100	0	0	0
PA2156	738	99	0	0	0
PA4317	738	100	0	0	0
PA0544	744	100	0	0	0
PA2803	744	100	0	0	0
PA5520	744	100	0	0	0
PA4972	747	100	0	0	0
PA3750	750	97	0	0	0
PA0309	753	81	2	1	0
PA1030	756	100	0	0	-1
PA0492	759	100	0	0	0
PA1012	759	100	0	0	0
PA4445	759	100	0	0	0
PA5532	759	100	0	0	0
PA1762	762	100	0	0	0
PA4312	762	100	0	0	0

5. Supplementary data

PA1195	765	100	0	0	0
PA2411	765	100	0	0	1
PA5028	768	100	0	0	0
PA2872	771	100	0	0	0
PA1307	774	100	0	0	0
PA5135	774	99	1	0	1
PA1813	777	100	0	0	0
PA2168	777	100	0	0	0
PA2959	777	100	1	0	0
PA4824	777	100	0	0	0
PA4122	780	101	0	2	0
PA4699	780	100	0	0	0
PA0862	783	100	0	0	0
PA1501	783	100	0	0	0
PA3680	786	100	0	0	0
PA0642	789	100	0	0	0
PA1166	789	100	0	0	0
PA3797	795	100	0	0	0
PA4382	795	100	0	0	0
PA0480	798	100	0	0	0
PA2871	798	100	0	0	0
PA4045	798	100	0	1	-1
PA1732	801	100	0	1	0
PA3127	804	100	0	0	0
PA3505	804	100	0	0	0
PA5194	804	100	0	0	0
PA3251	810	100	0	0	0
PA1621	813	100	0	0	0
PA2074	813	100	0	0	0
PA3419	813	100	0	0	0
PA0735	816	100	0	0	0
PA3293	816	100	2	0	0
PA3598	816	100	0	0	0
PA4516	816	100	0	0	0
PA1938	822	101	0	0	5
PA4632	822	100	0	0	0
PA0356	825	100	0	0	0
PA0878	828	100	0	0	0
PA3226	828	100	0	0	0
PA0539	831	100	0	0	0
PA0935	831	100	0	0	0
PA4030	831	100	0	0	0
PA4106	831	100	0	0	0
PA1140	837	100	0	0	0
PA1291	840	100	0	1	0
PA5180	840	100	0	0	0
PA0987	843	100	1	0	0
PA2707	846	100	0	0	0
PA1539	849	100	0	0	3

5. Supplementary data

PA3787	849	100	0	1	0
PA5343	852	100	0	0	0
PA3283	855	100	1	0	0
PA0469	858	100	0	0	0
PA3132	858	100	0	0	0
PA3240	858	100	0	0	0
PA4788	858	100	0	0	0
PA1622	861	100	0	0	0
PA2418	861	100	0	0	0
PA4465	861	100	2	0	0
PA2745	864	100	0	0	0
PA4872	864	99	2	0	0
PA1018	867	95	1	0	0
PA2915	867	100	1	2	0
PA3037	867	100	1	0	0
PA4200	867	100	0	0	0
PA1688	870	100	1	0	0
PA3509	870	100	0	0	0
PA5087	870	100	0	0	0
PA1135	876	100	0	0	0
PA3323	876	100	0	0	0
PA0495	879	100	0	0	0
PA5488	879	100	0	0	0
PA5513	879	100	0	0	0
PA5088	882	100	0	0	0
PA1239	885	84	1	0	4
PA4069	885	100	0	0	0
PA0057	888	100	0	0	0
PA3200	888	100	0	0	0
PA2823	891	100	0	0	1
PA3912	891	100	0	0	0
PA3994	891	100	0	0	0
PA2661	894	100	0	0	0
PA3623	894	100	0	0	0
PA4717	894	100	0	0	0
PA0485	897	100	1	0	0
PA3429	897	100	0	0	1
PA3772	897	100	0	0	0
PA5539	897	100	0	0	0
PA3886	900	100	0	0	0
PA5363	900	100	1	0	0
PA2086	903	100	0	0	0
PA3695	906	100	0	0	0
PA1231	909	95	0	0	0
PA1638	909	100	0	0	0
PA2474	912	100	0	0	0
PA2689	915	100	0	0	0
PA2875	918	100	0	0	0
PA4656	918	61	0	0	0

5. Supplementary data

PA0100	921	99	2	0	0
PA2421	921	100	0	1	0
PA4404	924	100	0	0	0
PA1517	927	100	0	0	1
PA2452	927	100	0	0	0
PA2017	930	100	0	0	0
PA4509	930	100	0	0	0
PA4908	933	99	1	1	0
PA1209	936	100	1	0	0
PA0858	939	100	0	0	0
PA3071	939	100	0	0	0
PA0829	942	88	2	0	0
PA2599	945	94	0	0	-1
PA1205	948	100	2	1	0
PA0468	951	100	0	0	0
PA3301	951	100	0	0	0
PA0955	957	100	0	0	0
PA2595	957	100	0	0	0
PA1213	960	100	5	1	0
PA2211	960	100	2	0	0
PA2440	963	100	0	0	0
PA4437	963	100	0	0	0
PA2293	966	93	0	1	0
PA0543	969	87	2	0	0
PA3445	972	83	1	1	0
PA2610	975	84	0	1	0
PA0496	978	100	0	0	0
PA5396	978	100	0	0	0
PA3070	981	90	0	1	0
PA3087	981	100	0	1	0
PA0064	984	100	0	0	0
PA1680	984	100	0	0	0
PA4657	984	99	4	1	0
PA0360	987	101	2	2	0
PA3518	987	93	2	0	0
PA3586	987	100	0	0	0
PA0319	990	100	0	0	0
PA0368	999	100	0	0	0
PA3449	1002	92	2	1	0
PA4391	1002	100	0	0	0
PA4604	1005	100	3	1	0
PA0498	1008	88	0	2	0
PA3513	1008	102	5	1	0
PA3619	1008	100	0	0	0
PA4040	1008	100	0	2	0
PA4322	1008	100	0	0	0
PA3868	1011	100	2	0	0
PA0308	1020	96	5	1	0
PA2223	1020	100	1	0	1

5. Supplementary data

PA4952	1020	100	0	0	0
PA3073	1023	100	1	1	0
PA3981	1023	100	0	0	0
PA1763	1026	93	0	0	0
PA4631	1026	100	1	0	0
PA2993	1029	93	3	1	1
PA1605	1035	100	1	0	0
PA2793	1035	100	1	1	0
PA3492	1035	100	2	1	0
PA1640	1038	98	0	0	0
PA3519	1038	100	1	0	0
PA2581	1041	99	1	1	0
PA0732	1044	100	0	0	0
PA2549	1044	100	0	0	0
PA0599	1062	100	2	0	0
PA1293	1062	93	1	1	0
PA4372	1065	93	2	1	0
PA3615	1071	97	1	0	0
PA3515	1074	100	4	0	0
PA2172	1077	99	0	1	0
PA3076	1080	96	6	1	0
PA2660	1083	100	3	1	0
PA3969	1086	100	1	1	0
PA3481	1095	86	2	0	0
PA4438	1095	94	0	0	0
PA3080	1098	95	0	0	0
PA4673	1101	94	5	3	0
PA2218	1104	87	2	0	0
PA2695	1104	96	0	0	0
PA1356	1107	96	1	0	-1
PA0891	1113	78	0	0	0
PA3093	1119	78	0	0	0
PA3230	1125	92	0	0	0
PA2831	1128	98	0	2	0
PA2958	1134	88	0	0	0
PA3400	1134	90	0	0	0
PA3958	1140	91	3	3	0
PA5390	1155	96	2	0	0
PA0099	1161	84	2	1	0
PA3374	1164	89	0	0	0
PA2922	1170	91	2	1	0
PA3241	1170	79	1	1	1
PA3401	1173	84	2	0	0
PA2315	1176	85	0	2	0
PA1047	1179	91	2	2	0
PA1188	1182	75	0	0	0
PA3461	1197	74	0	1	0
PA0097	1200	93	7	1	-1
PA2328	1200	87	2	0	0

5. Supplementary data

PA5535	1203	78	5	2	0
PA3734	1206	87	7	2	-1
PA2228	1212	76	0	0	0
PA4344	1221	84	4	1	0
pa0446	1224	75	1	0	0
PA4008	1224	84	1	0	0
PA2325	1236	82	0	0	0
PA1488	1239	80	0	1	0
PA4677	1239	82	0	0	0
PA2682	1242	84	0	5	0
PA1450	1260	86	1	4	0
PA4065	1266	85	5	5	13
PA0333	1272	59	2	0	0
PA0726	1275	78	2	0	0
PA2091	1284	75	0	0	0
PA5133	1287	79	1	0	0
pa4011	1314	73	1	0	0
PA2530	1326	84	6	4	0
PA2613	1326	76	0	0	0
PA3464	1326	78	0	5	0
PA0451	1332	60	0	0	0
PA1791	1332	75	0	0	0
PA2927	1332	82	0	1	0
PA3043	1332	79	2	0	0
PA3170	1335	77	0	1	0
PA0667	1344	79	3	4	1
PA1451	1344	75	3	1	0
PA0142	1350	77	1	2	0
PA2729	1350	83	1	2	0
PA3238	1362	73	0	0	0
PA5106	1362	78	1	0	0
PA5209	1365	76	1	0	0
PA4115	1386	74	1	0	0
PA2004	1392	70	1	0	0
PA3919	1392	72	4	0	0
PA5113	1395	72	1	1	0
PA1918	1401	77	1	1	0
PA3614	1404	79	2	3	0
PA3424	1407	76	0	0	0
PA1888	1410	70	2	1	0
PA1730	1413	76	3	1	0
PA2529	1434	73	3	0	0
PA4474	1443	61	0	0	0
PA2283	1458	79	4	5	0
PA4958	1464	69	3	3	0
PA5136	1482	69	1	0	0
PA0371	1488	68	0	2	0
PA4308	1491	68	2	3	0
PA5290	1494	61	2	2	0

PA4961	1539	53	0	0	0
PA1915	1548	67	3	1	0
PA4701	1563	65	0	1	-1
PA5310	1590	66	3	0	0
PA1214	1599	68	5	0	0
PA1764	1599	62	4	0	0
PA3310	1656	63	0	0	0
PA0049	1662	61	1	1	0
PA2075	1662	63	2	5	0
PA1865	1680	57	12	3	0
PA1972	1704	67	3	2	0
PA0007	1707	61	1	0	0
PA3716	1707	64	2	3	0
PA4163	1710	54	0	0	0
PA5567	1737	54	0	1	0
PA2448	1743	59	1	1	0
PA3074	1761	51	0	0	0
PA2567	1764	60	1	1	0
PA3233	1800	56	3	1	0
PA4517	1803	54	8	0	0
PA1383	1806	59	0	0	0
PA1797	1833	52	5	1	0
PA2044	1875	56	0	0	0
PA3923	1926	54	0	1	0
PA1433	1953	54	0	0	0
PA0391	1968	52	1	0	0
PA4929	2043	51	3	0	0
PA1689	2103	50	0	0	0
PA0454	2202	49	1	10	0
PA2984	2226	43	1	1	0
PA1046	2274	41	0	0	0
pa1115	2325	44	0	0	0
PA2072	2595	29	0	0	0
PA0788	3126	32	0	0	0

*Alignment coverage represents a length of alignment between the Sanger sequencing result and a match (reference) in the *P. aeruginosa* genome relative to the expected gene size.

Δ coordinates represent a difference in chromosomal coordinates between the expected gene and a reference in the genome.

Table S3. Positive Sanger sequencing results of genes ≥ 1000 bp obtained with the reverse primer.

Gene name	Gene length [bp]	Alignment coverage [%]*	Mismatches	Gaps	Δ coordinates [#]
PA1415	729	98	0	0	3
PA2086	903	60	10	2	-3
PA3449	1002	76	0	0	3
PA0308	1020	48	3	0	-3
PA1186	1020	94	3	0	-3
PA3500	1020	80	0	0	3

5. Supplementary data

PA2309	1023	83	2	1	3
PA3492	1035	88	3	3	-3
PA1640	1038	93	0	0	3
PA0069	1059	96	9	3	-3
PA4362	1059	88	4	1	-3
PA1293	1062	68	1	0	3
PA4372	1065	62	0	0	-3
PA2330	1068	66	0	0	3
PA3615	1071	77	0	0	-3
PA3076	1080	64	7	0	-3
PA3969	1086	77	2	0	-3
PA3481	1095	83	2	0	3
PA3080	1098	82	3	0	3
PA2695	1104	81	2	1	3
PA1356	1107	73	1	2	-3
PA3230	1125	63	3	1	3
PA3400	1134	69	1	0	3
PA3958	1140	82	2	1	-3
PA1112	1149	51	2	2	-3
PA5390	1155	74	1	0	3
PA0099	1161	80	1	20	-3
PA2630	1170	85	3	0	-3
PA2922	1170	81	5	1	-3
PA3241	1170	43	1	2	3
PA3401	1173	78	2	1	3
PA1047	1179	58	2	0	-3
PA1188	1182	70	1	0	-3
PA2705	1182	67	1	0	3
PA2662	1194	81	1	0	3
PA3461	1197	70	3	0	-3
PA0097	1200	78	1	2	-3
PA5535	1203	79	1	1	3
PA2221	1206	68	3	0	-3
PA2691	1206	68	5	1	3
PA3734	1206	56	3	0	-3
PA2228	1212	55	0	0	3
PA0446	1224	74	1	0	3
PA4008	1224	68	2	0	-3
PA2325	1236	80	1	0	-3
PA2346	1236	81	9	3	-3
PA1488	1239	77	3	1	3
PA4677	1239	69	0	0	3
PA2682	1242	65	3	1	-3
PA1450	1260	50	1	0	-3
PA0587	1272	73	6	0	3
PA0726	1275	59	0	0	-3
PA1513	1278	52	1	0	3
PA5133	1287	33	3	1	-3
PA4011	1314	72	5	0	-4

5. Supplementary data

PA4186	1320	76	12	3	-3
PA2613	1326	75	3	3	3
PA3464	1326	46	2	0	3
PA1791	1332	68	4	1	3
PA2927	1332	78	6	0	-3
PA3043	1332	69	4	1	-3
PA1451	1344	54	1	0	-3
PA0142	1350	63	2	1	-3
PA2729	1350	61	2	0	-3
PA3238	1362	60	0	0	-3
PA1416	1383	60	1	1	3
PA4115	1386	68	4	1	-3
PA2004	1392	69	5	1	3
PA5113	1395	39	2	0	3
PA1567	1398	66	4	1	3
PA1918	1401	64	4	2	3
PA3614	1404	61	3	0	-3
PA3424	1407	59	5	3	-3
PA1888	1410	36	0	0	3
PA4371	1422	55	4	0	-3
PA5136	1482	57	0	1	-3
PA0371	1488	65	3	2	3
PA4308	1491	52	1	1	3
PA4961	1539	36	0	0	-3
PA1915	1548	56	2	2	3
PA4701	1563	51	0	0	-3
PA1214	1599	48	1	1	3
PA1972	1704	47	0	1	-3
PA0007	1707	54	4	0	-3
PA3716	1707	52	4	1	3
PA4163	1710	49	0	1	-3
PA3074	1761	48	0	0	-3
PA2567	1764	36	0	2	-8
PA3670	1848	53	5	3	3
PA3923	1926	45	2	0	3
PA4929	2043	36	1	1	-3
PA0454	2202	44	4	1	3
PA2984	2226	42	4	0	3
PA1115	2325	19	2	0	3
PA0788	3126	23	1	1	3

*Alignment coverage represents a length of alignment between the Sanger sequencing result and a match (reference) in the *P. aeruginosa* genome relative to the expected gene size.

Δ coordinates represent a difference in chromosomal coordinates between the expected gene and a reference in the genome.

Table S4. Organization of GUFs expressed from corresponding pGUF constructs in DWP and analyzed by dot-blot and hydrolase assays.

HY I	1	2	3	4	5	6	7	8	9	10	11	12
A	PA2228	PA2871	PA5519	PA2218	PA1089	PA3797	PA1888	PA0947	PA1597	PA1089	PA2871	PA1763
B	PA4968	PA1593	PA0431	PA1797	PA1935	PA0469	PA0065	PA5329	PA2814	PA4968	PA0449	PA4717
C	PA3756	PA2283	medium ctrl	PA2803	PA5396	PA2698	PA4404	PA3941	PA1166	PA1239	PA1433	PA2581
D	PA1675	PA5281	PA0959	PA1307	PA0492	PA1450	PA2044	PA1291	PA3301	PA3564	PA1202	PA0496
E	PA0308	PA5209	PA5396	PA3564	PA3301	PA3941	PA0480	PA3681	PA3464	PA3251	PA4965	PA2750
F	PA0469	PA3981	PA0351	PA0368	PA3727	PA1012	PA2728	PA2831	PA5177	PA2764	P_A3829	PA1193
G	PA2419	PA2411	PA2682	PA3614	PA4382	PA5177	PA1047	PA1938	PA1356	PA3623	PA3969	PA0480
H	PA3518	PA5488	PA0333	P_A3755	PA1732	PA2086	P_A3754*	P-A1370*	P_A4699*	P_A2839*	pGUF	PlaF

HY II	1	2	3	4	5	6	7	8	9	10	11	12
A	PA2228	PA2693					PA3785					PA2452
B	PA4677	PA0758	PA0858	PA3509	PA4312	PA5246	PA3994	PA5363	PA0201	PA2636	P_A3082	PA5222
C	PA3750	PA2471	PA2168	P_A4500	PA2922	PA5133	PA2503	PA3958	PA1677	PA1434	PA2984	medium ctrl
D	PA3323	PA4200	PA0990	PA0451	PA5194	PA4830	PA3461	PA0878	PA3283	PA0862	PA0371	PA3238
E	PA2230	PA4923	PA4048	PA2221	PA0468	PA3951	PA1573	PA3255	PA4017	PA4437	PA3953	PA1188
F	PA0100	PA0310	PA0726	PA5481	PA1567	PA0891	PA3772	PA1018	PA4360	PA3074	PA2632	PA0829
G	PA2156	PA0587	PA2309	PA1219	PA0639	PA2111	PA3580	PA3445	PA4961	PA3682	PA1112	PA1688
H	PA4792	PA4390	PA2610	PA2705	PA2503	PA2286	PA0145	PA3288	PA3075	PA4045	pGUF	PlaF

HY III	1	2	3	4	5	6	7	8	9	10	11	12
A	PA2689	PA2693	PA3259	PA3519	PA0732	PA1746	PA1788	PA5088	PA0565	PA2102	PA3240	PA3615
B	PA1140	PA1791	medium ctrl	PA2293	PA2418	PA2941	PA3513	PA3664	PA4069	PA4008	PA4163	PA4532
C	PA5330	PA0360	PA0387	PA3619	PA1488	PA0145	PA3598	PA3923	PA4631	PA5532	PA0055	PA1495
D	PA0741	PA2182	PA1205	PA1206	PA1841	PA2017	PA2530	PA2474	PA2974	PA3716	PA4336	PA5086
E	PA2595	PA2613	PA0484	PA2693	PA2729	PA1210	PA2972	PA3080	PA1918	PA2141	PA3238	PA3731
F	PA4115	PA3868	PA4620	PA5245	PA0144	PA4908	PA4478	PA0987	PA1214	PA1274	PA1689	PA1885
G	pa1115	PA2660	PA2328	PA3230	PA3481	PA3618	PA4106	PA3424	PA4465	PA4612	PA4040	PA4121
H	PA5481	PA5535	PA2134	PA0735	PA1219	PA1357	PA1559	PA2106	PA4517	PA0319	pGUF	PlaF

HY IV	1	2	3	4	5	6	7	8	9	10	11	12
A	PA1688	PA5087	PA2498	PA1972	PA2632	PA4516		pGUF				
B	PA3772	PA2067	PA2993	PA1915	PA3693	PA0356		PlaF				
C	PA2074	PA0145	PA1211	PA5136	PA1009	PA0671	PA0731					
D	PA0629	PA0560	PA2745	PA1605	PA4118	PA3071						
E	PA2075	PA5390	PA2110	PA3449	PA4788	PA3492						
F	PA0006	PA2529	PA4474	PA3419	PA5520	PA4841	PA1906					
G		PA1831	PA2707	PA4802	PA1894	PA5395						
H	PA2067	PA3429	PA3074	PA3919	PA2421							

HY V	1	2	3	4	5	6	7	8	9	10	11	12
A	PA3093	PA0543	PA0013	PA0404	PA1135	PA1213	PA2211	PA2315	PA2625	PA4679	PA5028	PA4308
B	PA4673	PA5113	PA5176	PA5547	PA0788	PA0832	PA0935	PA1167	PA1198	PA0978	PA1517	PA1878
C	PA2872	PA0495	PA0976	PA2301	PA3332	PA4372	PA5135	PA5371	PA0335	PA1568	PA0049	PA0462
D	PA0868	PA1035	PA1558	PA1762	PA1768	PA2823	PA3066	PA4122	PA5130	PA5196	PA5343	PA5391
E	PA0127	PA0544	PA1111	PA1293	PA1638	PA1730	PA2927	PA3472	PA3499	PA4012	PA4030	PA4093
F	PA4510	PA4604	PA5106	PA0988	PA1616	PA1640	PA2172	PA0457	PA2801	PA2875	PA3070	PA3130
G	PA3787	PA3037	PA3076	PA3180	PA3200	PA3241	PA3734	PA5392	PA0142	PA0589	PA1143	PA1289
H	PA1575	PA1680	PA1767	PA2375	PA2451	PA2959	PA3374	PA3470	PA3856	pGUF	medium ctrl	PlaF

HY VI	1	2	3	4	5	6	7	8	9	10	11	12
A	PA4011	PA2223	PA5310	PA1506	PA1280	PA0391	PA2958	PA3170	PA5513	PA4458	PA4952	PA3846
B	PA4065	PA5079	PA5551	PA0057	PA1733	PA3172	PA0562	PA1813	PA1621	PA3226	PA3586	PA4322
C	PA4440	PA4972	PA5290	PA2072	PA3132	PA1622	PA0968	PA1792	PA5202	PA1835	PA1594	PA0474
D	PA0957	PA1451	PA1518	PA1506	PA2769	PA3912	PA2539	PA3741	PA3310	PA4701	PA5026	PA4391
E	PA2661	PA3695	PA3043	PA1209	PA3087	PA4509	medium ctrl	PA2567	PA5180	PA1622	PA4966	PA3073
F	PA4639	PA4010	PA0925	PA5347	PA4656	PA1966	PA3505	PA5144	PA0731	PA2189	PA2120	PA0315
G	PA1501	PA3886	PA3127	PA5303	PA2440	PA1428	PA5339	PA1906	PA3978	PA1539	PA4438	PA1062
H										pGUF	medium ctrl	PlaF

*Genes with the wrong orientation that were not analyzed in dot-blot or hydrolase assays.

Table S5. PUFs with low activities in hydrolase enzyme screening.

Gene	Well - plate	Enzyme activity	% difference to plate average + st. dev.*		% difference to pGUF#		Dot-blot
			assay 1	assay 2	assay 1	assay 2	
PA0049	C11 - HY V	lipase (pNPD)	2	3	13	15	-
PA0142	G9 - HY V	lipase (pNPD)	3	2	15	14	-
PA0319	H10 - HY III	lipase (pNPD)	2	6	-1	3	+
PA0333	H3 - HY I	phospholipase C	10	78	16	231	+
PA0457	F8 - HY V	phosphatase	3	4	16	19	+
PA0484	E3 - HY III	phospholipase A	6	12	11	51	+
PA0496	D12 - HY I	lipase (GTD)	3	5	10	10	-
PA0543	A2 - HY V	phosphatase	3	9	16	24	-
PA0543	A2 - HY V	glucosidase	2	2	2	5	-
PA0629	D1 - HY IV	lipase (pNPD)	2	124	15	163	+
PA0629	D1 - HY IV	phospholipase C	5	7	32	31	+
PA0741	D1 - HY III	esterase	2	8	42	7	+
PA0788	B5 - HY V	glucosidase	2	9	2	12	-
PA0868	D1 - HY V	thioesterase	1	7	107	23	-
PA0935	B7 - HY V	glucosidase	0,4	3	0,4	6	-
PA0987	F8 - HY III	phospholipase A	1	0,04	5	35	+
PA1167	B8 - HY V	lipase (GTD)	3	149	19	363	-
PA1193	F12 - HY I	lipase (GTD)	8	11	15	16	-
PA1198	B9 - HY V	lipase (pNPD)	7	7	20	20	+
PA1198	B9 - HY V	glucosidase	3	11	3	14	+
PA1206	D4 - HY III	phospholipase A	5	0,4	10	35	+
PA1210	E6 - HY III	phospholipase A	6	19	11	60	+
PA1239	C10 - HY I	phospholipase C	8	16	13	185	+
PA1356	G9 - HY I	thioesterase	8	6	9	1943	+
PA1433	C11 - HY I	thioesterase	2	16	3	2126	-
PA1488	C5 - HY III	glucosidase	7	4	35	31	+
PA1506	A4 - HY VI	thioesterase	1	8	32	56	+
PA1517	B11 - HY V	lipase (pNPD)	6	13	18	26	+
PA1517	B11 - HY V	phosphatase	8	3	21	17	+
PA1517	B11 - HY V	phosphodiesterase	8	15	20	41	+
PA1517	B11 - HY V	glucosidase	2	5	2	8	+
PA1616	F5 - HY V	phosphatase	6	5	19	20	+
PA1616	F5 - HY V	phospholipase C	5	3	21	18	+
PA1688	A1 - HY IV	esterase	3	3	24	15	+
PA1732	H5 - HY I	phosphodiesterase	6	23	-25	17	+
PA1733	B5 - HY VI	thioesterase	6	19	39	72	-
PA1788	A7 - HY III	phosphodiesterase	2	16	24	31	+
PA1878	B12 - HY V	phosphatase	8	2	21	17	-
PA1915	B4 - HY IV	phosphatase	6	5	16	-3	+
PA1918	E9 - HY III	glucosidase	3	16	29	46	-

PA1935	B5 - HY I	phosphatase	8	4	-33	31	+
PA1935	B5 - HY I	thioesterase	5	12	6	2051	+
PA2067	H1 - HY IV	esterase	8	9	30	22	-
PA2067	H1 - HY IV	phospholipase C	10	13	38	38	-
PA2067	B2 - HY IV	thioesterase	0,1	11	49	-1	+
PA2074	C1 - HY IV	thioesterase	0,5	7	49	-4	+
PA2086	H6 - HY I	phosphodiesterase	7	2	-25	1	+
PA2106	H8 - HY III	lipase (pNPD)	10	11	7	9	+
PA2189	F10 - HY VI	thioesterase	4	6	36	53	-
PA2211	A7 - HY V	phosphodiesterase	3	5	14	28	-
PA2228	A1 - HY II	esterase	7	9	17	n.d.	+
PA2440	A9 - HY II	phospholipase A	6	43	55	52	+
PA2440	G5 - HY VI	phospholipase C	7	29	0,2	33	-
PA2581	C12 - HY I	esterase	2	3	-4	-12	-
PA2595	E1 - HY III	glucosidase	2	4	28	31	+
PA2625	A9 - HY V	glucosidase	4	6	4	10	-
PA2660	G2 - HY III	phospholipase A	4	13	8	53	-
PA2661	E1 - HY VI	phosphatase	7	4	55	66	+
PA2682	G3 - HY I	phosphodiesterase	2	3	-28	3	+
PA2689	A1 - HY III	protease	8	7	11	55	+
PA2689	A1 - HY III	lipase (pNPD)	10	14	6	11	+
PA2693	A2 - HY III	lipase (pNPD)	1	2	-2	0,2	-
PA2705	H4 - HY II	phosphodiesterase	9	8	9	17	+
PA2801	F9 - HY V	glucosidase	3	7	3	10	+
PA2839	H10 - HY I	phosphodiesterase	9	22	-23	17	-
PA2972	E7 - HY III	phospholipase A	9	6	14	43	+
PA3074	H3 - HY IV	phosphodiesterase	6	9	39	40	+
PA3074	H3 - HY IV	thioesterase	8	10	60	-1	+
PA3230	G4 - HY III	lipase (pNPD)	2	8	-1	6	+
PA3230	G4 - HY III	lipase (GTD)	0,1	19	13	24	+
PA3240	A11 - HY III	esterase	2	11	43	11	+
PA3251	E10 - HY I	phospholipase C	3	8	8	180	+
PA3323	D1 - HY II	phosphatase	4	15	11	25	+
PA3464	E9 - HY I	phospholipase A	2	2	32	-6	+
PA3472	E8 - HY V	phosphatase	2	1	15	15	-
PA3615	A12 - HY III	esterase	6	23	49	26	+
PA3619	C4 - HY III	glucosidase	2	6	29	33	+
PA3682	G10 - HY II	lipase (GTD)	1	3	22	-17	+
PA3695	E2 - HY VI	glucosidase	7	4	2	3	+
PA3756	C1 - HY I	lipase (GTD)	10	9	17	14	+
PA3772	B1 - HY IV	esterase	6	7	28	20	+
PA3772	B1 - HY IV	phosphodiesterase	8	11	41	42	+
PA3886	G2 - HY VI	lipase (GTD)	1	6	66	-47	-

PA3919	H4 - HY IV	phospholipase A	7	31	67	-31	+
PA3941	C8 - HY I	lipase (GTD)	2	2	9	6	+
PA3981	F2 - HY I	lipase (GTD)	7	4	14	9	-
PA4121	G12 - HY III	lipase (pNPD)	2	7	-1	5	+
PA4163	B11 - HY III	glucosidase	4	1	31	27	-
PA4404	C7 - HY I	phospholipase A	9	0,3	40	-8	+
PA4465	G9 - HY III	phosphatase	3	16	-368	46	-
PA4509	E6 - HY VI	phosphodiesterase	2	8	51	65	+
PA4639	F1 - HY VI	phosphatase	9	9	58	74	+
PA4639	F1 - HY VI	glucosidase	3	7	-2	5	+
PA4677	B1 - HY II	phosphodiesterase	1	18	1	27	+
PA4699	H9 - HY I	lipase (GTD)	9	7	17	12	+
PA4802	G4 - HY IV	phospholipase A	9	3	70	-46	+
PA4961	G9 - HY II	phospholipase C	8	21	109	14	+
PA4968	B1 - HY I	glucosidase	0,2	0,1	259	170	-
PA5028	A11 - HY V	lipase (pNPD)	7	8	19	21	-
PA5088	A8 - HY III	phosphodiesterase	6	2	29	15	+
PA5144	F8 - HY VI	lipase (GTD)	4	44	72	-28	-
PA5176	B3 - HY V	phosphatase	2	4	15	19	-
PA5180	E9 - HY VI	phosphatase	5	9	52	74	-
PA5303	G4 - HY VI	lipase (GTD)	5	2	73	-49	-
PA5347	F4 - HY VI	phosphatase	1	4	47	66	+
PA5347	F4 - HY VI	glucosidase	2	8	-3	6	+
PA5481	H1 - HY III	phospholipase A	10	11	15	50	+
PA5519	A3 - HY I	phosphatase	6	27	-34	59	-

*The percentage increase in activity of sample relative to plate (higher than plate) was calculated by dividing the difference between sample activity and the sum of average activity and st. dev. of the plate with the absolute value of a sum of average activity and st.dev of the plate.

#The percentage increase in activity of the sample relative to pGUF (higher than pGUF) was calculated by dividing the difference between sample activity and pGUF activity with the absolute value of pGUF activity.

PUFs whose expression was confirmed by dot-blot analysis are marked with the plus. n.d.=not determined.

6. References

1. Gomila, M., *et al.*, *Phylogenomics and systematics in Pseudomonas*. Front Microbiol, 2015. **6**: p. 214.
2. Diggle, S.P. and M. Whiteley, *Microbe profile: Pseudomonas aeruginosa: opportunistic pathogen and lab rat*. Microbiology (Reading, England), 2020. **166**(1): p. 30-33.
3. Kukavica-Ibrulj, I., *et al.*, *In vivo growth of Pseudomonas aeruginosa strains PAO1 and PA14 and the hypervirulent strain LESB58 in a rat model of chronic lung infection*. J Bacteriol, 2008. **190**(8): p. 2804-2813.
4. Wu, W., *et al.*, *Pseudomonas aeruginosa*, in *Molecular medical microbiology*, 2015. Academic Press. p. 753-767.
5. Driscoll, J.A., S.L. Brody, and M.H. Kollef, *The epidemiology, pathogenesis and treatment of Pseudomonas aeruginosa Infections*. Drugs, 2007. **67**(3): p. 351-368.
6. Bodey, G.P., *et al.*, *Infections caused by Pseudomonas aeruginosa*. Rev Infect Dis, 1983. **5**(2): p. 279-313.
7. Osmon, S., *et al.*, *Hospital mortality for patients with bacteremia due to Staphylococcus aureus or Pseudomonas aeruginosa*. Chest, 2004. **125**(2): p. 607-616.
8. Harbarth, S., *et al.*, *Epidemiology and prognostic determinants of bloodstream infections in surgical intensive care*. Arch Sur, 2002. **137**(12): p. 1353-1359.
9. Mikkelsen, H., R. McMullan, and A. Filloux, *The Pseudomonas aeruginosa reference strain PA14 displays increased virulence due to a mutation in ladS*. PloS one, 2011. **6**(12): p. e29113.
10. Stover, C.K., *et al.*, *Complete genome sequence of Pseudomonas aeruginosa PAO1, an opportunistic pathogen*. Nature, 2000. **406**(6799): p. 959-964.
11. Huang, W., *et al.*, *PAMDB: a comprehensive Pseudomonas aeruginosa metabolome database*. Nucleic Acids Res, 2018. **46**(D1): p. D575-D580.
12. Moore, N.M. and M.L. Flaws, *Epidemiology and pathogenesis of Pseudomonas aeruginosa infections*. Clin Lab Sci, 2011. **24**(1): p. 43.
13. Klockgether, J. and B. Tümmler, *Recent advances in understanding Pseudomonas aeruginosa as a pathogen*. F1000Res, 2017. **6**.
14. Crone, S., *et al.*, *The environmental occurrence of Pseudomonas aeruginosa*. APMIS, 2020. **128**(3): p. 220-231.
15. Rada, B. and T. L. Leto, *Pyocyanin effects on respiratory epithelium: relevance in Pseudomonas aeruginosa airway infections*. Trends Microbiol, 2013. **21**(2): p. 73-81.
16. Robinson, R.K., *Encyclopedia of food microbiology*, 2014. Academic press.
17. Meyer, J.-M., *Pyoverdines: pigments, siderophores and potential taxonomic markers of fluorescent Pseudomonas species*. Arch Microbiol, 2000. **174**(3): p. 135-142.
18. Reyes, E., *et al.*, *Identification of Pseudomonas aeruginosa by pyocyanin production on tech agar*. J Clin Microbiol, 1981. **13**(3): p. 456-458.
19. Bielecki, P., *et al.*, *Towards understanding Pseudomonas aeruginosa burn wound infections by profiling gene expression*. Biotechnol Lett, 2008. **30**(5): p. 777-790.
20. Balasubramanian, D., *et al.*, *A dynamic and intricate regulatory network determines Pseudomonas aeruginosa virulence*. Nucleic Acids Res, 2013. **41**(1): p. 1-20.
21. Rocha, A.J., *et al.*, *Pseudomonas aeruginosa: virulence factors and antibiotic resistance genes*. Braz Arch Biol Technol, 2019. **62**: p. e19180503
22. Vasil, M.L., *Pseudomonas aeruginosa: biology, mechanisms of virulence, epidemiology*. J Pediatr, 1986. **108**(5): p. 800-805.
23. Dolan, S.K., *Current knowledge and future directions in developing strategies to combat Pseudomonas aeruginosa infection*. J Mol Biol, 2020. **432**(20): p. 5509-5528.
24. Coggan, K.A. and M.C. Wolfgang, *Global regulatory pathways and cross-talk control Pseudomonas aeruginosa environmental lifestyle and virulence phenotype*. Curr Issues Mol Biol, 2012. **14**(2): p. 47-70.

25. Jurado-Martín, I., M. Sainz-Mejías, and S. McClean, *Pseudomonas aeruginosa: An audacious pathogen with an adaptable arsenal of virulence factors*. Int J Mol Sci, 2021. **22**(6).
26. Rosa, R.L., H. Johansen, and S. Molin, *Convergent Metabolic Specialization through Distinct Evolutionary Paths in Pseudomonas aeruginosa*. mBio, 2018. **9**.
27. Bianconi, I., et al., *Comparative genomics and biological characterization of sequential Pseudomonas aeruginosa isolates from persistent airways infection*. BMC genomics, 2015. **16**(1): p. 1-13.
28. Jimenez, P.N., et al., *The multiple signaling systems regulating virulence in Pseudomonas aeruginosa*. Microbiol Mol Biol Rev, 2012. **76**(1): p. 46-65.
29. Moradali, M.F., S. Ghods, and B.H. Rehm, *Pseudomonas aeruginosa Lifestyle: A paradigm for adaptation, survival, and persistence*. Front Cell Infect Microbiol, 2017. **7**: p. 39.
30. Pesci, E.C., et al., *Quinolone signaling in the cell-to-cell communication system of Pseudomonas aeruginosa*. PNAS, 1999. **96**(20): p. 11229-11234.
31. Burrows, L.L., *Pseudomonas aeruginosa twitching motility: type IV pili in action*. Annu Rev Microbiol, 2012. **66**: p. 493-520.
32. Talà, L., et al., *Pseudomonas aeruginosa orchestrates twitching motility by sequential control of type IV pili movements*. Nature Microbiol, 2019. **4**(5): p. 774-780.
33. Heiniger, R.W., et al., *Infection of human mucosal tissue by Pseudomonas aeruginosa requires sequential and mutually dependent virulence factors and a novel pilus-associated adhesin*. Cell Microbiol, 2010. **12**(8): p. 1158-73.
34. Burrows, L.L., *Pseudomonas aeruginosa Twitching Motility: Type IV Pili in Action*. Annu Rev Microbiol, 2012. **66**(1): p. 493-520.
35. Kadurugamuwa, J.L. and T.J. Beveridge, *Natural release of virulence factors in membrane vesicles by Pseudomonas aeruginosa and the effect of aminoglycoside antibiotics on their release*. J Antimicrob Chemother, 1997. **40**(5): p. 615-21.
36. Persat, A., et al., *Type IV pili mechanochemically regulate virulence factors in Pseudomonas aeruginosa*. PNAS, 2015. **112**(24): p. 7563-7568.
37. Alarcon, I., D.J. Evans, and S.M.J. Fleiszig, *The role of twitching motility in Pseudomonas aeruginosa exit from and translocation of corneal epithelial cells*. IOVS, 2009. **50**(5): p. 2237-2244.
38. Tolker-Nielsen, T., *Pseudomonas aeruginosa biofilm infections: from molecular biofilm biology to new treatment possibilities*. APMIS Suppl, 2014. **122**: p. 1-51.
39. Comolli, J.C., et al., *Pseudomonas aeruginosa gene products PilT and PilU are required for cytotoxicity in vitro and virulence in a mouse model of acute pneumonia*. Infect Immun, 1999. **67**(7): p. 3625.
40. Haiko, J. and B. Westerlund-Wikström, *The role of the bacterial flagellum in adhesion and virulence*. Biol (Basel), 2013. **2**(4): p. 1242-67.
41. Duan, Q., et al., *Flagella and bacterial pathogenicity*. J Basic Microbiol, 2013. **53**(1): p. 1-8.
42. Sampedro, I., et al., *Pseudomonas chemotaxis*. FEMS Microbiol Rev, 2015. **39**(1): p. 17-46.
43. Schwarzer, C., H. Fischer, and T.E. Machen, *Chemotaxis and binding of Pseudomonas aeruginosa to scratch-wounded human cystic fibrosis airway epithelial cells*. PLoS One, 2016. **11**(3): p. e0150109.
44. Garcia, M., et al., *Pseudomonas aeruginosa flagellum is critical for invasion, cutaneous persistence and induction of inflammatory response of skin epidermis*. Virulence, 2018. **9**(1): p. 1163-1175.
45. Feldman, M., et al., *Role of flagella in pathogenesis of Pseudomonas aeruginosa pulmonary infection*. Infect Immun, 1998. **66**(1): p. 43-51.
46. Haiko, J. and B. Westerlund-Wikström, *The role of the bacterial flagellum in adhesion and virulence*. Biol, 2013. **2**(4): p. 1242-1267.
47. Bucior, I., J.F. Pielage, and J.N. Engel, *Pseudomonas aeruginosa pili and flagella mediate distinct binding and signaling events at the apical and basolateral surface of airway epithelium*. PLoS Pathog, 2012. **8**(4): p. e1002616.

48. Ketko, A.K., et al., *Surfactant protein A binds flagellin enhancing phagocytosis and IL-1 β production*. PLoS One, 2013. **8**(12): p. e82680.
49. Stanislavsky, E.S. and J.S. Lam, *Pseudomonas aeruginosa antigens as potential vaccines*. FEMS Microbiol Rev, 1997. **21**(3): p. 243-277.
50. Miao, E.A., et al., *TLR5 and Ipaf: dual sensors of bacterial flagellin in the innate immune system*. Semin Immunopathol, 2007. **29**(3): p. 275-88.
51. Amiel, E., et al., *Pseudomonas aeruginosa evasion of phagocytosis is mediated by loss of swimming motility and is independent of flagellum expression*. Infect Immun, 2010. **78**(7): p. 2937-2945.
52. Mahenthiralingam, E., M.E. Campbell, and D.P. Speert, *Nonmotility and phagocytic resistance of Pseudomonas aeruginosa isolates from chronically colonized patients with cystic fibrosis*. Infect Immun, 1994. **62**(2): p. 596-605.
53. Huszczyński, S.M., J.S. Lam, and C.M. Khursigara, *The role of Pseudomonas aeruginosa lipopolysaccharide in bacterial pathogenesis and physiology*. Pathogens, 2019. **9**(1).
54. Nikaido, H., *Molecular basis of bacterial outer membrane permeability revisited*. Microbiol Mol Biol Rev, 2003. **67**(4): p. 593-656.
55. Schletter, J., et al., *Molecular mechanisms of endotoxin activity*. Arch Microbiol, 1995. **164**(6): p. 383-389.
56. Alshalchi, S.A. and G.G. Anderson, *Expression of the lipopolysaccharide biosynthesis gene lpxD affects biofilm formation of Pseudomonas aeruginosa*. Arch Microbiol, 2015. **197**(2): p. 135-145.
57. Engels, W., et al., *Role of lipopolysaccharide in opsonization and phagocytosis of Pseudomonas aeruginosa*. Infect Immun, 1985. **49**(1): p. 182-189.
58. Mann, E.E. and D.J. Wozniak, *Pseudomonas biofilm matrix composition and niche biology*. FEMS Microbiol Rev, 2012. **36**(4): p. 893-916.
59. Leid, J.G., et al., *The exopolysaccharide alginate protects Pseudomonas aeruginosa biofilm bacteria from IFN- γ -mediated macrophage killing*. J Immun, 2005. **175**(11): p. 7512-7518.
60. Ghafoor, A., I.D. Hay, and B.H. Rehm, *Role of exopolysaccharides in Pseudomonas aeruginosa biofilm formation and architecture*. Appl Environ Microbiol, 2011. **77**(15): p. 5238-5246.
61. Gellatly, S.L. and R.E. Hancock, *Pseudomonas aeruginosa: new insights into pathogenesis and host defenses*. Pathog Dis, 2013. **67**(3): p. 159-173.
62. Madsen, J.S., et al., *The interconnection between biofilm formation and horizontal gene transfer*. FEMS Immunol Med Microbiol, 2012. **65**(2): p. 183-195.
63. Chua, S.L., et al., *Dispersed cells represent a distinct stage in the transition from bacterial biofilm to planktonic lifestyles*. Nature Comm, 2014. **5**(1): p. 1-12.
64. Bonnardel, F., et al., *UniLectin3D, a database of carbohydrate binding proteins with curated information on 3D structures and interacting ligands*. Nucleic Acids Res, 2019. **47**(D1): p. D1236-D1244.
65. Winzer, K., et al., *The Pseudomonas aeruginosa lectins PA-IL and PA-IIL are controlled by quorum sensing and by RpoS*. J Bacteriol, 2000. **182**(22): p. 6401-6411.
66. Grishin, A.V., et al., *Pseudomonas aeruginosa lectins as targets for novel antibacterials*. Acta Naturae, 2015. **7**(2): p. 29-41.
67. Funken, H., et al., *Specific association of lectin LecB with the surface of Pseudomonas aeruginosa: role of outer membrane protein OprF*. PLoS One, 2012. **7**(10) p. e46857.
68. Chemani, C., et al., *Role of LecA and LecB lectins in Pseudomonas aeruginosa-induced lung injury and effect of carbohydrate ligands*. Infect Immun, 2009. **77**(5): p. 2065-2075.
69. Loris, R., et al., *Structural basis of carbohydrate recognition by the lectin LecB from Pseudomonas aeruginosa*. J Mol Biol, 2003. **331**(4): p. 861-870.
70. Imberty, A., et al., *Structures of the lectins from Pseudomonas aeruginosa: insights into the molecular basis for host glycan recognition*. Microb Infect, 2004. **6**(2): p. 221-228.
71. Tielker, D., et al., *Pseudomonas aeruginosa lectin LecB is located in the outer membrane and is involved in biofilm formation*. Microbiol, 2005. **151**(5): p. 1313-1323.

72. Johansson, E.M.V., et al., *Inhibition and dispersion of Pseudomonas aeruginosa biofilms by glycopeptide dendrimers targeting the fucose-specific lectin LecB*. Chem Biol, 2008. **15**(12): p. 1249-1257.
73. Sonawane, A., J. Jyot, and R. Ramphal, *Pseudomonas aeruginosa LecB is involved in pilus biogenesis and protease IV activity but not in adhesion to respiratory mucins*. Infect Immun, 2006. **74**(12): p. 7035-7039.
74. Gilboa-Garber, N. and D. Sudakevitz, *The hemagglutinating activities of Pseudomonas aeruginosa lectins PA-IL and PA-III exhibit opposite temperature profiles due to different receptor types*. FEMS Immun Med Microbiol, 1999. **25**(4): p. 365-369.
75. Bleves, S., et al., *Protein secretion systems in Pseudomonas aeruginosa: a wealth of pathogenic weapons*. Int J Med Microbiol, 2010. **300**(8): p. 534-543.
76. Pena, R.T., et al., *Relationship Between Quorum Sensing and Secretion Systems*. Front Microbiol, 2019. **10**: p. 1100.
77. Filloux, A., *Protein secretion systems in Pseudomonas aeruginosa: an essay on diversity, evolution, and function*. Front Microbiol, 2011. **2**: p. 155.
78. Kanonenberg, K., et al., *Type I secretion system—it takes three and a substrate*. FEMS Microbiol Lett, 2018. **365**(11).
79. Michel, G.P. and R. Voulhoux, *The type II secretory system (T2SS) in Gram-negative bacteria: a molecular nanomachine for secretion of Sec and Tat-dependent extracellular proteins*. In Bacterial secreted proteins: secretory mechanisms and role in pathogenesis, Caister Academic Press, 2009: p. 67-92.
80. Bardoel, B.W., et al., *Inhibition of Pseudomonas aeruginosa virulence: characterization of the AprA–AprI interface and species selectivity*. J Mol Biol, 2012. **415**(3): p. 573-583.
81. Zhao, K., et al., *TesG is a type I secretion effector of Pseudomonas aeruginosa that suppresses the host immune response during chronic infection*. Nat Microbiol, 2019. **4**(3): p. 459-469.
82. Olson, J.C. and D. Ohman, *Efficient production and processing of elastase and LasA by Pseudomonas aeruginosa require zinc and calcium ions*. J Bacteriol, 1992. **174**(12): p. 4140-4147.
83. Nomura, K., et al., *Pseudomonas aeruginosa elastase causes transient disruption of tight junctions and downregulation of PAR-2 in human nasal epithelial cells*. Resp Res, 2014. **15**(1): p. 1-13.
84. Rosenau, F., et al., *Lipase LipC affects motility, biofilm formation and rhamnolipid production in Pseudomonas aeruginosa*. FEMS Microbiol Lett, 2010. **309**(1): p. 25-34.
85. Funken, H., et al., *The lipase LipA (PA2862) but not LipC (PA4813) from Pseudomonas aeruginosa influences regulation of pyoverdine production and expression of the sigma factor PvdS*. J Bacteriol, 2011. **193**(20): p. 5858-5860.
86. Terada, L.S., et al., *Pseudomonas aeruginosa hemolytic phospholipase C suppresses neutrophil respiratory burst activity*. Infect Immun, 1999. **67**(5): p. 2371-6.
87. Holm, B.A., et al., *Inhibition of pulmonary surfactant function by phospholipases*. J App Physiol, 1991. **71**(1): p. 317-321.
88. Filloux, A., et al., *Phosphate regulation in Pseudomonas aeruginosa: cloning of the alkaline phosphatase gene and identification of phoB-and phoR-like genes*. Mol Gen Genet, 1988. **212**(3): p. 510-513.
89. Pavlovskis, O., B. Iglewski, and M. Pollack, *Mechanism of action of Pseudomonas aeruginosa exotoxin A in experimental mouse infections: adenosine diphosphate ribosylation of elongation factor 2*. Infect Immun, 1978. **19**(1): p. 29-33.
90. Folders, J., et al., *Identification of a chitin-binding protein secreted by Pseudomonas aeruginosa*. J Bacteriol, 2000. **182**(5): p. 1257-1263.
91. Anantharajah, A., M.-P. Mingeot-Leclercq, and F. Van Bambeke, *Targeting the type three secretion system in Pseudomonas aeruginosa*. Trends Pharma Sci, 2016. **37**(9): p. 734-749.
92. Kida, Y., et al., *A novel secreted protease from Pseudomonas aeruginosa activates NF-κB through protease-activated receptors*. Cell Microbiol, 2008. **10**(7): p. 1491-1504.

93. Wilhelm, S., et al., *The autotransporter esterase EstA of Pseudomonas aeruginosa is required for rhamnolipid production, cell motility, and biofilm formation*. J Bacteriol, 2007. **189**(18): p. 6695-6703.
94. Qu, J., et al., *Persistent Bacterial Coinfection of a COVID-19 Patient Caused by a Genetically Adapted Pseudomonas aeruginosa Chronic Colonizer*. Front Cell Infect Microbiol, 2021. **11**: p. 641920.
95. Salacha, R., et al., *The Pseudomonas aeruginosa patatin-like protein PlpD is the archetype of a novel Type V secretion system*. Environ Microbiol, 2010. **12**(6): p. 1498-1512.
96. Sana, T.G., B. Berni, and S. Bleves, *The T6SSs of Pseudomonas aeruginosa strain PAO1 and their effectors: beyond bacterial-cell targeting*. Front Cell Infect Microbiol, 2016. **6**: p. 61.
97. Wandersman, C. and P. Delepelaire, *Bacterial iron sources: from siderophores to hemophores*. Annu Rev Microbiol, 2004. **58**: p. 611-647.
98. Jayaseelan, S., D. Ramaswamy, and S. Dharmaraj, *Pyocyanin: production, applications, challenges and new insights*. World J Microbiol Biotechnol, 2014. **30**(4): p. 1159-68.
99. Hall, S., et al., *Cellular effects of pyocyanin, a secreted virulence factor of Pseudomonas aeruginosa*. Toxins, 2016. **8**(8): p. 236.
100. Ran, H., D.J. Hassett, and G.W. Lau, *Human targets of Pseudomonas aeruginosa pyocyanin*. PNAS, 2003. **100**(24): p. 14315-14320.
101. Gardner, P.R., *Superoxide production by the mycobacterial and pseudomonad quinoid pigments phthiocol and pyocyanine in human lung cells*. Arch Biochem Biophys, 1996. **333**(1): p. 267-74.
102. O'Malley, Y.Q., et al., *Subcellular localization of Pseudomonas pyocyanin cytotoxicity in human lung epithelial cells*. Am J Physiol Lung Cell Mol Physiol, 2003. **284**(2): p. L420-L430.
103. Rada, B. and T.L. Leto, *Pyocyanin effects on respiratory epithelium: relevance in Pseudomonas aeruginosa airway infections*. Trends Microbiol, 2013. **21**(2): p. 73-81.
104. Zeng, B., et al., *Heat shock protein DnaJ in Pseudomonas aeruginosa affects biofilm formation via pyocyanin production*. Microorganisms, 2020. **8**(3): p. 395-399.
105. Nutman, J., et al., *Studies on the mechanism of T cell inhibition by the Pseudomonas aeruginosa phenazine pigment pyocyanine*. J Immunol, 1987. **138**(10): p. 3481-3487.
106. Machan, Z., et al., *Interaction between Pseudomonas aeruginosa and Staphylococcus aureus: description of an antistaphylococcal substance*. J Med Microbiol, 1991. **34**(4): p. 213-217.
107. Hassan, H.M. and I. Fridovich, *Mechanism of the antibiotic action pyocyanine*. J Bacteriol, 1980. **141**(1): p. 156-163.
108. McClure, C.D. and N.L. Schiller, *Inhibition of macrophage phagocytosis by Pseudomonas aeruginosa rhamnolipids in vitro and in vivo*. Cur Microbiol, 1996. **33**(2): p. 109-117.
109. Read, R.C., et al., *Effect of Pseudomonas aeruginosa rhamnolipids on mucociliary transport and ciliary beating*. J Appl Physiol, 1992. **72**(6): p. 2271-2277.
110. Davey, M.E., N.C. Caiazza, and G.A. O'Toole, *Rhamnolipid surfactant production affects biofilm architecture in Pseudomonas aeruginosa PAO1*. J Bacteriol, 2003. **185**(3): p. 1027-1036.
111. Kapoor, G., S. Saigal, and A. Elongavan, *Action and resistance mechanisms of antibiotics: A guide for clinicians*. J Anaesthesiol Clinic Pharmacol, 2017. **33**(3): p. 300-305.
112. Bermingham, A. and J.P. Derrick, *The folic acid biosynthesis pathway in bacteria: evaluation of potential for antibacterial drug discovery*. BioEssays, 2002. **24**(7): p. 637-648.
113. Poirel, L., A. Jayol, and P. Nordmann, *Polymyxins: Antibacterial activity, susceptibility testing, and resistance mechanisms encoded by plasmids or chromosomes*. Clin Microbiol Rev, 2017. **30**(2): p. 557-596.
114. Wright, G.D., *Q&A: Antibiotic resistance: where does it come from and what can we do about it?* BMC Biol, 2010. **8**(1): p. 1-6.
115. Sriramulu, D., *Evolution and impact of bacterial drug resistance in the context of cystic fibrosis disease and nosocomial settings*. Microbiol Insights, 2013. **6**: p. MBI. S10792.

116. Ayukekbong, J.A., M. Ntemgwa, and A.N. Atabe, *The threat of antimicrobial resistance in developing countries: causes and control strategies*. Antimicrob Resist Infect Control, 2017. **6**(1): p. 1-8.
117. Brauner, A., et al., *Distinguishing between resistance, tolerance and persistence to antibiotic treatment*. Nat Rev Microbiol, 2016. **14**(5): p. 320-330.
118. Levin-Reisman, I., et al., *Epistasis between antibiotic tolerance, persistence, and resistance mutations*. Proc Natl Acad Sci USA, 2019. **116**(29): p. 14734-14739.
119. Pacios, O., et al., *Strategies to combat multidrug-resistant and persistent infectious diseases*. Antibiotics, 2020. **9**(2): p. 65.
120. Tenover, F.C., *Mechanisms of antimicrobial resistance in bacteria*. Amer J Med, 2006. **119**(6): p. S3-S10.
121. Pang, Z., et al., *Antibiotic resistance in Pseudomonas aeruginosa: mechanisms and alternative therapeutic strategies*. Biotechn Advan, 2019. **37**(1): p. 177-192.
122. Bellido, F., et al., *Reevaluation, using intact cells, of the exclusion limit and role of porin OprF in Pseudomonas aeruginosa outer membrane permeability*. J Bacteriol, 1992. **174**(16): p. 5196-5203.
123. Lambert, P., *Mechanisms of antibiotic resistance in Pseudomonas aeruginosa*. J RCoc Med, 2002. **95**(41): p. 22-28.
124. Trimble, M.J., et al., *Polymyxin: Alternative Mechanisms of Action and Resistance*. CSH Perspect Med, 2016. **6**(10): p. a025288.
125. Falagas, M.E., P.I. Rafailidis, and D.K. Matthaiou, *Resistance to polymyxins: mechanisms, frequency and treatment options*. Drug Res Updat, 2010. **13**(4-5): p. 132-138.
126. Macfarlane, E.L., A. Kwasnicka, and R.E. Hancock, *Role of Pseudomonas aeruginosa PhoP-PhoQ in resistance to antimicrobial cationic peptides and aminoglycosides*. Microbiol, 2000. **146**(10): p. 2543-2554.
127. Alcalde-Rico, M., et al., *Role of the multidrug resistance efflux pump MexCD-OprJ in the Pseudomonas aeruginosa quorum sensing response*. Front Microbiol, 2018. **9**: p. 2752.
128. Daury, L., et al., *Tripartite assembly of RND multidrug efflux pumps*. Nat Comm, 2016. **7**(1): p. 1-8.
129. Langendonk, R.F., D.R. Neill, and J.L. Fothergill, *The building blocks of antimicrobial resistance in Pseudomonas aeruginosa: Implications for current resistance-breaking therapies*. Front Cell Infect Microbiol, 2021. **11**(307).
130. Richardot, C., et al., *Carbapenem resistance in cystic fibrosis strains of Pseudomonas aeruginosa as a result of amino acid substitutions in porin OprD*. Int J Antimicrob Agent, 2015. **45**(5): p. 529-532.
131. Bruchmann, S., et al., *Quantitative contributions of target alteration and decreased drug accumulation to Pseudomonas aeruginosa fluoroquinolone resistance*. Antimicrob Agent Chemother, 2013. **57**(3): p. 1361-1368.
132. Doi, Y. and Y. Arakawa, *16S ribosomal RNA methylation: emerging resistance mechanism against aminoglycosides*. Clin Infect Dis, 2007. **45**(1): p. 88-94.
133. Yaeger, L.N., et al., *How to kill Pseudomonas—emerging therapies for a challenging pathogen*. Ann N Y Acad Sci, 2021. **1496**(1): p. 59-81.
134. Hall, C.W. and T.-F. Mah, *Molecular mechanisms of biofilm-based antibiotic resistance and tolerance in pathogenic bacteria*. FEMS Microbiol Rev, 2017. **41**(3): p. 276-301.
135. Moradali, M.F., S. Ghods, and B.H. Rehm, *Pseudomonas aeruginosa lifestyle: a paradigm for adaptation, survival, and persistence*. Front Cell Infect Microbiol, 2017. **7**: p. 39.
136. Batoni, G., et al., *Use of antimicrobial peptides against microbial biofilms: advantages and limits*. Cur Med Chem, 2011. **18**(2): p. 256-279.
137. Ciofu, O. and T. Tolker-Nielsen, *Tolerance and resistance of Pseudomonas aeruginosa biofilms to antimicrobial agents—How P. aeruginosa can escape antibiotics*. Front Microbiol, 2019. **10**: p. 913.

138. Zhou, J., et al., *Identification of a toxin-antitoxin system that contributes to persister formation by reducing NAD in Pseudomonas aeruginosa*. Microorg, 2021. **9**(4): p. 753-759.
139. Lascols, C., et al., *Type II topoisomerase mutations in clinical isolates of Enterobacter cloacae and other enterobacterial species harbouring the qnrA gene*. Int J Antimicrob Agent, 2007. **29**(4): p. 402-409.
140. Pai, H., et al., *Carbapenem resistance mechanisms in Pseudomonas aeruginosa clinical isolates*. Antimicrob Agent Chemother, 2001. **45**(2): p. 480-484.
141. Rice, L.B., *Federal funding for the study of antimicrobial resistance in nosocomial pathogens: no ESKAPE*. J Infect Dis, 2008. **197**(8): p. 1079-1081.
142. Gill, E.E., O.L. Franco, and R.E. Hancock, *Antibiotic adjuvants: diverse strategies for controlling drug-resistant pathogens*. Chem Biol Drug Des, 2015. **85**(1): p. 56-78.
143. Cassini, A., et al., *Attributable deaths and disability-adjusted life-years caused by infections with antibiotic-resistant bacteria in the EU and the European Economic Area in 2015: a population-level modelling analysis*. Lancet Infect Dis, 2019. **19**(1): p. 56-66.
144. Bassetti, M., et al., *How to manage Pseudomonas aeruginosa infections*. Drugs Cont, 2018. **7**.
145. Gonçalves, I.R., et al., *Carbapenem-resistant Pseudomonas aeruginosa: association with virulence genes and biofilm formation*. Braz J Microbiol, 2017. **48**(2): p. 211-217.
146. Tümmler, B., *Emerging therapies against infections with Pseudomonas aeruginosa*. F1000Res, 2019. **8**.
147. Tacconelli, E., et al., *Discovery, research, and development of new antibiotics: the WHO priority list of antibiotic-resistant bacteria and tuberculosis*. Lancet Infect Dis, 2018. **18**(3): p. 318-327.
148. Tankhiwale, S., *Beta-lactamases in P. aeruginosa: a threat to clinical therapeutics*. Curr Pediat Res, 2016.
149. Vaara, M., *Polymyxin derivatives that sensitize Gram-negative bacteria to other antibiotics*. Mol (Basel, Switzerland), 2019. **24**(2): p. 249.
150. Askoura, M., et al., *Efflux pump inhibitors (EPIs) as new antimicrobial agents against Pseudomonas aeruginosa*. Lib J Med, 2011. **6**(1).
151. Van Bambeke, F. and V.J. Lee, *Inhibitors of bacterial efflux pumps as adjuvants in antibiotic treatments and diagnostic tools for detection of resistance by efflux*. Recent Pat Antiinfect Drug Discov, 2006. **1**(2): p. 157-175.
152. Zimmermann, S., et al., *Clinically approved drugs inhibit the Staphylococcus aureus multidrug NorA efflux pump and reduce biofilm formation*. Front Microbiol, 2019. **10**: p. 2762.
153. Lamers, R.P., J.F. Cavallari, and L.L. Burrows, *The efflux inhibitor phenylalanine-arginine beta-naphthylamide (PAβN) permeabilizes the outer membrane of Gram-negative bacteria*. PLoS One, 2013. **8**(3): p. e60666.
154. Ferrer-Espada, R., et al., *A permeability-increasing drug synergizes with bacterial efflux pump inhibitors and restores susceptibility to antibiotics in multi-drug resistant Pseudomonas aeruginosa strains*. Sci Rep, 2019. **9**(1): p. 1-12.
155. Watkins, W.J., et al., *The relationship between physicochemical properties, in vitro activity and pharmacokinetic profiles of analogues of diamine-containing efflux pump inhibitors*. Bioorg Med Chem Lett, 2003. **13**(23): p. 4241-4244.
156. Siriyong, T., et al., *Conessine as a novel inhibitor of multidrug efflux pump systems in Pseudomonas aeruginosa*. BMC Compl Alternat Med, 2017. **17**(1): p. 1-7.
157. Mitchell, C.J., T.A. Stone, and C.M. Deber, *Peptide-based efflux pump inhibitors of the small multidrug resistance protein from Pseudomonas aeruginosa*. Antimicrob Agent Chemother, 2019. **63**: p.9.
158. Furiga, A., et al., *Impairment of Pseudomonas aeruginosa biofilm resistance to antibiotics by combining the drugs with a new quorum-sensing inhibitor*. Antimicrob Agents Chemother, 2015. **60**(3): p. 1676-86.
159. Ray, V.A., et al., *Anti-Psl targeting of Pseudomonas aeruginosa biofilms for neutrophil-mediated disruption*. Sci Rep, 2017. **7**(1): p. 1-12.

160. Martinez, M., *et al.*, *Synergistic and antibiofilm activity of the antimicrobial peptide P5 against carbapenem-resistant Pseudomonas aeruginosa*. Biochim Biophys Acta - Biomembr, 2019. **1861**(7): p. 1329-1337.
161. Frederiksen, B., *et al.*, *Effect of aerosolized rhDNase (Pulmozyme) on pulmonary colonization in patients with cystic fibrosis*. Acta Paediatr, 2006. **95**(9): p. 1070-4.
162. Narayanaswamy, V.P., *et al.*, *Novel glycopolymer eradicates antibiotic-and CCCP-induced persister cells in Pseudomonas aeruginosa*. Front Microbiol, 2018. **9**: p. 1724.
163. Pan, J., *et al.*, *Reverting antibiotic tolerance of Pseudomonas aeruginosa PAO1 persister cells by (Z)-4-bromo-5-(bromomethylene)-3-methylfuran-2 (5 H)-one*. PloS one, 2012. **7**(9): p. e45778.
164. Al Hussein, L., A. Maleki, and M. Al Marjani, *Antisense mqsR-PNA as a putative target to the eradication of Pseudomonas aeruginosa persisters*. New Microb New Infect, 2021. **41**: p. 100868.
165. Imperi, F., L. Leoni, and P. Visca, *Antivirulence activity of azithromycin in Pseudomonas aeruginosa*. Front Microbiol, 2014. **5**: p. 178.
166. Clatworthy, A.E., E. Pierson, and D.T. Hung, *Targeting virulence: a new paradigm for antimicrobial therapy*. Nat Chem Biol, 2007. **3**(9): p. 541-548.
167. Asadi, A., *et al.*, *A review on anti-adhesion therapies of bacterial diseases*. Infect, 2019. **47**(1): p. 13-23.
168. Huebinger, R.M., *et al.*, *Targeting bacterial adherence inhibits multidrug-resistant Pseudomonas aeruginosa infection following burn injury*. Sci Rep, 2016. **6**(1): p. 1-8.
169. Boukerb, A.M., *et al.*, *Antiadhesive properties of glycoclusters against Pseudomonas aeruginosa lung infection*. J Med Chem, 2014. **57**(24): p. 10275-10289.
170. Sui, S.J.H., *et al.*, *Raloxifene attenuates Pseudomonas aeruginosa pyocyanin production and virulence*. Int J Antimicrob Agent, 2012. **40**(3): p. 246-251.
171. Bythell-Douglas, R., *Structural biology of hydrolase enzymes*. Ph.D. Thesis, The University of Western Australia, 2013.
172. McDonald, A.G., S. Boyce, and K.F. Tipton, *Enzyme classification and nomenclature*. eLS, 2015. p. 1-11.
173. Kovacic, F., *et al.*, *Classification of lipolytic enzymes from bacteria*. In Aerobic Utilization of Hydrocarbons, Oils, and Lipids, 2019. **24**: p. 255-289.
174. Gao, F. and R.R. Zhang, *Enzymes are enriched in bacterial essential genes*. PloS one, 2011. **6**(6): p. e21683.
175. Kovačić, F., *et al.*, *Structural and functional characterisation of TesA-a novel lysophospholipase A from Pseudomonas aeruginosa*. PloS one, 2013. **8**(7): p. e69125.
176. Larsen, E.M. and R.J. Johnson, *Microbial esterases and ester prodrugs: An unlikely marriage for combating antibiotic resistance*. Drug Dev Res, 2019. **80**(1): p. 33-47.
177. Lopes, D.B., *et al.*, *Lipase and esterase: to what extent can this classification be applied accurately?* Food Sci Technol, 2011. **31**(3): p. 603-613.
178. Sandoval, G. (editor), *Lipases and phospholipases. Methods and protocols*. 2018: Springer.
179. Schmiel, D.H. and V.L. Miller, *Bacterial phospholipases and pathogenesis*. Microb Infect, 1999. **1**(13): p. 1103-1112.
180. Leščić Ašler, I., *et al.*, *Probing enzyme promiscuity of SGNH hydrolases*. Chem biochem, 2010. **11**(15): p. 2158-2167.
181. Perraud, Q., *et al.*, *A key role for the periplasmic PfeE esterase in iron acquisition via the siderophore enterobactin in Pseudomonas aeruginosa*. ACS Chem Biol, 2018. **13**(9): p. 2603-2614.
182. Zieliński, M., *et al.*, *Structural and functional insights into esterase-mediated macrolide resistance*. Nat Comm, 2021. **12**(1): p. 1-9.
183. Kim, Y.-H., C.-J. Cha, and C.E. Cerniglia, *Purification and characterization of an erythromycin esterase from an erythromycin-resistant Pseudomonas sp.* FEMS Microbiol Lett, 2002. **210**(2): p. 239-244.

184. Nardini, M., *et al.*, *Crystal structure of Pseudomonas aeruginosa lipase in the open conformation: the prototype for family I. 1 of bacterial lipases*. J Biol Chem, 2000. **275**(40): p. 31219-31225.
185. Dollinger, P., *Lipase-specific Foldase-aided Folding of Lipase A from Pseudomonas aeruginosa*. Heinrich-HeineUniversität Düsseldorf, 2019. Inaugural Dissertation.
186. Aloulou, A., *et al.*, *Phospholipases: an overview*. Lipases and phospholipases, 2012: p. 63-85.
187. Gendrin, C., *et al.*, *Structural basis of cytotoxicity mediated by the type III secretion toxin ExoU from Pseudomonas aeruginosa*. PLoS Path, 2012. **8**(4): p. e1002637.
188. Sawa, T., *et al.*, *Pseudomonas aeruginosa type III secretory toxin ExoU and its predicted homologs*. Toxins, 2016. **8**(11): p. 307.
189. da Mata Madeira, P.V., *et al.*, *Structural basis of lipid targeting and destruction by the type V secretion system of Pseudomonas aeruginosa*. J Mol Biol, 2016. **428**(9): p. 1790-1803.
190. Jiang, F., *et al.*, *The Pseudomonas aeruginosa type VI secretion PGAP1-like effector induces host autophagy by activating endoplasmic reticulum stress*. Cell reports, 2016. **16**(6): p. 1502-1509.
191. Gao, X., *et al.*, *Structure-based prototype peptides targeting the Pseudomonas aeruginosa Type VI secretion system effector as a novel antibacterial strategy*. Front Cell Infect Microbiol, 2017. **7**(411).
192. Flores-Díaz, M., *et al.*, *Bacterial sphingomyelinases and phospholipases as virulence factors*. Microbiol Mol Biol Rev, 2016. **80**(3): p. 597-628.
193. Truan, D., *et al.*, *High-level over-expression, purification, and crystallization of a novel phospholipase C/sphingomyelinase from Pseudomonas aeruginosa*. Protein Expr Purif, 2013. **90**(1): p. 40-46.
194. Jones, R.A., *et al.*, *Phosphorus stress induces the synthesis of novel glycolipids in Pseudomonas aeruginosa that confer protection against a last-resort antibiotic*. ISME J, 2021: p. 1-12.
195. Jiang, F., *et al.*, *A Pseudomonas aeruginosa type VI secretion phospholipase D effector targets both prokaryotic and eukaryotic cells*. Cell Host Microb, 2014. **15**(5): p. 600-610.
196. Boulant, T., *et al.*, *Higher prevalence of PldA, a Pseudomonas aeruginosa trans-kingdom H2-Type VI secretion system effector, in clinical isolates responsible for acute infections and in multidrug resistant strains*. Front Microbiol, 2018. **9**(2578).
197. Gonzalez, C.F., *et al.*, *Structure and activity of the Pseudomonas aeruginosa hotdog-fold thioesterases PA5202 and PA2801*. Biochem J, 2012. **444**(3): p. 445-455.
198. Yokoyama, T., *et al.*, *Structure and function of a Campylobacter jejuni thioesterase Cj0915, a hexameric hot dog fold enzyme*. Biochim Biophys Acta - Prot Proteomic, 2009. **1794**(7): p. 1073-1081.
199. Montavon, T.J. and S.D. Bruner, *Nonribosomal peptide synthetases*, in *Comprehensive Natural Products II*, H.-W. Liu and L. Mander, Editors. 2010, Elsevier: Oxford. p. 619-655.
200. Swarbrick, C., *et al.*, *Structure, function, and regulation of thioesterases*. Prog Lipid Res, 2020: p. 101036.
201. Reimmann, C., *et al.*, *PchC thioesterase optimizes nonribosomal biosynthesis of the peptide siderophore pyochelin in Pseudomonas aeruginosa*. J Bacteriol, 2004. **186**(19): p. 6367-6373.
202. Drees, S.L. and S. Fetzner, *PqsE of Pseudomonas aeruginosa acts as pathway-specific thioesterase in the biosynthesis of alkylquinolone signaling molecules*. Chem Biol, 2015. **22**(5): p. 611-618.
203. Mukherjee, S., *et al.*, *The PqsE and RhIR proteins are an autoinducer synthase–receptor pair that control virulence and biofilm development in Pseudomonas aeruginosa*. PNAS, 2018. **115**(40): p. E9411-E9418.
204. Kuznetsova, E., *et al.*, *Enzyme genomics: Application of general enzymatic screens to discover new enzymes*. FEMS Microbiol Rev, 2005. **29**(2): p. 263-279.
205. Sajid, A., *et al.*, *Protein phosphatases of pathogenic bacteria: role in physiology and virulence*. Annu Rev Microbiol, 2015. **69**: p. 527-547.

206. Ueda, A. and T.K. Wood, *Connecting quorum sensing, c-di-GMP, pel polysaccharide, and biofilm formation in Pseudomonas aeruginosa through tyrosine phosphatase TpbA (PA3885)*. PLoS Pathog, 2009. **5**(6): p. e1000483.
207. Ueda, A. and T.K. Wood, *Tyrosine phosphatase TpbA of Pseudomonas aeruginosa controls extracellular DNA via cyclic diguanylic acid concentrations*. Environ Microbiol Rep, 2010. **2**(3): p. 449-455.
208. Djeghader, A., et al., *Crystallization and preliminary X-ray diffraction analysis of a high-affinity phosphate-binding protein endowed with phosphatase activity from Pseudomonas aeruginosa PAO1*. Acta Cryst Sec F, 2013. **69**(10): p. 1143-1146.
209. Matange, N., *Revisiting bacterial cyclic nucleotide phosphodiesterases: cyclic AMP hydrolysis and beyond*. FEMS Microbiol Lett, 2015. **362**(22): p. fnv183.
210. Matange, N., M. Podobnik, and S.S. Visweswariah, *Metallophosphoesterases: structural fidelity with functional promiscuity*. Biochem J, 2015. **467**(2).
211. Fuchs, E.L., et al., *In V itro and In Vivo Characterization of the Pseudomonas aeruginosa Cyclic AMP (cAMP) Phosphodiesterase CpdA, Required for cAMP Homeostasis and Virulence Factor Regulation*. J Bacteriol, 2010. **192**(11): p. 2779-2790.
212. Vermassen, A., et al., *Cell Wall Hydrolases in Bacteria: Insight on the Diversity of Cell Wall Amidases, Glycosidases and Peptidases Toward Peptidoglycan*. Front Microbiol, 2019. **10**(331).
213. Davies, G. and B. Henrissat, *Structures and mechanisms of glycosyl hydrolases*. Structure, 1995. **3**(9): p. 853-859.
214. Acebrón, I., et al., *Catalytic cycle of the N-acetylglucosaminidase NagZ from Pseudomonas aeruginosa*. J Amer Chem Soc, 2017. **139**(20): p. 6795-6798.
215. Ho, L.A., et al., *A mechanism-based GlcNAc-inspired cyclophellitol inactivator of the peptidoglycan recycling enzyme NagZ reverses resistance to β -lactams in Pseudomonas aeruginosa*. Chem Comm, 2018. **54**(75): p. 10630-10633.
216. Dhar, S., et al., *Cell-wall recycling and synthesis in Escherichia coli and Pseudomonas aeruginosa – their role in the development of resistance*. J Med Microbiol, 2018. **67**(1): p. 1-21.
217. Baker, P., et al., *Characterization of the Pseudomonas aeruginosa glycoside hydrolase PslG reveals that its levels are critical for Psl polysaccharide biosynthesis and biofilm formation*. J Biol Chem, 2015. **290**(47): p. 28374-28387.
218. Yu, S., et al., *PslG, a self-produced glycosyl hydrolase, triggers biofilm disassembly by disrupting exopolysaccharide matrix*. Cell Res, 2015. **25**(12): p. 1352-1367.
219. Mechetin, G.V., et al., *Inhibitors of DNA glycosylases as prospective drugs*. Int J Mol Sci, 2020. **21**(9): p. 3118.
220. Culp, E. and G.D. Wright, *Bacterial proteases, untapped antimicrobial drug targets*. J Antibiot, 2017. **70**(4): p. 366-377.
221. Frees, D., L. Brøndsted, and H. Ingmer, *Bacterial proteases and virulence*. In Regulated proteolysis in microorganisms, Springer Link, 2013: p. 161-192.
222. Galdino, A.C.M., et al., *Pseudomonas aeruginosa and its arsenal of proteases: weapons to battle the host*. In Pathophysiological Aspects of proteases, Springer Link, 2017: p. 381-397.
223. Sherman, M. and A. Goldberg, *Involvement of molecular chaperones in intracellular protein breakdown*. In Stress-inducible cellular responses, Springer Link, 1996: p. 57-78.
224. Fernández, L., et al., *Role of intracellular proteases in the antibiotic resistance, motility, and biofilm formation of Pseudomonas aeruginosa*. Antimicrob Agents Chemother, 2012. **56**(2): p. 1128-1132.
225. Breidenstein, E.B., et al., *The Lon protease is essential for full virulence in Pseudomonas aeruginosa*. PloS one, 2012. **7**(11): p. e49123.
226. Heywood, A. and I.L. Lamont, *Cell envelope proteases and peptidases of Pseudomonas aeruginosa: multiple roles, multiple mechanisms*. FEMS Microbiol Rev, 2020. **44**(6): p. 857-873.

227. Papp-Wallace, K.M., et al., *Ceftazidime-Avibactam in Combination With Fosfomycin: A Novel Therapeutic Strategy Against Multidrug-Resistant Pseudomonas aeruginosa*. J Infect Dis, 2019. **220**(4): p. 666-676.
228. Seo, J. and A.J. Darwin, *The Pseudomonas aeruginosa periplasmic protease CtpA can affect systems that impact its ability to mount both acute and chronic infections*. Infect Immun, 2013. **81**(12): p. 4561-4570.
229. Yakhnina, A.A., H.R. McManus, and T.G. Bernhardt, *The cell wall amidase AmiB is essential for Pseudomonas aeruginosa cell division, drug resistance and viability*. Mol Microbiol, 2015. **97**(5): p. 957-973.
230. Gupta, V., *An update on newer beta-lactamases*. India J Med Res, 2007. **126**(5): p. 417-421.
231. Bush, K. and G.A. Jacoby, *Updated functional classification of β -actamases*. Antimicrob Agents Chemother, 2010. **54**(3): p. 969-976.
232. Treepong, P., et al., *Global emergence of the widespread Pseudomonas aeruginosa ST235 clone*. Clin Microbiol Infect, 2018. **24**(3): p. 258-266.
233. Balasubramanian, D., et al., *The regulatory repertoire of Pseudomonas aeruginosa AmpC β -lactamase regulator AmpR includes virulence genes*. PloS One, 2012. **7**(3): p. e34067.
234. Schnoes, A.M., et al., *Annotation error in public databases: misannotation of molecular function in enzyme superfamilies*. PLoS Comp Biol, 2009. **5**(12): p. e1000605-e1000605.
235. Roberts, R.J., et al., *An experimental approach to genome annotation. American Academy of Microbiology Colloquia Reports*, in *An experimental approach to genome annotation: a colloquium of the American Academy of Microbiology, 2004, Washington DC*.
236. Brown, E.D. and G.D. Wright, *Antibacterial drug discovery in the resistance era*. Nature, 2016. **529**(7586): p. 336-343.
237. Zrieq, R., et al., *Genome-wide screen of Pseudomonas aeruginosa in Saccharomyces cerevisiae identifies new virulence factors*. Front Cell Infect Microbiol, 2015. **5**: p. 81.
238. Bakheet, T.M. and A.J. Doig, *Properties and identification of antibiotic drug targets*. BMC Bioinformat, 2010. **11**(1): p. 1-10.
239. Winsor, G.L., et al., *Pseudomonas Genome Database: facilitating user-friendly, comprehensive comparisons of microbial genomes*. Nucleic Acids Res, 2009. **37**(suppl_1): p. D483-D488.
240. Kelley, L.A., et al., *The Phyre2 web portal for protein modeling, prediction and analysis*. Nat Prot, 2015. **10**(6): p. 845-858.
241. Hirokawa, T., S. Boon-Chieng, and S. Mitaku, *SOSUI: classification and secondary structure prediction system for membrane proteins*. Bioinformatics (Oxford, England), 1998. **14**(4): p. 378-379.
242. Schneider, C.A., W.S. Rasband, and K.W. Eliceiri, *NIH Image to ImageJ: 25 years of image analysis*. Nat Meth, 2012. **9**(7): p. 671-675.
243. Hall, T. *BioEdit: a user-friendly biological sequence alignment editor and analysis program for Windows 95/98/NT*. in Nucleic Acids Symp. Ser. 1999.
244. Korbie, D.J. and J.S. Mattick, *Touchdown PCR for increased specificity and sensitivity in PCR amplification*. Nat Prot, 2008. **3**(9): p. 1452.
245. Crowe, J., et al., *Improved cloning efficiency of polymerase chain reaction (PCR) products after proteinase K digestion*. Nucleic Acids Res, 1991. **19**(1): p. 184.
246. Gallet, B., F. Bernaudat, and T. Vernet, *Large scale purification of linear plasmid DNA for efficient high throughput cloning*. WILEY-VCH Verlag, 2010. **5**(9): p. 978-985.
247. Gibson, D.G., et al., *Enzymatic assembly of DNA molecules up to several hundred kilobases*. Nat Meth, 2009. **6**(5): p. 343-345.
248. Russell, D.W. and J. Sambrook, *Molecular cloning: a laboratory manual*. Vol. 1. 2001: Cold Spring Harbor Laboratory Cold Spring Harbor, NY.
249. Bertani, G., *Lysogeny at mid-twentieth century: P1, P2, and other experimental systems*. J Bacteriol, 2004. **186**(3): p. 595-600.
250. Hanahan, D., *Studies on transformation of Escherichia coli with plasmids*. J Mol Biol, 1983. **166**(4): p. 557-580.

251. Studier, F.W. and B.A. Moffatt, *Use of bacteriophage T7 RNA polymerase to direct selective high-level expression of cloned genes*. J Mol Biol, 1986. **189**(1): p. 113-130.
252. Miroux, B. and J.E. Walker, *Over-production of proteins in Escherichia coli: mutant hosts that allow synthesis of some membrane proteins and globular proteins at high levels*. J Mol Biol, 1996. **260**(3): p. 289-298.
253. Holloway, B., V. Krishnapillai, and A. Morgan, *Chromosomal genetics of Pseudomonas*. Microbiol Rev, 1979. **43**(1): p. 73.
254. Held, K., et al., *Sequence-verified two-allele transposon mutant library for Pseudomonas aeruginosa PAO1*. J Bacteriol, 2012. **194**(23): p. 6387-6389.
255. Kovach, M.E., et al., *Four new derivatives of the broad-host-range cloning vector pBBR1MCS, carrying different antibiotic-resistance cassettes*. Gene, 1995. **166**(1): p. 175-176.
256. Sanders, E.R., *Aseptic laboratory techniques: plating methods*. J Vis Exp, 2012(63): p. e3064.
257. Hills, A.E., *Spectroscopy in Biotechnology Research and Development*. Academic Press, 2017. p. 198-202.
258. Sambrook, J. and D.W. Russell, *The inoue method for preparation and transformation of competent E. coli: "ultra-competent" cells*. CSH Protoc, 2006. **2006**(1): p. 10.1101.
259. Riley, L.M., et al., *Structural and functional characterization of Pseudomonas aeruginosa AlgX: role of AlgX in alginate acetylation*. J Biol Chem, 2013. **288**(31): p. 22299-22314.
260. Putra, S.E.D., et al., *Dealing with large sample sizes: comparison of a new one spot dot blot method to western blot*. Clin Lab, 2014. **60**(11): p. 1871-1877.
261. Laemmli, U.K., *Cleavage of structural proteins during the assembly of the head of bacteriophage T4*. Nature, 1970. **227**(5259): p. 680-685.
262. Sambrook, J. and D.W. Russell, *SDS-polyacrylamide gel electrophoresis of proteins*. CSH Protoc, 2006. **2006**(4): p. pdb. prot4540.
263. Towbin, H., T. Staehelin, and J. Gordon, *Electrophoretic transfer of proteins from polyacrylamide gels to nitrocellulose sheets: procedure and some applications*. PNAS, 1979. **76**(9): p. 4350-4354.
264. Jaeger, K.-E. and F. Kovacic, *Determination of lipolytic enzyme activities*, in *Pseudomonas Methods and Protocols*, A. Filloux and J.-L. Ramos, Editors. 2014, Springer New York: New York, NY. p. 111-134.
265. Kuznetsova, E., et al., *Enzyme genomics: Application of general enzymatic screens to discover new enzymes*. FEMS Microbiol Rev, 2005. **29**(2): p. 263-79.
266. Kurioka, S. and M. Matsuda, *Phospholipase C assay using p-nitrophenylphosphorylcholine together with sorbitol and its application to studying the metal and detergent requirement of the enzyme*. Anal Biochem, 1976. **75**(1): p. 281-289.
267. Bücher, K.S., et al., *Monodisperse sequence-controlled α -l-fucosylated glycooligomers and their multivalent inhibitory effects on LecB*. Macromol Biosci, 2018. **18**(12): p. 1800337.
268. O'Toole, G.A., *Microtiter dish biofilm formation assay*. J Vis Exp, 2011(47): p. 2437.
269. Koch, G., et al., *Assessing Pseudomonas virulence with nonmammalian host: Galleria mellonella*, in *Pseudomonas Methods and Protocols*. 2014, Springer. p. 681-688.
270. Sui, S.J.H., et al., *The association of virulence factors with genomic islands*. PloS One, 2009. **4**(12): p. e8094.
271. Winsor, G.L., et al., *Enhanced annotations and features for comparing thousands of Pseudomonas genomes in the Pseudomonas genome database*. Nucleic Acids Res, 2016. **44**(D1): p. D646-653.
272. Babic, N. and F. Kovacic, *Predicting drug targets by homology modelling of Pseudomonas aeruginosa proteins of unknown function*. PLoS One, 2021. **16**(10): p. e0258385.
273. Lee, S.A., et al., *General and condition-specific essential functions of Pseudomonas aeruginosa*. PNAS USA, 2015. **112**(16): p. 5189-5194.
274. Kelley, L.A., et al., *The Phyre2 web portal for protein modeling, prediction and analysis*. Nat Protoc, 2015. **10**: p. 845-858.

275. Kelley, L.A., et al., *The Phyre2 web portal for protein modeling, prediction and analysis*. Nat Protoc, 2015. **10**(6): p. 845-858.
276. Kovach, M.E., et al., *Four new derivatives of the broad-host-range cloning vector pBBR1MCS, carrying different antibiotic-resistance cassettes*. Gene, 1995. **166**(1): p. 175-6.
277. Obranić, S., F. Babić, and G. Maravić-Vlahoviček, *Improvement of pBBR1MCS plasmids, a very useful series of broad-host-range cloning vectors*. Plasmid, 2013. **70**(2): p. 263-267.
278. Kovacic, F., et al., *A membrane-bound esterase PA2949 from Pseudomonas aeruginosa is expressed and purified from Escherichia coli*. FEBS Open Bio, 2016. **6**(5): p. 484-493.
279. Ahmad, S., et al., *Substrate access mechanism in a novel membrane-bound phospholipase A of Pseudomonas aeruginosa concordant with specificity and regioselectivity*. bioRxiv, 2021.doi: <https://doi.org/10.1101/2021.06.29.450291>.
280. Mokhonova, E.I., et al., *Forceful large-scale expression of "problematic" membrane proteins*. Biochem Biophys Res Comm, 2005. **327**(3): p. 650-655.
281. Tsai, C.J.-Y., J.M.S. Loh, and T. Proft, *Galleria mellonella infection models for the study of bacterial diseases and for antimicrobial drug testing*. Virulence, 2016. **7**(3): p. 214-229.
282. Gerlt, J.A., *Tools and strategies for discovering novel enzymes and metabolic pathways*. Perspect Sci, 2016. **9**: p. 24-32.
283. Antczak, M., M. Michaelis, and M.N. Wass, *Environmental conditions shape the nature of a minimal bacterial genome*. Nature Comm, 2019. **10**(1): p. 1-13.
284. Roberts, R.J., et al., *An experimental approach to genome annotation*. American Academy of Microbiology Colloquia Reports, in *An experimental approach to genome annotation: a colloquium of the American Academy of Microbiology, 2004, Washington DC*.
285. Gerlt, J.A., et al., *The enzyme function initiative*. Biochem, 2011. **50**(46): p. 9950-9962.
286. Babic, N. and F. Kovacic, *Predicting drug targets by homology modelling of Pseudomonas aeruginosa proteins of unknown function*. PLOS ONE, 2021. **16**(10): p. e0258385.
287. Hardison, R.C., *Comparative genomics*. PLoS Biol, 2003. **1**(2): p. E58-E58.
288. Pandey, G., V. Kumar, and M. Steinbach, *Computational approaches for protein function prediction: A survey*, 2006.
289. Allen, J.P., et al., *A comparative genomics approach identifies contact-dependent growth inhibition as a virulence determinant*. PNAS, 2020. **117**(12): p. 6811.
290. Huynen, M., T. Dandekar, and P. Bork, *Differential genome analysis applied to the species-specific features of Helicobacter pylori*. FEBS Letters, 1998. **426**(1): p. 1-5.
291. Sakharkar, K.R., M.K. Sakharkar, and V.T. Chow, *A novel genomics approach for the identification of drug targets in pathogens, with special reference to Pseudomonas aeruginosa*. In Silico Biol, 2004. **4**(3): p. 355-60.
292. Lee, S.A., et al., *General and condition-specific essential functions of Pseudomonas aeruginosa*. PNAS, 2015. **112**(16): p. 5189.
293. Kadurugamuwa, J. and T. Beveridge, *Natural release of virulence factors in membrane vesicles by Pseudomonas aeruginosa and the effect of aminoglycoside antibiotics on their release*. J Antimicrob Chemother, 1997. **40**(5): p. 615-621.
294. Higdon, R., B. Louie, and E. Kolker, *Modeling sequence and function similarity between proteins for protein functional annotation*. Proc Int Symp High Perform Distrib Comput, 2010. **2010**: p. 499-502.
295. Pandey, G., V. Kumar, and M. Steinbach, *Computational approaches for protein function prediction: A survey*. Twin Cities: Department of Computer Science and Engineering, University of Minnesota, 2006. **1**.
296. Whisstock, J.C. and A.M. Lesk, *Prediction of protein function from protein sequence and structure*. Q Rev Biophys, 2003. **36**(3): p. 307-340.
297. Teichmann, S.A., A.G. Murzin, and C. Chothia, *Determination of protein function, evolution and interactions by structural genomics*. Curr Opin Struct Biol, 2001. **11**(3): p. 354-363.

298. Heinemann, U., *Structural genomics: structure-to-function approaches*, in *encyclopedia of genomics and proteomics in molecular medicine*. 2006, Springer Berlin Heidelberg: Berlin, Heidelberg. p. 1810-1816.
299. Babic, N. and F. Kovacic, *Predicting drug targets by homology modelling of Pseudomonas aeruginosa proteins of unknown function*. PloS one, 2021. **16**(10): p. e0258385.
300. Mao, C., et al., *Functional assignment of Mycobacterium tuberculosis proteome revealed by genome-scale fold-recognition*. Tuberculosis, 2013. **93**(1): p. 40-46.
301. Antczak, M., M. Michaelis, and M.N. Wass, *Environmental conditions shape the nature of a minimal bacterial genome*. Nature Comm, 2019. **10**(1): p. 3100.
302. Houston, S., et al., *Functional insights from proteome-wide structural modeling of Treponema pallidum subspecies pallidum, the causative agent of syphilis*. BMC Struct Biol, 2018. **18**(1): p. 1-18.
303. Sousounis, K., et al., *Conservation of the three-dimensional structure in non-homologous or unrelated proteins*. Hum Genomics, 2012. **6**(1): p. 10.
304. Loewenstein, Y., et al., *Protein function annotation by homology-based inference*. Genome Biol, 2009. **10**(2): p. 207.
305. Xu, X., P. Zhao, and S.-J. Chen, *Vfold: a web server for RNA structure and folding thermodynamics prediction*. PloS one, 2014. **9**(9): p. e107504.
306. Ohse, M., et al., *Effects of plasmid DNA sizes and several other factors on transformation of Bacillus subtilis ISW1214 with plasmid DNA by electroporation*. Biosci Biotechnol Biochem, 1995. **59**(8): p. 1433-1437.
307. Rosano, G.L. and E.A. Ceccarelli, *Recombinant protein expression in Escherichia coli: advances and challenges*. Front Microbiol, 2014. **5**(172).
308. Liang, T., et al., *Construction of T7-like expression system in Pseudomonas putida KT2440 to enhance the heterologous expression level*. Front Chem, 2021. **9**(556).
309. Jia, B. and C.O. Jeon, *High-throughput recombinant protein expression in Escherichia coli: current status and future perspectives*. Open Biol, 2016. **6**(8): p. 160196.
310. Wong, C.F., et al., *Construction of new genetic tools as alternatives for protein overexpression in Escherichia coli and Pseudomonas aeruginosa*. Iran J Biotechnol, 2017. **15**(3): p. 194-200.
311. Troeschel, S.C., et al., *Novel broad host range shuttle vectors for expression in Escherichiacoli, Bacillus subtilis and Pseudomonas putida*. J Biotechnol, 2012. **161**(2): p. 71-9.
312. Nora, L.C., et al., *The art of vector engineering: towards the construction of next-generation genetic tools*. Microb Biotechnol, 2019. **12**(1): p. 125-147.
313. Kovacic, F., et al., *A membrane-bound esterase PA2949 from Pseudomonas aeruginosa is expressed and purified from Escherichia coli*. FEBS open bio, 2016. **6**(5): p. 484-493.
314. Bleffert, F., et al., *Pseudomonas aeruginosa esterase PA2949, a bacterial homolog of the human membrane esterase ABHD6: expression, purification and crystallization*. Acta CrystF, 2019. **75**(4): p. 270-277.
315. Schweizer, H.P., *Vectors to express foreign genes and techniques to monitor gene expression in Pseudomonads*. Curr Opin Biotechnol, 2001. **12**(5): p. 439-45.
316. Wong, C.F., et al., *Construction of new genetic tools as alternatives for protein overexpression in Escherichia coli and Pseudomonas aeruginosa*. Iran J Biotechnol, 2017. **15**(3): p. 194.
317. Kato, Y., *Extremely low leakage expression systems using dual transcriptional-translational control for toxic protein production*. Int J Mol Sci, 2020. **21**(3): p. 705.
318. Lu, S.-E., B.K. Scholz-Schroeder, and D.C. Gross, *Construction of pMEKm12, an expression vector for protein production in Pseudomonas syringae*. FEMS Microbiol Lett, 2002. **210**(1): p. 115-121.
319. Qiu, D., et al., *PBAD-based shuttle vectors for functional analysis of toxic and highly regulated genes in Pseudomonas and Burkholderia spp. and other bacteria*. App Environ Microbiol, 2008. **74**(23): p. 7422-7426.
320. Fakruddin, M., et al., *Critical factors affecting the success of cloning, expression, and mass production of enzymes by recombinant E. coli*. ISRN Biotechnol, 2013. **2013**: p. 590587.

321. Na, G., et al., *A low-copy-number plasmid for retrieval of toxic genes from BACs and generation of conditional targeting constructs*. Mol Biotechnol, 2013. **54**(2): p. 504-514.
322. Jahn, M., et al., *Copy number variability of expression plasmids determined by cell sorting and droplet digital PCR*. Microb Cell Fact, 2016. **15**(1): p. 211-211.
323. Bleffert, F., et al., *Evidence for a bacterial Lands cycle phospholipase A: Structural and mechanistic insights into membrane phospholipid remodeling*. bioRxiv, 2021: p. 2021.06.22.448587.
324. LaBaer, J., et al., *The Pseudomonas aeruginosa PAO1 Gene Collection*. Genome Res, 2004. **14**(10b): p. 2190-2200.
325. Brandner, C.J., et al., *The ORFeome of Staphylococcus aureus v 1.1*. BMC Genomics, 2008. **9**: p. 321.
326. Dricot, A., et al., *Generation of the Brucella melitensis ORFeome version 1.1*. Genome Res, 2004. **14**(10B): p. 2201-2206.
327. Maier, C.J., et al., *Construction of a highly flexible and comprehensive gene collection representing the ORFeome of the human pathogen Chlamydia pneumoniae*. BMC Genomics, 2012. **13**: p. 632.
328. Murthy, T., et al., *A Full-Genomic Sequence-Verified Protein-Coding Gene Collection for Francisella tularensis*. PLOS ONE, 2007. **2**(6): p. e577.
329. Rolfs, A., et al., *Production and sequence validation of a complete full length ORF collection for the pathogenic bacterium Vibrio cholerae*. PNAS, 2008. **105**(11): p. 4364-4369.
330. Nagase, T., et al., *Exploration of human ORFeome: high-throughput preparation of ORF clones and efficient characterization of their protein products*. DNA Res, 2008. **15**: p. 137 - 149.
331. Festa, F., et al., *High-throughput cloning and expression library creation for functional proteomics*. Proteomics, 2013. **13**(9): p. 1381-1399.
332. Klockgether, J., et al., *Pseudomonas aeruginosa genomic structure and diversity*. Front Microbiol, 2011. **2**(150).
333. Kolmodin, L.A. and D.E. Birch, *Polymerase chain reaction. Basic principles and routine practice*. Methods Mol Biol, 2002. **192**: p. 3-18.
334. Farrell, E.M. and G. Alexandre, *Bovine serum albumin further enhances the effects of organic solvents on increased yield of polymerase chain reaction of GC-rich templates*. BMC research notes, 2012. **5**(1): p. 1-8.
335. Terpe, K., *Overview of bacterial expression systems for heterologous protein production: from molecular and biochemical fundamentals to commercial systems*. Appl Microbiol Biotechnol, 2006. **72**(2): p. 211-222.
336. Kwon, S.K., et al., *Comparative genomics and experimental evolution of Escherichia coli BL21(DE3) strains reveal the landscape of toxicity escape from membrane protein overproduction*. Sci Rep, 2015. **5**(1): p. 16076.
337. Vincentelli, R. and C. Romier, *Expression in Escherichia coli: becoming faster and more complex*. Curr Opin Struct Biol, 2013. **23**(3): p. 326-334.
338. Knaust, R.K. and P. Nordlund, *Screening for soluble expression of recombinant proteins in a 96-well format*. Anal Biochem, 2001. **297**(1): p. 79-85.
339. Vincentelli, R., et al., *Automated expression and solubility screening of His-tagged proteins in 96-well format*. Anal Biochem, 2005. **346**(1): p. 77-84.
340. Ahmad, S., et al., *Substrate access mechanism in a novel membrane-bound phospholipase A of Pseudomonas aeruginosa concordant with specificity and regioselectivity*. J Chem Inf Model, 2021. **61**(11): p. 5626-5643.
341. Weiler, A.J., et al., *Novel intracellular phospholipase B from Pseudomonas aeruginosa with activity towards endogenous phospholipids affects biofilm assembly*. bioRxiv, 2021. doi: <https://doi.org/10.1101/2021.06.15.448513>.
342. Eisenstein, E., et al., *Biological function made crystal clear - annotation of hypothetical proteins via structural genomics*. Curr Opin Biotechnol, 2000. **11**(1): p. 25-30.

343. Baumann, M., R. Stürmer, and U.T. Bornscheuer, *A high-throughput-screening method for the identification of active and enantioselective hydrolases*. *Angew Chem Int Ed*, 2001. **40**(22): p. 4201-4204.
344. Coughlan, L., et al., *Biotechnological applications of functional metagenomics in the food and pharmaceutical industries*. *Front microbiol*, 2015. **6**(672).
345. Thies, S., et al., *Metagenomic discovery of novel enzymes and biosurfactants in a slaughterhouse biofilm microbial community*. *Sci Rep*, 2016. **6**(1): p. 27035.
346. Molitor, R., et al., *Agar plate-based screening methods for the identification of polyester hydrolysis by Pseudomonas species*. *Microb Biotechnol*, 2020. **13**(1): p. 274-284.
347. Goddard, J.-P. and J.-L. Reymond, *Enzyme assays for high-throughput screening*. *Curr Opin Biotechnol*, 2004. **15**(4): p. 314-322.
348. Xiao, H., Z. Bao, and H. Zhao, *High throughput screening and selection methods for directed enzyme evolution*. *Ind Eng Chem Res*, 2015. **54**(16): p. 4011-4020.
349. Braun, P. and J. LaBaer, *High throughput protein production for functional proteomics*. *Trends Biotechnol*, 2003. **21**(9): p. 383-388.
350. Singh, A., et al., *Protein recovery from inclusion bodies of Escherichia coli using mild solubilization process*. *Microb cell factories*, 2015. **14**(1): p. 1-10.
351. Phizicky, E.M., et al., *Biochemical genomics approach to map activities to genes*. *Meth Enzymol*, 2002. **350**: p. 546-559.
352. Reymond, J.-L., *Enzyme assays: high-throughput screening, genetic selection and fingerprinting*. 2006: John Wiley & Sons.
353. Lescic Asler, I., et al., *Probing enzyme promiscuity of SGNH hydrolases*. *Chembiochem*, 2010. **11**(15): p. 2158-67.
354. Weiler, A.J., et al., *Novel intracellular phospholipase B from Pseudomonas aeruginosa with activity towards endogenous phospholipids affects biofilm assembly*. *bioRxiv*, 2021. doi: <https://doi.org/10.1101/2021.06.15.448513>.
355. Perraud, Q., et al., *A key role for the periplasmic PfeE esterase in iron acquisition via the siderophore enterobactin in Pseudomonas aeruginosa*. *ACS Chem Biol*, 2018. **13**(9): p. 2603-2614.
356. UniProt, C., *UniProt: the universal protein knowledgebase in 2021*. *Nucleic Acids Res*, 2021. **49**(D1): p. D480-D489.
357. Wagner, U.G., et al., *EstB from Burkholderia gladioli: a novel esterase with a beta-lactamase fold reveals steric factors to discriminate between esterolytic and beta-lactam cleaving activity*. *Protein Sci*, 2002. **11**(3): p. 467-78.
358. Arpigny, J.L. and K.E. Jaeger, *Bacterial lipolytic enzymes: classification and properties*. *Biochem J*, 1999. **343 Pt 1**(Pt 1): p. 177-83.
359. Liberati, N.T., et al., *An ordered, nonredundant library of Pseudomonas aeruginosa strain PA14 transposon insertion mutants*. *Proc Natl Acad Sci U S A*, 2006. **103**(8): p. 2833-8.
360. Petersen, E.I., et al., *A novel esterase from Burkholderia gladioli which shows high deacetylation activity on cephalosporins is related to beta-lactamases and DD-peptidases*. *J Biotechnol*, 2001. **89**(1): p. 11-25.
361. Choi, D.S., et al., *Proteomic analysis of outer membrane vesicles derived from Pseudomonas aeruginosa*. *Proteomics*, 2011. **11**(16): p. 3424-9.
362. Cox, A.J., et al., *Cloning and characterisation of the Pasteurella multocida ahpA gene responsible for a haemolytic phenotype in Escherichia coli*. *Vet Microbiol*, 2000. **72**(1-2): p. 135-52.
363. Lee, S.A., et al., *General and condition-specific essential functions of Pseudomonas aeruginosa*. *PNAS USA*, 2015. **112**(16): p. 5189-5194.
364. Son, M.S., et al., *In vivo evidence of Pseudomonas aeruginosa nutrient acquisition and pathogenesis in the lungs of cystic fibrosis patients*. *Infect Immun*, 2007. **75**(11): p. 5313-5324.
365. Cox, A.J., et al., *Cloning and characterisation of the Pasteurella multocida ahpA gene responsible for a haemolytic phenotype in Escherichia coli*. *Vet Microbiol*, 2000. **72**(1-2): p. 135-52.

366. Ruiz, C., et al., *Helicobacter pylori* EstV: identification, cloning, and characterization of the first lipase isolated from an epsilon-proteobacterium. *Appl Environ Microbiol*, 2007. **73**(8): p. 2423-2431.
367. Rao, L., et al., A thermostable esterase from *Thermoanaerobacter tengcongensis* opening up a new family of bacterial lipolytic enzymes. *Biochim Biophys Acta*, 2011. **1814**(12): p. 1695-702.
368. Lescic Asler, I., et al., Probing enzyme promiscuity of SGNH hydrolases. *Chembiochem*, 2010. **11**(15): p. 2158-67.
369. Henry, J.T. and S. Crosson, Ligand-binding PAS domains in a genomic, cellular, and structural context. *Annu Rev Microbiol*, 2011. **65**: p. 261-286.
370. Chan, C., et al., Structural basis of activity and allosteric control of diguanylate cyclase. *PNAS*, 2004. **101**(49): p. 17084-17089.
371. Bellini, D., et al., Dimerisation induced formation of the active site and the identification of three metal sites in EAL-phosphodiesterases. *Sci Rep*, 2017. **7**: p. 42166-42166.
372. Möglich, A., R.A. Ayers, and K. Moffat, Structure and Signaling Mechanism of Per-ARNT-Sim Domains. *Structure*, 2009. **17**(10): p. 1282-1294.
373. Ryjenkov, D.A., et al., Cyclic diguanylate is a ubiquitous signaling molecule in bacteria: insights into biochemistry of the GGDEF protein domain. *J Bacteriol Res*, 2005. **187**(5): p. 1792-1798.
374. Galperin, M.Y., A.N. Nikolskaya, and E.V. Koonin, Novel domains of the prokaryotic two-component signal transduction systems. *FEMS Microbiol Lett*, 2001. **203**(1): p. 11-21.
375. Liu, C., et al., Insights into biofilm dispersal regulation from the crystal structure of the PAS-GGDEF-EAL region of RbdA from *Pseudomonas aeruginosa*. *J Bacteriol Res*, 2018. **200**(3): p. e00515-17.
376. Kulesekara, H., et al., Analysis of *Pseudomonas aeruginosa* diguanylate cyclases and phosphodiesterases reveals a role for bis-(3'-5')-cyclic-GMP in virulence. *PNAS USA*, 2006. **103**(8): p. 2839-2844.
377. Liu, C., et al., Insights into biofilm dispersal regulation from the crystal structure of the PAS-GGDEF-EAL region of RbdA from *Pseudomonas aeruginosa*. *J Bacteriol Res*, 2018. **200**(3): p. e00515-17.
378. Phippen, C.W., et al., Formation and dimerization of the phosphodiesterase active site of the *Pseudomonas aeruginosa* MorA, a bi-functional c-di-GMP regulator. *FEBS letters*, 2014. **588**(24): p. 4631-4636.
379. Mantoni, F., et al., Insights into the GTP-dependent allosteric control of c-di-GMP hydrolysis from the crystal structure of PA0575 protein from *Pseudomonas aeruginosa*. *The FEBS journal*, 2018. **285**(20): p. 3815-3834.
380. Devamani, T., et al., Catalytic promiscuity of ancestral esterases and hydroxynitrile lyases. *J Am Chem Soc*, 2016. **138**(3): p. 1046-56.
381. Zheng, H., et al., Identification of integrator-PP2A complex (INTAC), an RNA polymerase II phosphatase. *Science*, 2020. **370**(6520).
382. Greber, B.J., et al., The complete structure of the human TFIIH core complex. *Elife*, 2019. **8**: p. e44771.
383. Das, A.K., P.T. Cohen, and D. Barford, The structure of the tetratricopeptide repeats of protein phosphatase 5: implications for TPR-mediated protein-protein interactions. *EMBO Rep*, 1998. **17**(5): p. 1192-1199.
384. Cervený, L., et al., Tetratricopeptide repeat motifs in the world of bacterial pathogens: role in virulence mechanisms. *Infect Immun*, 2013. **81**(3): p. 629-35.
385. Wang, S., et al., Dissecting the role of VicK phosphatase in aggregation and biofilm formation of *Streptococcus mutans*. *J Dent Res*, 2021. **100**(6): p. 631-638.
386. Park, J., et al., Structural basis for nucleotide-independent regulation of acyl-CoA thioesterase from *Bacillus cereus* ATCC 14579. *Int J Biol Macromol*, 2021. **170**: p. 390-396.
387. Burns, B., G. Mendz, and S. Hazell, Methods for the measurement of a bacterial enzyme activity in cell lysates and extracts. *Biol Proced online*, 1998. **1**: p. 17-26.

388. Jamal, M., et al., *Bacterial biofilm and associated infections*. J Chin Med Assoc, 2018. **81**(1): p. 7-11.
389. Jencks, W.P., *On the attribution and additivity of binding energies*. PNAS, 1981. **78**(7): p. 4046-4050.
390. Weber, M., A. Bujotzek, and R. Haag, *Quantifying the rebinding effect in multivalent chemical ligand-receptor systems*. J Chem Phys, 2012. **137**(5): p. 054111.
391. Morvan, F., et al., *Fucosylated pentaerythrityl phosphodiester oligomers (PePOs): automated synthesis of DNA-based glycoclusters and binding to Pseudomonas aeruginosa lectin (PA-III)*. Bioconjug Chem, 2007. **18**(5): p. 1637-1643.
392. Berthet, N., et al., *High affinity glycodendrimers for the lectin LecB from Pseudomonas aeruginosa*. Bioconjug Chem, 2013. **24**(9): p. 1598-1611.
393. Smadhi, M., et al., *Expeditive synthesis of trithiotriazine-cored glycoclusters and inhibition of Pseudomonas aeruginosa biofilm formation*. Beilstein J Org Chem, 2014. **10**(1): p. 1981-1990.
394. Kitov, P.I. and D.R. Bundle, *On the nature of the multivalency effect: a thermodynamic model*. J Am Chem Soc, 2003. **125**(52): p. 16271-16284.
395. Kolomiets, E., et al., *Glycopeptide dendrimers with high affinity for the fucose-binding lectin LecB from Pseudomonas aeruginosa*. ChemMedChem, 2009. **4**(4): p. 562-569.
396. Sabin, C., et al., *Binding of different monosaccharides by lectin PA-III from Pseudomonas aeruginosa: thermodynamics data correlated with X-ray structures*. FEBS letters, 2006. **580**(3): p. 982-987.
397. Johansson, E.M., et al., *Inhibition and dispersion of Pseudomonas aeruginosa biofilms by glycopeptide dendrimers targeting the fucose-specific lectin LecB*. Chem Biol, 2008. **15**(12): p. 1249-57.